DENDRITIC CELLS CONTRIBUTE TO PERIVASCULAR ADIPOSE TISSUE DYSFUNCTION IN TYPE 2 DIABETES

A Dissertation presented to the Faculty of the Graduate School

University of Missouri

In Partial Fulfillment of

The Requirements for the Degree

Doctor of Philosophy

By

TIANYI QIU

Dr. Michael A. Hill, Dissertation Supervisor

July 2017

The undersigned, appointed by the dean of the Graduate School,

Have examined the dissertation entitled

DENDRITIC CELLS CONTRIBUTE TO PERIVASCULAR ADIPOSE TISSUE DYSFUNCTION IN TYPE 2 DIABETES

Presented by Tianyi Qiu

A candidate for the degree of Doctor of Philosophy

And hereby certify that, in their opinion, it is worthy of acceptance.

Dr. Michael A. Hill

Dr. Ronald J. Korthuis

Dr. James R. Sowers

Dr. Michael J. Davis

ACKNOWLEDGEMENTS

My most cordial gratitude is given to my mentor, Dr. Michael Hill. I came from University of Wuhan in China with little background knowledge about microcirculation area. Surprisingly, Dr. Hill accepted me in his lab and introduced me into the fantastic microcirculation world. He gradually taught me basic research concepts and showed me the practical techniques of microcirculation functional studies. He also guided me into the correct research direction by inspiring me with interesting questions. Usually after a small discussion, I had a very clear picture on my experiments. I also appreciated that he sincerely encouraged students to attend different symposiums, which greatly built up my confidence on my research project. I do feel very grateful that my mentor always supported our students' research even when the funding was tight, so that my project could be completed successfully.

I also want to express my deep gratitude to my co-mentor Dr. Ronald J. Korthuis. When I was first enrolled into our department, I chose to stay in Dr. Cuihua Zhang's lab for my PhD life. Unfortunately, Dr. Zhang passed away due to her health issue during my first PhD year. I felt very sad about the death of Dr. Zhang and at the same time worried about my PhD progress. At this moment, Dr. Korthuis introduced me into Dr. Hill's lab, which opened an opportunity to continue my study. Also, I would like to sincerely appreciate the financial support from Dr. Korthuis for my last year's research. Without his kindly assistance, I could not finish my project on time. Meanwhile, I would like to thank my other committee members, Dr. Sowers and Dr. Davis. During the progress of my project, they offered me very valuable and insightful suggestions and made me think deeper in my project.

Finally, I would like to thank Dr. Ming Li, who was one of Dr. Hill's lab members. I was surprised by her vast knowledge of cell and molecular biology techniques. She was so kind that she never felt exhausted to explain those technique mechanisms and assist students on problem-shooting during experiments. With her help, I successfully mastered PCR, flow cytometry and

immunohistochemistry principles and procedures, which largely promoted the progress of my research. I also want to thank Dr. Nourian Zahra and Dr. Yan Yang for their excellent assistance in data analysis.

Last but not least, I want to thank my parents and husband for their spiritual support during the hardship of my PhD life.

TABLE OF CONTENTS

LIST OF FIGURES

Figure **Pages**

LIST OF TABLES

Tables **Pages**

LIST OF ABBREVIATIONS

ACC1	acetyl-CoA carboxylase 1
ACh	acetylcholine
ADRF	adipocyte-derived relaxing factor
AH	pericardial adipose tissue
α-GalCer	α-galactosylceramide
AMPK	AMP- activated protein kinase
Ang	angiotensin
ANOVA	analysis of variance
APC	antigen presenting cell
ATA	periaortic adipose tissue
ATM	adipose tissue macrophage
BMI	body mass index
CD40L	CD40 ligand
CLS	crown-like structure
CSE	cystathionine γ-lyase
CT	threshold cycle
DTR	diphtheria toxin receptor
eNOS	endothelial nitric oxide synthase
ERK	extracellular signal-regulated protein kinase
ET-1	endothelin-1
4-AP	4-aminopyridine
Flt3l	FMS-like tyrosine kinase 3 ligand
GAPDH	glyceraldehyde 3-phosphate dehydrogenase
GLUT4	glucose transporter type 4
H_2O_2	hydrogen peroxide

H_2S	hydrogen sulfide
IFN-γ	interferon gamma
IKKβ	IκB kinase β
IL-1β	interleukin 1 β
IL-1R1	interleukin 1 receptor type 1
IL-2	interleukin 2
IL-4	interleukin 4
IL-5	interleukin 5
IL-6	interleukin 6
IL-8	interleukin 8
IL-10	interleukin 10
IL-13	interleukin 13
IL-17	interleukin 17
IL-22	interleukin 22
IL-33	interleukin 33
ILC2	lymphoid type 2 cell
iNKT	invariant natural killer T cell
IRS	insulin-receptor substrate
iTreg	induced regulatory T cell
JNK	JUN N-terminal kinase
Kv channel	voltage-dependent potassium channel
LAD	left anterior descending coronary artery
LXR α	liver X receptor α
MA	mesenteric artery
MAIT	mucosal associated invariant T cell
MAPK	mitogen-activated protein kinase

MAT	mesenteric adipose tissue
MCP-1	monocyte chemo attractant protein-1
MCP-3	monocyte chemo attractant protein-3
MHC	major histocompatibility complex
NADPH	nicotinamide adenine dinucleotide phosphate
NEFA	non-esterified fatty acid
NF-κB	nuclear factor-κB
NKT	natural killer T cell
NLRP3 protein 3	nucleotide-binding domain, leucine-rich repeat containing
NO	nitric oxide
PE	phenylephrine
PPAR-γ	peroxisome proliferation-activated receptor γ
PPAR-α	peroxisome proliferation-activated receptor α
PSS	physiological saline solution
PVAT	perivascular adipose tissue
qPCR	quantitative polymerase chain reaction
ROS	reactive oxygen species
SOD	superoxide dismutase
STAT	signaling transducer and activator of transcription protein
TA	thoracic aorta
TBS	Tris-Buffered Saline
TCR	T cell receptor
T2DM	type 2 diabetes
TGF-β	transforming growth factor β
Th1	T helper cell
TLR4	toll like receptor 4

TNF-α	tumor necrosis factor alpha
Treg	regulatory T cell
SEM	standard error of the mean
SCD1	stearoyl CoA desaturase-1
VAT	visceral adipose tissue
WHO	world health organization

DENDRITIC CELLS CONTRIBUTE TO PERIVASCULAR ADIPOSE TISSUE DYSFUNCTION IN TYPE 2 DIABETES

Tianyi Qiu

ABSTRACT

T2DM is a chronic disease characterized by low-grade inflammation in adipose tissue. Recent investigations have shown that a variety of immune cells can accumulate in adipose tissue contributing to the development of chronic inflammation. To date focus has been placed on specific immune cell populations including B and T lymphocytes, M1 macrophages, neutrophils, mast cells and natural killer cells. However, it remains uncertain about the exact immune cell populations in adipose tissue during T2DM. The dendritic cell is a potent antigen presenting cell that has been demonstrated to participate in the chronic inflammation associated with multiple diseases, including autoimmune disease, atherosclerosis and type 1 diabetes. Thus, it was hypothesized that dendritic cells would also play a role in the development of chronic inflammation elicited by T2DM. Firstly, our data obtained in *db/db* mice (T2DM murine model) provide evidence that dendritic cells do, indeed, accumulate in multiple depots of perivascular and visceral adipose tissue. Importantly, the dendritic cells target the adipose tissue rather than accumulating within the vascular wall, accompanied with increased production of pro-inflammatory factors TNF-α and IL-6 in adipose tissue. Secondly, depletion of dendritic cells within adipose tissue in *db/db* (db^{Flt3l-}/ db^{Flt3l-}) mice attenuated the pro-inflammatory environment. As perivascular adipose tissue exerts anti-contractile actions and potentiates vasorelaxation under physiological conditions, we examined the effects of fat from *db/db* mice on vascular function. The data showed that in *db/db* mice, both of these 'vaso-protective' effects were lost at early (6-10 weeks) and later (18-22 weeks) stages of T2DM in the presence of inflamed mesenteric adipose tissue. Depletion of dendritic cells in db^{Flt3l-}/ db^{Flt3l-} mice greatly attenuated inflammation in perivascular adipose tissue (decreased secretion of TNF-α and IL-6) compared to the *db/db* and partially restored vascular function. Collectively, our studies demonstrate that the accumulation of dendritic cells in adipose tissue contributes to the pathogenesis of chronic

inflammation in T2DM, resulting in impairment of anti-contractile and pro-relaxant actions of perivascular adipose tissue. Deletion of dendritic cells restores these physiological actions of adipose tissue.

CHAPTER I

EFFECTS OF PERIVASCULAR ADIPOSE TISSUE DYSFUNCTION ON BLOOD VESSELS IN TYPE 2 DIABETES

1.1 Role of adipose tissue in the pathological development of obesity and T2DM

Obesity is a pathological condition that has been commonly considered as a body mass index (BMI) greater than 30 kg per m^2. This phenomenon of inappropriately increased body weight has drawn more and more attention from all over the world, since the prevalence of obesity is gradually increasing not only in developed western countries, but also in many developing countries (for example China, Pacific Islands and the Middle East). Importantly, this interest has been heightened as obesity has been linked to a series of severe consequences, such as type 2 diabetes (T2DM) and cardiovascular diseases. Thus, it was reported in 2012 that approximately 9.3% of the population in United States (29.1 million Americans) have been diagnosed with T2DM (Olanipekun, Salemi et al. 2016). From an economic perspective, the overall cost of T2DM in 2012 had reached 245 billion dollars in United States. The escalating costs for treatment of T2DM have greatly stimulated research efforts to identify underlying mechanisms and potential therapies for both obesity and T2DM.

The main causes of morbidity and mortality in T2DM relate to both macro-vascular and micro-vascular complications. Macro-vascular complications consist of coronary artery occlusion, cerebrovascular stroke and kidney failure, while microvascular complications include retinopathy, diabetic foot ulcer and neuropathy (Liu, Fu et al. 2010). Vascular endothelial cell dysfunction appears to precede the development of the vascular complications and has become a possible early marker in their diagnosis (Hwang and Kim 2014). This vascular endothelial dysfunction is characterized by impairment of endothelial-dependent relaxation in both small resistance (Zhang, Potter et al. 2011) and large conduit arteries (Lee, Zhang et al. 2012). Amongst a number of

hypotheses, it is believed that hyperglycemia and hyperlipidemia in T2DM result in the overproduction of reactive oxygen species (ROS) and pro-inflammatory cytokines, which lead to an uncoupling of endothelial nitric oxide synthase (eNOS) and a decrease of overall nitric oxide (NO) bioavailability (Hwang and Kim 2014). As NO is a physiological mediator of endothelial-dependent relaxation, decreased availability is believed to underlie vascular dysfunction in T2DM.

Two critical features in obesity contribute to the development of overt T2DM (Guilherme, Virbasius et al. 2008). The first feature is impaired insulin responsiveness of skeletal muscle while the other one relates to the failure of pancreatic islet β-cells to produce the required amount of 'functional' insulin to maintain normal fasting blood glucose levels. These two features highlight the pivotal role of insulin resistance in the pathological progression from obesity to T2DM. It is generally accepted that the release of multiple free fatty acids, especially non-esterified fatty acid (NEFA) is the primary culprit responsible for insulin resistance development in skeletal muscle and pancreatic islet β-cell dysfunction (Kahn, Hull et al. 2006, Guilherme, Virbasius et al. 2008). This notion has been demonstrated in T2DM patients that lowering of circulating free fatty acids by acipimox, a long-acting anti-lipolytic drug, leads to a decrease in insulin resistance and improvement of glucose tolerance (Santomauro, Boden et al. 1999, Bajaj, Suraamornkul et al. 2005). The source of free fatty acids now has been found in adipose tissue and it is believed that adipose tissue is the key modulator of lipid and glucose metabolism in the whole body scale (Guilherme, Virbasius et al. 2008). Under physiological conditions, adipose tissue sequesters free fatty acids causing their circulating concentrations to be relatively low. This action of adipose tissue effectively restricts fatty acid toxicity on insulin sensitivity (Guilherme, Virbasius et al. 2008). In contrast, in the obese state, the size of adipocytes is enlarged to increase their capability for fatty acid storage. Initially, this compensatory response effectively controls the increment of circulating fatty acid concentration. However, as obesity continues to develop, the increase in adipocyte size becomes ineffective in buffering circulating fatty acids, eventually leading to insulin resistance formation (Lewis, Carpentier et al. 2002).

Importantly as obesity develops, the function of adipose tissue as an endocrine/paracrine organ becomes compromised. In particular, the secretion of multiple biologically active molecules is affected. Anti-inflammatory cytokines including adiponectin and leptin, have been shown to decline in obese adipose tissue (Dandona, Aljada et al. 2004) whereas pro-inflammatory cytokines, such as tumor necrosis factor alpha (TNF-α), interleukin 6 (IL-6) and monocyte chemoattractant protein-1 (MCP-1), have been reported to be increased (Dandona, Aljada et al. 2004). The role of TNF-α in modulating adiposity has been suggested to involve activation of both IκB kinase β (IKKβ)/nuclear factor-κB (NF-κB) and JUN N-terminal kinase (JNK) intracellular pathways to elicit insulin resistance (Moller 2000, Dandona, Aljada et al. 2004, Shoelson, Lee et al. 2006). The proposed mechanisms include accelerated lipolysis with increased circulating free fatty acids, decreased protein synthesis of glucose transporter type 4 (GLUT4) and insulin receptors, inhibition of insulin receptor auto-phosphorylation, acute inhibition of insulin-stimulated glucose transport (Moller 2000). Similarly, high IL-6 expression is also associated with insulin resistance development. IL-6 shares the same downstream molecular signaling pathway with TNF-α, resulting in decreased synthesis of GLUT-4 and insulin-receptor substrate (IRS), a marked reduction of insulin-stimulated tyrosine phosphorylation and peroxisome proliferation-activated receptor γ (PPAR-γ), but it has no effect on insulin receptor tyrosine phosphorylation (Rotter, Nagaev et al. 2003). Conversely, adiponectin potentiates insulin sensitivity in peripheral tissues by activating fatty acid oxidation through both AMP activated protein kinase (AMPK) and peroxisome proliferation-activated receptor α (PPAR-α) dependent intracellular pathways (Kadowaki, Yamauchi et al. 2006, Scherer 2006).

1. 2. Interplay between adipose tissue and T2DM: implication of distinct immune cells.

As mentioned in the previous section, adipose tissue in T2DM undergoes progressive inflammation favoring a pro-inflammatory response that is accompanied by increased production of inflammatory factors and a decreased production of anti-inflammatory mediators. The underlying mechanism to explain this alteration in secretion profile in T2DM adipose tissue has

gained more and more research interest from global scientists (Franco Nitta 2013, Seijkens, Kusters et al. 2014, Grant and Dixit 2015). Interestingly, a number of such investigations have shown that inflammation in obese adipose tissue is highly associated with the recruitment of various immune cells (Huh, Park et al. 2014). The following sections introduce the roles of different immune cells implicated in the development of adipose tissue inflammation during obesity.

1.2.1. Macrophages in adipose tissue

The macrophage is an indispensable immune cell that participates in the foreign pathogen defense (Parkin and Cohen 2001). It plays an important role in both innate and acquired immunities, which are two major compartments of the immune system. Resident macrophages in peripheral tissues are derived from monocytes leaving the circulation by extravasation (Gordon and Taylor 2005). In innate immunity, resident macrophages promptly arrive at infected sites and defend against foreign antigens and coordinate leukocyte infiltration (Gordon and Taylor 2005). Macrophages are responsible for the clearance of foreign antigens through phagocytosis and subsequent degradation of apoptotic cells, microbes and possibly neoplastic cells (Gordon and Taylor 2005). In adaptive immunity, macrophages function as antigen presenting cells, which deliver antigens to immune effector cells, such as T and B lymphocytes. Activated T and B lymphocytes help to clear residual antigens that are missed by macrophages in innate immunity, by the release of various cytotoxic cytokines and production of specific antibodies (Duffield 2003). Of note, macrophages are also capable of generating a variety of cytokines, chemokines, arachidonic acid metabolites and reactive radicals to eradicate lethal microbes. Such cytokines include TNF-α and IL-6 (Tejada-Simon and Pestka 1999).

Adipose tissue macrophages (ATM) are considered to be a special population of macrophages that are located in the stromal vascular fraction of adipose tissue and form a ring-like configuration called crown-like structure (CLS). Unfortunately, a definitive nomenclature for ATM is still lacking (McNelis and Olefsky 2014). However, the $F4/80^{+}CD11b^{+}$ cell population is commonly considered to be ATMs (Zeyda and Stulnig 2007). ATM is generally divided into two

subtypes: M1 and M2 types. M1 type of ATM is referred as being pro-inflammatory while the M2 type is referred as an anti-inflammatory ATM. Under physiological conditions, M2 ATMs are the primary tissue-resident macrophage and maintain adipose tissue homeostasis by secretion of anti-inflammatory mediators, such as IL-10. In contrast, during the development of obesity, M2 ATMs progressively switch to the M1 type and promote the pro-inflammatory state in adipose tissue by releasing multiple inflammatory factors, such as TNF-α, interleukin 1 β (IL-1β), IL-6, interferon gamma (IFN-γ) and leukotriene B4 (Zeyda and Stulnig 2007). The presence of TNF-α and IL-6 in adipose tissue has been confirmed to inhibit insulin receptor auto-phosphorylation and attenuate the insulin signaling cascade, which eventually promotes the development of the insulin resistant state as outlined above (Hajer, van Haeften et al. 2008). Thus it is now generally accepted that ATMs are the key effector cell in the propagation of inflammation caused by obesity (McNelis and Olefsky 2014, Boutens and Stienstra 2016). It has been demonstrated that depletion of M1 macrophages in high fat diet induced mice resulted in the restoration of anti-inflammatory mediator IL-10 levels in visceral adipose tissue (Lumeng, Bodzin et al. 2007). Another piece of evidence also showed that ablation of M1 macrophages not only markedly reduced pro-inflammatory cytokines IL-6 and MCP-1 production in obese adipose tissue, but also normalized glucose tolerance and insulin sensitivity in high fat diet induced mice (Patsouris, Li et al. 2008). In summary, these results suggested that M1 macrophages are the upstream regulator of inflammatory cytokine generation in obese adipose tissue.

1.2.2. B lymphocytes in adipose tissue

In contrast to macrophages, B lymphocytes are both generated and differentiated within bone marrow. After maturation, B lymphocytes migrate to various peripheral tissues including lymphoid and non-lymphoid organs. The humoral immune system in murine models consists of at least two subsets of matured B lymphocytes: referred to as B1 and B2 cell populations (Kaminski and Stavnezer 2006). B1 lymphocytes are predominantly distributed to the peritoneal and pleural cavities, while B2 lymphocytes are located in the spleen, lymph nodes and Peyer's patches in the intestine (Martin and Kearney 2001). Apart from different locations, the role of B1 lymphocytes in humoral responses also differs from that of B2 lymphocytes. B1 lymphocytes are responsible for

antibody production preferentially in a T lymphocyte-independent manner, whereas B2 lymphocytes generate various antibodies through the activation of T lymphocytes. Despite these differences in characteristics between B1 and B2 lymphocytes, the principal function of B lymphocytes is to generate diverse antibodies against a number of soluble antigens and foreign microorganisms.

In regard to the role of B lymphocytes within adipose tissue, it is has been shown that they infiltrate into inflamed visceral adipose tissue of mice fed with high fat diet (Duffaut, Galitzky et al. 2009, Winer, Winer et al. 2011). This accumulation of B lymphocytes has been demonstrated to contribute to systemic insulin resistance development (Duffaut, Galitzky et al. 2009, Winer, Winer et al. 2011). Three distinct mechanisms have been proposed by which B lymphocytes modulate insulin resistance in obesity. The first mechanism is through cytokine production. Thus, isolated B lymphocytes from T2DM subjects secrete greater amounts of the pro-inflammatory factor interleukin 8 (IL-8) into the circulation compared to that of non-diabetic individuals (Jagannathan, McDonnell et al. 2010). The increased levels of serum IL-8 are associated with insulin resistance development and a reduction of skeletal muscle capillary density during the pathological course of T2DM (Sharabiani, Vermeulen et al. 2011, Amir Levy, Ciaraldi et al. 2015). Moreover, serum levels of anti-inflammatory factor IL-10 have been reported to be relatively low in T2DM subjects (van Exel, Gussekloo et al. 2002). These B lymphocyte infiltration-dependent differences in cytokine production promote local and systemic inflammatory responses. The second mechanism is through modulation of T lymphocytes, which is linked to the B lymphocyte being a member of the antigen-presenting cell family. In diet-induced obese mice, B lymphocytes present antigens to T lymphocytes in a major histocompatibility complex (MHC) dependent manner (Winer, Winer et al. 2011). In obese visceral adipose tissue, MHC I molecules expressed on B lymphocytes present antigens to $CD8^+$ T cells, whereas MHC II molecules on B lymphocytes exhibit antigens to $CD4^+$ T cells (Winer, Winer et al. 2011). Local insulin resistance in obese adipose tissue becomes worse, accompanied with the rise of IFN-γ production, after both $CD4^+$ and $CD8^+$ T cells are activated (Mallat 2011). The third mechanism is through B lymphocyte antibody production. Published data from Winer (Winer, Winer et al. 2011) suggested that a specific intracellular

antigen involved in protein trafficking between Golgi apparatus and endoplasmic reticulum, stimulates B lymphocyte to proliferate and produce multiple antibodies in obese adipose tissue from mice fed with high fat diet. It is also recognized that B1 lymphocytes generate IgM antibody, which promotes the activation of anti-inflammatory M2 macrophages and regulates the inflammatory reaction in obese adipose tissue from high fat diet induced mice (Mallat 2011). In contrast, B2 lymphocytes are responsible for the production of pro-inflammatory IgG autoantibodies, which capture auto-antigen and form an antigen-antibody complex (Mallat 2011). This complex cross-links to Fc receptors expressed on the surface of macrophages and further stimulates inflammatory macrophages to produce pro-inflammatory cytokine TNF-α. Moreover, antigen-antibody complexes also activate the complement pathway, which exacerbates adipose tissue inflammation and remodeling. In a high fat diet induced murine model, the release of IgM antibodies is decreased while IgG antibody production is increased in both serum and visceral adipose tissue (Winer, Winer et al. 2011). Depletion of B lymphocytes in adipose tissue results in the switching of M2 to M1 inflammatory macrophages and a reduction of $CD8^+$T cells, leading to amelioration of glucose intolerance in diet-induced obese mice (Winer, Winer et al. 2011). In summary, B lymphocytes promote the development of an inflammatory state in obese adipose tissue through the increasing production of pro-inflammatory cytokines and antibodies, as well as the interaction with T lymphocytes.

1.2.3. T lymphocytes in adipose tissue

Adipose tissue is also known to contain another important and large group of immune cells - T lymphocytes. T lymphocytes can be primarily divided into two types: $CD4^+$ and $CD8^+$ T lymphocytes. Also, other small clusters of T lymphocytes, which are not included in either $CD4^+$ or $CD8^+$ T lymphocyte populations, have been found in murine adipose tissue, such as natural killer T cells (NKT) and mucosal-associated invariant T cells (MAIT). In the following sections, these subtypes will be covered in detail.

1.2.3.1 $CD4^+$T cells in adipose tissue

$CD4^+$ T cells represent a major type of T lymphocytes in the immune system from both human and mice. They are activated by antigens presented by class II MHC molecules located on the surface of antigen presenting cells (APCs). Effector $CD4^+$ T cells can then differentiate into four different subtypes, including T helper (Th) 1, Th2, Th17, and induced regulatory T (iTreg) cells (Zhu, Yamane et al. 2010). Th1 cells are characterized by IFN-γ secretion, but also can produce interleukin 2 (IL-2) (Fernandez-Botran, Sanders et al. 1988), TNF-α and lymph toxin (Kagami, Rizzo et al. 2010). Th2 cells are characterized by the release of IL-4, interleukin 5 (IL-5) and IL-13 (Fort, Cheung et al. 2001). Th17 cells are signified by the secretion of interleukin 17 (IL-17) and interleukin 22 (IL-22) (Liang, Tan et al. 2006). However, there is no specific cytokine exclusively secreted by iTreg cells. The proliferation and differentiation of those effector Th cell populations have been confirmed to be triggered by a family of special molecules called signaling transducer and activator of transcription proteins (STAT). It is known that activation of STAT1 protein is indispensable in Th1 cell differentiation and IFN-γ production (Lighvani, Frucht et al. 2001, Afkarian, Sedy et al. 2002). STAT3 protein has also been demonstrated to participate in Th17 cell differentiation and maintenance (Bettelli, Carrier et al. 2006, Mangan, Harrington et al. 2006). The activation of STAT 6 protein is necessary for Th2 cell differentiation and expansion (Shimoda, van Deursen et al. 1996, Takeda, Tanaka et al. 1996).

At present, only three $CD4^+$ T cell populations have been identified in murine adipose tissue, including Th1, Th2 and Th17 cells. In visceral adipose tissue of diet-induced obese mice, the $CD4^+Foxp3^+$Th1 cell compartment was discovered to outnumber the static $CD4^+Foxp3^-$Th2 cell compartment, resulting in an increased ratio of Th1 to Th2 cells (Winer, Chan et al. 2009). The accumulation of Th1 cells induces the development of M1 pro-inflammatory macrophages in adipose tissue by the secretion of IL-6 and TNF-α. Conversely, Th2 cells secrete IL-4 and IL-13 and promote macrophage differentiation into the anti-inflammatory M2 phenotype (Odegaard, Ricardo-Gonzalez et al. 2007, Tiemessen, Jagger et al. 2007). The increase of Th1 to Th2 ratio in obese adipose tissue facilitates macrophage polarization from anti-inflammatory M2 into pro-inflammatory M1 phenotype, further exacerbating the inflammatory state in obese adipose tissue. Apart from macrophages, $CD4^+$T cells also interact with surrounding adipocytes and induce the

production of pro-inflammatory factors TNF-α and IL-1β (Ilan, Maron et al. 2010). In human studies, obese subjects with insulin resistance have elevated $CD4^+$T lymphocytes in visceral adipose tissue, particularly Th17 cells (Fabbrini, Cella et al. 2013). These cells are responsible for the production of IL-17, which inhibits glucose metabolism in skeletal muscle and reduces insulin sensitivity in liver. However, the function of iTreg cells still remains unclear. In summary, $CD4^+$ T cells facilitate the inflammatory state in obese adipose tissue by recruitment of more M1 macrophages and stimulation of adipocytes to generate multiple pro-inflammatory cytokines.

1.2.3.2. $CD8^+$ T cells in adipose tissue

$CD8^+$ T cells belong to an important T lymphocyte subset that controls and eradicates viral, bacterial and protozoan infections in adaptive immunity. These cells can recognize and then be activated by MHC class I molecules ubiquitously located on the surface of nucleated cells (Gallucci and Matzinger 2001). Once activated, effector $CD8^+$ T cells clear up host cells bearing intracellular pathogens by releasing large quantities of cytokines, including TNF-α and IL-1β (Gallucci and Matzinger 2001).

Emerging evidence has demonstrated that $CD8^+$T cells accumulate in visceral adipose tissue of diet-induced obese mice (Kintscher, Hartge et al. 2008, Rausch, Weisberg et al. 2008, Nishimura, Manabe et al. 2009, Jiang, Perrard et al. 2014, Khan, Dai Perrard et al. 2014). This accumulation of $CD8^+$T cells has been revealed to occur early in the development of obesity and is responsible for recruitment and activation of macrophages in visceral adipose tissue (Nishimura, Manabe et al. 2009). This action is conducted by substantial secretions of interferon-inducible protein-10, MCP-1 and monocyte chemo attractant protein-3 (MCP-3). Incubation of adipocytes with $CD8^+$T cells up-regulates CD11a expression on $CD8^+$T cells, which in turn promotes more $CD8^+$T cells to infiltrate adipose tissue (Jiang, Perrard et al. 2014). The inhibitory effect of CD8 specific antibodies successfully ameliorates the pro-inflammatory state of obese adipose tissue and improves both glucose and insulin tolerance reactions in diet-induced obese mice (Nishimura, Manabe et al. 2009). The role of $CD8^+$T cells in adipose tissue inflammation appears to be much smaller in human obesity than in mice (Yang, Youm et al. 2010). A significant

but small increment of $CD8^+$T cells was detected in obese visceral adipose tissue from humans (Yang, Youm et al. 2010). In summary, accumulation of $CD8^+$T cells in adipose tissue promotes the development of inflammatory state and deteriorates glucose intolerance in obese murine models, yet with little effects on human obesity.

1.2.3.3 Treg cells in adipose tissue

The general immune response can be classified into two forms. The first is the induction of the immune reaction while the second relates the suppression of immune reaction. Under physiological conditions, these two forms are evenly balanced. One subtype of $CD4^+$ T cells, $FOXP3^+CD4^+$ $CD25^+$ T cells, defined as regulatory T cells (Treg) constitute only 5-20% of the overall $CD4^+$ T cell compartment (Zheng and Rudensky 2007, Cipolletta, Kolodin et al. 2011). Despite accounting for a small population, Treg cells play an important functional role in the negative regulation of immune responses (Teh, Vasanthakumar et al. 2015). Deficiency of Treg cells has been implicated in various autoimmune diseases, including multiple sclerosis, antigen induced arthritis, thyroiditis and eczema (Beissert, Schwarz et al. 2006).

Under steady state conditions, more than half of the Treg cell population is located in abdominal adipose tissue rather than lymphoid organs, including spleen and lymph nodes (Feuerer, Herrero et al. 2009). Emerging evidence has shown that during the development of obesity, a striking decrease of Treg cells occurs in visceral adipose tissue of both morbidly obese mice and humans (Deiuliis, Shah et al. 2011). Induction of Treg cell proliferation in visceral adipose tissue by administration of anti-CD3 antibody plus β-glucosylceramide has been shown to enhance production of anti-inflammatory mediators, such as IL-10 and transforming growth factor β (TGF-β) (Ilan, Maron et al. 2010). Moreover, systemic restoration of Treg cells attenuated hepatic fat accumulation and pancreatic hyperplasia together with lower levels of serum glucose and cholesterol (Ilan, Maron et al. 2010). The mechanisms of Treg cell reduction in obesity, however, are still unclear. It has been suggested that CD36 plays a role in the high fat diet-induced reduction of Treg cells in murine epididymal adipose tissue and mesenteric lymph nodes (Geys, Vranckx et al. 2015). Furthermore, it has been reported that in normal mice, resident

adipose tissue M2 type macrophages are, in part, responsible for the proliferation of Treg cells (Onodera, Fukuhara et al. 2015). In wild type mice, resident adipose tissue M2 macrophages up-regulate PPAR γ expression, which further induces the proliferation of Treg cells in abdominal adipose tissue. Conversely, pro-inflammatory M1 macrophages derived from obese adipose tissue blunt the production of PPAR γ and impair the differentiation and proliferation of Treg cells (Onodera, Fukuhara et al. 2015). In summary, Treg cells are responsible for anti-inflammatory cytokine production, but are decreased in adipose tissue during obesity development.

1.2.3.4. NKT cells in adipose tissue

NKT cells are a lineage of lymphocytes characterized by both T cell and natural killer cell features, expressing both αβ T cell receptor (TCR) and cell surface markers of natural killer cells (Bendelac, Savage et al. 2007). Based on TCRα chain expression and MHC restriction, NKT cells can be classified into three subtypes. Type I NKT cells, also termed invariant NKT (iNKT) cells, are characteristic of an invariant TCR α chain expression accompanied with a restricted subtype of TCR β chains. Type I NKT cells receive lipid antigens delivered by CD1d, which is a non-classical MHC-like antigen-presenting protein (Boes, Stoppelenburg et al. 2009). Type II NKT cells express variant TCRs and are capable of regulating multiple immune responses, such as autoimmunity suppression and tumor rejection inhibition (Godfrey, Stankovic et al. 2010). Type III NKT cells have diverse TCRα chains and do not rely on CD1d to present antigens. The predominant NKT cell population is the type I NKT (iNKT) cell, which in murine models is mainly found in the liver and thymus. Only a small fraction is resident in visceral adipose tissue (Schipper, Rakhshandehroo et al. 2012).

The iNKT cell has been reported to play a crucial role in the control of adipose tissue inflammation and metabolic intolerance in diet-induced obese mice (Ji, Sun et al. 2012). It was observed that the number of iNKT cells was significantly decreased in obese visceral adipose tissue and this was accompanied by infiltration of M1 macrophages (Ji, Sun et al. 2012). Marine sponge-derived α-galactosylceramide (α-GalCer) is a special lipid antigen that was used recently to specifically expand iNKT cell populations in a murine model (Bendelac, Savage et al. 2007).

Administration of α-GalCer not only proliferated adipose-resident iNKT cell populations and ameliorated systemic glucose intolerance (Ji, Sun et al. 2012), but also promoted M2 macrophage polarization in visceral adipose tissue from obese mice (Ji, Sun et al. 2012). This polarization was mediated by activation of IL-4 in adipose tissue (Ji, Sun et al. 2012), which further phosphorylated tyrosine residues of STAT6 and triggered the expansion of M2 macrophages (Ji, Sun et al. 2012). Restoration of iNKT cells in adipose tissue results in declining levels of pro-inflammatory factors IL-13 and IFN-γ in diet-induced obese mice (Schipper, Rakhshandehroo et al. 2012). However, some investigators also reported that activation of iNKT cells exacerbated glucose intolerance and promoted macrophage accumulation in adipose tissue as well as pro-inflammatory cytokine secretion, rather than ameliorated metabolic parameters (Ohmura, Ishimori et al. 2010). Given these disparate results, the role of iNKT cells in obese adipose tissue needs to be further explored.

1.2.3.5. MAIT cells in adipose tissue

MAIT cells are a novel unconventional subset of invariant T cells, which were discovered during the late 1980s in both human (Bender and Kabelitz 1990) and mice (Miescher, Howe et al. 1988). The MAIT cell displays neither CD4 nor CD8 molecules on the cellular surface. Moreover, the development of MAIT cells is not restricted by MHC molecules, but by the MHC related molecule, MR1 (Tilloy, Treiner et al. 1999). This characteristic leads to the recruitment of MAIT cells into intestinal lamina propria (Treiner, Duban et al. 2003), which acquires MR1 receptors. Further investigation of MAIT cells revealed that they also infiltrate the peripheral circulation, liver, and adipose tissue (Magalhaes, Pingris et al. 2015). The principal role of MAIT cells is to mediate anti-bacterial actions by releasing IFN-γ and IL-17 cytokines (Gold, Cerri et al. 2010).

Delving further into MAIT cells in obese humans, Carolan and colleagues have found that the distribution and secretion profile of MAIT cells are changed in human tissue (Carolan, Tobin et al. 2015). In healthy adults and children, MAIT cells were enriched in the circulation rather than adipose tissue. However, in obese individuals, circulating MAIT cells were depleted and instead recruited into adipose tissue. The MAIT cells in adipose tissue appeared to produce more pro-

inflammatory cytokine IL-17 rather than anti-inflammatory mediator IL-10. The IL-17^{+} MAIT cells have further been shown to be directly related to the degree of insulin resistance in obese humans (Fabbrini, Cella et al. 2013, Magalhaes, Pingris et al. 2015). It has also been reported that cytokine IL-17 suppresses adipocyte maturation and function by impairing gene expression of adipokines and adipose triglyceride lipase (Zuniga, Shen et al. 2010). Furthermore, IL-17 induces IL-6 generation in pre-adipocytes, which is known to induce insulin resistance in vivo and in vitro (Kern, Ranganathan et al. 2001, Rotter, Nagaev et al. 2003). Collectively, MAIT cells are involved in the promotion of inflammatory state in obese adipose tissue induced by high fat diet.

1.2.4. Eosinophils in adipose tissue

The eosinophil is another type of immune cell belonging to innate immune system. It is generated from hematopoietic stem cells in the bone marrow and later resides in various peripheral tissues and organs. Eosinophils play an important role in the defense of bacterial and parasitic invasion, as well as allergen-induced inflammatory responses (Rothenberg and Hogan 2006). Activated eosinophils kill bacteria by the release of tissue destructive granular molecules and extracellular traps composed of mitochondrial DNA. Similarly, parasitic infection is eliminated, in part, by eosinophil degranulation of major basic or cationic proteins (Bystrom, Amin et al. 2011). In the inflammatory response induced by allergens, eosinophils secrete cationic or tissue destructive proteins resulting in tissue or organ damage (Amin, Ludviksdottir et al. 2000).

In the perspective of adipose tissue immunity, eosinophils act as a negative regulator in modulating adipose tissue inflammation and metabolic dysfunction (Wu, Molofsky et al. 2011, Molofsky, Nussbaum et al. 2013). Under physiological conditions, the presence of the cytokine interleukin 33 (IL-33) has been demonstrated to facilitate the activation and secretion of a novel type of lymphocyte, innate lymphoid type 2 cells (ILC2s), in murine visceral adipose tissue (Molofsky, Nussbaum et al. 2013, Brestoff, Kim et al. 2015). The activated ILC2s are responsible for the secretion of IL-5, which promotes the recruitment of eosinophils from the circulation into visceral adipose tissue (Molofsky, Nussbaum et al. 2013). The eosinophils in adipose tissue are responsible for the secretion of IL-4, which then activates M2 polarization of macrophages (Wu,

Molofsky et al. 2011). This macrophage polarization promotes the anti-inflammatory, rather than pro-inflammatory, environment in visceral adipose tissue, resulting in restoration of metabolic disorders. In contrast, the number of eosinophils in visceral adipose tissue has been found to be decreased in high fat diet-induced obese mice (Wu, Molofsky et al. 2011). This reduction further impairs the M2 polarization of macrophages and finally leads to adipose tissue inflammation and impaired insulin sensitivity (Wu, Molofsky et al. 2011).

1.2.5. Dendritic cells in adipose tissue

Dendritic cells are potent antigen-presenting and processing cells that play a pivotal role in the orchestration of both innate and adaptive immune systems. They are also referred to as “sentinels” or “sensors” of the immune system because they are located in nearly every organ and maintain surveillance for a wide spectrum of environmental invaders (Steinman 2006). Once dendritic cells sense antigen invasion, they immediately migrate into the threatened region and capture, phagocytize, process and finally present these antigens on their surface (Banchereau and Steinman 1998). After activation by these antigens, dendritic cells leave the peripheral tissue and carry the antigens into lymphoid organs where they present antigens to B or T lymphocytes. Due to the essential signals provided by dendritic cells, B and T lymphocytes are stimulated and migrate through the peripheral circulation into attacked region, where invading antigens are recognized and subsequently cleared (Banchereau and Steinman 1998). Despite the relative paucity of dendritic cells, they have been suggested to play a role in the pathologies of atherosclerosis (Dieterlen, John et al. 2016) and type 1 diabetes (Besin, Gaudreau et al. 2008).

Dendritic cells have been shown to initiate and enhance the development of type 1 diabetes, including contribution to the onset of diabetes (Rosmalen, Leenen et al. 1997). The role of dendritic cells in the pathogenesis of type 1 diabetes appears to be associated with the activation of T lymphocytes (Machen, Harnaha et al. 2004). The full activation of T lymphocytes requires two signals provided by dendritic cells. The first signal is processed antigen presented by dendritic cells to the T cell receptor on T lymphocytes. This signal triggers T lymphocytes to increase the expression of CD40 ligand (CD40L) on their surface, which incites the second signal

referred to as ‘co-activation’ (Machen, Harnaha et al. 2004). Initially, CD40L on the T lymphocyte interacts with CD40 on dendritic cells. This event up-regulates CD80 and CD86 expression on dendritic cells, which then act as the second signal and engages CD28 on T lymphocyte. The combination of both first and second signals consequently leads to full activation of T lymphocytes, which subsequently mediates pancreatic β cell destruction and type 1 diabetic development. Several lines of evidence have shown that any disturbance in these two signals for T lymphocyte activation can result in suppression of type 1 diabetic development (Machen, Harnaha et al. 2004, Acharya, Dolgova et al. 2011).

In regard to mechanisms underlying obesity and T2DM, a contribution of dendritic cells has also been suggested (Bertola, Ciucci et al. 2012, Reynolds, McGillicuddy et al. 2012, Stefanovic-Racic, Yang et al. 2012). In a high fat diet-induced obese murine model, dendritic cells have been found to infiltrate hypertrophic adipose tissue (Reynolds, McGillicuddy et al. 2012). These high fat diet-derived dendritic cells are switched to a pro-inflammatory phenotype with enhanced production of inflammatory cytokines, including IL-1β, interleukin 1 receptor type 1 (IL-1R1), toll like receptor 4 (TLR4) and caspase-1 (Reynolds, McGillicuddy et al. 2012). It is believed that free fatty acids can directly prime the nucleotide-binding domain, leucine-rich repeat containing protein 3 (NLRP3) inflammasome via TLR4 on dendritic cells, which subsequently promote adipocyte inflammation and development of insulin resistance (Reynolds, McGillicuddy et al. 2012). Another line of evidence showed that dendritic cells contribute to the systemic metabolic response to obesity by promoting macrophage infiltration into adipose tissue (Stefanovic-Racic, Yang et al. 2012). Emerging studies also indicate that dendritic cells in obese adipose tissue induce T lymphocyte differentiation into Th17 cells which secrete IL-17 into peripheral tissues (Bertola, Ciucci et al. 2012). Although IL-17 has an anti-adipogenic property, the exact function of IL-17 in the pathogenesis of obesity remains unclear. Nevertheless, the expansion of Th17 cells has been shown to exacerbate autoimmunity in rodent disease models of colitis and autoimmune encephalomyelitis (Ahmed and Gaffen 2010). Taken together, although the exact mechanisms of dendritic cell recruitment into obese adipose tissue are still unknown, dendritic cells appear to play an important role in the pathological processes underlying obesity and T2DM.

1.2.6. Summary of the different immune cells in obese adipose tissue

From the above, it is apparent that when adipose tissue progresses to the obese state, the composition of various immune cells is altered. Greater numbers of B lymphocytes, $CD4^+$ and $CD8^+$ T lymphocytes, MAIT cells, M1 macrophages and dendritic cells accumulate in the obese adipose tissue, whereas fewer Treg cells, NKT cells, eosinophils and M2 macrophages are present. This alteration results in an imbalance in the secretion of pro-inflammatory and anti-inflammatory cytokines, as shown in **Fig1-1**. More pro-inflammatory factors TNF-α, IFN-γ, IL-1β, IL-6, IL-8, IL-13 and IL-17 are secreted in the obese adipose tissue while there is a reduction in anti-inflammatory factors, including IL-10, IL-4 and TGF-β. Ultimately, the inflammatory state in obese adipose tissue that results from immune cell imbalance leads to the development of insulin resistance and progression to overt T2DM.

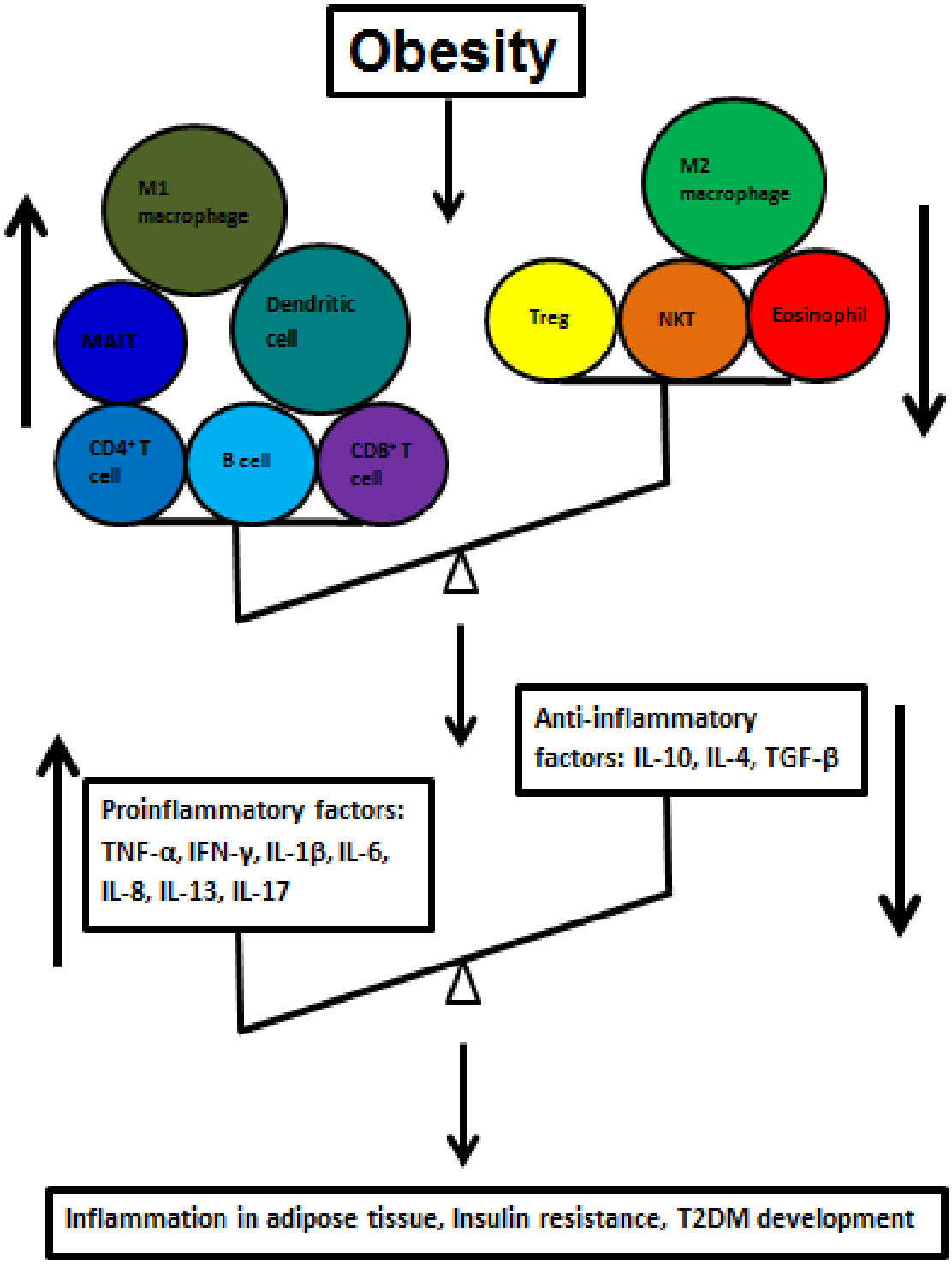

Figure1-1. Obesity induces immune cell infiltration and inflammatory state in adipose tissue.

1.3. Role of Perivascular Adipose Tissue (PVAT) in T2DM

PVAT is defined as the adipose tissue directly surrounding blood vessels without any separation from the adventitia of vasculature (Eringa, Bakker et al. 2012). According to this definition, PVAT includes epicardial adipose tissue, periaortic adipose tissue, mesenteric adipose tissue, perirenal adipose tissue and adipose tissue around orbital arteries. PVAT differs from visceral adipose tissue (VAT) mainly by the different fat distribution in that VAT is typically located at the abdominal cavity of human or animal models (Ng, Wai et al. 2012). Apart from these differences, both VAT and PVAT can be histologically divided into two compartments: namely, adipocytes and the stromal vascular fraction. The stromal vascular fraction is a specialized term encompassing the remainder of cells in adipose tissue apart from adipocytes. It is enriched with various cell populations, such as pre-adipocytes, mesenchymal stem cells, vascular progenitor cells, hematopoietic stem cells, pericytes, fibroblasts, smooth muscle cells, endothelial cells and blood cells (Bourin, Bunnell et al. 2013). In addition, VAT or PVAT contains a network of capillaries, sympathetic and parasympathetic nerve systems, which are capable of delivering information to the central nervous system (Gu and Xu 2013). During the development of T2DM, immune cells, such as macrophages, B or T lymphocytes infiltrate into the stromal vascular fraction portion of VAT or PVAT (Feldon, O'Loughlin C et al. 2006, Police, Thatcher et al. 2009).

1.3.1 Versatility in PVAT function

It has become gradually accepted that PVAT has a number of effects on surrounding blood vessels. PVAT not only provides structural support and insulation to vasculature, but also secretes a variety of factors that affect the pathophysiological function of the vasculature it encases. Cultured PVAT cells have been shown to differentiate into mesenchymal stem cells and then obtain migratory property (Crisan, Yap et al. 2008). Visfatin, a novel protein factor that was identified in PVAT, has been demonstrated to inhibit vascular smooth muscle cell contraction and enhance vascular smooth muscle cell proliferation (Wang, Xu et al. 2009). Interestingly, adiponectin secreted from epicardial adipose tissue has been confirmed to protectively maintain the sinus rhythm following cardiac surgery (Kourliouros, Karastergiou et al. 2011). Importantly,

PVAT has been documented to influence vascular function in both canine (Noblet, Owen et al. 2015) and swine animal models (Payne, Bohlen et al. 2009). Under physiological conditions, the presence of PVAT attenuates vascular contraction induced by a variety of pharmacological vasoconstrictors, including phenylephrine and 5-hydroxytryptamine (Gao, Lu et al. 2007). The mechanism behind this phenomenon is associated with the release of a reservoir of vasoactive substances generated within PVAT (Lastra and Manrique 2015). These vasoactive factors include adiponectin, angiotensin 1-7, hydrogen peroxide (H_2S), leptin, nitric oxide (NO) and the yet to be fully characterized, adipocyte-derived relaxing factor (ADRF). The overall effect on vascular function from those vasoactive molecules is beneficial to vasodilatory rather than vasoconstriction responses. The mechanisms behind ADRF involves both endothelial-dependent and vascular smooth muscle cell-dependent relaxation (Gao 2007). This anti-contractile effect on vasculature has been suggested to be essential for vascular resistance maintenance under physiological conditions (Gollasch and Dubrovska 2004, Gao 2007).

1.3.2. Loss of anti-contractile effect of PVAT in obesity

Under physiological conditions, the anti-contractile effect of PVAT is increased in relation to the amount of PVAT (Verlohren, Dubrovska et al. 2004). As such, it is conceivable that the anti-contractile effect of obese PVAT also would be increased. However, in obesity, both the structure and function of PVAT are considerably changed. The anti-contractile action of obese PVAT has been shown to be severely impaired in various animal models (Gao, Holloway et al. 2005). In obese rats, increased adiposity of peri-aortic adipose tissue attenuates thoracic aorta relaxation. Similarly, a diminished anti-contractile effect in mesenteric arteries was observed in New Zealand obese mice (Fesus, Dubrovska et al. 2007). Notably, this anti-contractile effect in mesenteric arteries declined with age (and duration) in New Zealand obese mice. In an obese Ossabaw swine model, despite an increase in weight of epicardial adipose tissue, adenosine-induced vasodilation was attenuated by impairment of calcium-dependent potassium channels and voltage-dependent K_V7 channels (Noblet, Owen et al. 2015). In this context, an imbalance in secretion of pro-inflammatory and anti-inflammatory cytokines was observed in PVAT of obese

animals (Vieira-Potter, Lee et al. 2015). Further, increased production of pro-inflammatory factors, such as IL-6 and MCP-1, has been shown to diminish the anti-contractile effect of PVAT (Rajsheker, Manka et al. 2010). The possible mechanisms leading to impairment of anti-contractile effect of obese PVAT will be discussed in the following sections in detail.

1.3.2.1. Impairment of ADRF in obesity

Under normal conditions, healthy PVAT generates an unidentified factor which has been named ADRF. This factor (or factors), acting in a paracrine manner, promotes relaxation responses in the adjacent vasculature. It was first reported by Löhn et al (Lohn, Dubrovska et al. 2002) that ADRF is a transferrable and vasoactive group of compounds that relax pre-contracted rat aorta isolated from adherent PVAT. It is an active regulator of arterial tone by antagonism of contraction shown by donor-acceptor transfer bioassays (Lohn, Dubrovska et al. 2002). Moreover, Löhn et al described ADRF as a special group of proteins rather than a collection of lipids. Their experiment showed that ADRF is inactivated by high temperature (greater than 65°C) and not bound by serum albumin, which suggests that it is not a fatty acid. Interestingly, the secretion of ADRF from PVAT is dependent on external Ca^{2+} concentration and can be inhibited by either protein kinase A or tyrosine kinase inhibitors (Lohn, Dubrovska et al. 2002). In contrast, the production of ADRF and the resultant relaxation are independent of functional adenosine, leptin, vanilloid, cannabinoid and cyclooxygenase pathway; calcitonin gene-related peptide receptors; cytochrome P450 pathway; the formation of NO; or the endothelium (Lohn, Dubrovska et al. 2002). Evidence does, however, suggest that the modulation of arterial tone exerted by ADRF involves the activation of different potassium channels on vascular smooth muscle cells. Pharmacological experiments from Löhn et al demonstrated that the anti-contractile effect of PVAT from rat aorta is diminished by the presence of the ATP-dependent potassium channel inhibitor glibenclamide (Lohn, Dubrovska et al. 2002). Bath bioassay experiments using PVAT from around human internal thoracic artery have suggested that calcium-dependent potassium channel inhibitor tetraethylammonium chloride significantly blocks the relaxation induced by PVAT (Gao, Zeng et al. 2005). Recently, accumulating evidence supports an interaction between

ADRF and potassium channels on vascular smooth muscle cells (Weston, Egner et al. 2013, Zavaritskaya, Zhuravleva et al. 2013, Noblet, Owen et al. 2015). Thus, it is considered that the release of ADRF from adjacent PVAT activates different potassium channels, including voltage-gated potassium channels, ATP-dependent potassium channels and Ca^{2+}-activated potassium channels on vascular smooth muscle cells, resulting in hyperpolarization and relaxation of smooth muscle cells.

In obese conditions, the anti-contractile effect from PVAT is impaired in both animals (Owen, Witzmann et al. 2013, Noblet, Owen et al. 2015) and humans (Meijer, Serne et al. 2015). Accumulating evidence suggests that voltage-gated potassium channels (Berwick, Dick et al. 2013), Ca^{2+}-activated potassium channels (Borbouse, Dick et al. 2009) and ATP-dependent potassium channels (Climent, Simonsen et al. 2014) may all be impaired in the microcirculation of obese animals. This effect is attributable to the loss of ADRF. In addition to a role for potassium channels, it has been shown that inhibition of cyclooxygenase in obese PVAT significantly restores the anti-contractile effect on thoracic aorta (Meyer, Fredette et al. 2013). It is believed that inhibition of cyclooxygenase reduces the production of vasoconstrictors and promotes the restoration of ADRF generation in PVAT. Overall, loss of ADRF and dysfunctional potassium channels appear to be involved in the impairment of PVAT anti-contractile effects in obesity.

1.3.2.2. Decrease of NO and H_2S in obese PVAT

NO and H_2S are two different gaseous molecules that have been suggested to participate in the anti-contractile effects of PVAT. Under physiological conditions, NO is produced by both endothelial cells lining blood vessels and PVAT. It has been well-known that endothelial cell NO synthase is responsible for the generation of NO that subsequently elicits endothelial cell-dependent acetylcholine-induced relaxation responses in both large conduit (Rees, Palmer et al. 1989) and small resistance vessels (Kubes, Suzuki et al. 1991). Notably, recent investigations have indicated that adipocytes within PVAT can also express NO synthase and generate bioactive NO into adjacent vasculature (Xia, Horke et al. 2016). Interestingly, NO produced by PVAT plays a pivotal role in the endothelium-independent, anti-contractile function of PVAT by

pharmacological inhibition of NO synthase on vascular endothelial cells (Aghamohammadzadeh, Unwin et al. 2016). Under obese conditions, it has long been believed that impaired endothelium-dependent vasodilation in small vessels from obese animals is due to the reduction of NO bioavailability derived from endothelial cells (Perticone, Ceravolo et al. 2001). However, further investigations of obesity suggest that NO production from PVAT is also reduced in the late stages of obesity (Xia, Horke et al. 2016). This decrease in NO production is associated with impaired anti-contractile effects of obese PVAT (Bussey, Withers et al. 2016). Interestingly, during the early stage of obesity, NO production is increased in PVAT (Aghamohammadzadeh, Unwin et al. 2016). This abnormal situation is believed to be an adaptive reaction to the development of obesity, but the exact underlying mechanism is still unclear. With the progression of obesity, adaptive NO overproduction in PVAT is reduced to undetectable levels (Aghamohammadzadeh, Unwin et al. 2016). Moreover, leptin has been confirmed to stimulate NO production in PVAT (Gil-Ortega, Stucchi et al. 2010). Consistent with this, leptin deficient *ob/ob* mice did not exhibit NO production within adipocytes of PVAT (Gil-Ortega, Stucchi et al. 2010). However, restoration of leptin expression in *ob/ob* mice promoted NO generation in PVAT(Gil-Ortega, Stucchi et al. 2010).

Apart from NO, H_2S is also generated within PVAT, as has been shown in both periaortic and mesenteric adipose tissues (Fang, Zhao et al. 2009, Schleifenbaum, Kohn et al. 2010). H_2S is synthesized from L-homocysteine or L-cysteine by cystathionine β-synthase, cysteine aminotransferase, or cystathionine γ-lyase (CSE), as well as 3- mercaptopyruvate sulfur transferase (Kimura 2014). Within PVAT, CSE is the main source of H_2S production (Schleifenbaum, Kohn et al. 2010). Recently, H_2S has been considered as one element in the ADRF family (Gollasch 2012), due to its role in mediating anti-contractile effects of PVAT(Fang, Zhao et al. 2009). The mechanism of H_2S induced relaxation is considered to involve activation of different potassium channels in vascular smooth muscle cells, such as voltage-dependent potassium channels (Schleifenbaum, Kohn et al. 2010, Kohn, Schleifenbaum et al. 2012) and ATP dependent potassium channels (Zhao, Zhang et al. 2001). Moreover, H_2S can also stimulate endothelial NO synthase, promote NO production and finally enhance relaxation responses elicited by PVAT (Beltowski and Jamroz-Wisniewska 2014). In addition, H_2S can exert other

protective mechanisms to maintain healthy vascular homeostasis, such as inhibition of vascular smooth muscle cell proliferation (Li, Liu et al. 2013) and suppression of inflammatory reactions (Yu, Cui et al. 2014). Surprisingly, obesity does not appear to influence the sensitivity of vascular smooth muscle cells to H_2S (Beltowski 2013). However, 3 month-old, high calorie diet-induced obese mice have decreased H_2S production in adipose tissue compared to 1 month-old high calorie fed obese mice (Beltowski, Wojcicka et al. 2009). However, at present, there is no evidence to reveal a direct link between lower H_2S production and loss of anti-contractile effect of obese PVAT. Overall, obesity causes a reduction of NO and H_2S production within PVAT, which may contribute to the impairment of anti-contractile effects in obese PVAT.

1.3.2.3. Increased oxidative stress and inflammatory response in obese PVAT

The regulation of vascular function by PVAT under physiological and pathological conditions is not limited to the release of relaxing factors, such as ADRF. Most of the modulation in vasculature-PVAT system consists of a balance between anti-contractile and pro-contractile factors. Oxidative stress is characterized by the production of ROS, which are primarily composed of superoxide anion, hydrogen peroxide (H_2O_2) and hydroxyl radicals. In the vasculature-PVAT system, ROS is produced by various tissues, including PVAT (De Ciuceis, Amiri et al. 2005). Nicotinamide adenine dinucleotide phosphate (NADPH) oxidase is the major enzyme to produce ROS in the vasculature (Schiffrin 2008). This enzyme complex is also expressed in rat mesenteric adipose tissue (Gao, Takemori et al. 2006). NADPH oxidase within PVAT generates superoxide anion that activates tyrosine kinase and mitogen-activated protein kinase/extracellular signal-regulated protein kinase (MAPK/ERK) pathways in the vasculature, promoting arterial contractile rather than anti-contractile responses (Gao, Takemori et al. 2006). Superoxide anions can also be converted by superoxide dismutase (SOD) to H_2O_2. H_2O_2 is a vasoactive ROS that induces vasorelaxation response when endothelial and smooth muscle cell potassium channels are activated (Gil-Longo and Gonzalez-Vazquez 2005). Therefore, the overall outcome of vascular tone regulated by ROS is dependent on the relative production of both superoxide anion and H_2O_2.

A recent murine study showed that endothelial dysfunction in a high fat diet could be associated with the presence of PVAT (Chadderdon, Belcik et al. 2014). Further, impaired H_2O_2 production due to a reduction in SOD expression, contributes to the abolishment of anti-contractile effects of obese PVAT (Marchesi, Ebrahimian et al. 2009). In Ossabaw obese swine, anti-contractile effects mediated by H_2O_2 were also markedly decreased by the presence of coronary PVAT (Gao, Zeng et al. 2005). Another mechanism to explain excessive oxidative stress on vascular dysfunction has been explored (Marchesi, Ebrahimian et al. 2009). It is believed that in the presence of PVAT oxidative stress, uncoupled endothelial NO synthase produces superoxide anions rather than NO, resulting in reduction of NO bioavailability, endothelial dysfunction and vasoconstriction (Marchesi, Ebrahimian et al. 2009).

1.3.2.4. Dysregulation of PVAT-derived adipokines in obesity

Adipokines are a group of proteins secreted from adipocytes within PVAT in both a paracrine and endocrine manner (Ouwens, Sell et al. 2010). This protein family includes multiple components, such as leptin, adiponectin, resistin, chemerin, plasminogen activator inhibitor 1, adrenomedullin and visfatin (Ozen, Daci et al. 2015). Among them, leptin and adiponectin have received particular attention in a number of vascular diseases.

Leptin is a 167-amino acid paracrine-acting cytokine secreted by PVAT (Beltowski 2006). Recent studies have suggested that PVAT-derived leptin promotes a switch in vascular smooth muscle cell phenotype, from a contractile to synthetic phenotype (Li, Wang et al. 2014). This switch in phenotype appears to involve a p38 mitogen-activated protein kinase (MAPK)-dependent pathway and exacerbates vascular remodeling processes (Li, Wang et al. 2014). Interestingly, leptin has also been proposed to regulate vascular function by two distinct actions. On one hand, a very high concentration of leptin, much higher than concentrations seen in obesity, elicits a NO-dependent vasorelaxation response in isolated canine coronary arteries without any influence on coronary blood flow (Knudson, Dincer et al. 2005). On the other hand, obese epicardial PVAT- derived leptin blunts the coronary NO-dependent vasorelaxation response via a protein kinase C-β pathway (Payne, Borbouse et al. 2010). Further, improved

endothelial dependent relaxation responses elicited by PVAT are seen in the presence of a leptin antagonist (Payne, Borbouse et al. 2010). Collectively, the available data are inconsistent, leading to the conclusion that the exact mechanism of leptin on vascular function requires further exploration.

Adiponectin is another important adipokine implicated in the cross-talk between PVAT and the vasculature. Adiponectin is a 244-amino acid polypeptide primarily secreted by adipocytes within PVAT. It has been demonstrated that adiponectin activates and up-regulates endothelial NO synthase, leading to increasing NO production and its beneficial effects on the cardiovascular system (Chen, Montagnani et al. 2003, Hattori, Suzuki et al. 2003). Furthermore, recent investigation has shown that PVAT-derived adiponectin stimulates Ca^{2+}-activated potassium channels on vascular smooth muscle cells and mediates anti-contractile effects on vascular tone (Lynch, Withers et al. 2013). However, this anti-contractile capacity induced by adiponectin is lost in obesity during the development of adipocyte hypertrophy (Greenstein, Khavandi et al. 2009). Additional evidence also shows that the loss of PVAT anti-contractile function correlates with lower levels of adiponectin in obese rat and human PVAT (Aghamohammadzadeh, Unwin et al. 2015). Incubation of inflamed internal mammary artery with 10 µg/mL adiponectin for 6 hours has been shown to induce endothelial cell synthase phosphorylation and augment tetrahydrobiopterin bioavailability, eventually restoring endothelial cell synthase coupling (Margaritis, Antonopoulos et al. 2013). Induced release of adiponectin through administration of atrial natriuretic peptide has also been shown to activate adiponectin receptors on vascular smooth muscle cells, leading to downstream events including the phosphorylation of endothelial NO synthase, subsequent NO signaling and endothelium-dependent relaxation with the presence of PVAT(Withers, Simpson et al. 2014). Overall, the available data suggest that adiponectin is a vaso-protective cytokine that participates in the anti-contractile function of PVAT and is beneficial for the maintenance of vascular antioxidant state in cardiovascular diseases.

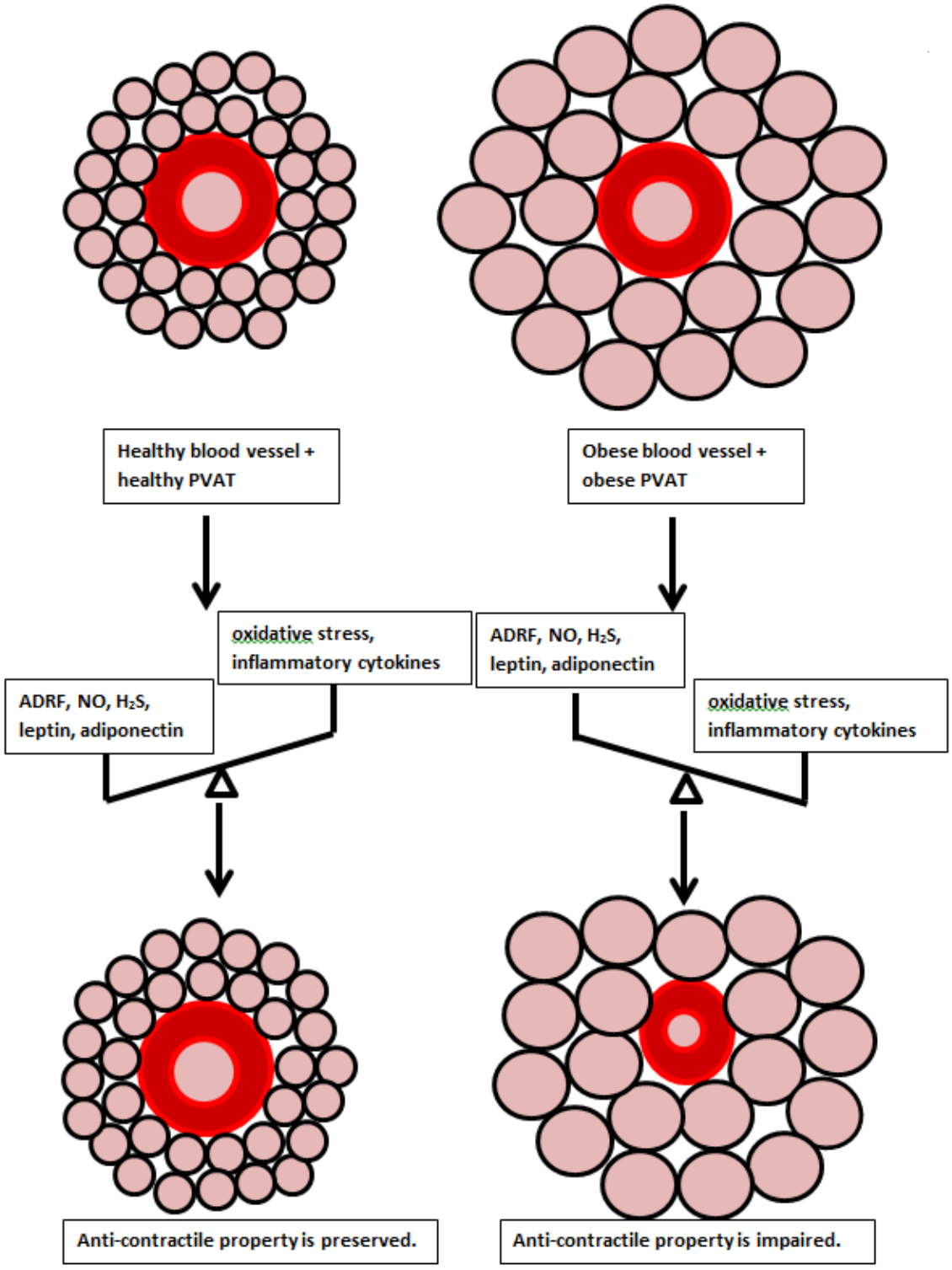

Figure 1.2. Role of PVAT in vascular function from both healthy and obese condition.

Aspects of the above discussion are summarized in **Figure 1-2.** Under physiological conditions, PVAT surrounding blood vessels provides a number of vasoactive anti-contractile factors, including ADRF, NO, H_2S, leptin, adiponectin. These PVAT-derived factors act at a local level to attenuate vasoconstriction responses. Conversely, in obese conditions, expanded PVAT exhibits a higher degree of oxidative stress and inflammatory cytokines, as opposed to anti-contractile factors of the normal state. Thus inflamed PVAT alters the balance between vasoconstriction and vasodilation.

1.4. Immune cell infiltration and vascular dysfunction

It is generally accepted that T2DM is characterized by chronic low grade inflammation and vascular dysfunction (Stehouwer, Gall et al. 2002). As discussed, considerable evidence also suggests that alteration to the normal crosstalk between PVAT and blood vessels underlies cardiovascular disease present in T2DM (Szasz, Bomfim et al. 2013, Even, Dulak-Lis et al. 2014). As shown in **Figure 1-2**, the PVAT-derived vasoactive molecules are accompanied by a background amount of Treg cell, NKT cell, eosinophils and M2 macrophages (see also **Figure 1-1**). Importantly, the presence of these immune cells contributes to the maintenance of an anti-inflammatory environment in adipose tissue favoring the normal function of the PVAT-derived vasoactive molecules (Even, Dulak-Lis et al. 2014). Under T2DM conditions, PVAT undergoes hypertrophy and remodeling processes, which trigger M1 pro-inflammatory phenotypic polarization and infiltration/accumulation of macrophages as well as other immune cells, including B and T lymphocytes (Gu and Xu 2013). The change in PVAT immune cell composition also alters the secretion profile favoring both inflammatory response and oxidative stress, which impairs the anti-contractile function of PVAT and subsequently leads to vascular endothelial dysfunction (Gu and Xu 2013).

Withers et al. have suggested that macrophages within PVAT are responsible for the increase in contractility of small resistance arteries when incubated with inflamed PVAT (Withers, Agabiti-Rosei et al. 2011). Consistent with this, depletion of macrophages in inflamed PVAT restores the anti-contractile capacity of PVAT and maintains vascular contractility in small arteries

(Withers, Agabiti-Rosei et al. 2011). These results provide a direct link between vascular contractility induced by PVAT and macrophage accumulation. Surprisingly, there are no other studies which have explored the association between vascular contractility induced by PVAT and the recruitment of other immune cells to PVAT, including dendritic cells. Therefore, future investigations are required to unveil the relationship between vascular contractility induced by PVAT and accumulation of varying immune cells.

1.5. Rationale and Hypothesis

The prevalence of obesity is rising each year, and represents a major cause of global morbidity and mortality. Obesity is one of major risk factors for metabolic syndrome, insulin resistance and T2DM along with associated cardiovascular complications (Osborn and Olefsky 2012). However, the mechanisms of obesity and T2DM remain poorly understood and efficient therapeutic treatment against T2DM and cardiovascular complications are still deficient. Recent studies have shown that obesity is tightly associated with chronic low-grade inflammation, especially in the expanded adipose tissue (Weisberg, McCann et al. 2003). More pro-inflammatory cytokines , such as TNF-α and IL-6, are produced while fewer anti-inflammatory cytokines, such as adiponectin and IL-10, are generated (Franco Nitta 2013). This imbalance of pro-inflammatory and anti-inflammatory factors has recently been demonstrated to be associated with infiltration of multiple immune cells (including B and T lymphocytes, M1 macrophages and dendritic cells) into adipose tissue (Grant and Dixit 2015). Prior studies have confirmed that the pro-inflammatory cytokines, TNF-α (Zhang, Park et al. 2009) and IL-6 (Hartge, Unger et al. 2007), decrease NO bioavailability, resulting in impaired endothelial-dependent vascular dysfunction in obesity and T2DM. Further, these pro-inflammatory cytokines attenuate the anti-contractile function of PVAT on small arteries (Greenstein, Khavandi et al. 2009). These observations suggest a possible link between immune cell infiltration and ablation of anti-contractile activity of PVAT. Consistent with this, it has recently been demonstrated in rodent models that depletion of macrophages in inflamed adipose tissue restores anti-contractile capacity of PVAT on small resistance arteries (Withers, Agabiti-Rosei et al. 2011). However, the relationship between

dendritic cell infiltration into PVAT and the anti-contractile capacity of PVAT in obese and/or T2DM models is unknown. Thus studies described in this dissertation focused on the effects of dendritic cells on the anti-contractile response of PVAT from T2DM. The studies are divided into two main goals, which are fully discussed in the following sections.

The ***first goal*** of this work is to investigate whether dendritic cells are recruited into PVAT of T2DM and whether there is an alteration of inflammatory state of PVAT from T2DM. The following hypotheses were tested in Chapter II:

a. Dendritic cells are predominately located in the PVAT rather than in the vascular wall.
b. More dendritic cells accumulate in the PVAT derived from T2DM, compared to PVAT under physiological conditions.
c. More pro-inflammatory cytokines and fewer anti-inflammatory cytokines are produced in PVAT from T2DM.

The ***second goal*** of this work was to investigate whether dendritic cells are associated with the development of inflammatory state in adipose tissue from T2DM and whether infiltration of dendritic cells into PVAT was related to vascular dysfunction in T2DM. The following hypotheses were tested in Chapter III:

a. Genetic depletion of dendritic cells restores the balance between pro-inflammatory and anti-inflammatory cytokine production in PVAT from T2DM.
b. The anti-contractile function of PVAT on small arteries is diminished in T2DM rodent models, while dendritic cell depletion restores this function of PVAT.
c. There is a progressive age-dependent impairment in the anti-contractile effects of PVAT in T2DM model and this is prevented by depletion of dendritic cells.

REFERENCES

Acharya, A. P., N. V. Dolgova, C. Q. Xia, M. J. Clare-Salzler and B. G. Keselowsky (2011). "Adhesive substrates modulate the activation and stimulatory capacity of non-obese diabetic mouse-derived dendritic cells." Acta biomaterialia 7(1): 180-192.

Afkarian, M., J. R. Sedy, J. Yang, N. G. Jacobson, N. Cereb, S. Y. Yang, T. L. Murphy and K. M. Murphy (2002). "T-bet is a STAT1-induced regulator of IL-12R expression in naive $CD4^+$ T cells." Nat Immunol **3**(6): 549-557.

Aghamohammadzadeh, R., R. D. Unwin, A. S. Greenstein and A. M. Heagerty (2015). "Effects of Obesity on Perivascular Adipose Tissue Vasorelaxant Function: Nitric Oxide, Inflammation and Elevated Systemic Blood Pressure." J Vasc Res 52(5): 299-305.

Ahmed, M. and S. L. Gaffen (2010). "IL-17 in obesity and adipogenesis." Cytokine & growth factor reviews 21(6): 449-453.

Amin, K., D. Ludviksdottir, C. Janson, O. Nettelbladt, E. Bjornsson, G. M. Roomans, G. Boman, L. Seveus and P. Venge (2000). "Inflammation and structural changes in the airways of patients with atopic and nonatopic asthma. BHR Group." Am J Respir Crit Care Med **162**(6): 2295-2301.

Amir Levy, Y., T. P. Ciaraldi, S. R. Mudaliar, S. A. Phillips and R. R. Henry (2015). "Excessive secretion of IL-8 by skeletal muscle in type 2 diabetes impairs tube growth: potential role of PI3K and the Tie2 receptor." American Journal of Physiology - Endocrinology and Metabolism **309**(1): E22-E34.

Bajaj, M., S. Suraamornkul, A. Romanelli, G. W. Cline, L. J. Mandarino, G. I. Shulman and R. A. DeFronzo (2005). "Effect of a sustained reduction in plasma free fatty acid concentration on intramuscular long-chain fatty Acyl-CoAs and insulin action in type 2 diabetic patients." Diabetes 54(11): 3148-3153.

Banchereau, J. and R. M. Steinman (1998). "Dendritic cells and the control of immunity." Nature 392(6673): 245-252.

Bastard, J.-P., M. Maachi, C. Lagathu, M. J. Kim, M. Caron, H. Vidal, J. Capeau and B. Feve (2006). "Recent advances in the relationship between obesity, inflammation, and insulin resistance." European cytokine network 17(1): 4-12.

Beissert, S., A. Schwarz and T. Schwarz (2006). "Regulatory T cells." Journal of investigative dermatology **126**(1): 15-24.

Beltowski, J. (2006). "Leptin and atherosclerosis." Atherosclerosis 189(1): 47-60.

Beltowski, J. (2013). "Endogenous hydrogen sulfide in perivascular adipose tissue: role in the regulation of vascular tone in physiology and pathology." Can J Physiol Pharmacol 91(11): 889-898.

Beltowski, J. and A. Jamroz-Wisniewska (2014). "Hydrogen sulfide and endothelium-dependent vasorelaxation." Molecules 19(12): 21183-21199.

Beltowski, J., G. Wojcicka, A. Jamroz-Wisniewska and A. Marciniak (2009). "Resistance to acute NO-mimetic and EDHF-mimetic effects of leptin in the metabolic syndrome." Life Sci 85(15-16): 557-567.

Bendelac, A., P. B. Savage and L. Teyton (2007). "The biology of NKT cells." Annu. Rev. Immunol. **25**: 297-336.

Bender, A. and D. Kabelitz (1990). "$CD4^{-}CD8^{-}$ human T cells: phenotypic heterogeneity and activation requirements of freshly isolated "double-negative" T cells." Cell Immunol **128**(2): 542-554.

Bertola, A., T. Ciucci, D. Rousseau, V. Bourlier, C. Duffaut, S. Bonnafous, C. Blin-Wakkach, R. Anty, A. Iannelli and J. Gugenheim (2012). "Identification of adipose tissue dendritic cells correlated with obesity-associated insulin-resistance and inducing Th17 responses in mice and patients." Diabetes 61(9): 2238-2247.

Berwick, Z. C., G. M. Dick, H. A. O'Leary, S. B. Bender, A. G. Goodwill, S. P. Moberly, M. K. Owen, S. J. Miller, A. G. Obukhov and J. D. Tune (2013). "Contribution of electromechanical coupling between Kv and Ca v1.2 channels to coronary dysfunction in obesity." Basic Res Cardiol 108(5): 370.

Besin, G., S. Gaudreau, M. Menard, C. Guindi, G. Dupuis and A. Amrani (2008). "Thymic stromal lymphopoietin and thymic stromal lymphopoietin-conditioned dendritic cells induce regulatory T-cell differentiation and protection of NOD mice against diabetes." Diabetes 57(8): 2107-2117.

Bettelli, E., Y. Carrier, W. Gao, T. Korn, T. B. Strom, M. Oukka, H. L. Weiner and V. K. Kuchroo (2006). "Reciprocal developmental pathways for the generation of pathogenic effector TH17 and regulatory T cells." Nature **441**(7090): 235-238.

Boes, M., A. J. Stoppelenburg and F. C. Sille (2009). "Endosomal processing for antigen presentation mediated by CD1 and Class I major histocompatibility complex: roads to display or destruction." Immunology **127**(2): 163-170.

Borbouse, L., G. M. Dick, S. Asano, S. B. Bender, U. D. Dincer, G. A. Payne, Z. P. Neeb, I. N. Bratz, M. Sturek and J. D. Tune (2009). "Impaired function of coronary BK($_{Ca}$) channels in metabolic syndrome." Am J Physiol Heart Circ Physiol 297(5): H1629-1637.

Bourin, P., B. A. Bunnell, L. Casteilla, M. Dominici, A. J. Katz, K. L. March, H. Redl, J. P. Rubin, K. Yoshimura and J. M. Gimble (2013). "Stromal cells from the adipose tissue-derived stromal vascular fraction and culture expanded adipose tissue-derived stromal/stem cells: a joint statement of the International Federation for Adipose Therapeutics and Science (IFATS) and the International Society for Cellular Therapy (ISCT)." Cytotherapy 15(6): 641-648.

Boutens, L. and R. Stienstra (2016). "Adipose tissue macrophages: going off track during obesity." Diabetologia **59**(5): 879-894.

Bussey, C. E., S. B. Withers, R. G. Aldous, G. Edwards and A. M. Heagerty (2016). "Obesity-related perivascular adipose tissue damage is reversed by sustained weight loss in the rat." Arteriosclerosis, thrombosis, and vascular biology: ATVBAHA. 116.307210.

Brestoff, J. R., B. S. Kim, S. A. Saenz, R. R. Stine, L. A. Monticelli, G. F. Sonnenberg, J. J. Thome, D. L. Farber, K. Lutfy, P. Seale and D. Artis (2015). "Group 2 innate lymphoid cells promote beiging of white adipose tissue and limit obesity." Nature **519**(7542): 242-246.

Bystrom, J., K. Amin and D. Bishop-Bailey (2011). "Analysing the eosinophil cationic protein--a clue to the function of the eosinophil granulocyte." Respir Res **12**: 10.

Carolan, E., L. M. Tobin, B. A. Mangan, M. Corrigan, G. Gaoatswe, G. Byrne, J. Geoghegan, D. Cody, J. O'Connell, D. C. Winter, D. G. Doherty, L. Lynch, D. O'Shea and A. E. Hogan (2015). "Altered distribution and increased IL-17 production by mucosal-associated invariant T cells in adult and childhood obesity." J Immunol **194**(12): 5775-5780.

Chadderdon, S. M., J. T. Belcik, L. Bader, M. A. Kirigiti, D. M. Peters, P. Kievit, K. L. Grove and J. R. Lindner (2014). "Proinflammatory endothelial activation detected by molecular imaging in obese nonhuman primates coincides with onset of insulin resistance and progressively increases with duration of insulin resistance." Circulation 129(4): 471-478.

Chen, H., M. Montagnani, T. Funahashi, I. Shimomura and M. J. Quon (2003). "Adiponectin stimulates production of nitric oxide in vascular endothelial cells." J Biol Chem 278(45): 45021-45026.

Chen, Y., X. Xu, Y. Zhang, K. Liu, F. Huang, B. Liu and J. Kou (2016). "Diosgenin regulates adipokine expression in perivascular adipose tissue and ameliorates endothelial dysfunction via regulation of AMPK." J Steroid Biochem Mol Biol 155(Pt A): 155-165.

Cipolletta, D., D. Kolodin, C. Benoist and D. Mathis (2011). "Tissular T(regs): a unique population of adipose-tissue-resident $Foxp3^{+}CD4^{+}$ T cells that impacts organismal metabolism." Semin Immunol **23**(6): 431-437.

Climent, B., U. Simonsen and L. Rivera (2014). "Effects of obesity on vascular potassium channels." Curr Vasc Pharmacol 12(3): 438-452.

Crisan, M., S. Yap, L. Casteilla, C. W. Chen, M. Corselli, T. S. Park, G. Andriolo, B. Sun, B. Zheng, L. Zhang, C. Norotte, P. N. Teng, J. Traas, R. Schugar, B. M. Deasy, S. Badylak, H. J. Buhring, J. P. Giacobino, L. Lazzari, J. Huard and B. Peault (2008). "A perivascular origin for mesenchymal stem cells in multiple human organs." Cell Stem Cell 3(3): 301-313.

Dandona, P., A. Aljada and A. Bandyopadhyay (2004). "Inflammation: the link between insulin resistance, obesity and diabetes." Trends in immunology 25(1): 4-7.

De Ciuceis, C., F. Amiri, P. Brassard, D. H. Endemann, R. M. Touyz and E. L. Schiffrin (2005). "Reduced vascular remodeling, endothelial dysfunction, and oxidative stress in resistance arteries of angiotensin II-infused macrophage colony-stimulating factor-deficient mice: evidence

for a role in inflammation in angiotensin-induced vascular injury." Arterioscler Thromb Vasc Biol 25(10): 2106-2113.

Deiuliis, J., Z. Shah, N. Shah, B. Needleman, D. Mikami, V. Narula, K. Perry, J. Hazey, T. Kampfrath, M. Kollengode, Q. Sun, A. R. Satoskar, C. Lumeng, S. Moffatt-Bruce and S. Rajagopalan (2011). "Visceral adipose inflammation in obesity is associated with critical alterations in tregulatory cell numbers." PLoS One **6**(1): e16376.

Dieterlen, M. T., K. John, H. Reichenspurner, F. W. Mohr and M. J. Barten (2016). "Dendritic Cells and Their Role in Cardiovascular Diseases: A View on Human Studies." 2016: 5946807.

Duffaut, C., J. Galitzky, M. Lafontan and A. Bouloumie (2009). "Unexpected trafficking of immune cells within the adipose tissue during the onset of obesity." Biochem Biophys Res Commun **384**(4): 482-485.

Duffield, J. S. (2003). "The inflammatory macrophage: a story of Jekyll and Hyde." Clin Sci (Lond) **104**(1): 27-38.

Eringa, E. C., W. Bakker and V. W. van Hinsbergh (2012). "Paracrine regulation of vascular tone, inflammation and insulin sensitivity by perivascular adipose tissue." Vascular pharmacology 56(5): 204-209.

Even, S. E., M. G. Dulak-Lis, R. M. Touyz and A. Nguyen Dinh Cat (2014). "Crosstalk between adipose tissue and blood vessels in cardiometabolic syndrome: implication of steroid hormone receptors (MR/GR)." Horm Mol Biol Clin Investig 19(2): 89-101.

Fabbrini, E., M. Cella, S. A. McCartney, A. Fuchs, N. A. Abumrad, T. A. Pietka, Z. Chen, B. N. Finck, D. H. Han, F. Magkos, C. Conte, D. Bradley, G. Fraterrigo, J. C. Eagon, B. W. Patterson, M. Colonna and S. Klein (2013). "Association between specific adipose tissue $CD4^+$ T-cell populations and insulin resistance in obese individuals." Gastroenterology **145**(2): 366-374.e361-363.

Fang, L., J. Zhao, Y. Chen, T. Ma, G. Xu, C. Tang, X. Liu and B. Geng (2009). "Hydrogen sulfide derived from periadventitial adipose tissue is a vasodilator." J Hypertens 27(11): 2174-2185.

Feldon, S. E., W. O'Loughlin C, D. M. Ray, S. Landskroner-Eiger, K. E. Seweryniak and R. P. Phipps (2006). "Activated human T lymphocytes express cyclooxygenase-2 and produce proadipogenic prostaglandins that drive human orbital fibroblast differentiation to adipocytes." Am J Pathol 169(4): 1183-1193.

Feuerer, M., L. Herrero, D. Cipolletta, A. Naaz, J. Wong, A. Nayer, J. Lee, A. B. Goldfine, C. Benoist, S. Shoelson and D. Mathis (2009). "Lean, but not obese, fat is enriched for a unique population of regulatory T cells that affect metabolic parameters." Nat Med **15**(8): 930-939.

Fesus, G., G. Dubrovska, K. Gorzelniak, R. Kluge, Y. Huang, F. C. Luft and M. Gollasch (2007). "Adiponectin is a novel humoral vasodilator." Cardiovasc Res 75(4): 719-727.

Fort, M. M., J. Cheung, D. Yen, J. Li, S. M. Zurawski, S. Lo, S. Menon, T. Clifford, B. Hunte and R. Lesley (2001). "IL-25 induces IL-4, IL-5, and IL-13 and Th2-associated pathologies in vivo." Immunity **15**(6): 985-995.

Franco Nitta, C. (2013). "Crosstalk between adipocytes and immune cells in adipose tissue in an obese inflammatory state: role of contact-mediated signaling."

Gallucci, S. and P. Matzinger (2001). "Danger signals: SOS to the immune system." Curr Opin Immunol **13**(1): 114-119.

Gao, Y. J. (2007). "Dual modulation of vascular function by perivascular adipose tissue and its potential correlation with adiposity/lipoatrophy-related vascular dysfunction." Curr Pharm Des 13(21): 2185-2192.

Gao, Y. J., A. C. Holloway, Z. H. Zeng, G. E. Lim, J. J. Petrik, W. G. Foster and R. M. Lee (2005). "Prenatal exposure to nicotine causes postnatal obesity and altered perivascular adipose tissue function." Obesity research 13(4): 687-692.

Gao, Y. J., C. Lu, L. Y. Su, A. Sharma and R. Lee (2007). "Modulation of vascular function by perivascular adipose tissue: the role of endothelium and hydrogen peroxide." British journal of pharmacology 151(3): 323-331.

Gao, Y. J., K. Takemori, L. Y. Su, W. S. An, C. Lu, A. M. Sharma and R. M. Lee (2006). "Perivascular adipose tissue promotes vasoconstriction: the role of superoxide anion." Cardiovasc Res 71(2): 363-373.

Gao, Y. J., Z. H. Zeng, K. Teoh, A. M. Sharma, L. Abouzahr, I. Cybulsky, A. Lamy, L. Semelhago and R. M. Lee (2005). "Perivascular adipose tissue modulates vascular function in the human internal thoracic artery." J Thorac Cardiovasc Surg 130(4): 1130-1136.

Geys, L., C. Vranckx, H. R. Lijnen and I. Scroyen (2015). "CD36 deficiency blunts effects of diet on regulatory T cells in murine gonadal adipose tissue and mesenteric lymph nodes." Cell Immunol **298**(1-2): 33-36.

Gil-Longo, J. and C. Gonzalez-Vazquez (2005). "Characterization of four different effects elicited by H_2O_2 in rat aorta." Vascul Pharmacol 43(2): 128-138.

Gil-Ortega, M., P. Stucchi, R. Guzmán-Ruiz, V. Cano, S. Arribas, M. C. González, M. Ruiz-Gayo, M. S. Fernández-Alfonso and B. Somoza (2010). "Adaptative nitric oxide overproduction in perivascular adipose tissue during early diet-induced obesity." Endocrinology 151(7): 3299-3306.

Godfrey, D. I., S. Stankovic and A. G. Baxter (2010). "Raising the NKT cell family." Nature immunology **11**(3): 197-206.

Gold, M. C., S. Cerri, S. Smyk-Pearson, M. E. Cansler, T. M. Vogt, J. Delepine, E. Winata, G. M. Swarbrick, W. J. Chua, Y. Y. Yu, O. Lantz, M. S. Cook, M. D. Null, D. B. Jacoby, M. J. Harriff, D. A. Lewinsohn, T. H. Hansen and D. M. Lewinsohn (2010). "Human mucosal associated invariant T cells detect bacterially infected cells." PLoS Biol **8**(6): e1000407.

Gollasch, M. (2012). "Vasodilator signals from perivascular adipose tissue." Br J Pharmacol 165(3): 633-642.

Gollasch, M. and G. Dubrovska (2004). "Paracrine role for periadventitial adipose tissue in the regulation of arterial tone." Trends Pharmacol Sci 25(12): 647-653.

Gordon, S. and P. R. Taylor (2005). "Monocyte and macrophage heterogeneity." Nature Reviews Immunology **5**(12): 953-964.

Grant, R. W. and V. D. Dixit (2015). "Adipose tissue as an immunological organ." Obesity 23(3): 512-518.

Greenstein, A. S., K. Khavandi, S. B. Withers, K. Sonoyama, O. Clancy, M. Jeziorska, I. Laing, A. P. Yates, P. W. Pemberton and R. A. Malik (2009). "Local inflammation and hypoxia

abolish the protective anticontractile properties of perivascular fat in obese patients." Circulation 119(12): 1661-1670.

Gu, P. and A. Xu (2013). "Interplay between adipose tissue and blood vessels in obesity and vascular dysfunction." Rev Endocr Metab Disord 14(1): 49-58.

Guilherme, A., J. V. Virbasius, V. Puri and M. P. Czech (2008). "Adipocyte dysfunctions linking obesity to insulin resistance and type 2 diabetes." Nat Rev Mol Cell Biol 9(5): 367-377.

Hajer, G. R., T. W. van Haeften and F. L. Visseren (2008). "Adipose tissue dysfunction in obesity, diabetes, and vascular diseases." European heart journal **29**(24): 2959-2971.

Hartge, M. M., T. Unger and U. Kintscher (2007). "The endothelium and vascular inflammation in diabetes." Diabetes and Vascular Disease Research 4(2): 84-88.

Hattori, Y., M. Suzuki, S. Hattori and K. Kasai (2003). "Globular adiponectin upregulates nitric oxide production in vascular endothelial cells." Diabetologia 46(11): 1543-1549.

Huh, J. Y., Y. J. Park, M. Ham and J. B. Kim (2014). "Crosstalk between adipocytes and immune cells in adipose tissue inflammation and metabolic dysregulation in obesity." Mol Cells 37(5): 365-371.

Hwang, M. H. and S. Kim (2014). "Type 2 Diabetes: Endothelial dysfunction and Exercise." J Exerc Nutrition Biochem 18(3): 239-247.

Ilan, Y., R. Maron, A. M. Tukpah, T. U. Maioli, G. Murugaiyan, K. Yang, H. Y. Wu and H. L. Weiner (2010). "Induction of regulatory T cells decreases adipose inflammation and alleviates insulin resistance in ob/ob mice." Proc Natl Acad Sci U S A **107**(21): 9765-9770.

Jagannathan, M., M. McDonnell, Y. Liang, H. Hasturk, J. Hetzel, D. Rubin, A. Kantarci, T. E. Van Dyke, L. M. Ganley-Leal and B. S. Nikolajczyk (2010). "Toll-like receptors regulate B cell cytokine production in patients with diabetes." Diabetologia **53**(7): 1461-1471.

Ji, Y., S. Sun, S. Xia, L. Yang, X. Li and L. Qi (2012). "Short term high fat diet challenge promotes alternative macrophage polarization in adipose tissue via natural killer T cells and interleukin-4." J Biol Chem **287**(29): 24378-24386.

Ji, Y., S. Sun, A. Xu, P. Bhargava, L. Yang, K. S. Lam, B. Gao, C. H. Lee, S. Kersten and L. Qi (2012). "Activation of natural killer T cells promotes M2 Macrophage polarization in adipose

tissue and improves systemic glucose tolerance via interleukin-4 (IL-4)/STAT6 protein signaling axis in obesity." J Biol Chem **287**(17): 13561-13571.

Jiang, E., X. D. Perrard, D. Yang, I. M. Khan, J. L. Perrard, C. W. Smith, C. M. Ballantyne and H. Wu (2014). "Essential role of CD11a in $CD8^+$ T-cell accumulation and activation in adipose tissue." Arterioscler Thromb Vasc Biol **34**(1): 34-43.

Kadowaki, T., T. Yamauchi, N. Kubota, K. Hara, K. Ueki and K. Tobe (2006). "Adiponectin and adiponectin receptors in insulin resistance, diabetes, and the metabolic syndrome." The Journal of clinical investigation 116(7): 1784-1792.

Kagami, S., H. L. Rizzo, J. J. Lee, Y. Koguchi and A. Blauvelt (2010). "Circulating Th17, Th22, and Th1 cells are increased in psoriasis." Journal of Investigative Dermatology **130**(5): 1373-1383.

Kahn, S. E., R. L. Hull and K. M. Utzschneider (2006). "Mechanisms linking obesity to insulin resistance and type 2 diabetes." Nature 444(7121): 840-846.

Kaminski, D. A. and J. Stavnezer (2006). "Enhanced IgA class switching in marginal zone and B1 B cells relative to follicular/B2 B cells." J Immunol **177**(9): 6025-6029.

Kern, P. A., S. Ranganathan, C. Li, L. Wood and G. Ranganathan (2001). "Adipose tissue tumor necrosis factor and interleukin-6 expression in human obesity and insulin resistance." Am J Physiol Endocrinol Metab **280**(5): E745-751.

Khan, I. M., X. Y. Dai Perrard, J. L. Perrard, A. Mansoori, C. W. Smith, H. Wu and C. M. Ballantyne (2014). "Attenuated adipose tissue and skeletal muscle inflammation in obese mice with combined $CD4^+$ and $CD8^+$ T cell deficiency." Atherosclerosis **233**(2): 419-428.

Kimura, H. (2014). "Hydrogen sulfide and polysulfides as biological mediators." Molecules 19(10): 16146-16157.

Kintscher, U., M. Hartge, K. Hess, A. Foryst-Ludwig, M. Clemenz, M. Wabitsch, P. Fischer-Posovszky, T. F. Barth, D. Dragun, T. Skurk, H. Hauner, M. Bluher, T. Unger, A. M. Wolf, U. Knippschild, V. Hombach and N. Marx (2008). "T-lymphocyte infiltration in visceral adipose tissue: a primary event in adipose tissue inflammation and the development of obesity-mediated insulin resistance." Arterioscler Thromb Vasc Biol **28**(7): 1304-1310.

Knudson, J. D., U. D. Dincer, C. Zhang, A. N. Swafford, Jr., R. Koshida, A. Picchi, M. Focardi, G. M. Dick and J. D. Tune (2005). "Leptin receptors are expressed in coronary arteries, and hyperleptinemia causes significant coronary endothelial dysfunction." Am J Physiol Heart Circ Physiol 289(1): H48-56.

Kohn, C., J. Schleifenbaum, I. A. Szijarto, L. Marko, G. Dubrovska, Y. Huang and M. Gollasch (2012). "Differential effects of cystathionine-gamma-lyase-dependent vasodilatory H_2S in periadventitial vasoregulation of rat and mouse aortas." PLoS One 7(8): e41951.

Kourliouros, A., K. Karastergiou, J. Nowell, P. Gukop, M. Tavakkoli Hosseini, O. Valencia, V. Mohamed Ali and M. Jahangiri (2011). "Protective effect of epicardial adiponectin on atrial fibrillation following cardiac surgery." Eur J Cardiothorac Surg 39(2): 228-232.

Kubes, P., M. Suzuki and D. Granger (1991). "Nitric oxide: an endogenous modulator of leukocyte adhesion." Proceedings of the National Academy of Sciences 88(11): 4651-4655.

Lastra, G. and C. Manrique (2015). "Perivascular adipose tissue, inflammation and insulin resistance: link to vascular dysfunction and cardiovascular disease." Horm Mol Biol Clin Investig 22(1): 19-26.

Lee, S., H. Zhang, J. Chen, K. C. Dellsperger, M. A. Hill and C. Zhang (2012). "Adiponectin abates diabetes-induced endothelial dysfunction by suppressing oxidative stress, adhesion molecules, and inflammation in type 2 diabetic mice." Am J Physiol Heart Circ Physiol 303(1): H106-115.

Lewis, G. F., A. Carpentier, K. Adeli and A. Giacca (2002). "Disordered fat storage and mobilization in the pathogenesis of insulin resistance and type 2 diabetes." Endocrine reviews 23(2): 201-229.

Li, H., Y. P. Wang, L. N. Zhang and G. Tian (2014). "Perivascular adipose tissue-derived leptin promotes vascular smooth muscle cell phenotypic switching via p38 mitogen-activated protein kinase in metabolic syndrome rats." Exp Biol Med (Maywood) 239(8): 954-965.

Li, L., D. Liu, D. Bu, S. Chen, J. Wu, C. Tang, J. Du and H. Jin (2013). "Brg1-dependent epigenetic control of vascular smooth muscle cell proliferation by hydrogen sulfide." Biochim Biophys Acta 1833(6): 1347-1355.

Liang, S. C., X.-Y. Tan, D. P. Luxenberg, R. Karim, K. Dunussi-Joannopoulos, M. Collins and L. A. Fouser (2006). "Interleukin (IL)-22 and IL-17 are coexpressed by Th17 cells and cooperatively enhance expression of antimicrobial peptides." Journal of Experimental Medicine **203**(10): 2271-2279.

Lighvani, A. A., D. M. Frucht, D. Jankovic, H. Yamane, J. Aliberti, B. D. Hissong, B. V. Nguyen, M. Gadina, A. Sher, W. E. Paul and J. J. O'Shea (2001). "T-bet is rapidly induced by interferon-gamma in lymphoid and myeloid cells." Proc Natl Acad Sci U S A **98**(26): 15137-15142.

Liu, Z., C. Fu, W. Wang and B. Xu (2010). "Prevalence of chronic complications of type 2 diabetes mellitus in outpatients-a cross-sectional hospital based survey in urban China." Health and quality of life outcomes 8(1): 1.

Lohn, M., G. Dubrovska, B. Lauterbach, F. C. Luft, M. Gollasch and A. M. Sharma (2002). "Periadventitial fat releases a vascular relaxing factor." Faseb j 16(9): 1057-1063.

Lynch, F. M., S. B. Withers, Z. Yao, M. E. Werner, G. Edwards, A. H. Weston and A. M. Heagerty (2013). "Perivascular adipose tissue-derived adiponectin activates $BK_{(Ca)}$ channels to induce anticontractile responses." Am J Physiol Heart Circ Physiol 304(6): H786-795.

Machen, J., J. Harnaha, R. Lakomy, A. Styche, M. Trucco and N. Giannoukakis (2004). "Antisense oligonucleotides down-regulating costimulation confer diabetes-preventive properties to nonobese diabetic mouse dendritic cells." The Journal of Immunology 173(7): 4331-4341.

Magalhaes, I., K. Pingris, C. Poitou, S. Bessoles, N. Venteclef, B. Kiaf, L. Beaudoin, J. Da Silva, O. Allatif, J. Rossjohn, L. Kjer-Nielsen, J. McCluskey, S. Ledoux, L. Genser, A. Torcivia, C. Soudais, O. Lantz, C. Boitard, J. Aron-Wisnewsky, E. Larger, K. Clement and A. Lehuen (2015). "Mucosal-associated invariant T cell alterations in obese and type 2 diabetic patients." J Clin Invest **125**(4): 1752-1762.

Mallat, Z. (2011). "The B-side story in insulin resistance." Nat Med **17**(5): 539-540.

Mangan, P. R., L. E. Harrington, D. B. O'Quinn, W. S. Helms, D. C. Bullard, C. O. Elson, R. D. Hatton, S. M. Wahl, T. R. Schoeb and C. T. Weaver (2006). "Transforming growth factor-beta induces development of the T(H)17 lineage." Nature **441**(7090): 231-234.

Marchesi, C., T. Ebrahimian, O. Angulo, P. Paradis and E. L. Schiffrin (2009). "Endothelial nitric oxide synthase uncoupling and perivascular adipose oxidative stress and inflammation contribute to vascular dysfunction in a rodent model of metabolic syndrome." Hypertension 54(6): 1384-1392.

Margaritis, M., A. S. Antonopoulos, J. Digby, R. Lee, S. Reilly, P. Coutinho, C. Shirodaria, R. Sayeed, M. Petrou, R. De Silva, S. Jalilzadeh, M. Demosthenous, C. Bakogiannis, D. Tousoulis, C. Stefanadis, R. P. Choudhury, B. Casadei, K. M. Channon and C. Antoniades (2013). "Interactions between vascular wall and perivascular adipose tissue reveal novel roles for adiponectin in the regulation of endothelial nitric oxide synthase function in human vessels." Circulation 127(22): 2209-2221.

Martin, F. and J. F. Kearney (2001). "B1 cells: similarities and differences with other B cell subsets." Curr Opin Immunol **13**(2): 195-201.

Meijer, R. I., E. H. Serne, H. I. Korkmaz, D. L. van der Peet, M. P. de Boer, H. W. Niessen, V. W. van Hinsbergh, J. S. Yudkin, Y. M. Smulders and E. C. Eringa (2015). "Insulin-induced changes in skeletal muscle microvascular perfusion are dependent upon perivascular adipose tissue in women." Diabetologia 58(8): 1907-1915.

Meyer, M. R., N. C. Fredette, M. Barton and E. R. Prossnitz (2013). "Regulation of vascular smooth muscle tone by adipose-derived contracting factor." PLoS One 8(11): e79245.

McNelis, J. C. and J. M. Olefsky (2014). "Macrophages, immunity, and metabolic disease." Immunity **41**(1): 36-48.

Miescher, G. C., R. C. Howe, R. K. Lees and H. R. MacDonald (1988). "CD3-associated alpha/beta and gamma/delta heterodimeric receptors are expressed by distinct populations of $CD4^-$ $CD8^-$ thymocytes." J Immunol **140**(6): 1779-1782.

Moller, D. E. (2000). "Potential role of TNF-α in the pathogenesis of insulin resistance and type 2 diabetes." Trends in Endocrinology & Metabolism 11(6): 212-217.

Molofsky, A. B., J. C. Nussbaum, H. E. Liang, S. J. Van Dyken, L. E. Cheng, A. Mohapatra, A. Chawla and R. M. Locksley (2013). "Innate lymphoid type 2 cells sustain visceral adipose tissue eosinophils and alternatively activated macrophages." J Exp Med **210**(3): 535-549.

Nishimura, S., I. Manabe, M. Nagasaki, K. Eto, H. Yamashita, M. Ohsugi, M. Otsu, K. Hara, K. Ueki and S. Sugiura (2009). "CD8$^+$ effector T cells contribute to macrophage recruitment and adipose tissue inflammation in obesity." Nature medicine **15**(8): 914-920.

Ng, A. C., D. C. Wai, E. S. Tai, K. M. Ng and L. L. Chan (2012). "Visceral adipose tissue, but not waist circumference is a better measure of metabolic risk in Singaporean Chinese and Indian men." Nutrition and Diabetes 2: e38.

Noblet, J. N., M. K. Owen, A. G. Goodwill, D. J. Sassoon and J. D. Tune (2015). "Lean and Obese Coronary Perivascular Adipose Tissue Impairs Vasodilation via Differential Inhibition of Vascular Smooth Muscle K$^+$ Channels." Arterioscler Thromb Vasc Biol 35(6): 1393-1400.

Odegaard, J. I., R. R. Ricardo-Gonzalez, M. H. Goforth, C. R. Morel, V. Subramanian, L. Mukundan, A. Red Eagle, D. Vats, F. Brombacher, A. W. Ferrante and A. Chawla (2007). "Macrophage-specific PPARgamma controls alternative activation and improves insulin resistance." Nature **447**(7148): 1116-1120.

Ohmura, K., N. Ishimori, Y. Ohmura, S. Tokuhara, A. Nozawa, S. Horii, Y. Andoh, S. Fujii, K. Iwabuchi, K. Onoe and H. Tsutsui (2010). "Natural killer T cells are involved in adipose tissues inflammation and glucose intolerance in diet-induced obese mice." Arterioscler Thromb Vasc Biol **30**(2): 193-199.

Olanipekun, T. O., J. L. Salemi, M. C. Mejia de Grubb, S. J. Gonzalez and R. J. Zoorob (2016). "Clostridium difficile infection in patients hospitalized with type 2 diabetes mellitus and its impact on morbidity, mortality, and the costs of inpatient care." Diabetes Res Clin Pract 116: 68-79.

Onodera, T., A. Fukuhara, M. H. Jang, J. Shin, K. Aoi, J. Kikuta, M. Otsuki, M. Ishii and I. Shimomura (2015). "Adipose tissue macrophages induce PPARgamma-high FOXP3(+) regulatory T cells." Sci Rep **5**: 16801.

Osborn, O. and J. M. Olefsky (2012). "The cellular and signaling networks linking the immune system and metabolism in disease." Nature medicine 18(3): 363-374.

Ouwens, D. M., H. Sell, S. Greulich and J. Eckel (2010). "The role of epicardial and perivascular adipose tissue in the pathophysiology of cardiovascular disease." Journal of cellular and molecular medicine 14(9): 2223-2234.

Owen, M. K., F. A. Witzmann, M. L. McKenney, X. Lai, Z. C. Berwick, S. P. Moberly, M. Alloosh, M. Sturek and J. D. Tune (2013). "Perivascular adipose tissue potentiates contraction of coronary vascular smooth muscle: influence of obesity." Circulation 128(1): 9-18.

Ozen, G., A. Daci, X. Norel and G. Topal (2015). "Human perivascular adipose tissue dysfunction as a cause of vascular disease: Focus on vascular tone and wall remodeling." Eur J Pharmacol 766: 16-24.

Parkin, J. and B. Cohen (2001). "An overview of the immune system." The Lancet **357**(9270): 1777-1789.

Payne, G. A., H. G. Bohlen, U. D. Dincer, L. Borbouse and J. D. Tune (2009). "Periadventitial adipose tissue impairs coronary endothelial function via PKC-beta-dependent phosphorylation of nitric oxide synthase." Am J Physiol Heart Circ Physiol 297(1): H460-465.

Payne, G. A., L. Borbouse, S. Kumar, Z. Neeb, M. Alloosh, M. Sturek and J. D. Tune (2010). "Epicardial perivascular adipose-derived leptin exacerbates coronary endothelial dysfunction in metabolic syndrome via a protein kinase C-beta pathway." Arterioscler Thromb Vasc Biol 30(9): 1711-1717.

Perticone, F., R. Ceravolo, M. Candigliota, G. Ventura, S. Iacopino, F. Sinopoli and P. L. Mattioli (2001). "Obesity and body fat distribution induce endothelial dysfunction by oxidative stress protective effect of vitamin C." Diabetes 50(1): 159-165.

Police, S. B., S. E. Thatcher, R. Charnigo, A. Daugherty and L. A. Cassis (2009). "Obesity promotes inflammation in periaortic adipose tissue and angiotensin II-induced abdominal aortic aneurysm formation." Arterioscler Thromb Vasc Biol 29(10): 1458-1464.

Rajsheker, S., D. Manka, A. L. Blomkalns, T. K. Chatterjee, L. L. Stoll and N. L. Weintraub (2010). "Crosstalk between perivascular adipose tissue and blood vessels." Current opinion in pharmacology 10(2): 191-196.

Rausch, M. E., S. Weisberg, P. Vardhana and D. V. Tortoriello (2008). "Obesity in C57BL/6J mice is characterized by adipose tissue hypoxia and cytotoxic T-cell infiltration." Int J Obes (Lond) **32**(3): 451-463.

Rees, D., R. Palmer and S. Moncada (1989). "Role of endothelium-derived nitric oxide in the regulation of blood pressure." Proceedings of the National Academy of Sciences 86(9): 3375-3378.

Reynolds, C. M., F. C. McGillicuddy, K. A. Harford, O. M. Finucane, K. H. Mills and H. M. Roche (2012). "Dietary saturated fatty acids prime the NLRP3 inflammasome via TLR4 in dendritic cells—implications for diet-induced insulin resistance." Molecular nutrition & food research 56(8): 1212-1222.

Rosmalen, J. G., P. J. Leenen, J. D. Katz, J. S. Voerman and H. A. Drexhage (1997). Dendritic cells in the autoimmune insulitis in NOD mouse models of diabetes. Dendritic cells in fundamental and clinical immunology, Springer: 291-294.

Rothenberg, M. E. and S. P. Hogan (2006). "The eosinophil." Annu Rev Immunol **24**: 147-174.

Rotter, V., I. Nagaev and U. Smith (2003). "Interleukin-6 (IL-6) induces insulin resistance in 3T3-L1 adipocytes and is, like IL-8 and tumor necrosis factor-alpha, overexpressed in human fat cells from insulin-resistant subjects." J Biol Chem **278**(46): 45777-45784.

Santomauro, A. T., G. Boden, M. E. Silva, D. M. Rocha, R. F. Santos, M. J. Ursich, P. G. Strassmann and B. L. Wajchenberg (1999). "Overnight lowering of free fatty acids with Acipimox improves insulin resistance and glucose tolerance in obese diabetic and nondiabetic subjects." Diabetes 48(9): 1836-1841.

Scherer, P. E. (2006). "Adipose tissue from lipid storage compartment to endocrine organ." Diabetes 55(6): 1537-1545.

Schiffrin, E. L. (2008). "Oxidative stress, nitric oxide synthase, and superoxide dismutase: a matter of imbalance underlies endothelial dysfunction in the human coronary circulation." Hypertension 51(1): 31-32.

Schipper, H. S., M. Rakhshandehroo, S. F. van de Graaf, K. Venken, A. Koppen, R. Stienstra, S. Prop, J. Meerding, N. Hamers, G. Besra, L. Boon, E. E. Nieuwenhuis, D.

Elewaut, B. Prakken, S. Kersten, M. Boes and E. Kalkhoven (2012). "Natural killer T cells in adipose tissue prevent insulin resistance." J Clin Invest **122**(9): 3343-3354.

Schleifenbaum, J., C. Kohn, N. Voblova, G. Dubrovska, O. Zavarirskaya, T. Gloe, C. S. Crean, F. C. Luft, Y. Huang, R. Schubert and M. Gollasch (2010). "Systemic peripheral artery relaxation by KCNQ channel openers and hydrogen sulfide." J Hypertens 28(9): 1875-1882.

Seijkens, T., P. Kusters, A. Chatzigeorgiou, T. Chavakis and E. Lutgens (2014). "Immune cell crosstalk in obesity: a key role for costimulation?" Diabetes 63(12): 3982-3991.

Sharabiani, M. T., R. Vermeulen, C. Scoccianti, F. S. Hosnijeh, L. Minelli, C. Sacerdote, D. Palli, V. Krogh, R. Tumino, P. Chiodini, S. Panico and P. Vineis (2011). "Immunologic profile of excessive body weight." Biomarkers **16**(3): 243-251.

Shimoda, K., J. van Deursen, M. Y. Sangster, S. R. Sarawar, R. T. Carson, R. A. Tripp, C. Chu, F. W. Quelle, T. Nosaka, D. A. Vignali, P. C. Doherty, G. Grosveld, W. E. Paul and J. N. Ihle (1996). "Lack of IL-4-induced Th2 response and IgE class switching in mice with disrupted Stat6 gene." Nature **380**(6575): 630-633.

Shoelson, S. E., J. Lee and A. B. Goldfine (2006). "Inflammation and insulin resistance." The Journal of clinical investigation 116(7): 1793-1801.

Stefanovic-Racic, M., X. Yang, M. S. Turner, B. S. Mantell, D. B. Stolz, T. L. Sumpter, I. J. Sipula, N. Dedousis, D. K. Scott and P. A. Morel (2012). "Dendritic cells promote macrophage infiltration and comprise a substantial proportion of obesity-associated increases in $CD11c^{+}$ cells in adipose tissue and liver." Diabetes 61(9): 2330-2339.

Stehouwer, C. D., M.-A. Gall, J. W. Twisk, E. Knudsen, J. J. Emeis and H.-H. Parving (2002). "Increased urinary albumin excretion, endothelial dysfunction, and chronic low-grade inflammation in type 2 diabetes progressive, interrelated, and independently associated with risk of death." Diabetes 51(4): 1157-1165.

Steinman, R. M. (2006). "Linking innate to adaptive immunity through dendritic cells." Novartis Found Symp 279: 101-109; discussion 109-113, 216-109.

Steinman, R. M. and J. Banchereau (2007). "Taking dendritic cells into medicine." Nature 449(7161): 419-426.

Szasz, T., G. F. Bomfim and R. C. Webb (2013). "The influence of perivascular adipose tissue on vascular homeostasis." Vasc Health Risk Manag 9: 105-116.

Takeda, K., T. Tanaka, W. Shi, M. Matsumoto, M. Minami, S. Kashiwamura, K. Nakanishi, N. Yoshida, T. Kishimoto and S. Akira (1996). "Essential role of Stat6 in IL-4 signalling." Nature **380**(6575): 627-630.

Teh, P. P., A. Vasanthakumar and A. Kallies (2015). "Development and Function of Effector Regulatory T Cells." Prog Mol Biol Transl Sci **136**: 155-174.

Tejada-Simon, M. V. and J. J. Pestka (1999). "Proinflammatory cytokine and nitric oxide induction in murine macrophages by cell wall and cytoplasmic extracts of lactic acid bacteria." Journal of Food Protection® **62**(12): 1435-1444.

Tiemessen, M. M., A. L. Jagger, H. G. Evans, M. J. van Herwijnen, S. John and L. S. Taams (2007). "$CD4^+CD25^+Foxp3^+$ regulatory T cells induce alternative activation of human monocytes/macrophages." Proc Natl Acad Sci U S A **104**(49): 19446-19451.

Tilloy, F., E. Treiner, S. H. Park, C. Garcia, F. Lemonnier, H. de la Salle, A. Bendelac, M. Bonneville and O. Lantz (1999). "An invariant T cell receptor alpha chain defines a novel TAP-independent major histocompatibility complex class Ib-restricted alpha/beta T cell subpopulation in mammals." J Exp Med **189**(12): 1907-1921.

Treiner, E., L. Duban, S. Bahram, M. Radosavljevic, V. Wanner, F. Tilloy, P. Affaticati, S. Gilfillan and O. Lantz (2003). "Selection of evolutionarily conserved mucosal-associated invariant T cells by MR1." Nature **422**(6928): 164-169.

van Exel, E., J. Gussekloo, A. J. de Craen, M. Frolich, A. Bootsma-Van Der Wiel and R. G. Westendorp (2002). "Low production capacity of interleukin-10 associates with the metabolic syndrome and type 2 diabetes : the Leiden 85-Plus Study." Diabetes **51**(4): 1088-1092.

Verlohren, S., G. Dubrovska, S. Y. Tsang, K. Essin, F. C. Luft, Y. Huang and M. Gollasch (2004). "Visceral periadventitial adipose tissue regulates arterial tone of mesenteric arteries." Hypertension 44(3): 271-276.

Vieira-Potter, V. J., S. Lee, D. S. Bayless, R. J. Scroggins, R. J. Welly, N. J. Fleming, T. N. Smith, G. M. Meers, M. A. Hill, R. S. Rector and J. Padilla (2015). "Disconnect between

adipose tissue inflammation and cardiometabolic dysfunction in Ossabaw pigs." Obesity (Silver Spring) 23(12): 2421-2429.

Weisberg, S. P., D. McCann, M. Desai, M. Rosenbaum, R. L. Leibel and A. W. Ferrante (2003). "Obesity is associated with macrophage accumulation in adipose tissue." The Journal of clinical investigation 112(12): 1796-1808.

Weston, A. H., I. Egner, Y. Dong, E. L. Porter, A. M. Heagerty and G. Edwards (2013). "Stimulated release of a hyperpolarizing factor (ADHF) from mesenteric artery perivascular adipose tissue: involvement of myocyte BK_{Ca} channels and adiponectin." Br J Pharmacol 169(7): 1500-1509.

Winer, D. A., S. Winer, L. Shen, P. P. Wadia, J. Yantha, G. Paltser, H. Tsui, P. Wu, M. G. Davidson, M. N. Alonso, H. X. Leong, A. Glassford, M. Caimol, J. A. Kenkel, T. F. Tedder, T. McLaughlin, D. B. Miklos, H. M. Dosch and E. G. Engleman (2011). "B cells promote insulin resistance through modulation of T cells and production of pathogenic IgG antibodies." Nat Med **17**(5): 610-617.

Winer, S., Y. Chan, G. Paltser, D. Truong, H. Tsui, J. Bahrami, R. Dorfman, Y. Wang, J. Zielenski, F. Mastronardi, Y. Maezawa, D. J. Drucker, E. Engleman, D. Winer and H. M. Dosch (2009). "Normalization of obesity-associated insulin resistance through immunotherapy." Nat Med **15**(8): 921-929.

Withers, S. B., C. Agabiti-Rosei, D. M. Livingstone, M. C. Little, R. Aslam, R. A. Malik and A. M. Heagerty (2011). "Macrophage activation is responsible for loss of anticontractile function in inflamed perivascular fat." Arterioscler Thromb Vasc Biol 31(4): 908-913.

Withers, S. B., L. Simpson, S. Fattah, M. E. Werner and A. M. Heagerty (2014). "cGMP-dependent protein kinase (PKG) mediates the anticontractile capacity of perivascular adipose tissue." Cardiovasc Res 101(1): 130-137.

Wu, D., A. B. Molofsky, H. E. Liang, R. R. Ricardo-Gonzalez, H. A. Jouihan, J. K. Bando, A. Chawla and R. M. Locksley (2011). "Eosinophils sustain adipose alternatively activated macrophages associated with glucose homeostasis." Science **332**(6026): 243-247.

Xia, N., S. Horke, A. Habermeier, E. I. Closs, G. Reifenberg, A. Gericke, Y. Mikhed, T. Münzel, A. Daiber and U. Förstermann (2016). "Uncoupling of Endothelial Nitric Oxide Synthase in Perivascular Adipose Tissue of Diet-Induced Obese Mice." Arteriosclerosis, thrombosis, and vascular biology 36(1): 78-85.

Yang, H., Y. H. Youm, B. Vandanmagsar, A. Ravussin, J. M. Gimble, F. Greenway, J. M. Stephens, R. L. Mynatt and V. D. Dixit (2010). "Obesity increases the production of proinflammatory mediators from adipose tissue T cells and compromises TCR repertoire diversity: implications for systemic inflammation and insulin resistance." J Immunol **185**(3): 1836-1845.

Yu, X. H., L. B. Cui, K. Wu, X. L. Zheng, F. S. Cayabyab, Z. W. Chen and C. K. Tang (2014). "Hydrogen sulfide as a potent cardiovascular protective agent." Clin Chim Acta 437: 78-87.

Zavaritskaya, O., N. Zhuravleva, J. Schleifenbaum, T. Gloe, L. Devermann, R. Kluge, M. **Mladenov, M. Frey, H. Gagov, G. Fesus, M. Gollasch and R. Schubert** (2013). "Role of KCNQ channels in skeletal muscle arteries and periadventitial vascular dysfunction." Hypertension 61(1): 151-159.

Zeyda, M. and T. M. Stulnig (2007). "Adipose tissue macrophages." Immunology letters **112**(2): 61-67.

Zhang, H., Y. Park, J. Wu, X. ping Chen, S. Lee, J. Yang, K. C. Dellsperger and C. Zhang (2009). "Role of TNF-α in vascular dysfunction." Clinical Science 116(3): 219-230.

Zhang, H., B. J. Potter, J. M. Cao and C. Zhang (2011). "Interferon-gamma induced adipose tissue inflammation is linked to endothelial dysfunction in type 2 diabetic mice." Basic Res Cardiol 106(6): 1135-1145.

Zhang, Y., P. Yang, R. Cui, M. Zhang, H. Li, C. Qian, C. Sheng, S. Qu and L. Bu (2015). "Eosinophils Reduce Chronic Inflammation in Adipose Tissue by Secreting Th2 Cytokines and Promoting M2 Macrophages Polarization." Int J Endocrinol **2015**: 565760.

Zhao, W., J. Zhang, Y. Lu and R. Wang (2001). "The vasorelaxant effect of H_2S as a novel endogenous gaseous K_{ATP} channel opener." Embo j 20(21): 6008-6016.

Zheng, Y. and A. Y. Rudensky (2007). "Foxp3 in control of the regulatory T cell lineage." Nat Immunol **8**(5): 457-462.

Zhu, J., H. Yamane and W. E. Paul (2010). "Differentiation of effector CD4 T cell populations (*)." Annu Rev Immunol **28**: 445-489.

Zuniga, L. A., W. J. Shen, B. Joyce-Shaikh, E. A. Pyatnova, A. G. Richards, C. Thom, S. M. Andrade, D. J. Cua, F. B. Kraemer and E. C. Butcher (2010). "IL-17 regulates adipogenesis, glucose homeostasis, and obesity." J Immunol **185**(11): 6947-6959.

CHAPTER II

The Development of Type 2 Diabetes is Associated with Accumulation of CD11c^{+} Cells and Increased Production of Inflammatory Cytokines in Perivascular Adipose Tissue

2.1. ABSTRACT

Objective*:* It is well-accepted that obesity is associated with chronic inflammation and accumulation of multiple immune cells in adipose tissue. However, little information is available as to whether the development of type 2 diabetes (T2DM) is associated with imbalanced production of inflammatory factors and accumulation of $CD11c^+$ immunocytes, including dendritic cells and macrophages in perivascular adipose tissue. Therefore, our study aimed to determine whether $CD11c^+$ cells infiltrate into diabetic perivascular adipose tissue and whether diabetic perivascular adipose tissue exhibits an imbalance production of pro- and anti-inflammatory cytokines. Also, our study sought to test whether above changes would be impacted by disease progression.

Methods*:* *db/db* mice, a T2DM murine model, were divided into 6-10, 12-16, 18-22 and > 24 weeks groups, along with their corresponding DbHET controls. Regional vasculatures and associated perivascular adipose tissue were collected. Subsequently, mRNA expression of CD11c, pro-inflammatory (tumor necrosis factor α (TNF-α) and interleukin 6 (IL-6)) and anti-inflammatory markers (adiponectin and interleukin 10 (IL-10)) were determined by real-time PCR. Identification of $CD11c^+$ cells in adipose tissue was also performed by immunofluorescence staining and flow cytometry.

Results: CD11c mRNA expression in multiple adipose tissues from *db/db* mice dramatically increased compared to DbHET mice. In contrast, regional arteries expressed very low CD11c mRNA levels. Flow cytometry data confirmed the presence of more $CD11c^+F4/80^-$ and $CD83^+CD86^+$ dendritic cells accumulated in VAT from *db/db* mice compared to DbHET mice at both 6-10 and 18-22 weeks. Similarly, increasing numbers of $CD11c^+F4/80^+$ macrophages were also accumulated in VAT from *db/db* mice compared to controls at both age groups. In agreement with flow cytometry data, immunohistochemistry results showed the presence of more $CD11c^+$ cells in the stromal vascular fraction of VAT from *db/db* than DbHET mice at both 6-10 and 18-22 weeks. PCR data showed that pro-inflammatory cytokine TNF-α and IL-6 mRNA levels were higher in VAT and MAT from *db/db* mice compared to DbHET mice at both 6-10 and 18-22 weeks,

except that there was no significant difference of TNF-α expression between *db/db* and DbHET mice at 6-10 weeks. In contrast, mRNA levels of the anti-inflammatory cytokine adiponectin were lower in VAT from *db/db* mice than DbHET at both age groups. The decrease of adiponectin mRNA levels in MAT from *db/db* mice was only detected at 18-22 weeks. Interestingly, anti-inflammatory cytokine IL-10 mRNA levels were increased in VAT and MAT from *db/db*, compared to DbHET mice at both age groups. Moreover, IL-10 mRNA levels were increased in MAT from *db/db* mice at 18-22 weeks compared to 6-10 weeks.

Conclusion: In a model of T2DM, $CD11c^+$ cells accumulate in the stromal vascular fraction of perivascular adipose tissue rather than in the vasculature wall, per se. More $CD11c^+$ cells comprised of dendritic cells and M1 macrophages accumulated in diabetic adipose tissue. Moreover, increased pro-inflammatory cytokines and decreased anti-inflammatory mediators are produced in diabetic perivascular adipose tissue. This imbalanced production of inflammatory factors becomes more severe with the development of T2DM.

***Key Words*:** adipose tissue; type 2 diabetes; $CD11c^+$ cells; dendritic cells; macrophages; TNF-α; lL-6; adiponectin; IL-10.

2.2. Introduction

Obesity is defined as a pathological condition with a body-mass index (BMI) greater than 30 kg/m^2 (Flegal, Carroll et al. 2012). It has been reported that between the years of 1980 and 2013, the global incidence of obesity increased from 28.8% to 36.9% in men, and from 29.8% to 38% (Ng, Fleming et al. 2014). According to data from the world health organization (WHO) (Sundara Rajan and Longhi 2016), the prevalence of obesity in children and adolescents has also increased dramatically in the past two decades. The development of obesity has been demonstrated to be associated with a variety of complications, including coronary heart disease, hypertension, type 2 diabetes (T2DM), cancers, sleep apnea, gallstones, osteoarthritis and infertility (Kahn, Hull et al. 2006). The most devastating complication of the above is T2DM, as this is a risk factor for the development of life threatening cardio/cerebrovascular diseases, particularly seen as coronary heart disease and stroke (Schlienger 2013). Furthermore, diabetes became the 7^{th} leading cause of death in United States, causing more than 200 million civilian deaths in 2010 (Chamberlain, Rhinehart et al. 2016). As a result of these alarming statistics, worldwide health professionals are focusing their attention on research to discover effective interventions.

Growing evidence suggests that both obesity and T2DM share common pathological mechanisms (Ferreira, Silva et al. 2016, Genser, Casella Mariolo et al. 2016). Both diseases exhibit chronic low-grade, local and systemic, inflammation, which contribute to the pathogenesis of insulin resistance (Dandona, Aljada et al. 2004, Kahn, Hull et al. 2006). This chronic inflammation is characterized by an increase in expression of pro-inflammatory cytokines and a decrease in expression of anti-inflammatory factors. Specifically, evidence supports a role for pro-inflammatory cytokine tumor necrosis factor-alpha (TNF-α) in mediating insulin resistance in both human and rodent models (Pina, Armesto et al. 2015, Al-Mutairi and Shabaan 2016). Administration of a TNF-α blocker in T2DM patients (Al-Mutairi and Shabaan 2016) or genetic depletion of TNF-α ligand in mice (Uysal, Wiesbrock et al. 1997) partially ameliorates obesity-induced insulin resistance. Another inflammatory marker interleukin-6 (IL-6), also has been found

to induce insulin resistance in adipocytes (Rotter, Nagaev et al. 2003) and is strongly correlated with the occurrence of T2DM (Almuraikhy, Kafienah et al. 2016, Liu, Feng et al. 2016). Adiponectin, as an important anti-inflammatory cytokine, has been shown to increase insulin sensitivity in adipocytes and decrease insulin resistance in obese mice (Yamauchi, Kamon et al. 2001, Kadowaki, Yamauchi et al. 2006). Thus evidence supports the concept that T2DM is positively correlated with elevated levels of inflammatory cytokines TNF-α and IL-6, and negatively correlated with lower levels of adiponectin (Daniele, Guardado Mendoza et al. 2014, Liu, Feng et al. 2016).

Another feature of chronic inflammation in T2DM is increasing infiltration of immune cells, particularly macrophages, into adipose tissue (Ye, Gao et al. 2007). It has been demonstrated that diet-induced obesity leads to accumulation of macrophages in inflamed visceral adipose tissue (Weisberg, McCann et al. 2003, Lumeng, Bodzin et al. 2007). Moreover, these macrophages in obese adipose tissue are activated to switch their phenotype from M2 anti-inflammatory to M1 pro-inflammatory form (Curat, Wegner et al. 2006, Lumeng, Bodzin et al. 2007, Kraakman, Murphy et al. 2014). As an extension of this, it is thought that accumulated M1 macrophages are a prominent source of TNF-α and IL-6 production, which subsequently impair insulin signaling in adipocytes, leading to obesity-associated insulin resistance (Lumeng, Bodzin et al. 2007). Apart from macrophages, $CD8^+$ effector T cells also accumulate in epididymal adipose tissue in obese mice fed with a high-fat diet (Wu, Ghosh et al. 2007, Nishimura, Manabe et al. 2009). In contrast, the number of $CD4^+$ T cells and regulatory T cells are lower in adipose tissue of the obese mice. Interestingly, the recruitment of $CD8^+$ effector T cells has been shown to precede the infiltration of M1 macrophages into adipose tissue, which amplifies TNF-α production and aggravates adipose tissue inflammation (Nishimura, Manabe et al. 2009). Consistent with this, inhibition of $CD8^+$ T cells by treatment with neutralizing antibodies not only significantly reduced M1 macrophage accumulation in adipose tissue, but also decreased pro-inflammatory TNF-α and IL-6 secretion in epididymal fat pads. Importantly, this also resulted in improvement of glucose tolerance and reduction of insulin resistance in diet-induced obese mice (Nishimura, Manabe et al. 2009). Interestingly, B lymphocytes have also been found to infiltrate into obese

adipose tissue from high fat diet treated mice (DeFuria, Belkina et al. 2013, Shaikh, Haas et al. 2015). It is believed that B lymphocytes present antigens to T lymphocytes and activate both $CD8^+$ effector T lymphocytes and M1 macrophages (Shaikh, Haas et al. 2015). This maneuver amplifies the production of a series of pro-inflammatory cytokines and promotes the development of chronic inflammation as well as insulin resistance in adipose tissue of obese mice. With the investigation of potential mechanisms of obesity-associated insulin resistance, other types of immune cells have been discovered to participate in the chronic inflammation in adipose tissue, such as natural killer cells, mast cells and eosinophils (Franco Nitta 2013, Seijkens, Kusters et al. 2014). Thus it appears that in obesity, the interplay among these immune cells within adipose tissue orchestrates the secretions of pro-inflammatory and anti-inflammatory mediators, which promote the development of chronic inflammation and T2DM.

CD11c is an integrin alpha X chain protein expressed on the cell surface of lymphocytes, predominantly on dendritic cells and M1 macrophages. Dendritic cells are well known to locate in a variety of tissues, including brain (Shi, Shen et al. 2011), spleen (Yang, Hu et al. 2006), lung (Patsouris, Li et al. 2008), liver (Pillarisetty, Shah et al. 2004) and intestine (Schulz, Jaensson et al. 2009). Accumulated evidence has demonstrated that dendritic cells also infiltrate into the vascular wall and accelerate the progression of atherosclerosis in rodent models (McArdle, Mikulski et al. 2016, Rombouts, Ammi et al. 2016). To date, however, there is little evidence documenting a role for dendritic cells in the development of T2DM. It is also unclear whether dendritic cells accumulate in the vasculature or adipose tissue during the development of T2DM. Further, although it is known that M1 macrophages are recruited into adipose tissue in the context of diet-induced obesity, it is still uncertain whether M1 macrophages also infiltrate into perivascular adipose tissue in T2DM rodent models. Therefore, the purpose of this study was to determine whether $CD11c^+$ cells would be associated with the development of T2DM by using the *Lepr*^{db} mouse model, which is genetically depleted of leptin receptors. We hypothesized that the majority of $CD11c^+$ cells are recruited into perivascular adipose tissue in T2DM mice, rather than the vasculature. Moreover, the increased numbers of $CD11c^+$ cells in adipose tissue of T2DM is

hypothesized to be accompanied by increased secretion of pro-inflammatory cytokines and the decreased production of anti-inflammatory mediators.

2.3. Methods

Animal Model

Male and female heterozygous mice (m*Lepr*^{db}, DbHET mice) on C57BLKS/J background were purchased from Jackson Laboratory and used as breeding pairs to produce homozygous T2DM mice (*Lepr*^{db}, *db/db* mice) and DbHET mice. All the above mice were maintained on a normal rodent chow diet and housed in a temperature and humidity controlled (25°C) facility with a 12-hour light/dark cycle. Mice were subsequently divided into four age groups: 6-10 weeks, 12-16 weeks, 18-22 weeks and more than 24 weeks groups. Non-fasting blood glucose measurements were performed using ReliOn prime blood glucose monitoring system (ReliOn Company, WA, USA) on each mouse before administration of anesthesia. A surgical plane of anesthesia was induced by intraperitoneal injection of sodium Nembutal (60mg kg^{-1}) (Sigma Company, Cream Ridge, NJ, USA) (Kato, Kashiwagi et al. 2006) and then tissues were collected. Total body weight, intestinal mesentery weight and weights of various adipose tissues were recorded. Mice were euthanized after anesthesia and tissue collection. All animal procedures were conducted in accordance with protocols approved by the Laboratory Animal Care and Use Committee at University of Missouri, Columbia.

Measurement of mRNA expression

After anesthesia, the spleen and visceral (VAT), mesenteric (MAT), periaortic (ATA), and pericardial (AH) adipose tissues were collected along with segments of first or second order mesenteric arteries (MA), thoracic aorta (TA), left anterior descending coronary artery (LAD) were dissected and snap frozen in liquid N_2. Tissues were subsequently prepared for measurement of mRNA expression using real-time, quantitative, polymerase chain reaction (qPCR). Total RNA of VAT, MAT, ATA and AH were extracted by RNeasy lipid tissue mini kits (Qiagen Company, Valencia, CA, USA). Total RNA of spleen was similarly extracted by the RNeasy mini kit (Qiagen). Total RNA of MA and LAD were extracted by Arcturus Pico Pure RNA isolation kit (Life Technologies Company, Grand Island, NY, USA). Total RNA of TA was extracted by RNeasy

fibrous tissue mini kit (Qiagen). The quality and quantity of total RNA were measured using a Nano Drop ND-1000 Spectrophotometer (Nano Drop Technologies, Wilmington, DE). cDNA was reverse transcribed using equal amounts of total RNA by the SuperScript III First-Strand Synthesis System (Invitrogen Company, Grand Island, NY, USA). Amplification of cDNA was conducted using Platinum® SYBR® Green qPCR SuperMix-UDG (Invitrogen) and an iQ5 Real-Time PCR system (Bio-Rad company, Hercules, CA, USA). qPCR reactions were performed according to the following protocol: 2 minute reactions at 50° C and 95 °C followed by 40 cycles of 95°C 3s and 56°C 30s. Melting/dissociation curves were performed on each well to assure specificity of the amplicon product. “No template” cDNA was used as a negative control in each plate to detect contamination. The housekeeping gene glyceraldehyde 3-phosphate dehydrogenase (GAPDH) was used for internal normalization. Spleen cDNA from a male DbHET mouse at 12 weeks was used as a calibrator. The same calibrator sample was included in all PCR reactions together with cDNA samples from the various adipose tissue and blood vessel samples. Primers were used as follows in **Table.2-1**:

Table. 2-2. Properties of Primers for q PCR detection in DbHET and *db/db* mice

Target gene	Primer sequence	Amplification efficiency
CD11c	F:5’-CTGGATAGCCTTT CTTCTGCTG-3’ R:5’-GCACACTGTGTCC GAACTCA-3’	1.97
GAPDH	F:5’-AATGGTGAAGGTC GGTGTG-3’ R:5’-GTGGAGTCATACT GGAACATGTAG-3’	1.99
TNF-α	F:5’-GTCCCCAAAGGGA TGAGAAG-3’ R:5’-CACTTGGTGGTTT	1.98

	GCTACGA-3’	
IL-6	F:5’-CCGGAGAGGAGA CTTCACAG-3’ R:5’-TCCACGATTTCCC AGAGAAC-3’	1.98
Adiponectin	F:5’-GTCTCACCCTTAG GACCAAGAA-3’ R:5’-AGGTTGGATGGCA GGC-3’	1.99
IL-10	F:5’-ATGGCCTTGTAGA CACCTTG-3’ R:5’-GTCATCGATTTCT CCCCTGTG-3’	1.98

The mean threshold cycle (CT) values were calculated by the $2^{-\Delta\Delta CT}$ method ($\Delta\Delta CT=C_{T.CD11c}-C_{T.GAPDH}$) (Pfaffl 2001). Results were presented as fold change of transcripts for CD11c normalized to GAPDH, compared with the calibrator (defined as 1.0 fold). mRNA levels of TNF-α, IL-6, adiponectin and IL-10 were presented as fold change of transcripts for different inflammatory cytokines normalized to GAPDH, compared to DbHET mice at 6-10 weeks (defined as 1.0 fold).

Isolation of Stromal Vascular Fraction from Adipose Tissue

VAT was harvested from both *db/db* and DbHET mice at 6-10 and 18-22 weeks of age. The tissue was then placed in freshly prepared buffer containing 1x Phosphate Buffered Saline (Ca/Mg^{2+} free) (Gibco Company, Waltham, MA, USA), 0.5% bovine serum albumin (Sigma-Aldrich Company, Cream Ridge, NJ, USA) and 10mM $CaCl_2$. Sterile scissors were used to mince adipose tissue into fine particles (< 10 mg). Type II collagenase purified from Clostridium histolyticum (Sigma-Aldrich Company, Cream Ridge, NJ, USA) at a concentration of 2 mg/ml was added to the minced adipose tissue, mixed and incubated at 37° C (20 minutes) on an orbital shaker (Thermo Scientific Company, Philadelphia, PA, USA). Enzymatic digestion was terminated

by 1 mM EDTA. The solution was then passed through a sterile 100-µm nylon strainer (Fisher Scientific Company, Waltham, MA, USA) and the suspension centrifuged at 1600 rpm for 5 minutes at room temperature. The suspension was separated into two divisions. The upper layer or supernatant contained 'floating' cells and is referred to as the adipocyte-enriched fraction. The pellet was collected as the stromal vascular cell fraction. The stromal vascular fraction was then re-suspended in erythrocyte lysis buffer (Bio legend Company, San Diego, CA, USA) and incubated at room temperature for 5 minutes without shaking. 1x Phosphate Buffered Saline depleted of Ca^{2+} and Mg^{2+} was then added to the samples to terminate the lysis reaction. The suspension was subsequently centrifuged at 1600 rpm for 5 minutes at 4 °C and the pelleted cells were considered to be the erythrocyte-depleted stromal vascular fraction cells and re-suspended in 1x Phosphate Buffered Saline without Ca^{2+} and Mg^{2+}.

Flow Cytometry

The erythrocyte-depleted stromal vascular fraction was cooled in ice for 10 minutes and cell number determined using a hemcytometer. Cell survival was determined by Trypan blue (0.4% solution) (Sclen Cell Research Laboratories, Carlsbad, CA, USA). Cell survival rate was determined to be approximately 90%. After cell number and survival rate measurements, cells were centrifuged at 1600 rpm for 5 minutes at 4°C. After aspiration of the supernatant, pelleted cells were then re-suspended in flow cytometry staining buffer (E-bioscience Company, San Diego, CA, USA). After cells were washed twice with flow cytometry staining buffer, the final cell count was approximately 1 $\times 10^6$ cell counts/ml. To prevent non-specific binding of antibodies, Fc-blocker (1 µg/ml, sigma-Aldrich Company, Cream Ridge, NJ, USA) was added to the samples and then incubated in the refrigerator at 4 ° C for 15 minutes in the absence of light. Without any washing, the following antibodies and corresponding isotype controls in **Table 2-2** were incubated with above cells in the dark at 4°C for 45 minutes.

Table.3-2. Properties of antibodies for flow cytometry measurements in DbHET and *db/db* mice.

Antibody	Conjugated fluorochrome	Commercial Company	Dilution
CD11c antibody	APC (Allophycocyanin)	BD Pharmingen Company, San Jose, CA, USA	1:200
F4/80 antibody	PE (phycoerythrin)	E-bioscience Company, San Diego, CA, USA	1:400
CD83 antibody	APC	Bio legend Company, San Diego, CA, USA	1:200
CD86 antibody	PE	E-bioscience Company, San Diego, CA, USA	1:200

Following this, 2ml flow cytometry staining buffer was added to wash the cell samples. The suspension was then centrifuged at 1600 rpm at 4 ° C for 5 minutes and the pelleted cells re-suspended in 2 ml flow cytometry staining buffer. This washing procedure was repeated twice. Cells were then identified in CyAn ADP High-Performance Flow Cytometer according to the expression of fluorochromes. The Summit and Flowjo software were used to quantify $CD11c^{+}F4/80^{-}$ and $CD83^{+}CD86^{+}$ dendritic cell populations as well as the $CD11c^{+}F4/80^{+}$ macrophage population.

Immunohistochemical Identification of $CD11c^{+}$ cells

VAT was harvested from DbHET and *db/db* mice at 6-10 and 18-22 weeks and samples fixed in 10% formalin (Sigma Company, Cream Ridge, NJ, USA) for 18-24 hours. Tissue samples were then embedded in paraffin and cut into 5 µm thick sections (Wentworth, Naselli et al. 2010). Sections were then de-paraffinized with xylene and series concentrations of ethanol at 100%,

95%, 75% and 50%. After deparaffinization, all the sections were incubated in sodium citrate buffer (10mM Sodium Citrate, 0.05% Tween 20, pH 6.0) around 100° C for 20 minutes. Following this antigen retrieval step, VAT sections were incubated with 10% goat serum at room temperature for 1 hour to prevent nonspecific binding of the primary antibodies. Tissue sections were then incubated (4°C) overnight with hamster anti-mouse CD11c primary antibodies (1:200 dilution, Abcam Company, Cambridge, United Kingdom). After washing with TBS (Tris-Buffered Saline), VAT sections were incubated at room temperature for 3 hours with goat anti-hamster secondary antibodies conjugated with Texas-Red (1:1000 dilution, Abcam Company, Cambridge, United Kingdom). Nuclei were identified by DAPI (4', 6-diamidino-2-phenylindole) staining (1mg/ml) (Invitrogen, Carlsbad CA, USA). Fluorescence staining was visualized using an Olympus microscope (model IX81). To evaluate the presence of $CD11c^+$ cells in VAT, adipocytes and $CD11c^+$ cells were counted from 10 random high power view fields (×200) on each section (Kosteli, Sugaru et al. 2010, Zhang, Sugiyama et al. 2011). Six sections were collected from each mouse and the percentage of $CD11c^+$ cells for each sample expressed as the sum of the number of CD11c-expressing cells divided by the total number of surrounding adipocytes in each field of view (Kosteli, Sugaru et al. 2010).

Statistical Analysis

All data are presented as mean ± SEM. Basic parameters of mice and CD11c mRNA levels were analyzed with two-way Analysis of variance (ANOVA), while the flow cytometry data, immunohistochemistry analysis and inflammatory cytokine mRNA levels were analyzed by one-way ANOVA using Graph pad Prism 4.0 software (Graph pad Company, CA, USA). The post-hoc test used in one-way ANOVA was Tukey's test. The P value < 0.05 was considered statistically significant.

2.4. Results

Characteristics of regional perivascular adipose tissues

To determine the impact of diabetic duration on phenotypic changes of T2DM mice, *db/db* and DbHET mice were studied at 6-10 weeks, 12-16 weeks, 18-22 weeks and > 24 weeks of age. *db/db* mice had higher non-fasting glucose levels (**Fig. 2-1-B**) and were more obese than DbHET controls at each age group (**Fig. 2-1-A**). In addition to increased whole body weight, *db/db* mice exhibited increased weights of VAT (**Fig. 2-1-C**) and perivascular adipose tissue compared to DbHET mice (**Fig. 2-1-D-F**). VAT and perivascular adipose tissue weights did not, however, significantly change with age in T2DM mice. Taken together, *db/db* mice had higher body weight and non-fasting glucose levels than control mice, accompanied with heavier VAT and perivascular adipose tissue weights, including intestinal mesentery, AH, and ATA. However, those parameters were not significantly altered with the development of T2DM.

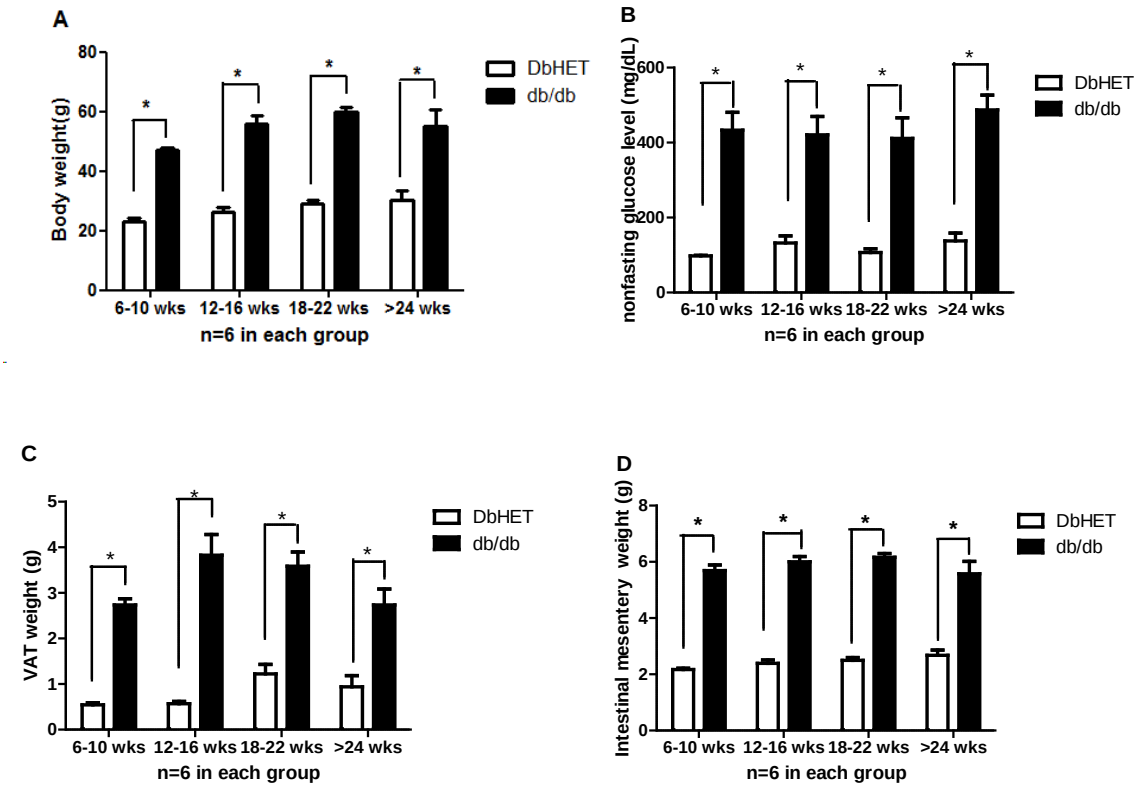

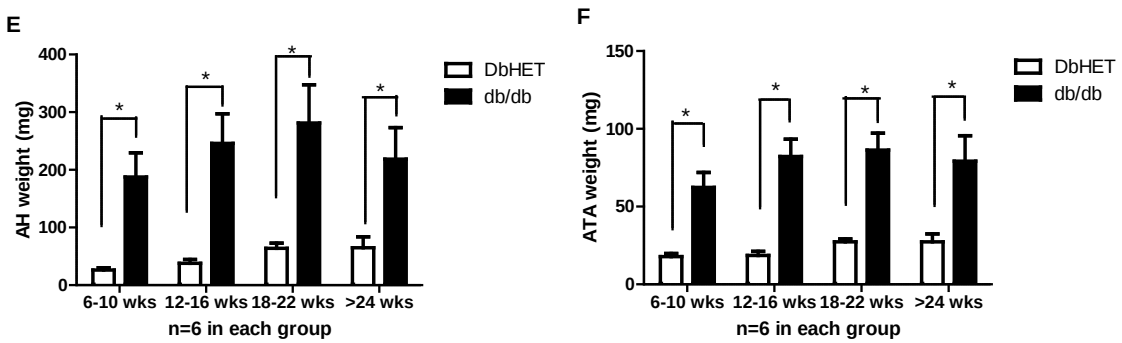

Figure 2-1. Basic characteristics of study groups. A-F: body weight **(A)**; non-fasting blood glucose **(B)**; VAT weight **(C)**; intestinal mesentery weight **(D)**; AH weight **(E)**; ATA weight **(F)** in heterozygous control (DbHET) and diabetic (*db/db*) mice. *db/db* mice showed greater body weight and increased non-fasting blood glucose level compared to DbHET mice. *db/db* mice exhibited significantly greater weights of intestinal mesentery and multiple perivascular adipose tissues compared to DbHET mice. These increases in these variables were similar, however, in all four age groups of *db/db* mice. Data are presented as mean ± SEM. * *P* <0.05 between *db/db* and DbHET mice.

Expression of CD11c mRNA levels on different vasculature

Since dendritic cells and macrophages have been found in the walls of blood vessels and have been implicated in both the induction and progression of inflammation in atherosclerosis of murine thoracic aorta (Chistiakov, Sobenin et al. 2015, Van Brussel, Ammi et al. 2015), we hypothesize that $CD11c^+$ cells also may accumulate in different vasculatures from T2DM mice. To test this postulation, regional arteries were collected from DbHET and *db/db* mice at four different age groups as aforementioned. RNA was extracted from all the samples and reverse-transcribed into cDNA. The cDNA samples were then transcribed and amplified into RNA via qPCR reactions. A spleen sample from a male mouse at 12 weeks was used as a calibrator for each PCR reaction. The purpose of calibrator was to compare CD11c m RNA expression between adipose tissue and their corresponding vasculature.

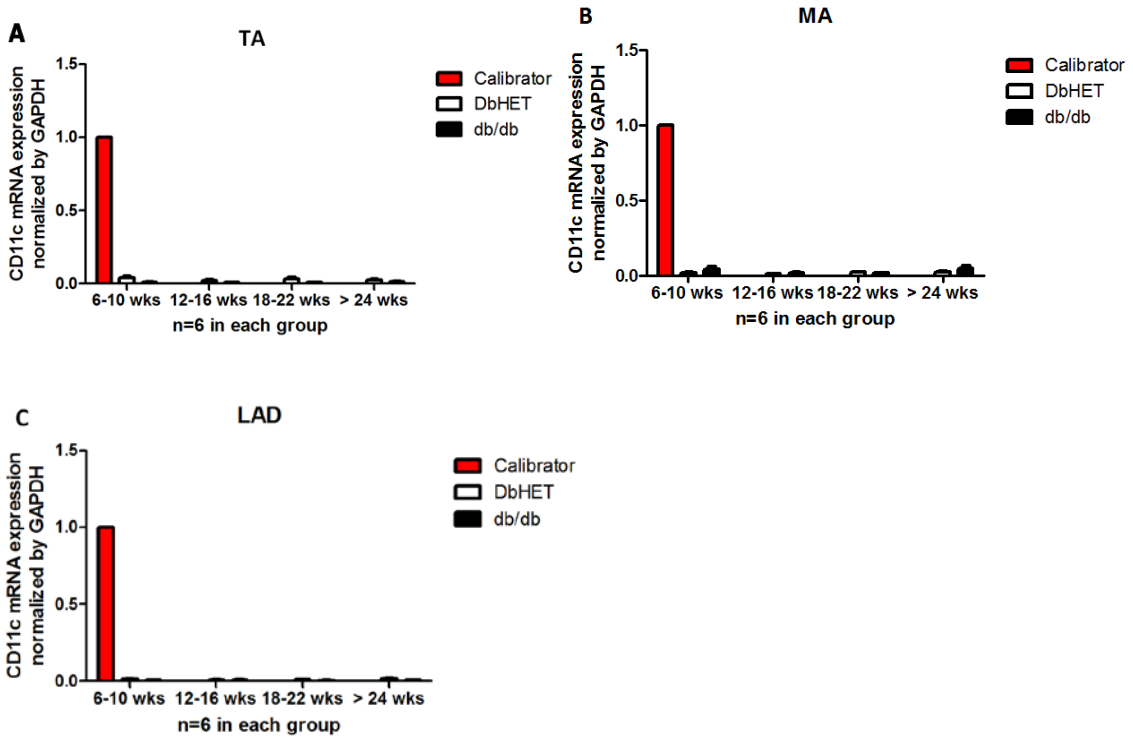

Figure 2-2. Vascular wall CD11c mRNA expression. A-C: In the vascular walls of TA **(A)**, MA **(B)** and LAD **(C),** no significant differences of CD11c mRNA expression were detected between DbHET and *db/db* mice at any age group examined. n=6 in each column, including 3 female and 3 male mice. Data were showed in means ± SEM.

Extremely low levels of CD11c mRNA expression were detected in the TA, MA and LAD samples from DbHET and *db/db* mice compared to the spleen calibrator (**Fig.2-2**). Furthermore, there were no significant differences of CD11c mRNA expression in vascular walls across T2DM duration in either DbHET or *db/db* mice.

Expression of mRNA for CD11c in regional perivascular adipose tissue samples

A growing body of evidence has demonstrated that adipose tissue harbors various immune cells in the development of obesity (Grant, Youm et al. 2013, Grant and Dixit 2015). It is hypothesized that $CD11c^{+}$ cells would also be recruited into perivascular adipose tissue in the

development of T2DM. To test this hypothesis, multiple perivascular adipose tissues were collected from both DbHET and *db/db* mice at the four different age groups. CD11c mRNA levels were again detected by qPCR. CD11c mRNA levels were strikingly increased in VAT (**Fig. 2-3-A**) and MAT (**Fig. 2-3-B**) of both DbHET and *db/db* mice, compared to the previously described splenic calibrator. Further, CD11c mRNA levels were significantly greater in VAT (**Fig. 2-3-A**), MAT (**Fig. 2-3-B**), AH (**Fig. 2-3-C**) and ATA (**Fig. 2-3-D**) from *db/db* mice compared to age-matched DbHET controls. Higher CD11c mRNA levels in AH of *db/db* mice (**Fig. 2-3-C**) were evident at the age greater than 18 weeks compared to DbHET controls. CD11c mRNA levels in VAT and MAT were higher in *db/db* mice at > 24 weeks, compared to *db/db* mice at 6-10 and 12-16 weeks groups, consistent with a duration of diabetes-dependent effect. In contrast, in DbHET mice, CD11c mRNA expression of VAT, MAT, AH and ATA remained constant among all the four age groups, suggesting the lack of an aging effect. Comparing CD11c mRNA levels of DbHET and *db/db* mice at > 24 weeks, the largest fraction of CD11c mRNA expression in *db/db* mice was located in VAT and MAT (**Fig. 2-3-E**). In contrast, CD11c mRNA levels in DbHET mice were comparable among VAT, MAT, AH and ATA, and significantly lower than *db/db* mice. Combined with the data in **Fig.2-2**, these results suggest that in this T2DM model, the majority of $CD11c^{+}$ cells accumulate in the perivascular adipose tissue, rather than in the vascular wall, itself.

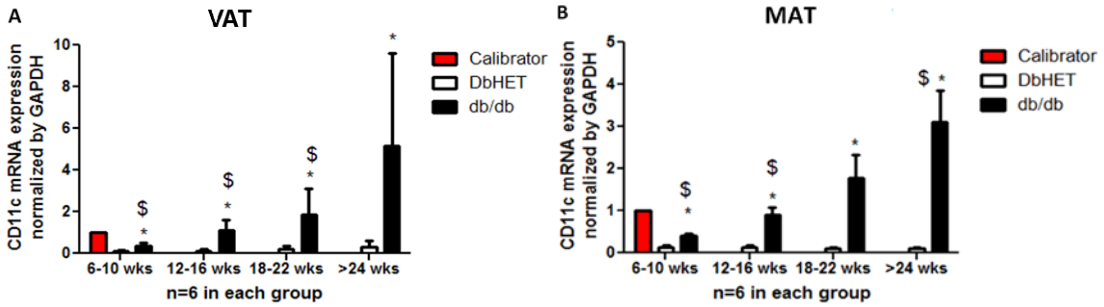

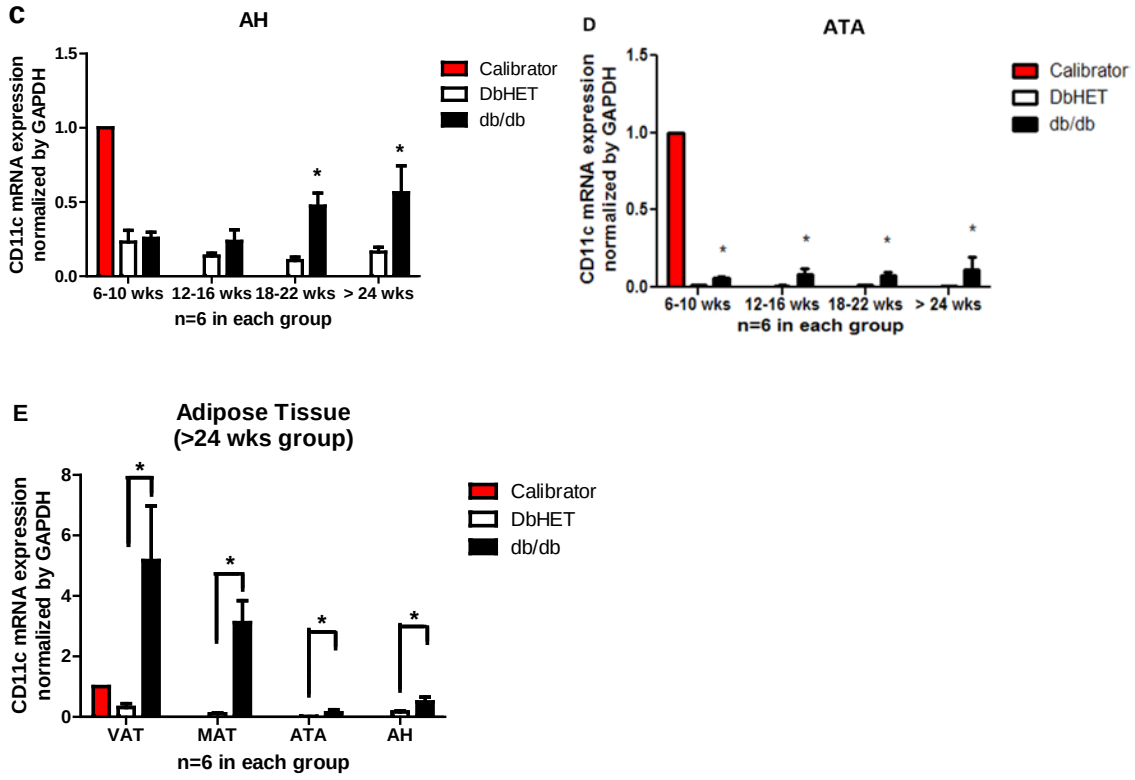

Figure 2-3. CD11c mRNA expression on different perivascular adipose tissue. A-B: Higher CD11c mRNA levels were observed in VAT (panel **A**) and MAT (panel **B**) from *db/db* than DbHET mice in all the age groups. **C**: *db/db* mice showed higher CD11c mRNA expression on AH than DbHET mice only at 18-22 and > 24 weeks groups. **D**: Higher CD11c mRNA levels were observed in ATA from *db/db* than DbHET mice at each age group. **E**: CD11c m RNA expression in VAT, MAT, AH and ATA from DbHET and *db/db* mice at > 24 weeks. n=6 in each column, including 3 female and 3 male mice. Data were showed in means ± SEM. *: $P < 0.05$ between *db/db* and DbHET mice. $: $P < 0.05$ among all the four age groups from *db/db* mice.

Quantification of CD11c$^+$ cells in VAT by flow cytometry

It has previously been shown that the majority of CD11c$^+$ cells consist of two different subsets of immune cells: dendritic cells and M1 macrophages (Kassim, Rajasagi et al. 2006, Li, Lu et al. 2010). Our previous data showed that CD11c mRNA levels were elevated in VAT obtained from *db/db* mice compared to DbHET mice. However, it is still unclear whether, in diabetes, the numbers of dendritic cells or M1 macrophages (or both) are increased in adipose tissue during the development of T2DM. To quantify the numbers of dendritic cells and M1

macrophages, flow cytometry was performed on VAT from both DbHET and *db/db* mice. In this study, we identified the dendritic cells with two combinations of cell surface molecular markers: $CD11c^{+}F4/80^{-}$ and $CD83^{+}CD86^{+}$ cells (Stefanovic-Racic, Yang et al. 2012). The M1 macrophages were identified as the $CD11c^{+}F4/80^{+}$ cells (Lumeng, Bodzin et al. 2007). In order to study the influence of duration of T2DM, we examined 6-10 and 18-22 weeks groups. As shown in **Fig. 2-4**, an approximate 2 fold increase in $CD11c^{+}F4/80^{-}$ dendritic cells (**Fig. 2-4-A, B**) and a 2.5 fold increase in $CD83^{+}CD86^{+}$dendritic cells (**Fig. 2-4-D, E**) were detected in VAT from *db/db* mice compared to DbHET at both 6-10 and 18-22 weeks. The numbers of $CD11c^{+}F4/80^{-}$ and $CD83^{+}CD86^{+}$dendritic cells in diabetic mice were similar in both the 6-10 and 18-22 week groups (**Fig. 2-4-A, B, 2-4-D, E**). Similarly, no significant differences in dendritic cell numbers were detected in DbHET at 6-10 and 18-22 weeks (**Fig 2-4-B, E**). Along with the increase in dendritic cells, *db/db* mice showed 2 fold increase of $CD11c^{+}F4/80^{+}$ M1 macrophages (**Fig. 2-4-A, C**) in VAT compared to DbHET controls. Similarly to the dendritic cell, there was no significant change in M1 macrophage numbers in VAT of *db/db* mice at both 6-10 and 18-22 weeks groups (**Fig. 2-4-A, C**). Furthermore, no significant differences in M1 macrophage numbers were apparent in DbHET mice between 6-10 and 18-22 week groups (**Fig. 2-4-A, C**). Collectively, the results suggest that, at protein levels, more $CD11c^{+}$ cells, including both dendritic cells and M1 macrophages were recruited into VAT of diabetic mice, compared to DbHET. However, there were no significant changes in $CD11c^{+}$ cell numbers in VAT with respect to duration of disease development.

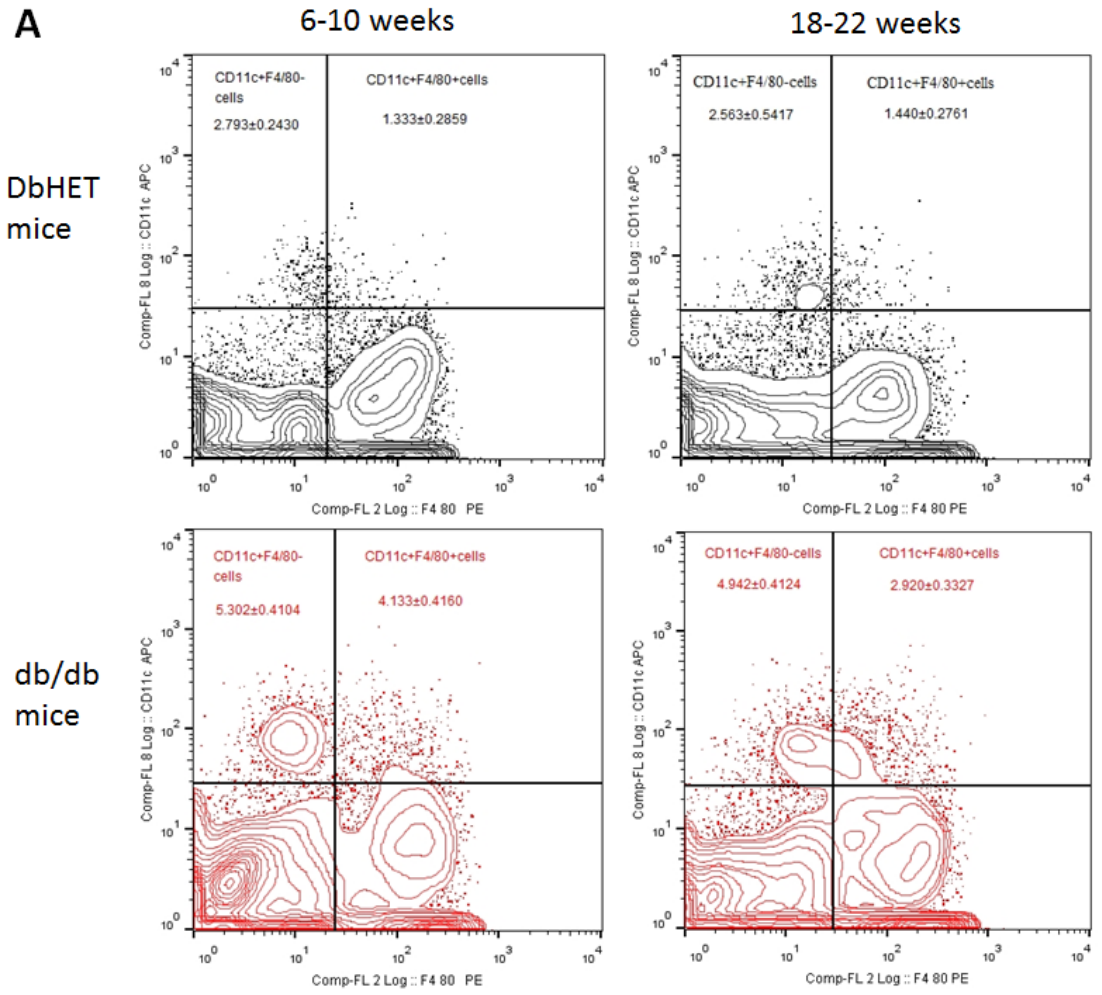

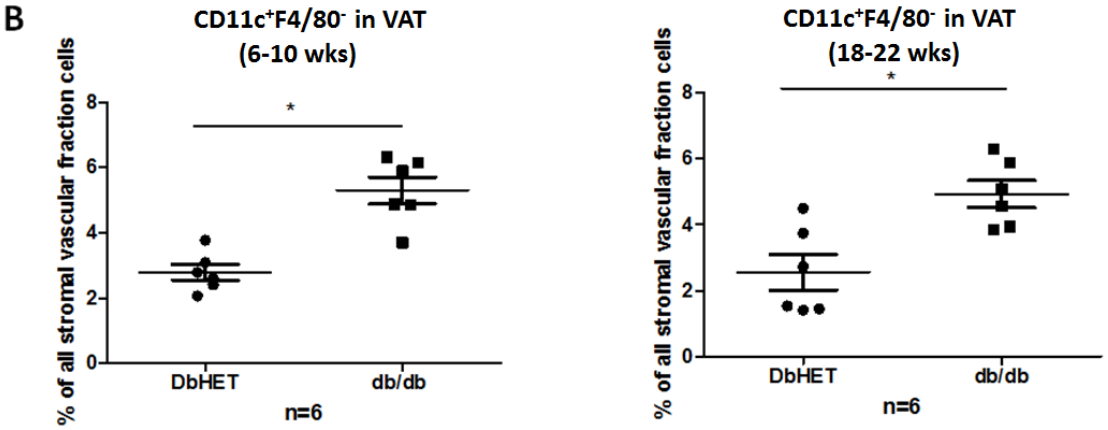

Mean ± SEM	2.793 ± 0.2430	5.302 ± 0.4104

Mean ± SEM	2.563 ± 0.5417	4.942 ± 0.4124

C

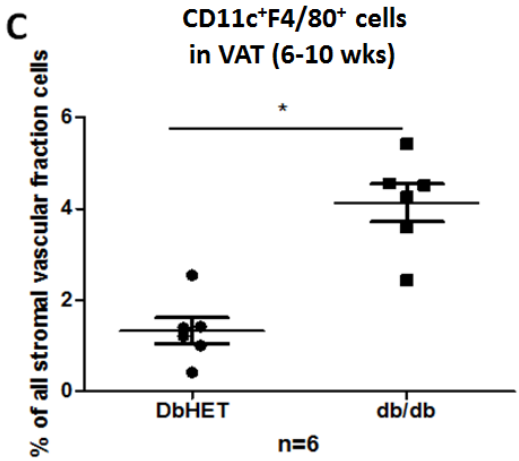

Mean ± SEM	1.333 ± 0.2859	4.133 ± 0.4160

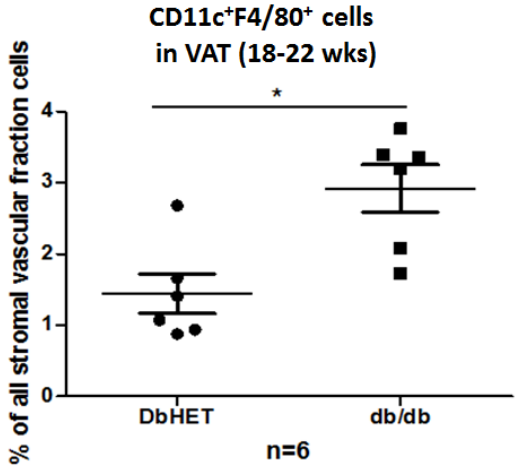

Mean ± SEM	1.440 ± 0.2761	2.920 ± 0.3327

D

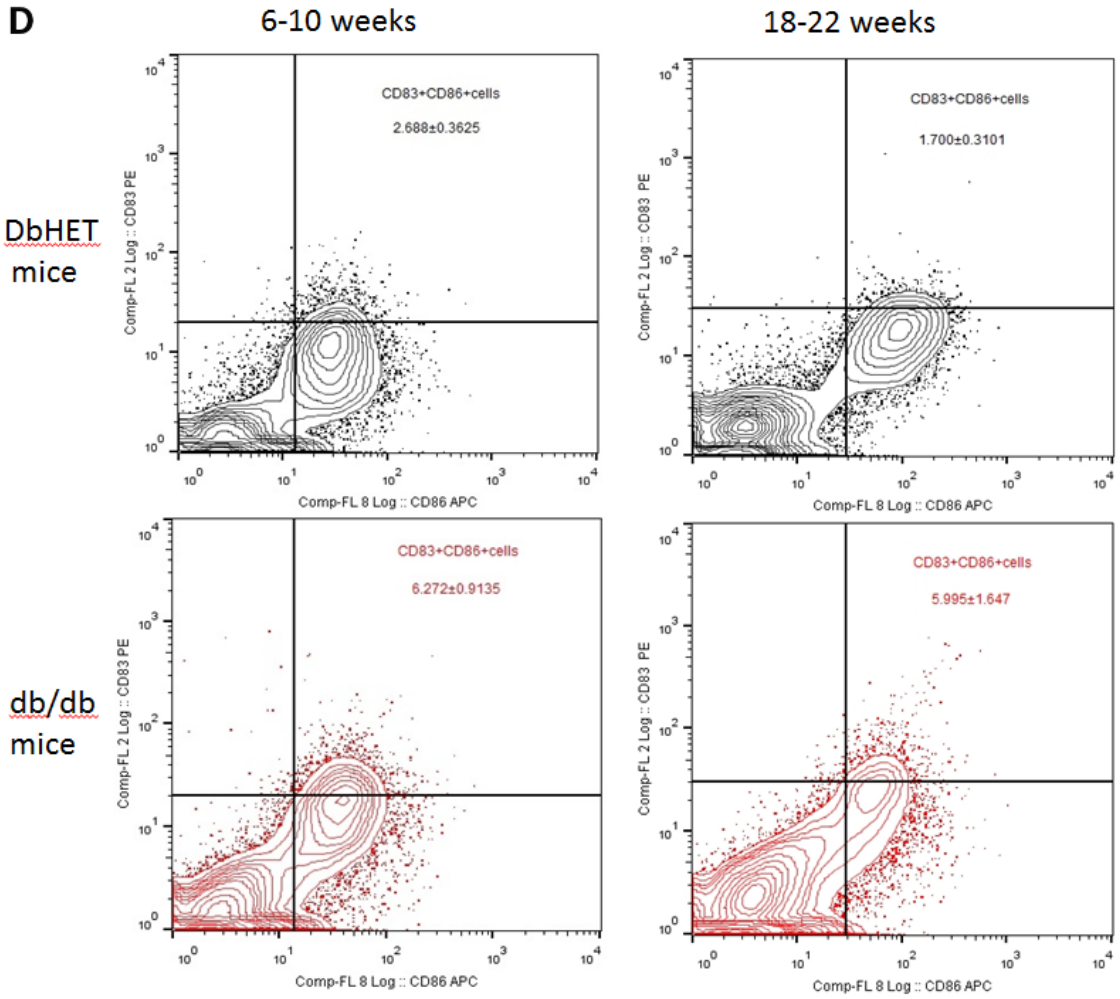

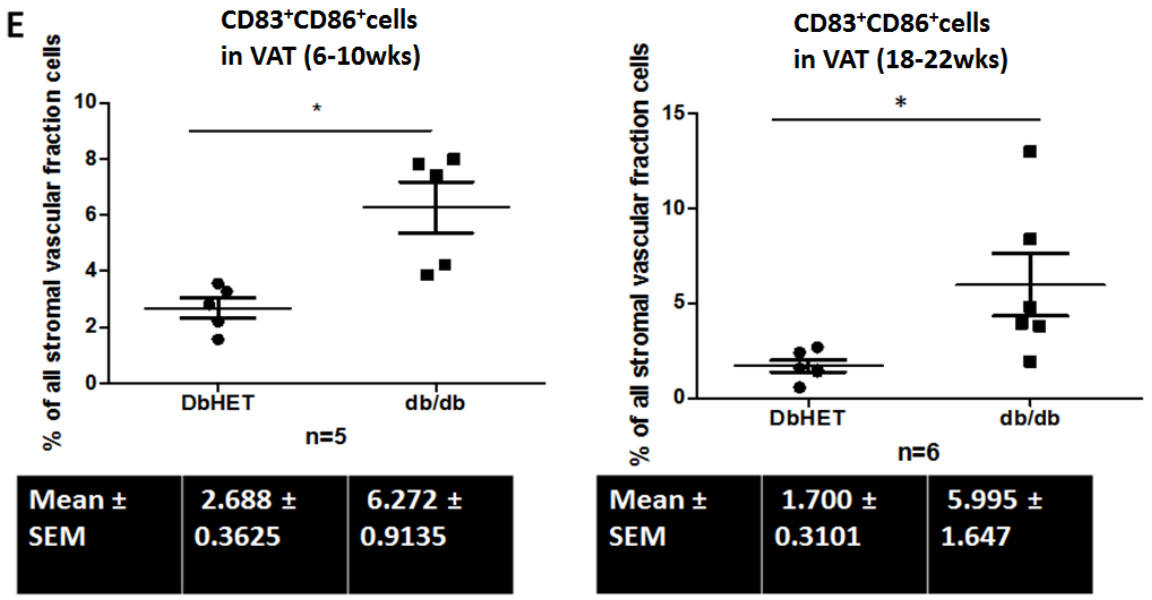

Figure. 2-4. Dendritic cells and M1 macrophages infiltrate into VAT in *db/db* mice at both 6-10 and 18-22 weeks. A: Identification of dendritic cells ($CD11c^+F4/80^-$ cells, in the left upper quadrant) and M1 macrophages ($CD11c^+F4/80^+$ cells, in the right upper quadrant) in flow cytometry analysis were shown. **B-C**: Dendritic cells and M1 macrophages were quantified as percentage of all stromal vascular fraction cells from VAT. No significant difference of $CD11c^+F4/80^-$ dendritic cells or $CD11c^+F4/80^+$ M1 macrophages was observed between 6-10 and 18-22 weeks in either DbHET or *db/db* mice. **D**: Identification of dendritic cells ($CD83^+CD86^+$ cells, in the right upper quadrant) in flow cytometry analysis was shown. **E**: Quantification of $CD83^+CD86^+$ dendritic cells as percentage of all stromal vascular fraction cells. There was no significant difference of $CD83^+CD86^+$ dendritic cells between 6-10 and 18-22 weeks in either DbHET and *db/db* mice. Data were shown in means ± SEM. * : $P <$ 0.05 between DbHET and *db/db* mice.

Immunohistochemical location of $CD11c^+$ cells in VAT

We next investigated the location of the $CD11c^+$ cell population within the adipose tissue by immunohistochemical examination in sections of VAT from *db/db* mice and DbHET control (6-10 and 18-22 week time-points). **Fig.2-5-A** depicts a bright field image for the membrane and shape of the adipocytes in VAT. In both DbHET and *db/db* mice, $CD11c^+$ cells were located within the stromal vascular fraction of VAT, between the adipocytes. To provide a quantitative measurement, the relative number of $CD11c^+$ cells was estimated by counting the number of positive signals (crown-like structure) and divided by the number of surrounding adipocytes in **Fig.2-5-B** (Hellmann, Tang et al. 2011, Zhang, Sugiyama et al. 2011). Consistent with our flow cytometry data, the immunohistochemical data showed that a greater number of $CD11c^+$ cells infiltrated into

VAT of *db/db* mice compared to that in DbHET controls; at both 6-10 and 18-22 weeks of age. Also consistent with the flow cytometry data, *db/db* mice at 6-10 weeks expressed similar numbers of $CD11c^+$ cells in VAT compared to *db/db* mice at 18-22 weeks. Similarly, there was no apparent difference in $CD11c^+$ cell numbers in VAT from DbHET mice between 6-10 and 18-22 weeks.

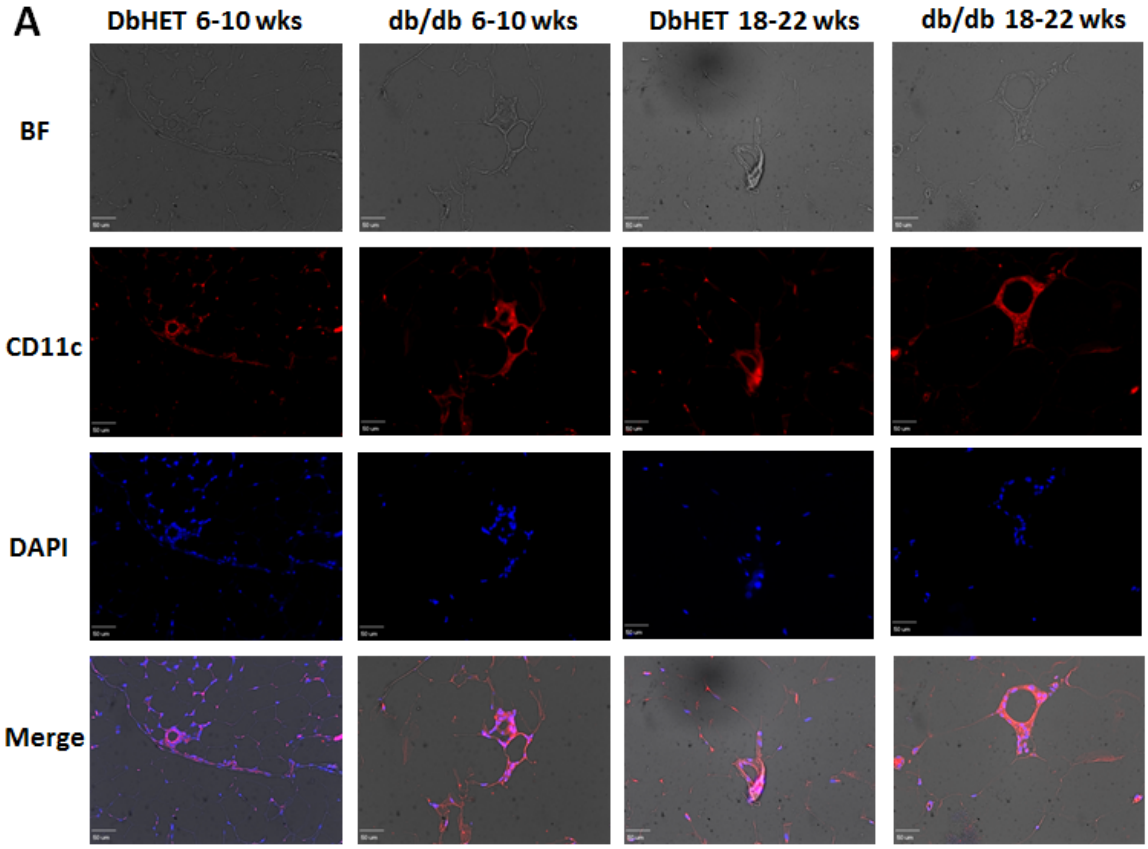

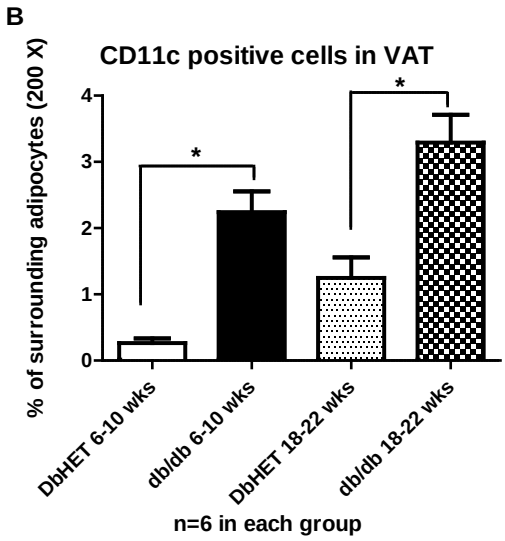

Figure 2-5. Distribution of CD11c+ cells in VAT of DbHET and *db/db* mice. A: Immunofluorescence staining of $CD11c^+$ cells in paraffin-embedded VAT sections from DbHET and *db/db* mice at both 6-10 and 18-22 weeks. BF = bright field vision of VAT. $CD11c^+$ cells were stained in Texas Red. Nuclei were stained in blue color (DAPI). Scale bar represented 50 μm. Sections from six mice were analyzed for each staining. **B**: Quantitative analysis of the extent of $CD11c^+$ cells infiltration into VAT. $CD11c^+$ cells were analyzed and plotted as the mean ± SEM from six independent experiments. n=6. There was no significant difference of $CD11c^+$ cells in VAT of *db/db* mice between 6-10 and 18-22 weeks. *: $P < 0.05$ between DbHET and *db/db* mice.

Effect of T2DM on Inflammatory cytokine mRNA expression in adipose tissue

Obesity is reported to be associated with altered adipokine production, which regulates systemic and local chronic inflammation (Wronkowitz, Romacho et al. 2014, Lastra and Manrique 2015). Since T2DM appears to share similar pathological process with obesity, it is conceivable that in diabetes, perivascular adipose tissue exhibits an inflammatory environment due to greater pro-inflammatory cytokine production together with diminished availability of anti-inflammatory mediators. In order to test this hypothesis, VAT and MAT were collected from *db/db* and DbHET mice at both 6-10 and 18-22 weeks of age. mRNA levels of pro-inflammatory cytokines TNF-α and IL-6, anti-inflammatory mediators adiponectin and IL-10, were subsequently detected by qPCR.

At both 6-10 and 18-22 weeks, a significant increase of TNF-α mRNA level was detected in VAT from *db/db* mice, compared to their respective DbHET controls (**Fig.2-6-A**). Moreover, *db/db* mice at 18-22 weeks expressed higher TNF-α mRNA level than *db/db* mice at 6-10 weeks. Similarly, IL-6 mRNA levels in VAT were increased in *db/db* mice at both 6-10 and 18-22 weeks, compared to DbHET controls. However, no significant change of IL-6 mRNA expression in VAT was detected in *db/db* mice between 6-10 and 18-22 weeks (**Fig.2-6-B**). As with anti-inflammatory mediator adiponectin mRNA expression, dramatically decreased levels were found in VAT from *db/db* mice, compared to DbHET mice at both age groups (**Fig. 2-6-C**). We did not, however, observe any significant change of adiponectin mRNA levels in VAT from *db/db* mice between 6-10 and 18-22 weeks of age. Unexpectedly, in contrast to adiponectin, we detected a significant increase of anti-inflammatory cytokine IL-10 mRNA level in VAT from *db/db* mice at 18-22 weeks compared to the DbHET control, whereas no significant change of IL-10 mRNA level was observed between *db/db* and DbHET mice at 6-10 weeks (**Fig.2-6-D**). In summary, VAT from diabetic mice shows increased mRNA expressions of pro-inflammatory cytokines TNF-α and IL-6, along with anti-inflammatory mediator IL-10. Conversely, a reduction of mRNA level of anti-inflammatory mediator adiponectin occurs in VAT from diabetic mice.

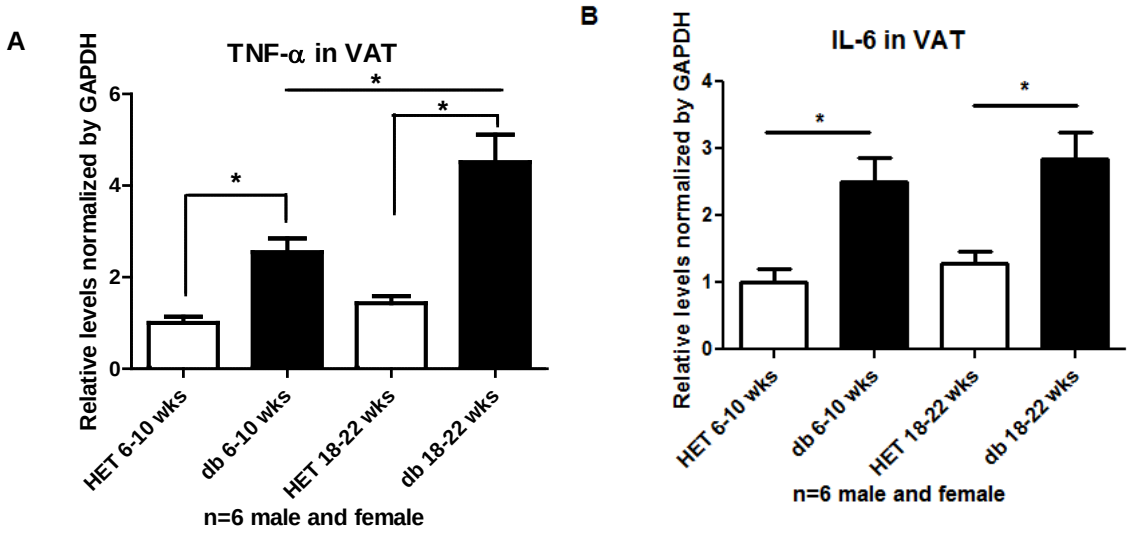

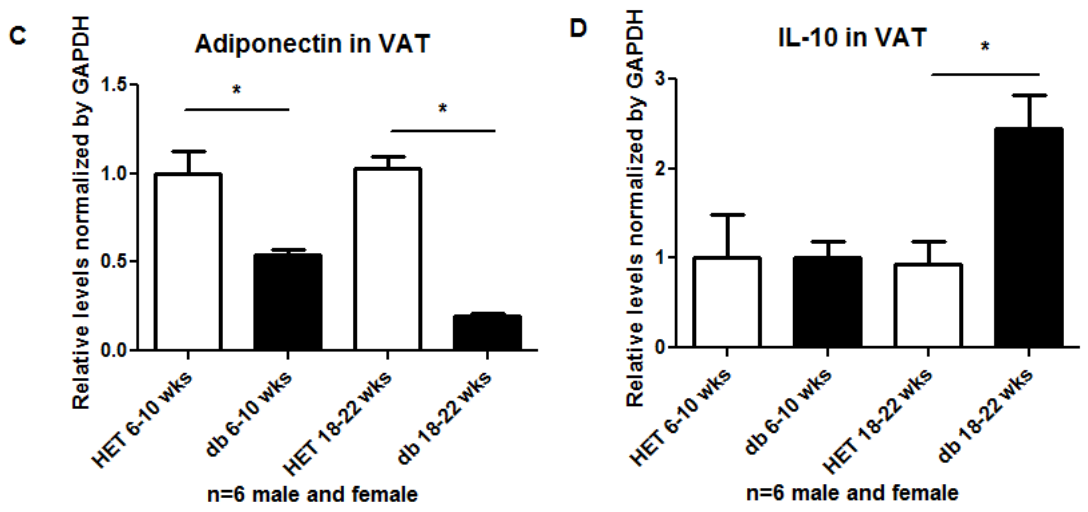

Figure 2-6. Gene expression of pro-inflammatory cytokines and anti-inflammatory mediators in VAT. A. Pro-inflammatory cytokine TNF-α mRNA levels of *db/db* and DbHET mice at both 6-10 and 18-22 weeks. **B**. Pro-inflammatory cytokine IL-6 mRNA levels of *db/db* and DbHET mice at both 6-10 and 18-22 weeks. **C**. Anti-inflammatory mediator adiponectin mRNA levels of *db/db* and DbHET mice at both 6-10 and 18-22 weeks. **D**. Anti-inflammatory mediator IL-10 mRNA levels of *db/db* and DbHET mice at both 6-10 and 18-22 weeks. Data were presented as the mean ± S.E.M. One way- ANOVA statistical analysis was performed. *: $P < 0.05$.

As shown in **Fig. 2-7-A**, a significantly increased level of TNF-α mRNA was found in MAT from *db/db* mice, compared to DbHET controls at 18-22 weeks. Additionally, *db/db* mice at 18-22 weeks had higher TNF-α mRNA level in MAT than *db/db* mice at 6-10 weeks, whereas no significant difference of TNF-α mRNA levels was observed between *db/db* and DbHET mice at 6-10 weeks. Similarly to VAT, increased IL-6 mRNA levels were found in MAT from *db/db* mice in comparison to DbHET controls at both age groups (**Fig. 2-7-B**). However, there was no significant difference of IL-6 expression in *db/db* mice between 6-10 and 18-22 weeks. Unexpectedly, no significant difference of adiponectin mRNA expression in MAT was observed between *db/db* and DbHET controls at 6-10 weeks. In contrast, in 18-22 weeks, *db/db* mice had significantly lower adiponectin mRNA levels in MAT than DbHET mice (**Fig. 2-7-C**). Interestingly, a significant higher IL-10 mRNA level was detected in *db/db* mice at 18-22 weeks, compared to their DbHET controls (**Fig. 2-7-D**). Meanwhile, *db/db* mice from 18-22 weeks had higher IL-10 mRNA expression in MAT than *db/db* mice from 6-10 weeks, whereas IL-10 mRNA expression was comparable between *db/db* and DbHET mice at 6-10 weeks. In summary, MAT from diabetic

mice have increased mRNA levels of pro-inflammatory cytokines TNF-α and IL-6, and fewer anti-inflammatory mediator adiponectin. Unexpectedly, anti-inflammatory cytokine IL-10 mRNA expression is elevated in MAT with the progression of T2DM.

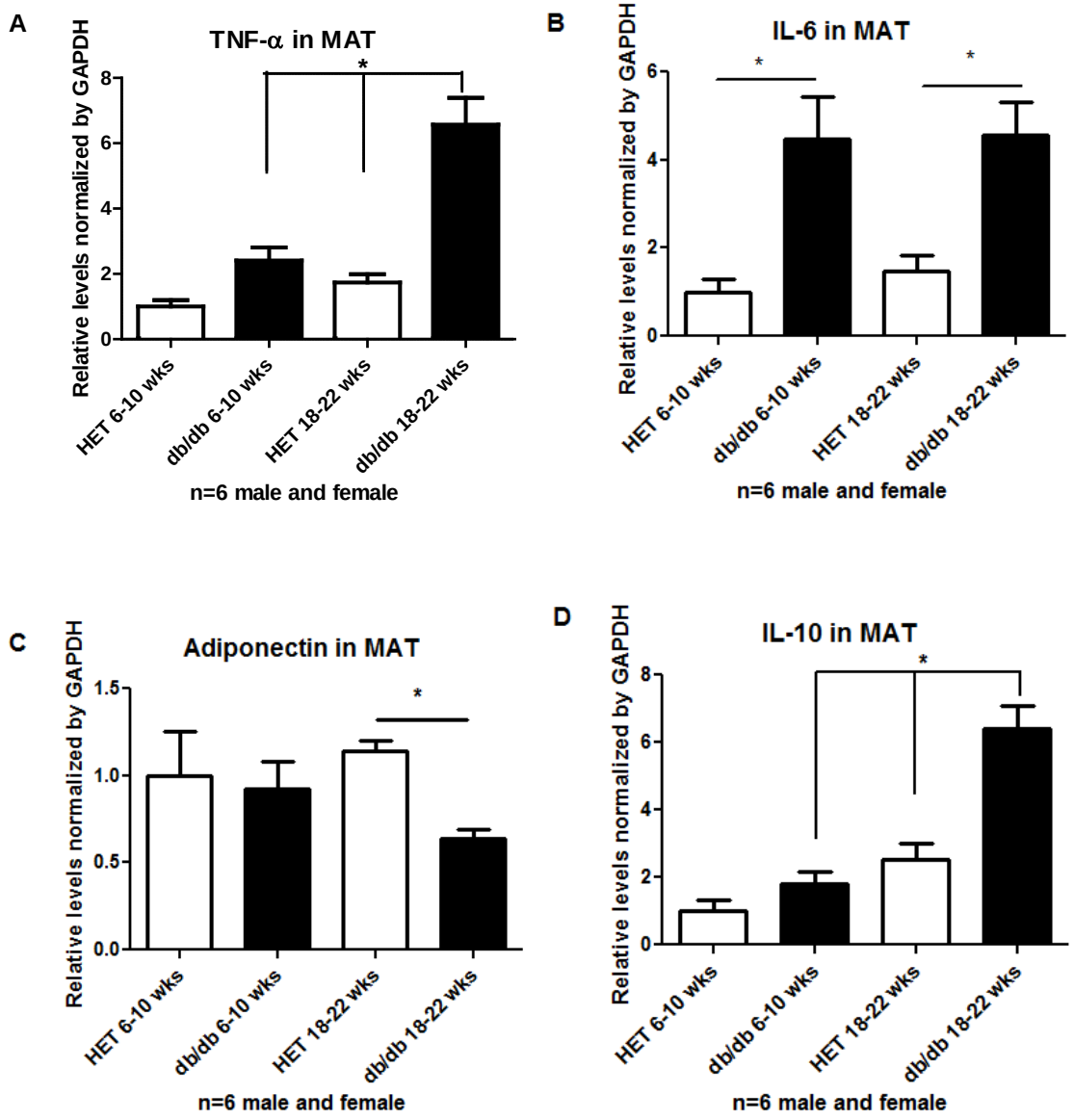

Figure 2-7. Gene expression of pro-inflammatory cytokines and anti-inflammatory mediators in MAT. A. Pro-inflammatory cytokine TNF-α gene expression of *db/db* and DbHET mice at both 6-10 and 18-22 weeks. **B**. Pro-inflammatory cytokine IL-6 gene expression of *db/db* and DbHET mice at both 6-10 and 18-22 weeks. **C**. Anti-inflammatory mediator adiponectin gene expression of *db/db* and DbHET mice at both 6-10 and 18-22 weeks. **D**. Anti-inflammatory mediator IL-10 gene expression of *db/db* and DbHET mice at both 6-10 and 18-22 weeks. Data were presented as the mean ± S.E.M. One way-ANOVA statistical analysis was performed. *: $P < 0.05$.

2.5. Discussion

The studies had three principal aims, the first being to identify whether $CD11c^+$ cells accumulated in the perivascular adipose tissue and/or in the vascular wall. The second aim was to determine whether more dendritic cells accumulated in perivascular adipose tissue over the duration of T2DM. The last aim was to examine whether a chronic state of inflammation was evident in perivascular adipose tissue and whether this was affected by the duration of T2DM. Our data indicate that $CD11c^+$ cells accumulate in perivascular adipose tissue rather than in the vascular wall. Further, a greater number of M1 macrophages and dendritic cells accumulate in VAT of diabetic mice compared to their normoglycemic, non-obese controls. Associated with this is an increased production of perivascular adipose tissue pro-inflammatory cytokines and decreased production of anti-inflammatory mediators found in T2DM animals.

Consistent with previous studies, *db/db* mice were much heavier than their heterozygote controls and this was accompanied by a large expansion of VAT and perivascular adipose tissues. With the progression of T2DM, total body weight and the expansion of adipose tissue remained constant, consistent with other reports (Koya, Haneda et al. 2000, Martinez-Botas, Anderson et al. 2000). In agreement with other findings, *db/db* mice exhibited significantly higher non-fasting glucose levels compared to DbHET mice, indicating that *db/db* mice qualified as a T2DM murine model in the current study (Koya, Haneda et al. 2000, Xie, Zhou et al. 2002).

Dendritic cells have been identified to cluster with T lymphocytes in atherosclerotic lesions of thoracic aorta at the early stage of atherosclerosis and are believed to promote plaque destabilization in murine models (Bobryshev 2005, Niessner, Sato et al. 2006). Moreover, M1 macrophages have also been reported to infiltrate into atherosclerotic plaques of murine aorta roots and human coronary arteries to promote plaque rupture in high fat diet models (Libby, Geng et al. 1996, Xu, Shah et al. 2001). Since $CD11c^+$ cells are primarily composed of dendritic cells and M1 macrophages, it is possible that $CD11c^+$ cells resident in the vasculature play a critical role in the pathological development of atherosclerosis. However, in the pathogenesis of obesity and T2DM, M1 macrophages accumulated in adipose tissue and activated the inflammatory

response, potentiating the development of chronic inflammation as well as insulin resistance in obese mice (Weisberg, McCann et al. 2003, Boutens and Stienstra 2016). It is acknowledged that atherosclerosis and diabetes share a similar pathological process related to chronic low grade inflammation (Beckman, Creager et al. 2002, Mangge, Schauenstein et al. 2004). It is possible that $CD11c^+$ cells could accumulate in either the vasculature or perivascular adipose tissue during the development of T2DM, but so far has not been studied. Thus, in the current study, both different vasculatures and corresponding perivascular adipose tissues along with VAT were collected to examine their CD11c mRNA expressions. Our qPCR data showed that extremely low CD11c mRNA levels were found on multiple types of blood vessels from both diabetic and heterozygous control mice, compared to a control mouse spleen calibrator. There was no significant difference of CD11c mRNA expression between diabetic and control mice. In contrast, much higher levels of CD11c mRNA expression, compared to the same calibrator, were detected in all collected perivascular adipose tissues as well as VAT from both diabetic and control mice. Diabetic mice had higher CD11c mRNA levels on adipose tissue than non-diabetic mice at all the four age groups. Our study is the first to compare the amount of CD11c mRNA expression between vasculature and perivascular adipose tissues over time in a murine T2DM model. Our data showed that the majority of $CD11c^+$ cells are resident in perivascular adipose tissue instead of the vasculature itself. With the development of T2DM, more $CD11c^+$ cells accumulated in perivascular adipose tissue from diabetic mice than control mice.

Our flow cytometry data indicated that both dendritic cells ($CD11c^+F4/80^-$ cells, $CD83^+CD86^+$ cells) and M1 macrophages ($CD11c^+F4/80^+$ cells) were elevated in VAT of diabetic mice than control mice in either 6-10 or 18-22 weeks. There was no significant increment of dendritic cells or M1 macrophages accumulation in VAT in the duration of T2DM. Those results implicated that $CD11c^+$ cells participated in the pathological process of T2DM at both early (6-10 weeks) and late (18-22 weeks) stages and the amount of $CD11c^+$ cells remained constant during the development of T2DM. However, these data were inconsistent with previous qPCR results, which showed an increment of CD11c mRNA expression in VAT and MAT over the duration of T2DM. It is possibly due to the increasing apoptosis of $CD11c^+$ cells in adipose tissue of T2DM, which in turn

stimulates more gene expression of $CD11c^+$ cells, as reflected by the increase of CD11c mRNA levels. It has been demonstrated that not only adipocytes undergo apoptosis in obese mice, but also T lymphocytes were prone to apoptosis in leptin-deficient obese mice, *db/db* mice (Fujita, Murakami et al. 2002, Fantuzzi 2005). Leptin, secreted from adipocytes, has been showed to protect macrophages, B and T lymphocytes from apoptosis and regulate the immune response in adipose tissue (Matarese, Moschos et al. 2005, Lolmede, Zakaroff-Girard et al. 2015). It is believed that in leptin-deficient obese mice, *db/db* mice, this suppression of apoptosis was eliminated. It is possible that the absence of increment of $CD11c^+$ cells in the duration of T2DM, detected by flow cytometry measurement, is due to the increasing apoptosis of infiltrated $CD11c^+$ cells in the adipose tissue from leptin-deficient mice.

Recently, evidence supports the concept that adipose tissue is an immunological organ involved in multiple aspects of hemostasis regulation (Huh, Park et al. 2014). Obesity has been reported to be associated with prominent inflammation in adipose tissue with infiltration of various immune cells, such as macrophages, neutrophils, mast cells, B and T lymphocytes (Seijkens, Kusters et al. 2014). The accumulation of those immune cells in obese adipose tissue has been reported to be responsible for high levels of pro-inflammatory factors including TNF-α, IFN-γ and IL-6, and low levels of anti-inflammatory mediators including IL-10 and IL-4 (Grant and Dixit 2015). However, little literature is available to show the alteration of those inflammatory markers in adipose tissue during the pathological process of T2DM. Here, in our study, we tried to reveal that alteration by measuring TNF-α, IL-6, adiponectin and IL-10 m RNA levels in different adipose tissues from both early (6-10 weeks) and late (18-22 weeks) stages of T2DM. Our qPCR data showed that in VAT and MAT, TNF-α mRNA levels were increased with the pathological progression of T2DM. Additionally, IL-6 mRNA levels were increased in VAT and MAT from diabetic mice, compared to control mice. However, there was no increment of IL-6 mRNA levels in the different age groups of diabetic mice. Collectively, more pro-inflammatory cytokines, TNF-α and IL-6 were produced in VAT and MAT from diabetic mice. This data were consistent with other reports, which revealed that circulating levels of TNF-α and IL-6 were elevated in T2DM patients and associated with insulin resistance development (Pedersen, Bruunsgaard et al. 2003, Mirza,

Hossain et al. 2012). As for the anti-inflammatory cytokine adiponectin, decreasing mRNA level was detected in VAT from diabetic mice at both age groups. However, decreasing mRNA levels of adiponectin in MAT were only detected in diabetic mice in the late stage of T2DM. This data is still consistent with other findings (Hotta, Funahashi et al. 2000, Hotta, Funahashi et al. 2001, Li, Shin et al. 2009). Unexpectedly, increasing mRNA levels of anti-inflammatory mediator IL-10 were found in both VAT and MAT of diabetic mice. Also, IL-10 mRNA level in MAT was increased in all age groups of diabetic mice. This result was still consistent with other findings, which showed that circulating IL-10 plasma levels were increased in overweight and obese chimpanzees (Nehete, Magden et al. 2014). Since IL-10 is considered as a classic anti-inflammatory cytokine that improves insulin sensitivity (Straczkowski, Kowalska et al. 2005), Esposito et al. has proposed that this elevation of IL-10 level in obese individuals was a compensatory response in order to suppress the increase of pro-inflammatory cytokine production (Esposito, Pontillo et al. 2003). Experiments from Esposito et al. also demonstrated that 1 year of physical activity plus body weight loss significantly reduced circulating IL-10 levels in obese objects (Esposito, Pontillo et al. 2003). Those findings supported our suggestion that the increase of IL-10 mRNA levels in VAT and MAT was due to the compensatory response to the progressive development of inflammation triggered by T2DM. Taken together, this imbalance production of pro-inflammatory factors and anti-inflammatory mediators in perivascular adipose tissue contributes to the local low-grade inflammation caused by T2DM (Zhang, Potter et al. 2011).

In conclusion, our data provide distinct insights into T2DM development, including $CD11c^{+}$ cells accumulation and chronic inflammation formation in perivascular adipose tissue. However, we still do not know the relationship between these two events in the development of T2DM. Since it has already been established that accumulation of M1 macrophages is responsible for this chronic inflammation in diabetic adipose tissue (Weisberg, McCann et al. 2003, Lumeng, Bodzin et al. 2007), it is possible that dendritic cells would also participate in the chronic inflammation of T2DM perivascular adipose tissue, which is one of the aims in the next chapter.

2.6. REFERENCES

Al-Mutairi, N. and D. Shabaan (2016). "Effects of tumor necrosis factor alpha inhibitors extend beyond psoriasis: insulin sensitivity in psoriasis patients with type 2 diabetes mellitus." Cutis **97**(3): 235-241.

Almuraikhy, S., W. Kafienah, M. Bashah, I. Diboun, M. Jaganjac, F. Al-Khelaifi, H. Abdesselem, N. A. Mazloum, M. Alsayrafi, V. Mohamed-Ali and M. A. Elrayess (2016). "Interleukin-6 induces impairment in human subcutaneous adipogenesis in obesity-associated insulin resistance." Diabetologia.

Beckman, J. A., M. A. Creager and P. Libby (2002). "Diabetes and atherosclerosis: epidemiology, pathophysiology, and management." Jama **287**(19): 2570-2581.

Bobryshev, Y. V. (2005). "Dendritic cells in atherosclerosis: current status of the problem and clinical relevance." European Heart Journal **26**(17): 1700-1704.

Boutens, L. and R. Stienstra (2016). "Adipose tissue macrophages: going off track during obesity." Diabetologia **59**(5): 879-894.

Chamberlain, J. J., A. S. Rhinehart, C. F. Shaefer, Jr. and A. Neuman (2016). "Diagnosis and Management of Diabetes: Synopsis of the 2016 American Diabetes Association Standards of Medical Care in Diabetes." Ann Intern Med **164**(8): 542-552.

Chistiakov, D. A., I. A. Sobenin, A. N. Orekhov and Y. V. Bobryshev (2015). "Myeloid dendritic cells: Development, functions, and role in atherosclerotic inflammation." Immunobiology.

Curat, C., V. Wegner, C. Sengenes, A. Miranville, C. Tonus, R. Busse and A. Bouloumie (2006). "Macrophages in human visceral adipose tissue: increased accumulation in obesity and a source of resistin and visfatin." Diabetologia **49**(4): 744-747.

Dandona, P., A. Aljada and A. Bandyopadhyay (2004). "Inflammation: the link between insulin resistance, obesity and diabetes." Trends in immunology **25**(1): 4-7.

Daniele, G., R. Guardado Mendoza, D. Winnier, T. V. Fiorentino, Z. Pengou, J. Cornell, F. Andreozzi, C. Jenkinson, E. Cersosimo, M. Federici, D. Tripathy and F. Folli (2014). "The inflammatory status score including IL-6, TNF-alpha, osteopontin, fractalkine, MCP-1 and

adiponectin underlies whole-body insulin resistance and hyperglycemia in type 2 diabetes mellitus." Acta Diabetol **51**(1): 123-131.

DeFuria, J., A. C. Belkina, M. Jagannathan-Bogdan, J. Snyder-Cappione, J. D. Carr, Y. R. Nersesova, D. Markham, K. J. Strissel, A. A. Watkins, M. Zhu, J. Allen, J. Bouchard, G. Toraldo, R. Jasuja, M. S. Obin, M. E. McDonnell, C. Apovian, G. V. Denis and B. S. Nikolajczyk (2013). "B cells promote inflammation in obesity and type 2 diabetes through regulation of T-cell function and an inflammatory cytokine profile." Proc Natl Acad Sci U S A **110**(13): 5133-5138.

Esposito, K., A. Pontillo, C. Di Palo, G. Giugliano, M. Masella, R. Marfella and D. Giugliano (2003). "Effect of weight loss and lifestyle changes on vascular inflammatory markers in obese women: a randomized trial." Jama **289**(14): 1799-1804.

Fantuzzi, G. (2005). "Adipose tissue, adipokines, and inflammation." Journal of Allergy and Clinical Immunology **115**(5): 911-919.

Ferreira, M. A., D. M. Silva, A. C. de Morais, Jr., J. F. Mota and P. B. Botelho (2016). "Therapeutic potential of green tea on risk factors for type 2 diabetes in obese adults - a review."

Flegal, K. M., M. D. Carroll, B. K. Kit and C. L. Ogden (2012). "Prevalence of obesity and trends in the distribution of body mass index among US adults, 1999-2010." Jama **307**(5): 491-497.

Franco Nitta, C. (2013). "Crosstalk between adipocytes and immune cells in adipose tissue in an obese inflammatory state: role of contact-mediated signaling."

Fujita, Y., M. Murakami, Y. Ogawa, H. Masuzaki, M. Tanaka, S. Ozaki, K. Nakao and T. Mimori (2002). "Leptin inhibits stress-induced apoptosis of T lymphocytes." Clinical & Experimental Immunology **128**(1): 21-26.

Gao, Y. J. (2007). "Dual modulation of vascular function by perivascular adipose tissue and its potential correlation with adiposity/lipoatrophy-related vascular dysfunction." Curr Pharm Des **13**(21): 2185-2192.

Genser, L., J. R. Casella Mariolo, L. Castagneto-Gissey, S. Panagiotopoulos and F. Rubino (2016). "Obesity, Type 2 Diabetes, and the Metabolic Syndrome: Pathophysiologic Relationships and Guidelines for Surgical Intervention." Surg Clin North Am **96**(4): 681-701.

Grant, R., Y. H. Youm, A. Ravussin and V. D. Dixit (2013). "Quantification of adipose tissue leukocytosis in obesity." Methods Mol Biol **1040**: 195-209.

Grant, R. W. and V. D. Dixit (2015). "Adipose tissue as an immunological organ." Obesity **23**(3): 512-518.

Hellmann, J., Y. Tang, M. Kosuri, A. Bhatnagar and M. Spite (2011). "Resolvin D1 decreases adipose tissue macrophage accumulation and improves insulin sensitivity in obese-diabetic mice." The FASEB Journal **25**(7): 2399-2407.

Hotta, K., T. Funahashi, Y. Arita, M. Takahashi, M. Matsuda, Y. Okamoto, H. Iwahashi, H. Kuriyama, N. Ouchi and K. Maeda (2000). "Plasma concentrations of a novel, adipose-specific protein, adiponectin, in type 2 diabetic patients." Arteriosclerosis, thrombosis, and vascular biology **20**(6): 1595-1599.

Hotta, K., T. Funahashi, N. L. Bodkin, H. K. Ortmeyer, Y. Arita, B. C. Hansen and Y. Matsuzawa (2001). "Circulating concentrations of the adipocyte protein adiponectin are decreased in parallel with reduced insulin sensitivity during the progression to type 2 diabetes in rhesus monkeys." Diabetes **50**(5): 1126-1133.

Huh, J. Y., Y. J. Park, M. Ham and J. B. Kim (2014). "Crosstalk between adipocytes and immune cells in adipose tissue inflammation and metabolic dysregulation in obesity." Mol Cells **37**(5): 365-371.

Kadowaki, T., T. Yamauchi, N. Kubota, K. Hara, K. Ueki and K. Tobe (2006). "Adiponectin and adiponectin receptors in insulin resistance, diabetes, and the metabolic syndrome." The Journal of clinical investigation **116**(7): 1784-1792.

Kahn, S. E., R. L. Hull and K. M. Utzschneider (2006). "Mechanisms linking obesity to insulin resistance and type 2 diabetes." Nature **444**(7121): 840-846.

Kassim, S. H., N. K. Rajasagi, X. Zhao, R. Chervenak and S. R. Jennings (2006). "In vivo ablation of CD11c-positive dendritic cells increases susceptibility to herpes simplex virus type 1 infection and diminishes NK and T-cell responses." J Virol **80**(8): 3985-3993.

Kato, H., H. Kashiwagi, M. Shiraga, S. Tadokoro, T. Kamae, H. Ujiie, S. Honda, S. Miyata, Y. Ijiri and J. Yamamoto (2006). "Adiponectin acts as an endogenous antithrombotic factor." Arteriosclerosis, thrombosis, and vascular biology **26**(1): 224-230.

Kosteli, A., E. Sugaru, G. Haemmerle, J. F. Martin, J. Lei, R. Zechner and A. W. Ferrante, Jr. (2010). "Weight loss and lipolysis promote a dynamic immune response in murine adipose tissue." J Clin Invest **120**(10): 3466-3479.

Koya, D., M. Haneda, H. Nakagawa, K. Isshiki, H. Sato, S. Maeda, T. Sugimoto, H. Yasuda, A. Kashiwagi, D. K. Ways, G. L. King and R. Kikkawa (2000). "Amelioration of accelerated diabetic mesangial expansion by treatment with a PKC beta inhibitor in diabetic db/db mice, a rodent model for type 2 diabetes." Faseb j **14**(3): 439-447.

Kraakman, M. J., A. J. Murphy, K. Jandeleit-Dahm and H. L. Kammoun (2014). "Macrophage polarization in obesity and type 2 diabetes: weighing down our understanding of macrophage function?" Front Immunol **5**: 470.

Lastra, G. and C. Manrique (2015). "Perivascular adipose tissue, inflammation and insulin resistance: link to vascular dysfunction and cardiovascular disease." Hormone molecular biology and clinical investigation **22**(1): 19-26.

Li, P., M. Lu, M. T. Nguyen, E. J. Bae, J. Chapman, D. Feng, M. Hawkins, J. E. Pessin, D. D. Sears, A. K. Nguyen, A. Amidi, S. M. Watkins, U. Nguyen and J. M. Olefsky (2010). "Functional heterogeneity of CD11c-positive adipose tissue macrophages in diet-induced obese mice." J Biol Chem **285**(20): 15333-15345.

Libby, P., Y. J. Geng, M. Aikawa, U. Schoenbeck, F. Mach, S. K. Clinton, G. K. Sukhova and R. T. Lee (1996). "Macrophages and atherosclerotic plaque stability." Current opinion in lipidology **7**(5): 330-335.

Liu, C., X. Feng, Q. Li, Y. Wang, Q. Li and M. Hua (2016). "Adiponectin, TNF-alpha and inflammatory cytokines and risk of type 2 diabetes: A systematic review and meta-analysis." Cytokine **86**: 100-109.

Lolmede, K., A. Zakaroff-Girard, C. Dray, M. L. Renoud, D. Daviaud, R. Burcelin, M. Lafontan, J. Galitzky and A. Bouloumie (2015). "Interrelationship between lymphocytes and leptin in fat depots of obese mice revealed by changes in nutritional status." J Physiol Biochem.

Lumeng, C. N., J. L. Bodzin and A. R. Saltiel (2007). "Obesity induces a phenotypic switch in adipose tissue macrophage polarization." The Journal of clinical investigation **117**(1): 175-184.

Mangge, H., K. Schauenstein, L. Stroedter, A. Griesl, W. Maerz and M. Borkenstein (2004). "Low grade inflammation in juvenile obesity and type 1 diabetes associated with early signs of atherosclerosis." Experimental and clinical endocrinology & diabetes: official journal, German Society of Endocrinology [and] German Diabetes Association **112**(7): 378-382.

Martinez-Botas, J., J. B. Anderson, D. Tessier, A. Lapillonne, B. H. Chang, M. J. Quast, D. Gorenstein, K. H. Chen and L. Chan (2000). "Absence of perilipin results in leanness and reverses obesity in Lepr(db/db) mice." Nat Genet **26**(4): 474-479.

Matarese, G., S. Moschos and C. S. Mantzoros (2005). "Leptin in immunology." The Journal of Immunology **174**(6): 3137-3142.

McArdle, S., Z. Mikulski and K. Ley (2016). "Live cell imaging to understand monocyte, macrophage, and dendritic cell function in atherosclerosis." J Exp Med **213**(7): 1117-1131.

Mirza, S., M. Hossain, C. Mathews, P. Martinez, P. Pino, J. L. Gay, A. Rentfro, J. B. McCormick and S. P. Fisher-Hoch (2012). "Type 2-diabetes is associated with elevated levels of TNF-alpha, IL-6 and adiponectin and low levels of leptin in a population of Mexican Americans: A cross-sectional study." Cytokine **57**(1): 136-142.

Nehete, P., E. R. Magden, B. Nehete, P. W. Hanley and C. R. Abee (2014). "Obesity related alterations in plasma cytokines and metabolic hormones in chimpanzees." International journal of inflammation **2014**.

Ng, M., T. Fleming, M. Robinson, B. Thomson, N. Graetz, C. Margono, E. C. Mullany, S. Biryukov, C. Abbafati, S. F. Abera, J. P. Abraham, N. M. Abu-Rmeileh, T. Achoki, F. S.

AlBuhairan, Z. A. Alemu, R. Alfonso, M. K. Ali, R. Ali, N. A. Guzman, W. Ammar, P. Anwari, A. Banerjee, S. Barquera, S. Basu, D. A. Bennett, Z. Bhutta, J. Blore, N. Cabral, I. C. Nonato, J. C. Chang, R. Chowdhury, K. J. Courville, M. H. Criqui, D. K. Cundiff, K. C. Dabhadkar, L. Dandona, A. Davis, A. Dayama, S. D. Dharmaratne, E. L. Ding, A. M. Durrani, A. Esteghamati, F. Farzadfar, D. F. Fay, V. L. Feigin, A. Flaxman, M. H. Forouzanfar, A. Goto, M. A. Green, R. Gupta, N. Hafezi-Nejad, G. J. Hankey, H. C. Harewood, R. Havmoeller, S. Hay, L. Hernandez, A. Husseini, B. T. Idrisov, N. Ikeda, F. Islami, E. Jahangir, S. K. Jassal, S. H. Jee, M. Jeffreys, J. B. Jonas, E. K. Kabagambe, S. E. Khalifa, A. P. Kengne, Y. S. Khader, Y. H. Khang, D. Kim, R. W. Kimokoti, J. M. Kinge, Y. Kokubo, S. Kosen, G. Kwan, T. Lai, M. Leinsalu, Y. Li, X. Liang, S. Liu, G. Logroscino, P. A. Lotufo, Y. Lu, J. Ma, N. K. Mainoo, G. A. Mensah, T. R. Merriman, A. H. Mokdad, J. Moschandreas, M. Naghavi, A. Naheed, D. Nand, K. M. Narayan, E. L. Nelson, M. L. Neuhouser, M. I. Nisar, T. Ohkubo, S. O. Oti, A. Pedroza, D. Prabhakaran, N. Roy, U. Sampson, H. Seo, S. G. Sepanlou, K. Shibuya, R. Shiri, I. Shiue, G. M. Singh, J. A. Singh, V. Skirbekk, N. J. Stapelberg, L. Sturua, B. L. Sykes, M. Tobias, B. X. Tran, L. Trasande, H. Toyoshima, S. van de Vijver, T. J. Vasankari, J. L. Veerman, G. Velasquez-Melendez, V. V. Vlassov, S. E. Vollset, T. Vos, C. Wang, X. Wang, E. Weiderpass, A. Werdecker, J. L. Wright, Y. C. Yang, H. Yatsuya, J. Yoon, S. J. Yoon, Y. Zhao, M. Zhou, S. Zhu, A. D. Lopez, C. J. Murray and E. Gakidou (2014). "Global, regional, and national prevalence of overweight and obesity in children and adults during 1980-2013: a systematic analysis for the Global Burden of Disease Study 2013." Lancet **384**(9945): 766-781.

Nguyen, D. M. and H. B. El-Serag (2010). "The epidemiology of obesity." Gastroenterol Clin North Am **39**(1): 1-7.

Niessner, A., K. Sato, E. L. Chaikof, I. Colmegna, J. J. Goronzy and C. M. Weyand (2006). "Pathogen-sensing plasmacytoid dendritic cells stimulate cytotoxic T-cell function in the atherosclerotic plaque through interferon-α." Circulation **114**(23): 2482-2489.

Nishimura, S., I. Manabe, M. Nagasaki, K. Eto, H. Yamashita, M. Ohsugi, M. Otsu, K. Hara, K. Ueki and S. Sugiura (2009). "$CD8^+$ effector T cells contribute to macrophage recruitment and adipose tissue inflammation in obesity." Nature medicine **15**(8): 914-920.

Patsouris, D., P.-P. Li, D. Thapar, J. Chapman, J. M. Olefsky and J. G. Neels (2008). "Ablation of CD11c-positive cells normalizes insulin sensitivity in obese insulin resistant animals." Cell metabolism **8**(4): 301-309.

Pedersen, M., H. Bruunsgaard, N. Weis, H. W. Hendel, B. U. Andreassen, E. Eldrup, F. Dela and B. K. Pedersen (2003). "Circulating levels of TNF-alpha and IL-6-relation to truncal fat mass and muscle mass in healthy elderly individuals and in patients with type-2 diabetes." Mechanisms of Ageing and Development **124**(4): 495-502.

Pfaffl, M. W. (2001). "A new mathematical model for relative quantification in real-time RT-PCR." Nucleic Acids Res **29**(9): e45.

Pillarisetty, V. G., A. B. Shah, G. Miller, J. I. Bleier and R. P. DeMatteo (2004). "Liver dendritic cells are less immunogenic than spleen dendritic cells because of differences in subtype composition." J Immunol **172**(2): 1009-1017.

Pina, T., S. Armesto, R. Lopez-Mejias, F. Genre, B. Ubilla, M. A. Gonzalez-Lopez, M. C. Gonzalez-Vela, A. Corrales, R. Blanco, M. T. Garcia-Unzueta, J. L. Hernandez, J. Llorca and M. A. Gonzalez-Gay (2015). "Anti-TNF-alpha therapy improves insulin sensitivity in non-diabetic patients with psoriasis: a 6-month prospective study." J Eur Acad Dermatol Venereol **29**(7): 1325-1330.

Rombouts, M., R. Ammi, I. Van Brussel, L. Roth, B. Y. De Winter, S. R. Vercauteren, J. M. Hendriks, P. Lauwers, P. E. Van Schil, G. R. De Meyer, E. Fransen, N. Cools and D. M. Schrijvers (2016). "Linking CD11b ($^{+}$) Dendritic Cells and Natural Killer T Cells to Plaque Inflammation in Atherosclerosis." Mediators Inflamm **2016**: 6467375.

Schulz, O., E. Jaensson, E. K. Persson, X. Liu, T. Worbs, W. W. Agace and O. Pabst (2009). "Intestinal CD103^{+}, but not CX3CR1^{+}, antigen sampling cells migrate in lymph and serve classical dendritic cell functions." J Exp Med **206**(13): 3101-3114.

Seijkens, T., P. Kusters, A. Chatzigeorgiou, T. Chavakis and E. Lutgens (2014). "Immune cell crosstalk in obesity: a key role for costimulation?" Diabetes **63**(12): 3982-3991.

Shaikh, S., K. Haas, M. Beck and H. Teague (2015). "The effects of diet-induced obesity on B cell function." Clinical & Experimental Immunology **179**(1): 90-99.

Shi, J. Q., W. Shen, J. Chen, B. R. Wang, L. L. Zhong, Y. W. Zhu, H. Q. Zhu, Q. Q. Zhang, Y. D. Zhang and J. Xu (2011). "Anti-TNF-alpha reduces amyloid plaques and tau phosphorylation and induces CD11c-positive dendritic-like cell in the APP/PS1 transgenic mouse brains." Brain Res **1368**: 239-247.

Stefanovic-Racic, M., X. Yang, M. S. Turner, B. S. Mantell, D. B. Stolz, T. L. Sumpter, I. J. Sipula, N. Dedousis, D. K. Scott and P. A. Morel (2012). "Dendritic cells promote macrophage infiltration and comprise a substantial proportion of obesity-associated increases in $CD11c^+$ cells in adipose tissue and liver." Diabetes **61**(9): 2330-2339.

Straczkowski, M., I. Kowalska, A. Nikolajuk, A. Krukowska and M. Gorska (2005). "Plasma Interleukin-10 Concentration Is Positively Related to Insulin Sensitivity in Young Healthy Individuals." Diabetes Care **28**(8): 2036-2037.

Sundara Rajan, S. and M. P. Longhi (2016). "Dendritic cells and adipose tissue." Immunology.

Szasz, T., G. F. Bomfim and R. C. Webb (2013). "The influence of perivascular adipose tissue on vascular homeostasis." Vasc Health Risk Manag **9**: 105-116.

Uysal, K. T., S. M. Wiesbrock, M. W. Marino and G. S. Hotamisligil (1997). "Protection from obesity-induced insulin resistance in mice lacking TNF-α function." Nature **389**(6651): 610-614.

Van Brussel, I., R. Ammi, M. Rombouts, N. Cools, S. R. Vercauteren, D. De Roover, J. M. Hendriks, P. Lauwers, P. E. Van Schil and D. M. Schrijvers (2015). "Fluorescent activated cell sorting: an effective approach to study dendritic cell subsets in human atherosclerotic plaques." J Immunol Methods **417**: 76-85.

Weisberg, S. P., D. McCann, M. Desai, M. Rosenbaum, R. L. Leibel and A. W. Ferrante (2003). "Obesity is associated with macrophage accumulation in adipose tissue." The Journal of clinical investigation **112**(12): 1796-1808.

Wentworth, J. M., G. Naselli, W. A. Brown, L. Doyle, B. Phipson, G. K. Smyth, M. Wabitsch, P. E. O'Brien and L. C. Harrison (2010). "Pro-inflammatory $CD11c^+CD206^+$ adipose tissue macrophages are associated with insulin resistance in human obesity." Diabetes **59**(7): 1648-1656.

Wronkowitz, N., T. Romacho, H. Sell and J. Eckel (2014). "Adipose tissue dysfunction and inflammation in cardiovascular disease." Front Horm Res **43**: 79-92.

Wu, H., S. Ghosh, X. D. Perrard, L. Feng, G. E. Garcia, J. L. Perrard, J. F. Sweeney, L. E. Peterson, L. Chan, C. W. Smith and C. M. Ballantyne (2007). "T-cell accumulation and regulated on activation, normal T cell expressed and secreted upregulation in adipose tissue in obesity." Circulation **115**(8): 1029-1038.

Xie, J. T., Y. P. Zhou, L. Dey, A. S. Attele, J. A. Wu, M. Gu, K. S. Polonsky and C. S. Yuan (2002). "Ginseng berry reduces blood glucose and body weight in db/db mice." Phytomedicine **9**(3): 254-258.

Xu, X. H., P. K. Shah, E. Faure, O. Equils, L. Thomas, M. C. Fishbein, D. Luthringer, X.-P. Xu, T. B. Rajavashisth and J. Yano (2001). "Toll-like receptor-4 is expressed by macrophages in murine and human lipid-rich atherosclerotic plaques and upregulated by oxidized LDL." Circulation **104**(25): 3103-3108.

Yamauchi, T., J. Kamon, H. Waki, Y. Terauchi, N. Kubota, K. Hara, Y. Mori, T. Ide, K. Murakami and N. Tsuboyama-Kasaoka (2001). "The fat-derived hormone adiponectin reverses insulin resistance associated with both lipoatrophy and obesity." Nature medicine **7**(8): 941-946.

Yang, L., Y. Hu and Y. Hou (2006). "Effects of 17beta-estradiol on the maturation, nuclear factor kappa B p65 and functions of murine spleen CD11c-positive dendritic cells." Mol Immunol **43**(4): 357-366.

Ye, J., Z. Gao, J. Yin and Q. He (2007). "Hypoxia is a potential risk factor for chronic inflammation and adiponectin reduction in adipose tissue of ob/ob and dietary obese mice." American Journal of Physiology - Endocrinology and Metabolism **293**(4): E1118-E1128.

Zhang, H., B. J. Potter, J. M. Cao and C. Zhang (2011). "Interferon-gamma induced adipose tissue inflammation is linked to endothelial dysfunction in type 2 diabetic mice." Basic Res Cardiol **106**(6): 1135-1145.

Zhang, L., T. Sugiyama, N. Murabayashi, T. Umekawa, N. Ma, Y. Kamimoto, Y. Ogawa and N. Sagawa (2011). "The inflammatory changes of adipose tissue in late pregnant mice." Journal of molecular endocrinology **47**(2): 157-165.

CHAPTER III

Depletion of perivascular adipose tissue dendritic cells Improves vascular dysfunction in type 2 diabetic mice

3.1. ABSTRACT

Objective: The aim of this study was to investigate the role of perivascular adipose tissue dendritic cells in the regulation of vascular function in T2DM mice.

Background: It is well known that impaired vasodilator responses and chronic local inflammation are evident in a number of metabolic disorders, including obesity and diabetes. The underlying mechanisms have recently been shown to involve the accumulation of multiple immune cell types, such as macrophages. However, the contribution of another important immune cell subtype, the dendritic cell, in the development of vascular dysfunction in T2DM has not been clarified.

Methods: DbHET controls, *db/db* T2DM mice, and dendritic cell depleted DbHET $^{Flt3l-/-}$ and db^{Flt3l-}/db^{Flt3l-} mice were used in the following studies. To first confirm the efficacy of dendritic cell ablation, visceral adipose tissue (VAT) was harvested from the above groups of mice and subjected to flow cytometry analysis. Glucose and insulin tolerance tests were conducted to investigate the effect of dendritic cell depletion on glucose homeostasis. Subsequently, the four groups of mice were divided into two age groups: 6-10 and 18-22 weeks of age. VAT and mesenteric adipose tissue (MAT) were collected to detect mRNA levels of pro-inflammatory cytokines TNF-α and lL-6, as well as the anti-inflammatory mediators, adiponectin and IL-10. Furthermore, ACh- induced vasorelaxation and PE- induced vasoconstriction were examined using first order mesenteric arteries incubated in the absence and presence of MAT isolated from above mice.

Results: Increased numbers of $CD11c^{+}F4/80^{-}$ and $CD83^{+}CD86^{+}$ dendritic cells accumulated in VAT from *db/db* mice, compared to DbHET controls. Depletion of Flt3l dramatically reduced dendritic cell numbers in VAT from db^{Flt3l-}/db^{Flt3l-} mice, indicating the suitability of this murine model. Glucose and insulin tolerance tests showed db^{Flt3l-}/db^{Flt3l-} mice had markedly lower glucose levels than *db/db* mice, while remaining elevated compared to DbHET and DbHET $^{Flt3l-/-}$

mice. Increased mRNA levels of pro-inflammatory factors, TNF-α and IL-6, as well as decreased levels of the anti-inflammatory cytokine, adiponectin, were found in VAT and MAT from *db/db*, compared to DbHET mice. The anti-inflammatory factor IL-10 was surprisingly increased in *db/db* mice possibly as compensation for the overproduction of pro-inflammatory factors. Depletion of dendritic cells significantly reduced TNF-α, IL-6 and IL-10 mRNA levels in VAT and MAT from db^{Flt3l-}/ db^{Flt3l-} mice compared to *db/db* mice without an apparent influence on adiponectin levels. Dendritic cell depletion during the early stage of T2DM further rescued impaired ACh-induced vasorelaxation and PE-induced vasoconstriction in mesenteric arteries resulting from MAT incubation.

Conclusion: Dendritic cells accumulate in the adipose tissue of T2DM mice. The presence of this population of immune cells leads to overproduction of pro-inflammatory cytokines, which contributes to impaired vasodilator and anti-contractile functions normally exerted by perivascular adipose tissue.

***Key Words*:** dendritic cells, perivascular adipose tissue, inflammation, vasorelaxation, anti-contractile function.

3.2. Introduction

The prevalence of obesity and type 2 diabetes (T2DM) in adults and children has increased dramatically in the last 20 years. While previously being largely associated with western societies, this is now occurring on a global scale. Further, the estimated total economic cost of obesity and T2DM is progressively increasing, approaching $92.6 billion dollars in 2002 and representing approximately 9% of the annual health expenditure in United States (Nguyen and El-Serag 2010). In terms of risk factors, it has been acknowledged that obesity is a major contributor to the development of T2DM and its cardiovascular complications (Creely, McTernan et al. 2007). Supporting this, approximately 80% of patients with T2DM are diagnosed with obesity. In particular, central obesity (characterized by increased waist circumference) is believed to be the primary cause of metabolic syndromes, such as T2DM (Greenstein, Khavandi et al. 2009).

Although adipose tissue has traditionally been considered as a relatively inert energy storage depot, it is now accepted that adipose tissue is also an active immunological organ capable of secreting a variety of bioactive molecules in a paracrine or endocrine manner under different pathological conditions (Yang, Graham et al. 2005, Grant and Dixit 2015). Many studies have now shown that obesity and T2DM are associated with a low-grade systemic inflammatory process (Zhang, Potter et al. 2011) and that adipose tissue contributes to the progression of this inflammation (Grant and Dixit 2015). Further, the inflammation is characterized by an imbalance in the production of pro-inflammatory and anti-inflammatory factors within adipose tissue (Creely, McTernan et al. 2007, Esser, Legrand-Poels et al. 2014). The levels of pro-inflammatory factors tumor necrosis factor alpha (TNF-α), interleukin 6 (IL-6), and monocyte chemo attractant protein-1(MCP-1) are elevated both systemically and in peripheral adipose tissue in the context of obesity (Zhang, Potter et al. 2011, Grant and Dixit 2015), whereas the level of the anti-inflammatory factor, adiponectin, is decreased in obese adipose tissue. The presence of TNF-α and IL-6 has been shown to impair glucose uptake and insulin action in peripheral tissues, such as skeletal muscle and liver, and this effect facilitates the development of insulin resistance and T2DM (Grant and Dixit 2015). Locally, in obese adipose tissue, these cytokines modulate adipocyte

lipolysis and potentiate inflammation by recruitment of inflammatory immune cells, such as macrophages, B and T lymphocytes (Guilherme, Virbasius et al. 2008, Winer, Chan et al. 2009, Winer, Winer et al. 2011). The accumulated immune cells subsequently become activated and secrete more pro-inflammatory cytokines (such as TNF-α, IL-6 and interferon-gamma (IFN-γ)) into obese adipose tissue. This facilitates the formation of a vicious circle, which further amplifies the inflammatory response that is thought to promote insulin resistance and ultimately contributes to the development of overt T2DM. Consistent with this, it has been reported that macrophage ablation results in normalization of insulin sensitivity in obese, insulin-resistant mice and is accompanied by lower levels of pro-inflammatory cytokines IL-6 and MCP-1 in obese adipose tissue (Patsouris, Li et al. 2008). Similarly, depletion of B (Winer, Winer et al. 2011) or T lymphocytes (Winer, Chan et al. 2009) in adipose tissue also restores insulin reactivity in obesity-associated insulin resistant mice. Collectively, in the context of obesity and T2DM, adipose tissue switches to an inflammatory profile with accumulation of various immune cells, leading to the development of insulin resistance.

Perivascular adipose tissue (PVAT) is defined as adipose tissue directly surrounding blood vessels and can thus be viewed as being continuous with the vascular adventitia (Eringa, Bakker et al. 2012). Accumulating evidence shows that under physiological conditions, the presence of PVAT opposes vascular constriction induced by pharmacological vasoconstrictors, such as serotonin (Chang, Milton et al. 2013, Gu and Xu 2013, Even, Dulak-Lis et al. 2014). This phenomenon is termed as the ‘anti-contractile’ property of PVAT. Consistent with this, co-incubation of PVAT with isolated arteries augments vascular relaxation induced by pharmacological vasodilators, such as acetylcholine (Wang, Luo et al. 2012, Meijer, Bakker et al. 2013). These anti-contractile and augmentation of vasorelaxation functions of PVAT appear to be mediated by a number of bioactive molecules secreted by PVAT, which are collectively termed as adipocyte-derived relaxing factors (ADRFs) (Even, Dulak-Lis et al. 2014, Oriowo 2015). However, the exact components of ADRFs are still unclear. It has been proposed that ADRFs might consist of adiponectin (Fesus, Dubrovska et al. 2007), hydrogen sulfide (H_2S) (Wojcicka, Jamroz-Wisniewska et al. 2011), nitric oxide (NO) (Gao, Lu et al. 2007) and/or angiotensin (Ang)1-7(Lee,

Lu et al. 2009). These vasoactive molecules except NO act on different potassium channels on vascular smooth muscle cells, causing membrane hyperpolarization and leading to an anti-contractile response (Malinowski, Deja et al. 2013, Tano, Schleifenbaum et al. 2014). Additionally, ADRFs act on endothelial cells and enhance vasorelaxation (Cheng, Ndisang et al. 2004, Goldstein and Scalia 2004). In contrast to the physiological state, obesity results in impairment of the anti-contractile activity of PVAT (Meijer, Bakker et al. 2013, Agabiti-Rosei, De Ciuceis et al. 2014), which has been implicated in local chronic inflammation and hypoxia caused by obesity (Greenstein, Khavandi et al. 2009). Increased TNF-α and IL-6 levels in PVAT largely abolished anti-contractile response induced by norepinephrine, while application of TNF-α antagonist, superoxide dismutase (SOD) or catalase rescued the anti-contractile reactivity from obese PVAT (Greenstein, Khavandi et al. 2009). Under obese conditions, the augmentation of vasorelaxation elicited by PVAT is also blunted, which can be partially restored by application of soluble adiponectin (Meijer, Bakker et al. 2013). Collectively, PVAT displays anti-contractile properties and augments vasorelaxation under physiological conditions, whereas in obesity local inflammation attenuates anti-contractile and augmentation of vasorelaxation of PVAT. As the accumulation of immune cells in obese adipose tissue results in an overproduction of inflammatory cytokines, it is conceivable that depletion of such cells would rescue the anti-contractile and augmentation of vasorelaxation in PVAT. However, to date this hypothesis has not been tested.

Dendritic cells are professional and potent antigen presenting cells characterized by tree-like extensions from the cell surface (Steinman 1991). Under physiological conditions, dendritic cells are generated from bone marrow hematopoietic stem cells and migrate into peripheral tissues acting as sentinels to surveillance the immune system (Steinman 1991). Once the immune system is insulted by foreign antigens, dendritic cells are usually the first immune cells to arrive at the site of insult and act to capture the foreign antigens. Further, the dendritic cells become activated and acquire the capacity to migrate from peripheral tissue to lymphoid organs, such as lymph nodes and spleen. In these organs, dendritic cells present processed antigens to immature B and T lymphocytes. Through this interaction, dendritic cells activate B and T effector

cells and direct them towards the site of insult where these effector cells eradicate foreign antigens and maintain immunological homeostasis (Steinman 2007). Defects in dendritic cell function have been shown to contribute to the pathological processes underlying a number of diseases, including cancer, immunodeficiency diseases (Vacas-Cordoba, Climent et al. 2014), autoimmune disease (Liao, Reihl et al. 2016), atherosclerosis (Dieterlen, John et al. 2016), and type 1 diabetes (Price and Tarbell 2015). Importantly, evidence suggests that in obesity dendritic cells have a weakened antigen presenting function and, instead, increase the capability for inflammatory cytokine secretion (Macia, Delacre et al. 2006). It is therefore possible that the accumulation of dendritic cells in obese adipose tissue contributes to the local production of inflammatory cytokines and contributes to the chronic inflammation seen in T2DM. If this is the case, the accumulation of dendritic cells in adipose tissue may play a role in the impairment of anti-contractile and augmentation of vasorelaxation caused by chronic inflammation in T2DM.

As a result of the above discussion, we proposed to examine the following hypotheses:

- That depletion of dendritic cells would reduce the production of pro-inflammatory cytokines and restore the secretion of anti-inflammatory mediators in obese PVAT from murine T2DM model.
- That accumulation of dendritic cells in adipose tissue is associated with vascular dysfunction caused by T2DM. Dendritic cell accumulation would impair the anti-contractile and augmentation of vasorelaxation elicited by obese PVAT.
- That there is a progressive (i.e. age/duration of diabetes-dependent) impairment of anti-contractile and enhanced vasorelaxation exerted by PVAT in a T2DM model.

3.3. Methods

Animal Models

Male and female homozygote T2DM mice (*Lepr*^{db}, *db/db* mice) and heterozygote controls (m *Lepr*^{db}, DbHET mice) on the same C57BLKS/J strain were purchased from Jackson Laboratory. Male and female Flt3l$^{-/-}$ mice, used as a murine model of dendritic cell depletion, were acquired from Taconic Farms (Stefanovic-Racic, Yang et al. 2012). To obtain T2DM mice depleted of dendritic cells, *db*$^{Flt3l-}$/ *db*$^{Flt3l-}$ mice, Flt3l$^{-/-}$ mice were cross-bred with m *Lepr*^{db} mice to generate m *Lepr*^{db} *Flt3l*$^{+/-}$ offspring. In the second generation, male m *Lepr*^{db} *Flt3l*$^{+/-}$ mice were bred with female m *Lepr*^{db} *Flt3l*$^{+/-}$ mice to generate the third hybrid generation m *Lepr*^{db} *Flt3l*$^{-/-}$ mice (abbreviated as DbHET $^{Flt3l-/-}$ mice). The DbHET $^{Flt3l-/-}$ mice were used as breeding pairs to generate DbHET $^{Flt3l-/-}$ and *db*$^{Flt3l-}$/ *db*$^{Flt3l-}$ mice which were later used in our studies. Male and female DbHET, *db/db,* DbHET $^{Flt3l-/-}$ and *db*$^{Flt3l-}$/ *db*$^{Flt3l-}$ mice were subdivided into two age groups: 6-10 and 18-22 weeks. All mice were housed in a constant temperature and humidity environment on a 12-hour light/dark cycle. All mice had ad libitum access to water and a standard chow diet. All the following procedures were approved by the Laboratory Animal Care Committee at University of Missouri, Columbia.

Glucose and insulin tolerance tests

Mice were deprived of food overnight for approximately 16 hours in preparation for glucose tolerance tests while mice were fasted for 4 hours before insulin tolerance tests. After the appropriate fasting procedure, tail tips of mice were cut with sterile scissors and baseline glucose levels measured by the ReliOn Prime glucometer (ReliOn Company, WA, USA). 20% glucose solution or 0.5 U/kg insulin (Humalin® R; Eli Lilly) were administered intraperitoneally (Lee, Park et al. 2011); volume was based on bodyweight. Blood glucose levels were taken from the initial tail cut at time 0, 30, 60, 90, and 120 minutes by gently massaging tail blood onto glucometer test strips.

Measurements of adipose tissue weights and non-fasting glucose levels

Weights of total body, intestinal mesentery, visceral adipose tissue (VAT), peri-aortic adipose tissue (ATA), pericardial adipose tissue (AH) from the above mice were measured on the same weight scale. Non-fasting blood glucose levels were measured by a ReliOn prime blood glucose monitoring system (ReliOn Company, WA, USA). Then all the mice were anesthetized with Nembutal (65mg/kg) (Sigma Company, Cream Ridge, NJ, USA) and euthanized under anesthesia (Kato, Kashiwagi et al. 2006).

Isolation of the Cellular Stromal Vascular Fraction from Adipose Tissue

The procedures for cell isolation from adipose tissue were described in detail previously in Chapter II. In brief, VAT was collected from DbHET, *db/db,* DbHET $^{Flt3l-/-}$and db^{Flt3l-}/ db^{Flt3l-} mice at 6-10 weeks. The VAT was placed in a freshly made solution of 1x Phosphate Buffered Saline (Ca/Mg^{2+} free)(Gibco Company, Waltham, MA, USA), 0.5% bovine serum albumin (Sigma Company, Cream Ridge, NJ, USA) and 10mM $CaCl_2$ and minced into fine particles (< 10 mg) using sterile scissors. 2 mg/ml type II collagenase (Sigma Company, Cream Ridge, NJ, USA) was added into the above solution and shaken at 37° C for 20 minutes. The enzymatic digestion was terminated by 1 mM EDTA and the solution was passed through 100-μm nylon strainers to remove undigested adipose tissue. The resulting suspension was centrifuged at 1600 rpm for 5 minutes at room temperature. The pellet was considered to be the stromal vascular fraction and was re-suspended in erythrocyte lysis buffer (Bio legend Company, San Diego, CA, USA). After removal of erythrocytes, the remaining cells were re-suspended in 1x Phosphate Buffered Saline without Ca^{2+} and Mg^{2+} for analysis by flow cytometry.

Flow Cytometry Analysis

Procedures for detecting dendritic cell and macrophage populations were similar to Chapter II. After determining cell number and survival rate of erythrocyte-depleted stromal vascular fraction cells, flow cytometry staining buffer (E-bioscience Company, San Diego, CA, USA) was used to wash those cells twice. Then 1 μg/ml Fc-blocker (Sigma Company, Cream Ridge, NJ, USA) was added into cell suspension to avoid non-specific binding of the primary antibodies.

After Fc-blocker incubation at 4 ° C in the dark for 15 minutes, cells subsequently underwent primary antibody incubation at the same environment for the following 45 minutes. The primary antibodies used in this experiment were list in **Table.3-1**.

Table.3-1. Properties of primary antibodies for flow cytometry measurements in DbHET, *db/db,* DbHET $^{Flt3l-/-}$ and db^{Flt3l-}/ db^{Flt3l-} mice.

Primary antibody	Dilution	Conjugated fluorophore	Company
Anti-CD11c	1:200	APC	BD Pharmingen Company
Anti-F4/80	1:400	PE	E-bioscience Company
Anti-CD83	1:200	PE	Bio legend Company
Anti-CD86	1:200	APC	E-bioscience Company

After washing with flow cytometry staining buffer twice, cells were assessed using the CyAn ADP High-Performance Flow Cytometer and Summit software. The final data were presented using Flowjo software. Dendritic cells were identified as $CD11c^{+}F4/80^{-}$ and $CD83^{+}CD86^{+}$ cell populations whereas macrophages were identified as $CD11c^{+}F4/80^{+}$ cell populations.

Inflammatory marker mRNA expression in adipose tissue

The protocols to detect mRNA levels of inflammatory factors were similar to that outlined in Chapter II. In brief, total RNA of VAT and mesenteric adipose tissue (MAT) was extracted using RNeasy lipid tissue mini kits (Qiagen Company, Valencia, CA, USA). Quality and quantity of the RNA preparations were measured by a Nano Drop ND-1000 Spectrophotometer (Nano Drop Technologies, Wilmington, DE). 100ng RNA was reversely transcribed into cDNA using the SuperScript III First-Strand Synthesis System (Invitrogen Company, Grand Island, NY, USA). Amplification of cDNA into mRNA was conducted by Platinum® SYBR® Green qPCR SuperMix-

UDG (Invitrogen Company, Grand Island, NY, USA) in an iQ5 Real-Time PCR system (Bio-Rad company, Hercules, CA, USA). Glyceraldehyde 3-phosphate dehydrogenase (GAPDH) was used for internal normalization. Inflammatory factor primers were used as follows:

Table. 3-2. Properties of Primers for q PCR detection in DbHET, *db/db,* DbHET $^{Flt3l-/-}$ and db^{Flt3l-}/ db^{Flt3l-} mice

Primers	Forward	Reverse
TNF-α	gtccccaaagggatgagaag	cacttggtggtttgctacga
IL-6	ccggagaggagacttcacag	tccacgatttcccagagaac
Adiponectin	gtctcacccttaggaccaagaa	aggttggatggcaggc
IL-10	atggccttgtagacaccttg	gtcatcgatttctcccctgtg
GAPDH	aatggtgaaggtcggtgtg	gtggagtcatactggaacatgtag

The mean threshold cycle (CT) values were calculated by the $2^{-\Delta\Delta CT}$ method ($\Delta\Delta CT=C_{T.CD11c}-C_{T.GAPDH}$) (Pfaffl 2001). Data were presented as fold change of a given transcript normalized to GAPDH, compared with DbHET mice (defined as 1.0-fold).

Immunohistochemistry

Immunohistochemistry was performed in a similar fashion to that described in chapter II. Briefly, VAT was harvested from DbHET, *db/db,* DbHET $^{Flt3l-/-}$ and db^{Flt3l-}/ db^{Flt3l-} mice at 18-22 weeks. Samples were fixed in 10% formalin (Sigma Company) for 18-24 hours, and then were embedded in paraffin and cut into 5 μm thick sections (Wentworth, Naselli et al. 2010). Sections were de-paraffinized with xylene and processed through a series of ethanol concentrations. Following antigen retrieval steps, VAT sections were incubated with blocking serum at room temperature for 1 hour to limit nonspecific bindings. Sections were then incubated overnight with rabbit anti-mouse TNF-α antibody (1:100 dilution, Abcam Company, Cambridge, United Kingdom) and goat anti-mouse perilipin antibody (1:50 dilution, Santa Cruz company, California, USA) at 4°C. After washing with Tris-buffered saline (TBS), sections were incubated at room temperature for 3 hours with goat anti-rabbit secondary antibody conjugated with Texas-Red (1:1000 dilution,

Abcam Company, Cambridge, United Kingdom) and donkey anti-goat secondary antibody conjugated with FITC (1:100 dilution, Santa Cruz Company, California, USA). Nuclei were identified by DAPI staining (Invitrogen, Carlsbad CA, USA). To evaluate the production of TNF-α in VAT, the number of positive signals from TNF-α along with surrounding adipocytes were calculated from 10 random ×200 view fields on each section (Kosteli, Sugaru et al. 2010, Zhang, Sugiyama et al. 2011). Six sections were collected from each mouse (Kosteli, Sugaru et al. 2010). The percentage of TNF-α for each sample was determined as the sum of the number of positive signals of TNF-α divided by the total number of surrounding adipocytes in each view field.

Functional assessment of mesenteric artery reactivity with or without MAT co-incubation

After mice (DbHET, *db/db,* DbHET $^{Flt3l-/-}$ and db^{Flt3l-}/ db^{Flt3l-} mice at both 6-10 and 18-22 weeks of age) reached a surgical plane of anesthesia, the intestinal mesentery was quickly excised and immediately placed in cold and freshly made physiological saline solution (PSS). PSS was composed of 4.69 mM KCl, 118.99 mM NaCl, 2.50 mM $CaCl_2$•$2H_2O$, 1.18 mM KH_2PO4, 1.17 mM $MgSO_4$•$7H_2O$, 14.9 mM $NaHCO_3$, 5.5 mM D-Glucose, and 0.03 mM EDTA. First order mesenteric arteries (MA) were dissected, cleaned of surrounding tissue and cut into rings approximately 2mm in length. Approximately 0.5 gram of MAT was saved in PSS solution for co-incubation experiments. The MA rings were carefully positioned between 2 stainless steel wires (diameter 17 μm) in organ chambers of a DMT wire myograph (model 610M; A&D Instruments) (Zhang, Potter et al. 2011). Tension was applied to the mounted MA rings to a trans mural pressure of approximately 100 mmHg (Zhang, Potter et al. 2011). Passive length-tension relationships of MA were then determined via a Power Lab system (AD instruments, CO, USA) (Lee, Yang et al. 2015). During the following experiments, the circumference of the MA rings was maintained constant and responses were examined under isometric condition. All MA rings were maintained in 37° C PSS aerated continuously with 95% air--5% CO_2 (Withers, Simpson et al. 2014).

After 30 minutes equilibration, MA rings were first challenged with 80mmol/L KCl and this procedure was repeated 3 times until a constant vasoconstriction was achieved. Next, contractile

responses to phenylephrine (PE) were investigated in a cumulative dose manner (PE; 10^{-9}—10^{-5} mol/L). Endothelium-dependent vasodilation in response to acetylcholine (ACh) was examined using a cumulative dose approach (ACh; 10^{-9}—10^{-5} mol/L) after ring segments were pre-contracted with PE (1×10^{-5} mol/L). PE-induced vasoconstriction responses were expressed as a percentage of the contraction to 80mmol/L KCl whereas ACh-induced vasorelaxation responses were calculated as a percentage of reduced contraction to PE. In adipose tissue co-incubation protocols, 0.5g MAT was placed directly in the organ bath chamber in which a given MA ring had been mounted. Co-incubation was performed for 1 hour, which was termed as "MAT incubation". MA rings mounted in organ chamber and not incubated with MAT, were termed as "time controls". After 1 hour incubation with MAT, PE-induced vasoconstriction and ACh-induced vasorelaxation were examined again to reveal the effects of MAT on vascular function. In order to test whether MAT effects could be reversed by washing, PE-induced vasoconstriction and ACh-induced vasorelaxation were repeated in both MAT incubation and time control groups after MA rings were washed with PSS for 1 hour (6 x 10mins).

MAT transfer bioassay experiments

The protocols were identical to the above functional assessment experiments, except for the preparation of MAT incubation. In these experiments, MAs from DbHET mice at 18-22 weeks were isolated and mounted in organ chambers. MAT from these DbHET mice was saved in PSS while MAT from *db/db* mice (18-22 weeks) was also saved in PSS. After determining PE-induced vasoconstriction and ACh-induced vasorelaxation without MAT incubation, one MA ring from DbHET mouse was co-incubated with 0.5g MAT from the same DbHET mouse, whereas an additional MA ring from the DbHET mouse was co-incubated with 0.5g MAT from *db/db* mouse. Additionally, a MA ring from DbHET mouse without MAT co-incubation was termed as a "time control". After the 1 hour co-incubation period, PE-induced vasoconstriction and ACh-induced vasorelaxation were investigated to reveal the MAT's effect on MA vascular function. Similarly, MA rings from DbHET$^{Flt3l-/-}$ mice at 18-22 weeks were mounted in organ chambers and set up three groups, including DbHET$^{Flt3l-/-}$ mice's MAT incubation, *db*$^{Flt3l-}$/ *db*$^{Flt3l-}$ mice's MAT incubation

and time control groups. PE-induced vasoconstriction and ACh-induced vasorelaxation were studied with and without MAT incubation.

Statistical Analysis

All the results were expressed as mean (SEM). Basic parameter measurements, flow cytometry data and PCR results were analyzed by one-way Analysis of Variance (ANOVA), along with Tukey's multiple comparison post-test. For the functional experiments and MAT transfer bioassay data, two-way ANOVA was performed, along with Bonferroni post-test. $P < 0.05$ was considered statistically significant in all of the studies.

3.4. Results

Total body and adipose tissue weights and glucose levels

Earlier studies have demonstrated that ablation of $CD11c^{+}$ cells (including dendritic cells and macrophages) normalizes insulin sensitivity in diet-induced obese mice (Probst, Tschannen et al. 2005, Patsouris, Li et al. 2008). Moreover, it has been shown that $Flt3l^{-/-}$ mice display increased metabolic rate and are protected against diet-induced obesity (Stefanovic-Racic, Yang et al. 2012). As DbHET $^{Flt3l-/-}$ and db^{Flt3l-}/ db^{Flt3l-} mice used in the present studies would also exhibit low blood glucose levels and high metabolic rate, non-fasting glucose levels, total body weight along with intestinal mesentery, VAT, AH and ATA weights were measured in DbHET, *db/db,* DbHET $^{Flt3l-/-}$ and db^{Flt3l-}/ db^{Flt3l-} mice (6-10 and 18-22 weeks of age). As shown in **Fig.3-1**, in the early stage of T2DM (6-10 weeks), *db/db* mice displayed significantly higher body weight, intestinal mesentery weight, VAT, AH and ATA weights, along with higher non-fasting glucose levels, compared to DbHET mice. Similar results were observed at the later stage of T2DM (18-22 weeks; **Fig.3-2).** Depletion of dendritic cells did not alter those parameters in either DbHET$^{Flt3l-/-}$ nor db^{Flt3l-}/ db^{Flt3l-} mice at 6-10 weeks, while at 18-22 weeks, dendritic cell depletion was associated with decreased intestinal mesentery (**Fig.3-2-C**) and VAT (**Fig.3-2-D**) weights and decreased non-fasting glucose levels (**Fig.3-2-B**). Glucose and insulin tolerance tests (**Fig.3-3**) performed at 18-22 weeks of age similarly showed significantly lower blood glucose levels in db^{Flt3l-}/ db^{Flt3l-} mice in comparison with *db/db* mice, but higher glucose levels in db^{Flt3l-}/ db^{Flt3l-} mice than DbHET or DbHET $^{Flt3l-/-}$ mice. These data indicated a partial restoration of insulin reactivity in diabetic mice after dendritic cell depletion. Collectively, the depletion of dendritic cells reduced intestinal mesentery and VAT weights, as well as decreased blood glucose levels in db^{Flt3l-}/ db^{Flt3l-} mice only at the late stage of T2DM.

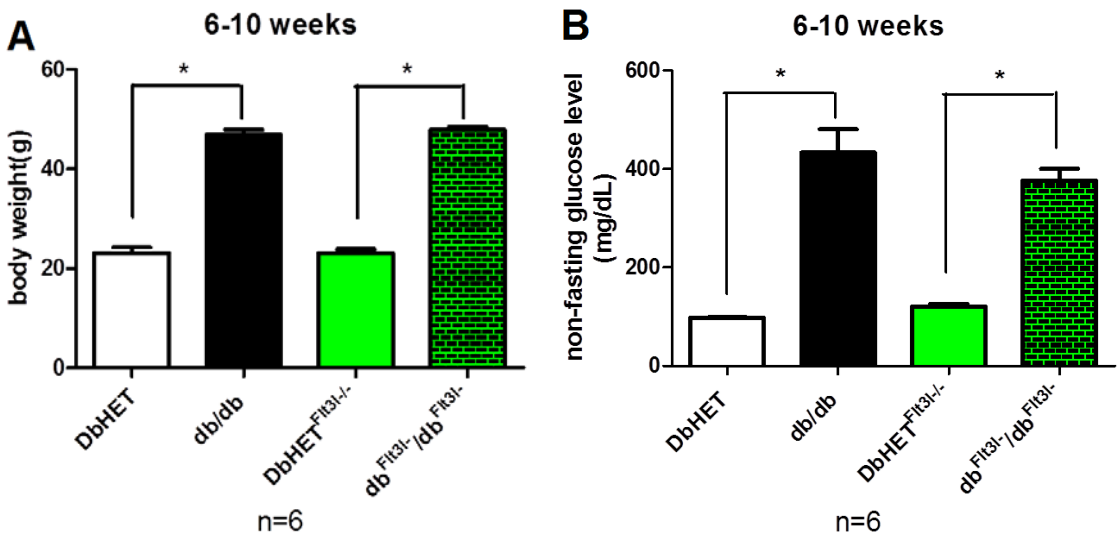
A
6-10 weeks
body weight(g)
60
40
20
0
*
*
DbHET
db/db
DbHET Flt3l-/-
db Flt3l-/db Flt3l-
n=6
B
6-10 weeks
non-fasting glucose level (mg/dL)
600
400
200
0
*
*
DbHET
db/db
DbHET Flt3l-/-
db Flt3l-/db Flt3l-
n=6

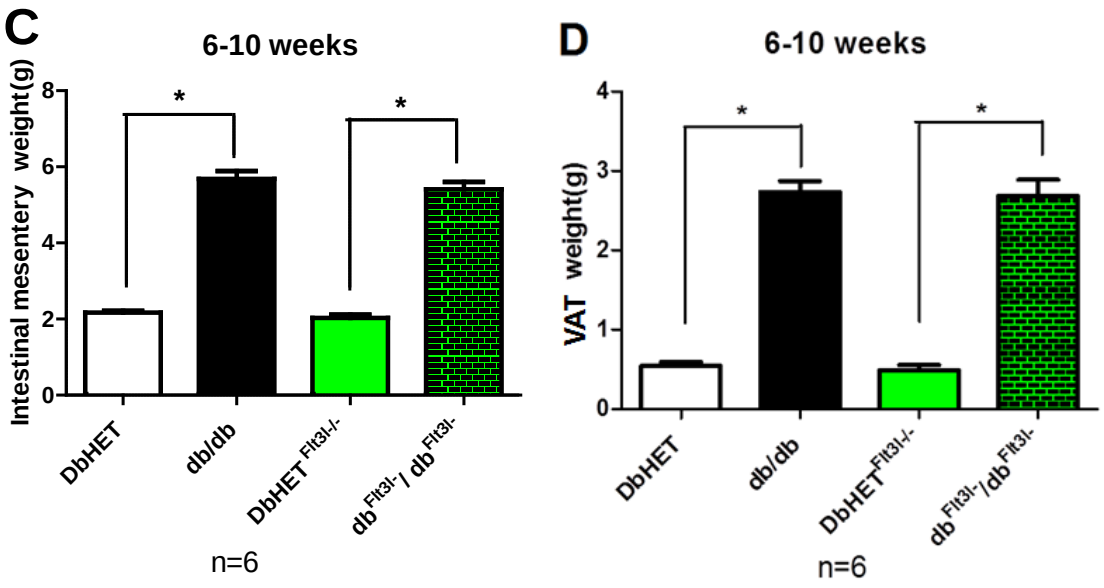
C
6-10 weeks
Intestinal mesentery weight(g)
8
6
4
2
0
*
*
DbHET
db/db
DbHET Flt3l-/-
db Flt3l-/ db Flt3l-
n=6
D
6-10 weeks
VAT weight(g)
4
3
2
1
0
*
*
DbHET
db/db
DbHET Flt3l-/-
db Flt3l-/db Flt3l-
n=6

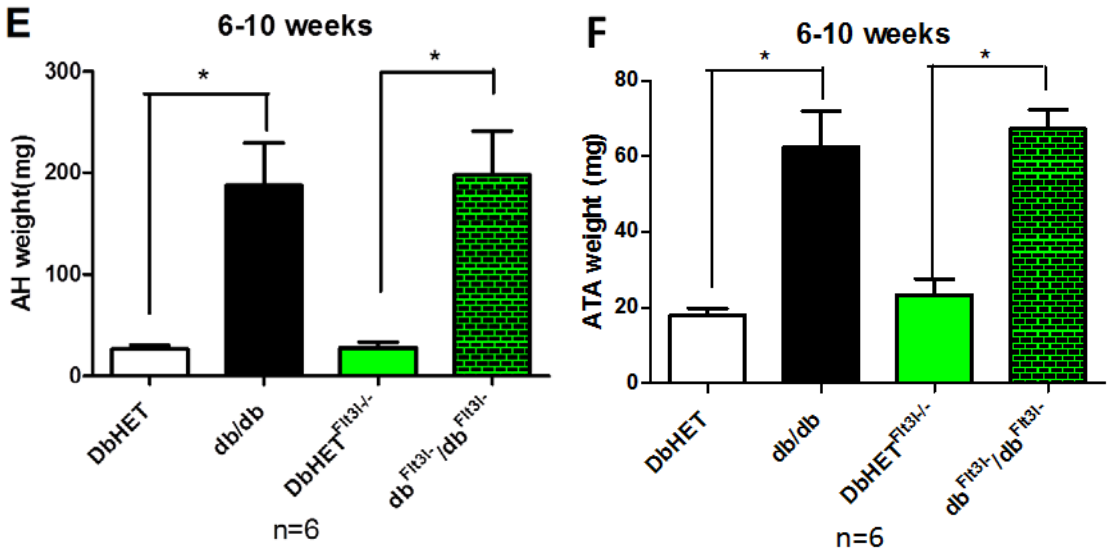

Figure.3-1. Total body and adipose tissue weights along with non-fasting glucose levels in experimental groups of mice (at 6-10 weeks) In the early stage of T2DM, *db/db* mice exhibited significantly heavier weights for total body **(A)**, intestinal mesentery **(C)**, VAT **(D)**, AH **(E)** and ATA **(F)**, compared to DbHET control mice. In addition, *db/db* mice showed dramatically higher non-fasting glucose levels **(B)** than controls. However, the depletion of Flt3l did not markedly affect those parameters in DbHET $^{Flt3l-/-}$ or db^{Flt3l-}/ db^{Flt3l-} mice. Data are shown as mean ± SEM. *: $P < 0.05$.

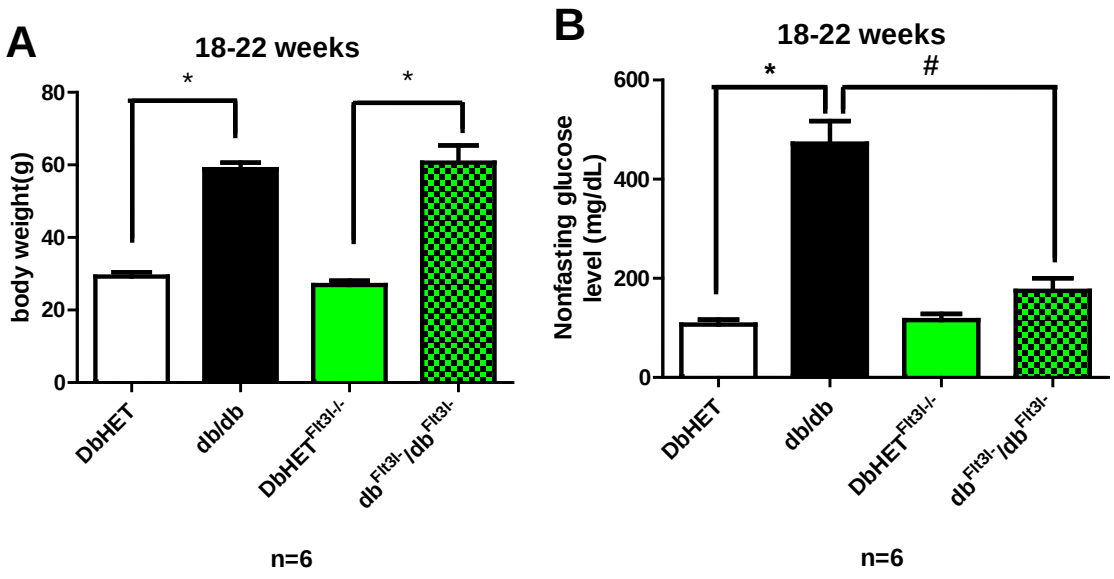

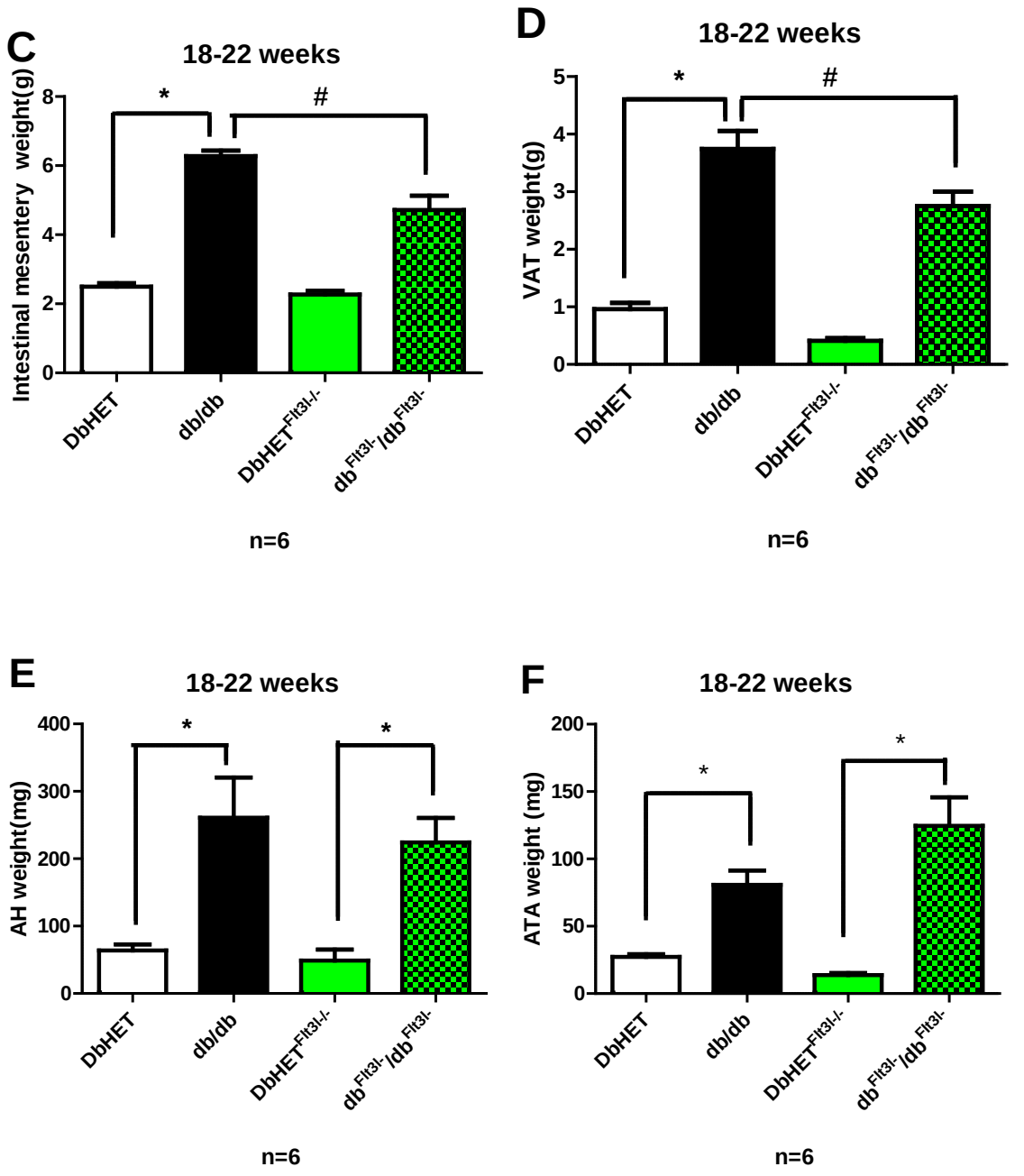

Figure. 3-2. Total body and adipose tissue weights along with non-fasting glucose levels in experimental groups of mice (at 18-22 weeks). In the later stage of T2DM, *db/db* mice exhibited significantly heavier weights of total body **(A)**, intestinal mesentery **(C)**, VAT **(D)**, AH **(E)** and ATA **(F)**, compared to DbHET controls. Further, *db/db* mice displayed markedly higher non-fasting glucose levels **(B)** than controls. In contrast to db^{Flt3l-}/ db^{Flt3l-} mice at 6-10 weeks, depletion of dendritic cells reduced intestinal mesentery **(C)** and VAT **(D)** weights along with non-fasting glucose levels **(B)** in db^{Flt3l-}/ db^{Flt3l-} mice at 18-22 weeks, without any influence on AH **(E)**, ATA **(F)** and total body weights **(A).** Depletion of dendritic cells did not affect those parameters in DbHET mice. Data are shown as mean ± SEM. *, #: $P < 0.05$.

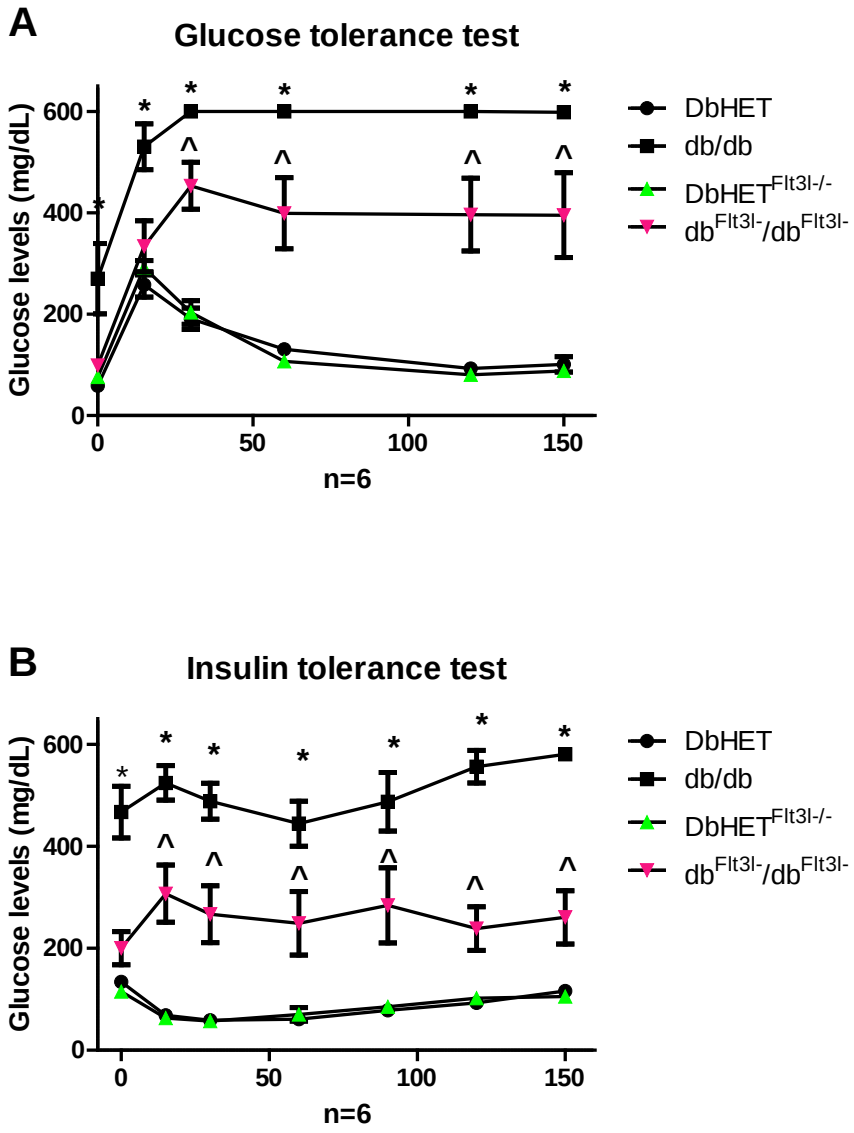

Figure.3-3. Glucose and insulin tolerance tests in experimental groups of mice at 18-22 weeks. During both tests, *db/db* mice had significantly higher glucose levels than DbHET, DbHET $^{Flt3l-/-}$ or db^{Flt3l-}/ db^{Flt3l-} mice. Although db^{Flt3l-}/ db^{Flt3l-} mice exhibited lower blood glucose levels than *db/db* mice, they had significantly higher glucose levels than DbHET or DbHET $^{Flt3l-/-}$ mice. No difference was found between DbHET and DbHET $^{Flt3l-/-}$ mice. *: *db/db* mice v.s. other three groups of mice. ^: db^{Flt3l-}/ db^{Flt3l-} mice v.s. DbHET or DbHET $^{Flt3l-/-}$ mice. Data are shown as mean ± SEM.

Flow cytometry measurements of markers for dendritic cell and macrophage populations in VAT

To confirm whether genetic depletion of Flt3l, in murine models, would lead to depletion of dendritic cells (without influence of macrophage populations), VAT samples from DbHET, *db/db,* DbHET $^{Flt3l-/-}$ and *db*$^{Flt3l-}$/ *db*$^{Flt3l-}$ mice were collected at 6-10 weeks. Dendritic cells were identified by two cell populations, CD11c^{+}F4/80^{-} and CD83^{+}CD86^{+} cell populations. The usage of two sets of markers allowed for more specific detection of dendritic cells. M1 macrophages were identified as the CD11c^{+}F4/80^{+} cell population. Flow cytometry analysis of VAT stromal vascular fraction showed, *db/db* mice had significantly increased levels of CD11c^{+}F4/80^{-} **(Fig.3-4-B)** and CD83^{+}CD86^{+} **(Fig.3-5-B)** dendritic cells than DbHET mice **(Fig.3-4-A, Fig.3-5-A)** at 6-10 weeks. Similarly, more CD11c^{+}F4/80^{+} macrophages were observed to accumulate in VAT from *db/db* mice **(Fig.3-4-B)**, compared to DbHET mice **(Fig.3-4-A)**. Genetic depletion of Flt3l significantly decreased CD11c^{+}F4/80^{-} **(Fig.3-4-C, D)** and CD83^{+}CD86^{+} **(Fig.3-5-C, D)** dendritic cell populations in VAT from DbHET $^{Flt3l-/-}$ and *db*$^{Flt3l-}$/ *db*$^{Flt3l-}$ mice. Our data also showed that CD11c^{+}F4/80^{-} **(Fig.3-4-E)** and CD83^{+}CD86^{+} **(Fig.3-5-E)** dendritic cells were comparable between DbHET $^{Flt3l-/-}$ and *db*$^{Flt3l-}$/ *db*$^{Flt3l-}$ mice. Importantly, Flt3l depletion did not significantly alter the number of CD11c^{+}F4/80^{+} macrophages in either DbHET $^{Flt3l-/-}$ **(Fig.3-4-C)** or *db*$^{Flt3l-}$/ *db*$^{Flt3l-}$ mice **(Fig.3-4-D)**. More CD11c^{+}F4/80^{+} macrophages infiltrated into VAT from *db*$^{Flt3l-}$/ *db*$^{Flt3l-}$ than DbHET $^{Flt3l-/-}$ mice **(Fig.3-4-F)**. Collectively, genetic depletion of Flt3l significantly reduced dendritic cell populations in VAT from DbHET $^{Flt3l-/-}$ and *db*$^{Flt3l-}$/ *db*$^{Flt3l-}$ mice, without any influence on the macrophage population. On the basis of these observations, DbHET $^{Flt3l-/-}$ and *db*$^{Flt3l-}$/ *db*$^{Flt3l-}$ mice were suitable in the following studies.

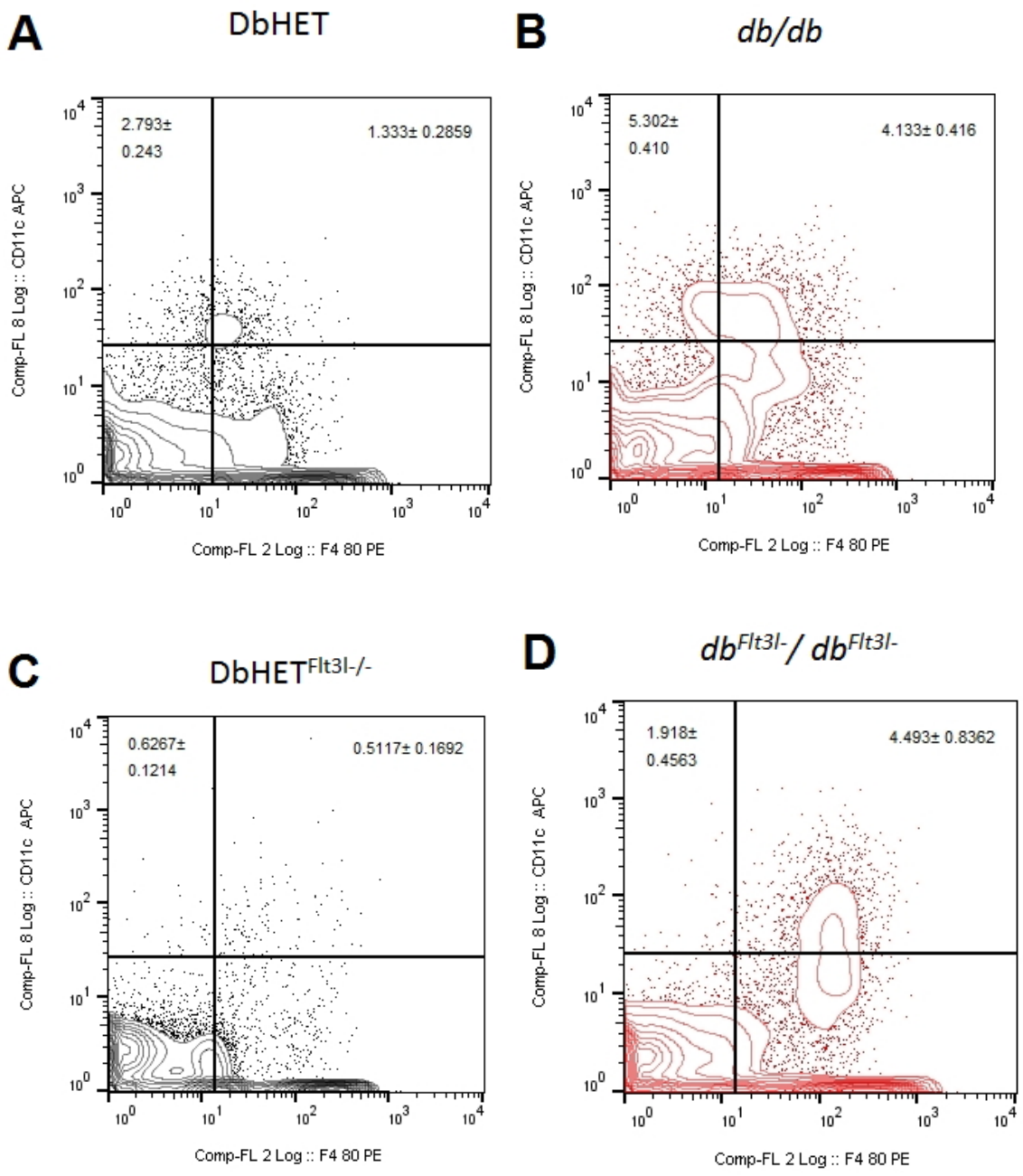
A
DbHET
2.793±
0.243
1.333± 0.2859
Comp-FL 8 Log :: CD11c APC
Comp-FL 2 Log :: F4 80 PE
B
db/db
5.302±
0.410
4.133± 0.416
Comp-FL 8 Log :: CD11c APC
Comp-FL 2 Log :: F4 80 PE
C
DbHET Flt3l-/-
0.6267±
0.1214
0.5117± 0.1692
Comp-FL 8 Log :: CD11c APC
Comp-FL 2 Log :: F4 80 PE
D
db Flt3l- / db Flt3l-
1.918±
0.4563
4.493± 0.8362
Comp-FL 8 Log :: CD11c APC
Comp-FL 2 Log :: F4 80 PE

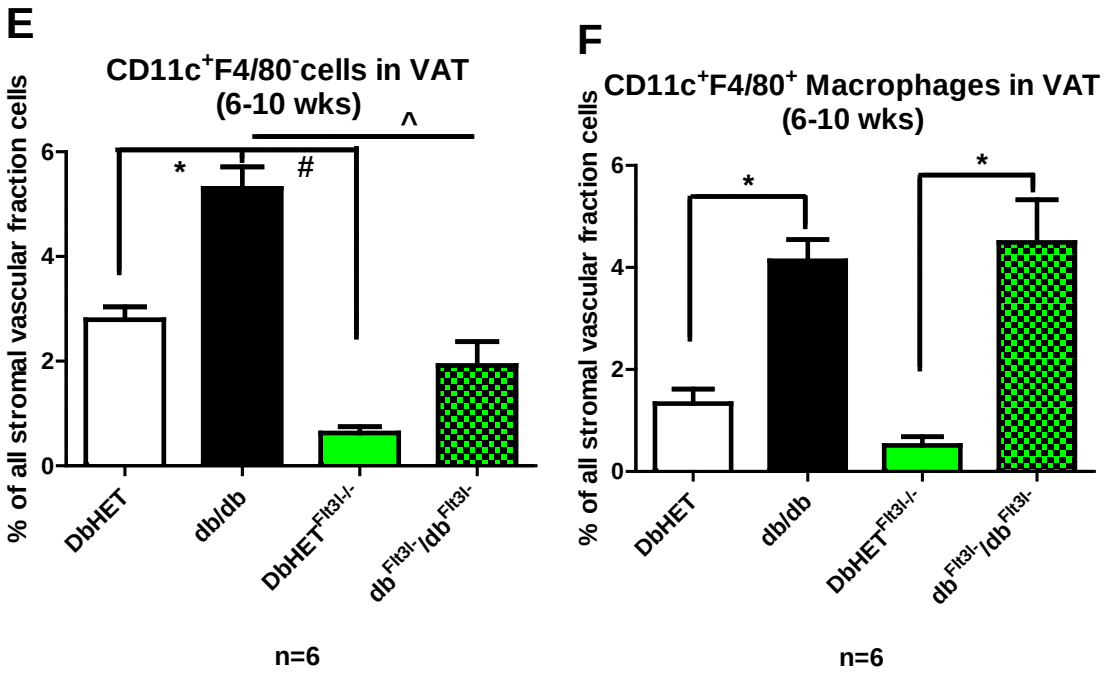

Figure.3-4. Flow cytometry data quantifying dendritic cell and macrophage populations in VAT from DbHET, *db/db*, DbHET $^{Flt3l-/-}$ and db^{Flt3l-}/db^{Flt3l-} mice (at 6-10 weeks). Panels **A-D** showed example flow cytometry data. More $CD11c^{+}F4/80^{-}$ dendritic cells (shown in the upper left quadrant) and $CD11c^{+}F4/80^{+}$ macrophages (shown in the upper right quadrant) accumulated in VAT from *db/db* mice **(B)** than DbHET mice **(A)**. Genetic depletion of Flt3l significantly decreased dendritic cell numbers in both DbHET $^{Flt3l-/-}$ **(C)** and db^{Flt3l-}/db^{Flt3l-} mice **(D)**. However, Flt3l depletion did not affect macrophage numbers in either DbHET $^{Flt3l-/-}$ **(C)** or db^{Flt3l-}/db^{Flt3l-} mice **(D)**. Panels **E** and **F** showed group data as mean ± SEM. *: $P < 0.05$. Between *db/db* and DbHET mice; between DbHET $^{Flt3l-/-}$ and db^{Flt3l-}/db^{Flt3l-} mice. #: $P < 0.05$. Between DbHET and DbHET $^{Flt3l-/-}$mice. ^: $P < 0.05$. Between *db/db* and db^{Flt3l-}/db^{Flt3l-} mice.

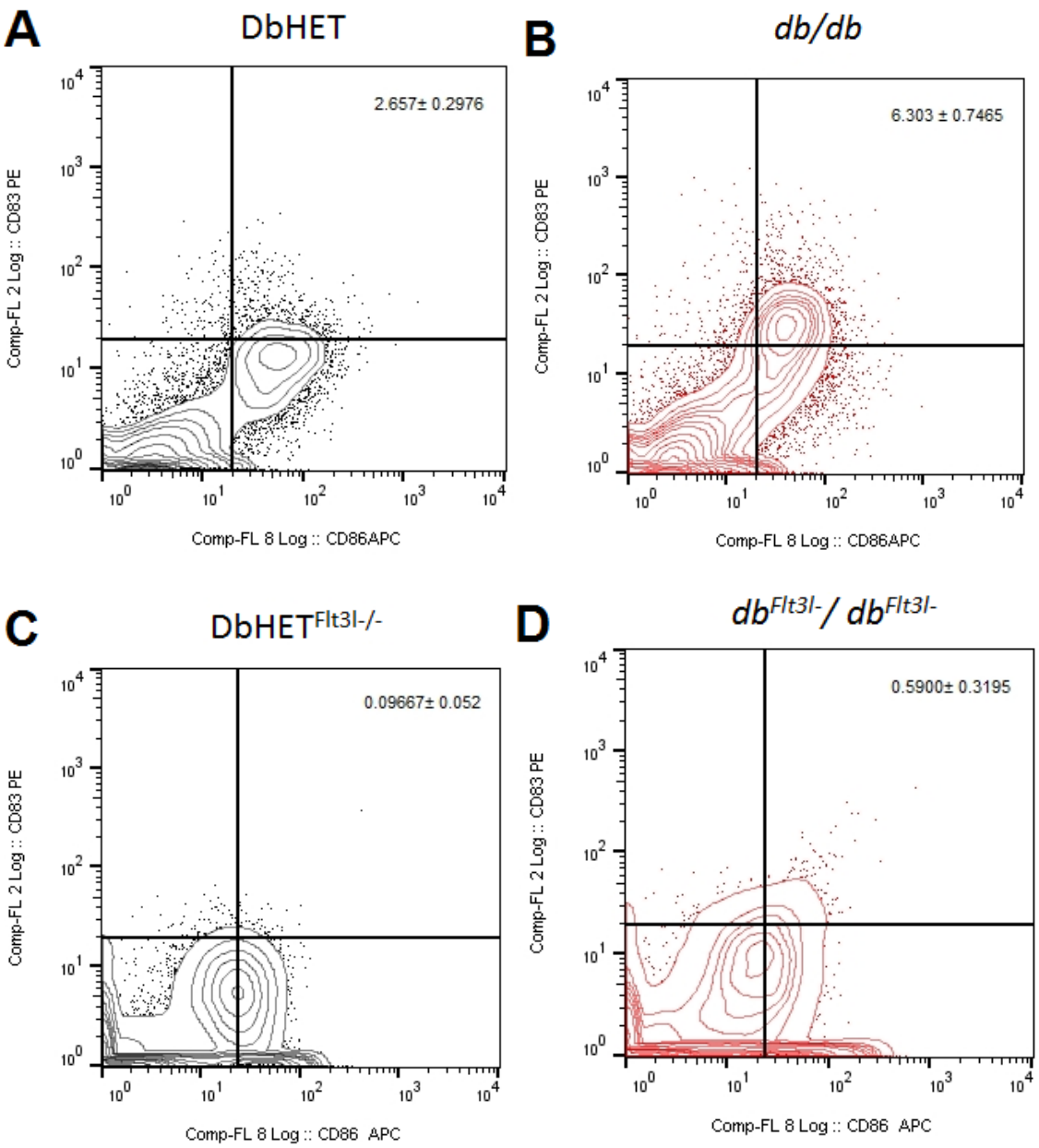
A
DbHET
2.657± 0.2976
Comp-FL 2 Log :: CD83 PE
Comp-FL 8 Log :: CD86APC
B
db/db
6.303 ± 0.7465
Comp-FL 2 Log :: CD83 PE
Comp-FL 8 Log :: CD86APC
C
DbHET Flt3l-/-
0.09667± 0.052
Comp-FL 2 Log :: CD83 PE
Comp-FL 8 Log :: CD86 APC
D
db Flt3l- / db Flt3l-
0.5900± 0.3195
Comp-FL 2 Log :: CD83 PE
Comp-FL 8 Log :: CD86 APC

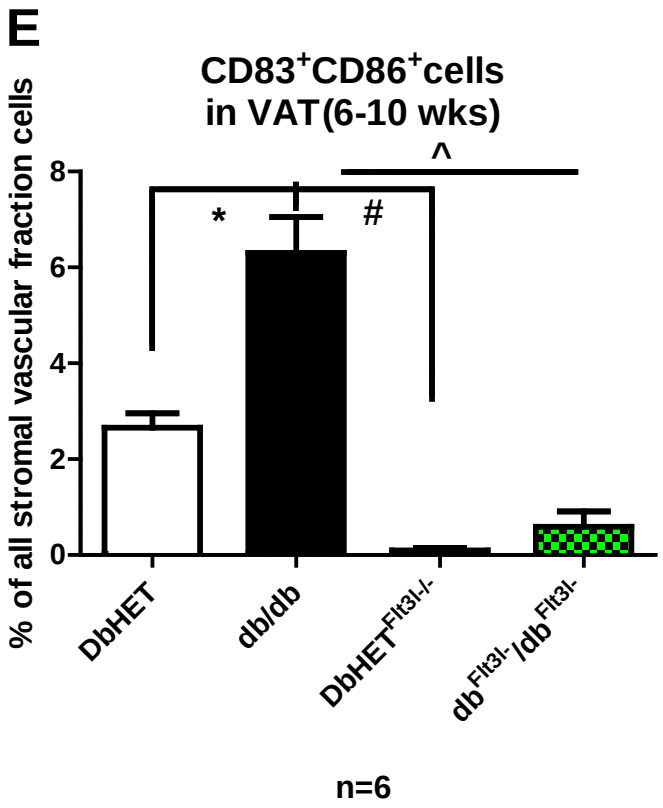

Figure.3-5. Flow cytometry data quantifying dendritic cell population in VAT from DbHET, *db/db,* DbHET $^{Flt3l-/-}$ and *db*$^{Flt3l-}$/ *db*$^{Flt3l-}$ mice (at 6-10 weeks). Panels **A-D** showed example flow cytometry data. More CD83^{+}CD86^{+} dendritic cells (shown in the upper right quadrant) accumulated in VAT from *db/db* mice **(B)** compared to DbHET mice **(A)**. Genetic Flt3l depletion significantly decreased dendritic cell population in both DbHET $^{Flt3l-/-}$ **(C)** or *db*$^{Flt3l-}$/ *db*$^{Flt3l-}$ mice **(D)**. Panels **E** showed group data as mean ± SEM. *: $P < 0.05$. Between *db/db* and DbHET mice. #: $P < 0.05$. Between DbHET and DbHET $^{Flt3l-/-}$mice. ^: $P < 0.05$. Between *db/db* and *db*$^{Flt3l-}$/ *db*$^{Flt3l-}$ mice.

mRNA expression for pro-inflammatory and anti-inflammatory factors

Earlier studies have shown that depletion of CD11c^{+} cells, in an obese murine model, led to a significant reduction of adipose tissue and systemic inflammation (Patsouris, Li et al. 2008). An improved inflammatory state was evident by decreased levels of pro-inflammatory cytokines TNF-α, IL-6 and MCP-1, and increased levels of anti-inflammatory factor, IL-10 (Patsouris, Li et al. 2008). We therefore hypothesized that depletion of Flt3l would significantly decrease production of pro-inflammatory cytokines while increasing availability of anti-inflammatory factors in adipose

tissue of genetically diabetic mice. In order to test this hypothesis, we used qPCR to measure mRNA levels of pro-inflammatory factors TNF-α and IL-6, along with anti-inflammatory mediators adiponectin and IL-10 mRNA levels in VAT and MAT from DbHET, *db/db*, DbHET $^{Flt3l-/-}$ and db^{Flt3l-}/ db^{Flt3l-} mice (aged 6-10 and 18-22 weeks). In the early stage of T2DM, mRNA levels for TNF-α and IL-6 were increased in VAT and MAT from *db/db* mice, compared to DbHET mice (**Fig.3-6**). Depletion of dendritic cells significantly decreased TNF-α and IL-6 levels in VAT and MAT from db^{Flt3l-}/ db^{Flt3l-} mice, except for IL-6 mRNA levels in VAT **(Fig.3-6-A,B,C,D)**. In contrast, mRNA levels of adiponectin were decreased in the VAT from *db/db* mice, compared to controls **(Fig.3-6-E)**. Depletion of dendritic cells did not restore adiponectin production in db^{Flt3l-}/ db^{Flt3l-} mice. Additionally, mRNA levels for adiponectin in MAT, along with IL-10 in VAT and MAT were not different between *db/db* and DbHET mice. Depletion of dendritic cells did not affect these patterns of results **(Fig.3-6-F, G, and H)**. In the later stage of T2DM, mRNA levels for TNF-α and IL-6 were increased in VAT and MAT from *db/db* mice, compared to controls **(Fig.3-7)**. Dendritic cell depletion significantly reduced TNF-α and IL-6 mRNA levels in VAT and MAT from db^{Flt3l-}/ db^{Flt3l-} mice **(Fig.3-7-A, B, C, D)**. TNF-α protein levels in VAT were consistent with the above findings **(Fig. 3-8)**. In contrast, mRNA levels for adiponectin were decreased in VAT and MAT from *db/db* mice, compared to controls **(Fig.3-7-E, F)**. However, depletion of dendritic cells did not restore adiponectin production in db^{Flt3l-}/ db^{Flt3l-} mice. Interestingly, mRNA levels of IL-10 were increased in VAT and MAT from *db/db* mice, compared to controls **(Fig.3-7-G, H)**. Dendritic cell depletion significantly reduced IL-10 mRNA levels only in MAT from db^{Flt3l-}/ db^{Flt3l-} mice **(Fig.3-7-H)**. Taken together, depletion of dendritic cells led to a reduction of pro-inflammatory factors and ameliorated chronic inflammation caused by T2DM.

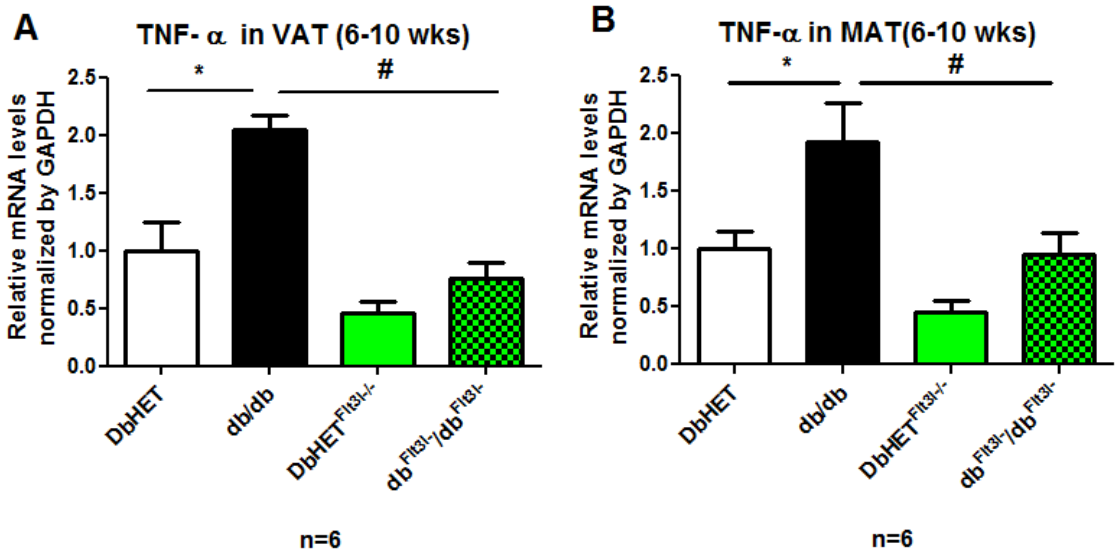
A
TNF- α in VAT (6-10 wks)
Relative mRNA levels normalized by GAPDH
2.5
2.0
1.5
1.0
0.5
0.0
*
#
DbHET
db/db
DbHET Flt3l-/-
db Flt3l-/db Flt3l-
n=6
B
TNF-α in MAT(6-10 wks)
Relative mRNA levels normalized by GAPDH
2.5
2.0
1.5
1.0
0.5
0.0
*
#
DbHET
db/db
DbHET Flt3l-/-
db Flt3l-/db Flt3l-
n=6

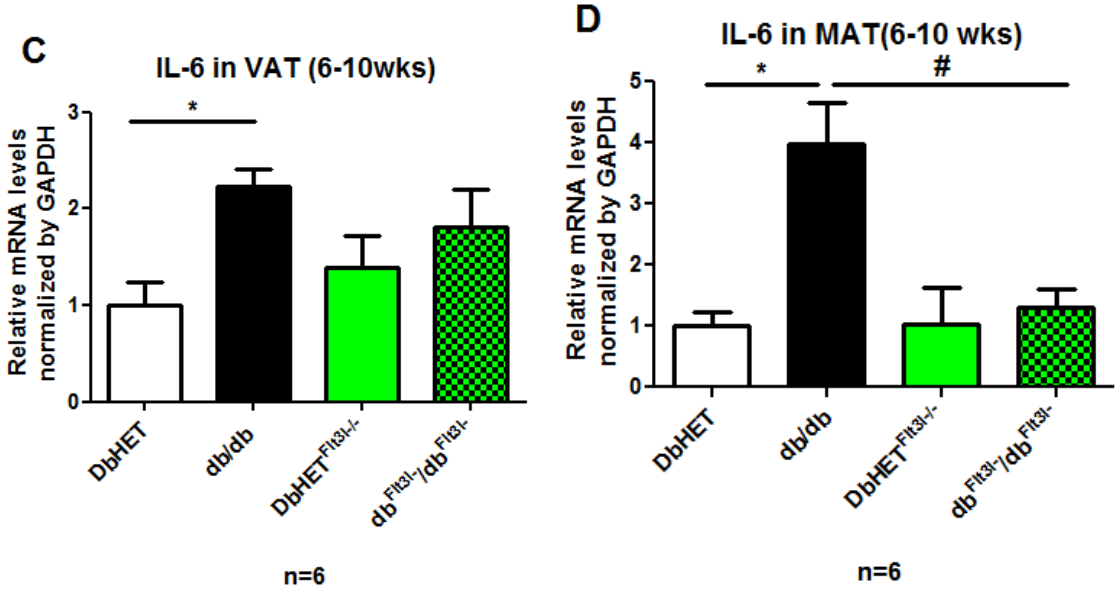
C
IL-6 in VAT (6-10wks)
Relative mRNA levels normalized by GAPDH
3
2
1
0
*
DbHET
db/db
DbHET Flt3l-/-
db Flt3l-/db Flt3l-
n=6
D
IL-6 in MAT(6-10 wks)
Relative mRNA levels normalized by GAPDH
5
4
3
2
1
0
*
#
DbHET
db/db
DbHET Flt3l-/-
db Flt3l-/db Flt3l-
n=6

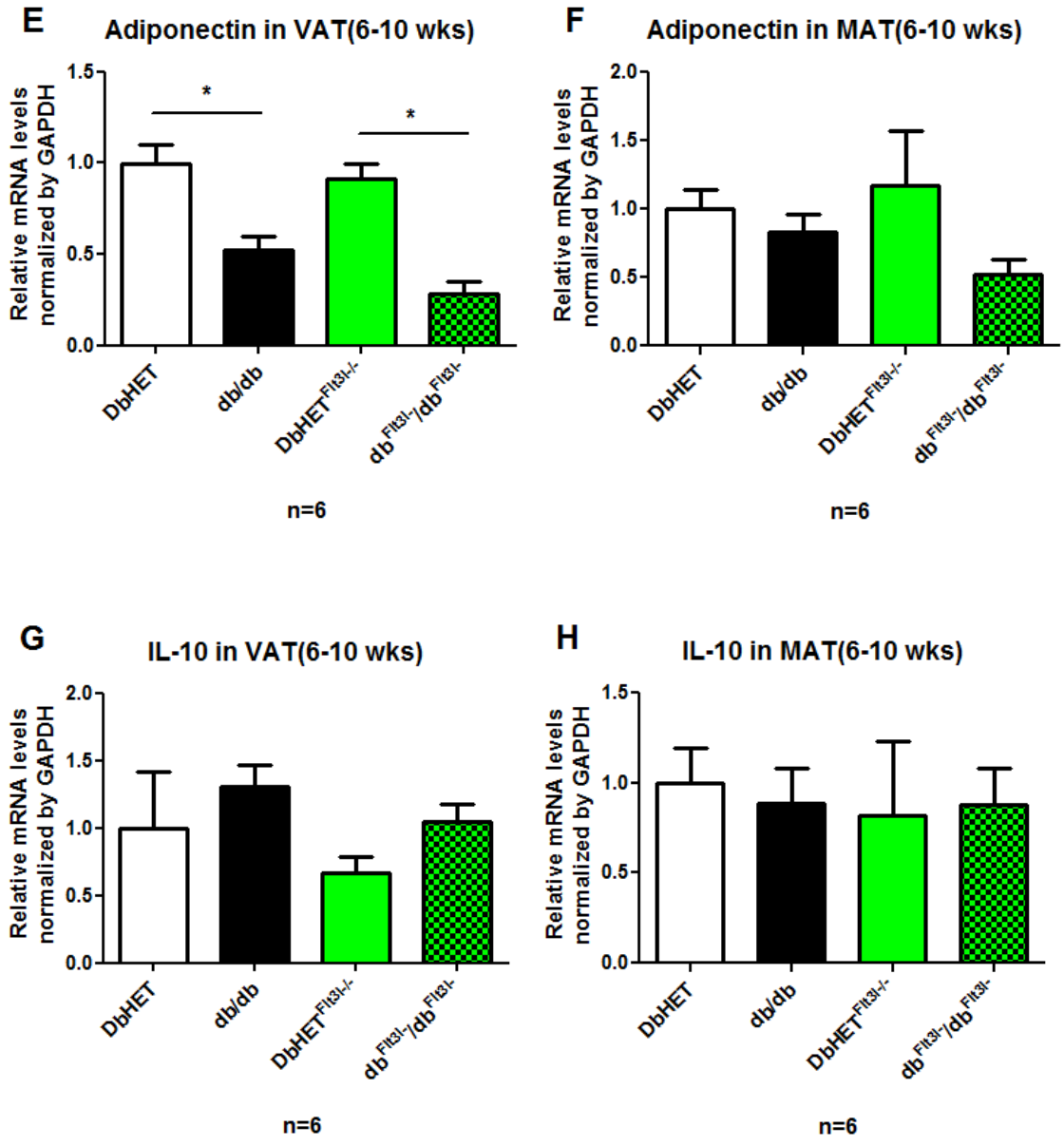

Figure. 3-6. mRNA expressions of inflammatory factors in VAT and MAT from DbHET, *db/db,* DbHET $^{Flt3l-/-}$ and *db*$^{Flt3l-}$/ *db*$^{Flt3l-}$ mice (at 6-10 weeks). Panels A-D showed increased mRNA levels of pro-inflammatory factors TNF-α **(A-B)** and IL-6 **(C-D)** in VAT and MAT from *db/db* mice compared to DbHET mice. Flt3l depletion significantly decreased TNF-α mRNA levels in diabetic VAT and MAT, while IL-6 levels were decreased only in diabetic MAT. Panel **E** showed that mRNA levels of the anti-inflammatory factor adiponectin were decreased in VAT from *db/db* mice, compared to DbHET mice. However, Flt3l depletion did not restore adiponectin production in *db/db* mice. Panel **F** showed adiponectin mRNA levels in MAT were similar in all four groups of mice. Panels **G-H** showed there was no significant difference of anti-inflammatory factor IL-10 levels in either VAT or MAT among all four groups of mice. Data are shown as mean ± SEM. *, #: $P < 0.05$.

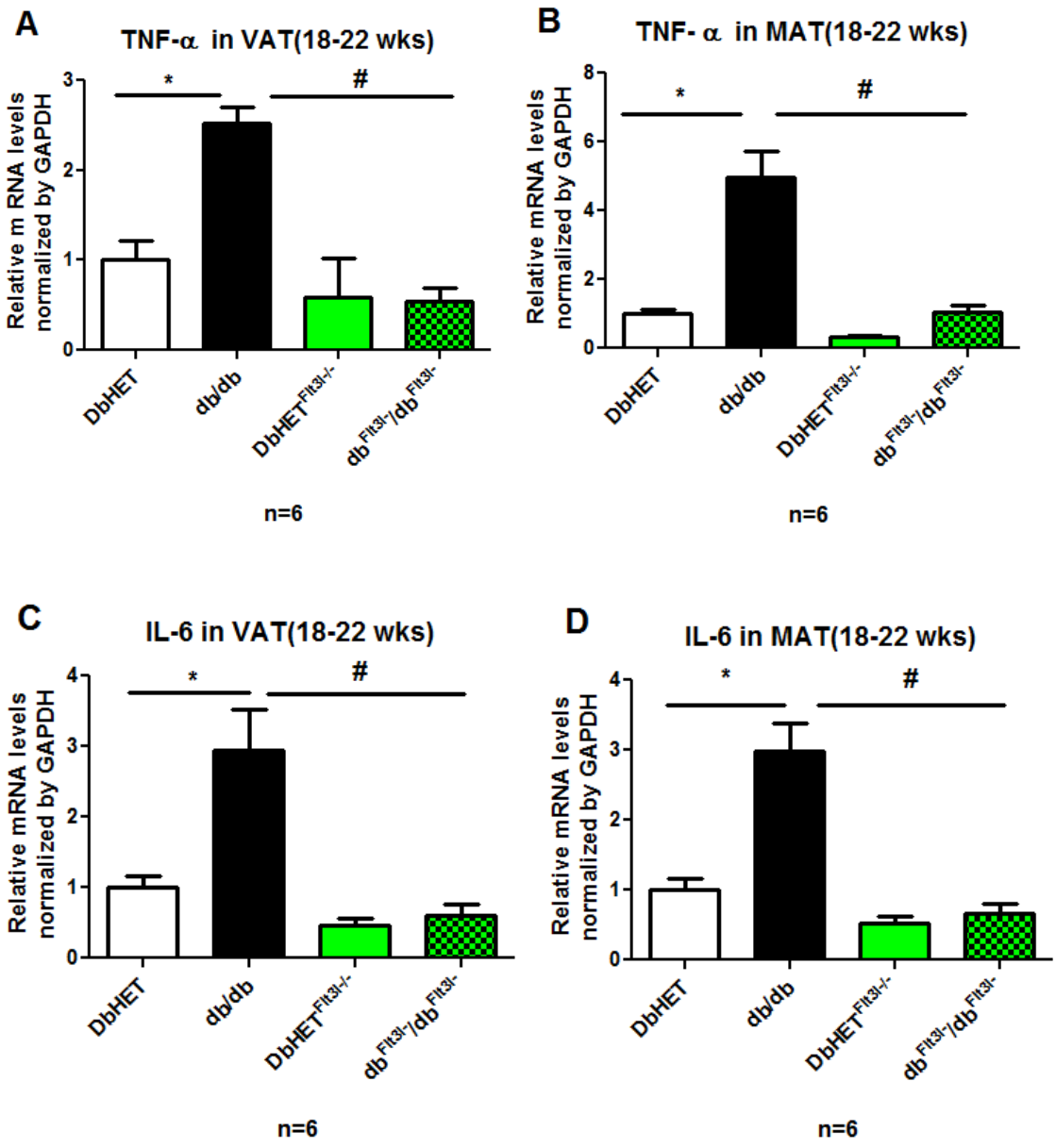
A
TNF-α in VAT(18-22 wks)
Relative m RNA levels normalized by GAPDH
*
#
DbHET
db/db
DbHET Flt3l-/-
db Flt3l-/db Flt3l-
n=6
B
TNF- α in MAT(18-22 wks)
Relative mRNA levels normalized by GAPDH
*
#
DbHET
db/db
DbHET Flt3l-/-
db Flt3l-/db Flt3l-
n=6
C
IL-6 in VAT(18-22 wks)
Relative mRNA levels normalized by GAPDH
*
#
DbHET
db/db
DbHET Flt3l-/-
db Flt3l-/db Flt3l-
n=6
D
IL-6 in MAT(18-22 wks)
Relative mRNA levels normalized by GAPDH
*
#
DbHET
db/db
DbHET Flt3l-/-
db Flt3l-/db Flt3l-
n=6

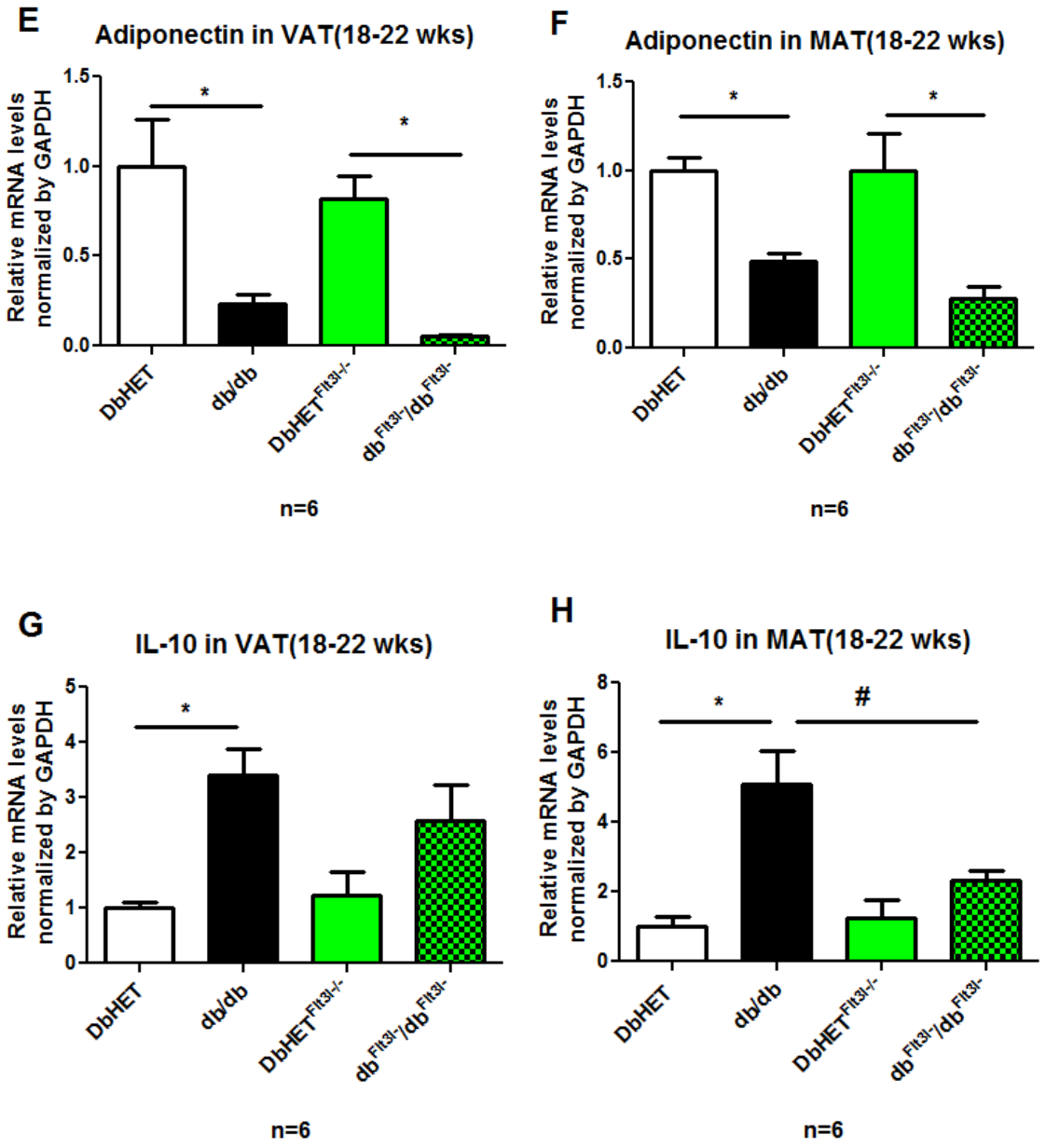

Figure. 3-7. mRNA expressions of inflammatory factors in VAT and MAT from DbHET, *db/db*, DbHET $^{Flt3l-/-}$ and *db* $^{Flt3l-}$/ *db* $^{Flt3l-}$ mice (at 18-22 weeks). Panels A-D showed increased TNF-α **(A-B)** and IL-6 **(C-D)** mRNA levels were found in VAT and MAT from *db/db* mice, compared to DbHET mice. Flt3l depletion significantly decreased TNF-α and IL-6 mRNA levels in diabetic VAT and MAT. Panels **E-F** showed decreased adiponectin mRNA levels in both VAT and MAT from *db/db* mice, compared to DbHET mice. However, Flt3l depletion did not restore adiponectin production in diabetic mice. Panels **G-H** showed increased IL-10 mRNA levels in VAT and MAT from *db/db* mice, compared to DbHET mice. Flt3l depletion significantly reduced IL-10 levels only in diabetic MAT. Data were shown as mean ± SEM. *, #: $P < 0.05$.

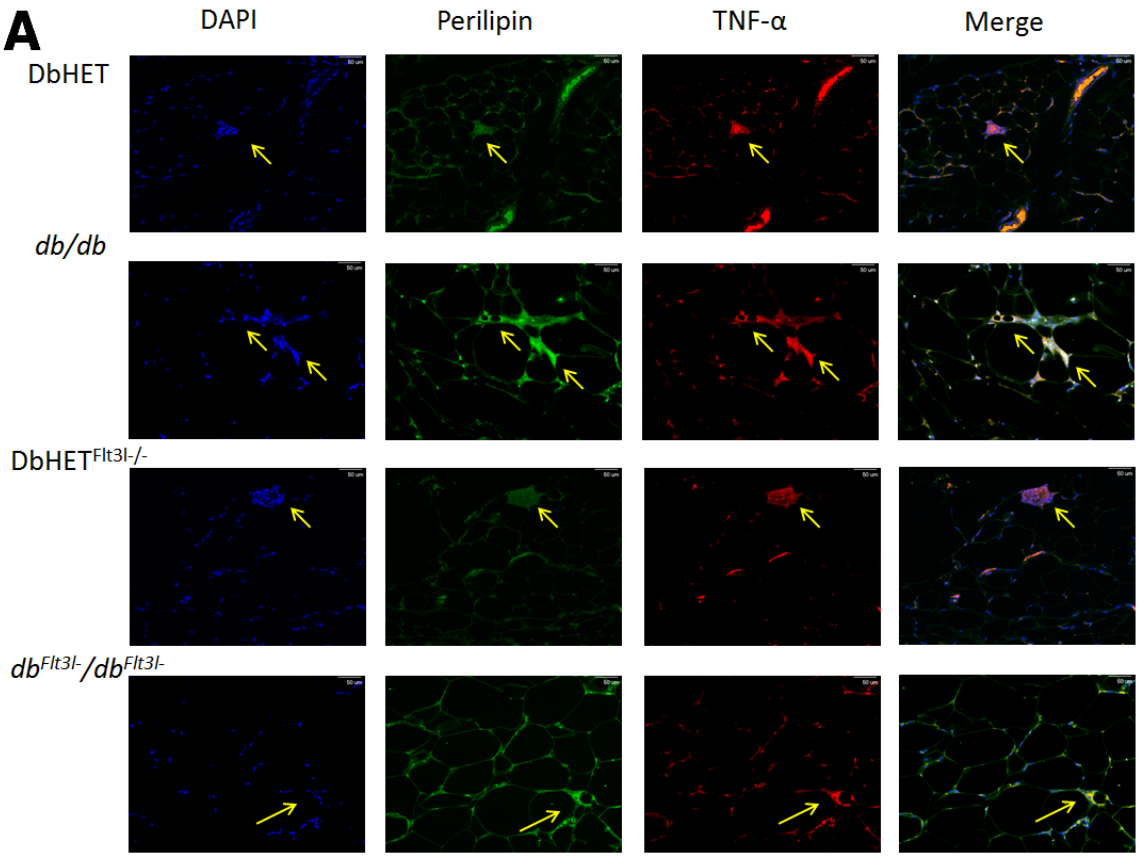
A
DAPI
Perilipin
TNF-α
Merge
DbHET
db/db
DbHET Flt3l-/-
db Flt3l-/db Flt3l-

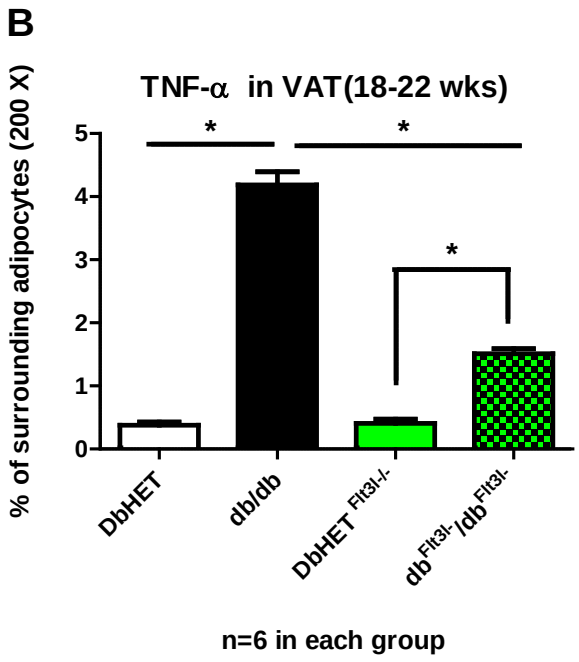
B
TNF-α in VAT(18-22 wks)
% of surrounding adipocytes (200 X)
0
1
2
3
4
5
*
*
*
DbHET
db/db
DbHET Flt3l-/-
db Flt3l-/db Flt3l-
n=6 in each group

Figure.3-8. TNF-α protein levels in VAT from DbHET, *db/db,* DbHET $^{Flt3l-/-}$ and *db*$^{Flt3l-}$/ *db*$^{Flt3l-}$ mice (at 18-22 weeks). (A) Immunofluorescent staining for perilipin and TNF-α in VAT. More TNF-α positive signals were found in *db/db* mice, compared to DbHET mice. However, depletion of dendritic cells significantly reduced TNF-α protein levels in *db*$^{Flt3l-}$/ *db*$^{Flt3l-}$ mice, compared to *db/db* mice. Nuclei were stained by DAPI while the outline of adipocytes was stained by perilipin. **(B)** Quantification of TNF-α positive signals in experimental groups of mice. Note that *db*$^{Flt3l-}$/ *db*$^{Flt3l-}$ mice produced more TNF-α than DbHET$^{Flt3l-/-}$ mice. No difference in TNF-α protein levels was observed between DbHET and DbHET$^{Flt3l-/-}$ mice. Data were shown as mean ± SEM. *: $P < 0.05$.

Effect of dendritic cell depletion in T2DM on vascular function

To investigate the effects of dendritic cell depletion on vascular function in T2DM, MAs from DbHET, *db/db,* DbHET $^{Flt3l-/-}$ and *db*$^{Flt3l-}$/ *db*$^{Flt3l-}$ mice (at 6-10 and 18-22 weeks) were examined by wire myograph. As shown in **Fig.3-9-A**, DbHET control mice show similar ACh-induced endothelial dependent vasorelaxation at 6-10 and 18-22 weeks. There was no significant difference in ACh-induced vasorelaxation between *db/db* and control mice at age 6-10 weeks. However, *db/db* mice at 18-22 weeks exhibited severely impaired ACh induced vasorelaxation in comparison with their corresponding controls (**Fig.3-9-A**). Thus, a progressive impairment of MA ACh-induced vasorelaxation was observed in the T2DM mice. In contrast to the impaired dilator response, there were no significant differences in PE-induced vasoconstriction between DbHET controls and *db/db* mice at either 6-10 or 18-22 weeks of age (**Fig.3-9-B).**

In additional studies, we investigated whether dendritic cell depletion in PVAT would affect vascular function of MA from DbHET and *db/db* mice (at both 6-10 and 18-22 weeks). At 6-10 weeks**,** there was no significant difference in ACh-induced vasorelaxation between DbHET and DbHET $^{Flt3l-/-}$ mice (**Fig.3-9-E)**. However, after dendritic cell depletion, *db*$^{Flt3l-}$/ *db*$^{Flt3l-}$ mice displayed significantly improved ACh-induced vasorelaxation relative to *db/db* mice. As shown in **Fig.3-9-G,** at 18-22 weeks there was still no significant difference in ACh-induced vasorelaxation between DbHET and DbHET $^{Flt3l-/-}$ mice. However, *db*$^{Flt3l-}$/ *db*$^{Flt3l-}$ mice showed restored ACh-induced vasorelaxation, compared to *db/db* mice. No significant difference of ACh-induced vasorelaxation was observed between DbHET $^{Flt3l-/-}$ and *db*$^{Flt3l-}$/ *db*$^{Flt3l-}$ mice at either 6-10 or 18-22

weeks (**Fig.3-9-C)**. Thus, dendritic cell depletion significantly restored ACh-induced vasorelaxation in *db/db* mice.

In regard to vasoconstrictor responses, no significant differences in PE-induced constriction were detected amongst DbHET, *db/db,* DbHET $^{Flt3l-/-}$ and db^{Flt3l-}/ db^{Flt3l-} mice at 6-10 weeks (**Fig.3-9-F)**. At 18-22 weeks**,** db^{Flt3l-}/ db^{Flt3l-} mice showed reduced PE-induced vasoconstriction compared to DbHET, *db/db* and DbHET $^{Flt3l-/-}$ mice (**Fig.3-9-H)**. Moreover, db^{Flt3l-}/db^{Flt3l-} mice at 18-22 weeks displayed reduced PE-induced vasoconstriction compared to db^{Flt3l-}/db^{Flt3l-} mice at 6-10 weeks (**Fig.3-9-D)**. Thus, depletion of dendritic cells did not affect PE induced vasoconstriction on MA in the early stage of T2DM, but significantly reduced vasoconstriction response in the late stage of T2DM. Taken together, in the duration of T2DM, ACh induced vasorelaxation was progressively impaired on MA, whereas PE induced vasoconstriction was not affected. However, dendritic cell depletion significantly restored vasorelaxation on MA in the duration of T2DM.

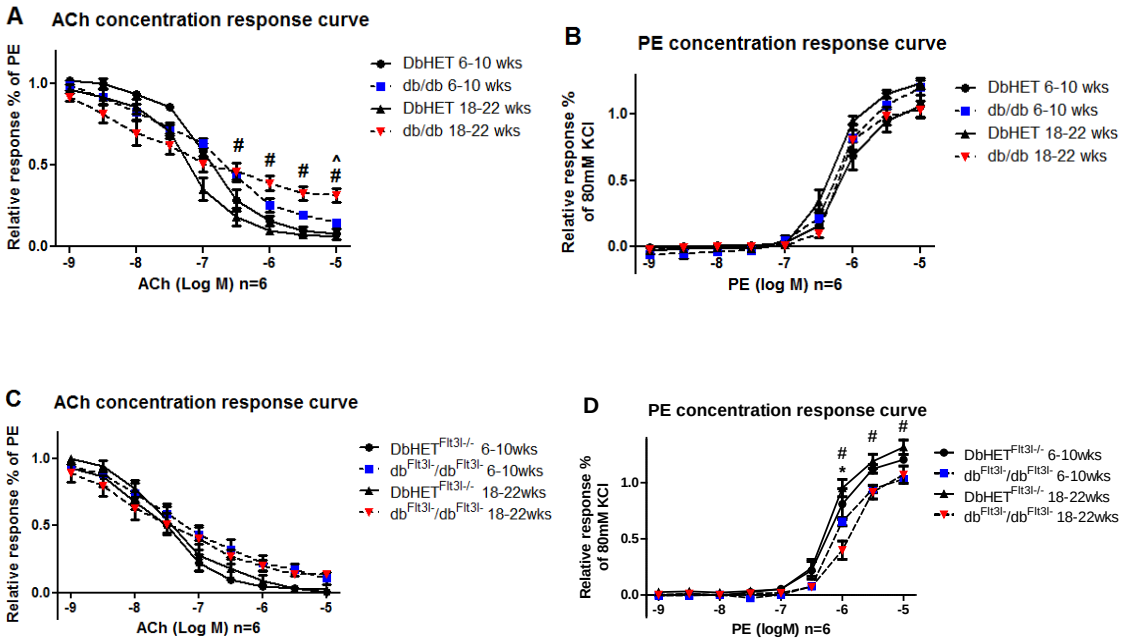

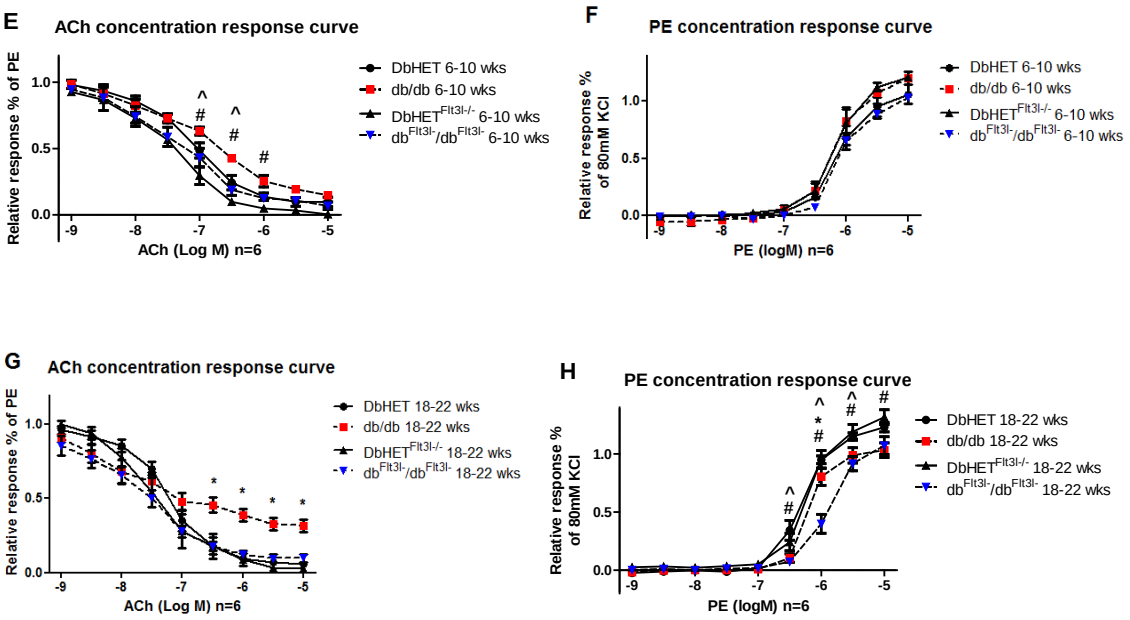

Figure. 3-9. ACh and PE concentration-response curves for MA from DbHET, *db/db,* DbHET $^{Flt3l-/-}$ and *db* $^{Flt3l-}$*/ db* $^{Flt3l-}$ mice at both 6-10 and 18-22 weeks of age. (A) *db/db* mice at 18-22 weeks had impaired ACh induced vasorelaxation response compared to DbHET mice and *db/db* mice at 6-10 weeks. #: $P < 0.05$. *db/db* mice at 18-22 weeks v.s. DbHET mice at 18-22 weeks. ^: $P < 0.05$. *db/db* mice at 18-22 weeks v.s. *db/db* mice at 6-10 weeks. **(B-C, F)** There was no significant difference of vasomotor response among all the four groups. **(D)** *db* $^{Flt3l-}$*/db* $^{Flt3l-}$ mice at 18-22 weeks presented reduced PE induced vasoconstriction in comparison with other mice. *: $P < 0.05$. *db* $^{Flt3l-}$ */db* $^{Flt3l-}$ mice at 18-22 weeks v.s. *db* $^{Flt3l-}$*/db* $^{Flt3l-}$ mice at 6-10 weeks. #: $P < 0.05$. *db* $^{Flt3l-}$ */db* $^{Flt3l-}$ mice at 18-22 weeks v.s. DbHET mice at 18-22 weeks. **(E)** DbHET $^{Flt3l-/-}$ and *db* $^{Flt3l-}$ */db* $^{Flt3l-}$ mice displayed better ACh induced vasorelaxation response than *db/db* mice at 6-10 weeks. #: $P < 0.05$. *db/db* mice v.s. DbHET $^{Flt3l-/-}$ mice. ^: $P < 0.05$. *db/db* mice v.s. *db* $^{Flt3l-}$*/db* $^{Flt3l-}$ mice. **(G)** *db/db* mice at 18-22 weeks had impaired ACh induced vasorelaxation. *: $P < 0.05$. *db/db* mice v.s. DbHET, DbHET $^{Flt3l-/-}$ and *db* $^{Flt3l-}$*/db* $^{Flt3l-}$ mice. **(H)** *db* $^{Flt3l-}$*/db* $^{Flt3l-}$ mice at 18-22 weeks displayed reduced PE induced vasoconstriction. #: $P < 0.05$. *db* $^{Flt3l-}$*/db* $^{Flt3l-}$ mice v.s. DbHET $^{Flt3l-/-}$ mice. *: $P < 0.05$. *db* $^{Flt3l-}$*/db* $^{Flt3l-}$ mice v.s. *db/db* mice. ^: $P < 0.05$. *db* $^{Flt3l-}$*/db* $^{Flt3l-}$ mice v.s. DbHET mice. All data was analyzed by Two-way ANOVA.

Effect of MAT incubation on vascular reactivity in DbHET mice at 6-10 and 18-22 weeks

Studies have shown that under physiological conditions, PVAT exerts an anti-contractile action on the adjacent vasculature (Fernández-Alfonso, Gil-Ortega et al. 2013, Even, Dulak-Lis et al. 2014). This effect of adipose tissue is considered to be mediated via paracrine and/or endocrine mechanisms. However, it is unclear whether this anti-contractile property is present in *db/db* and DbHET mice. Also, it is still unknown that whether this effect is age-dependent. To address these questions, first order MAs from DbHET mice were prepared and divided into two groups: namely, a time control and one co-incubation with MAT. Both groups subjected to cumulative concentrations of ACh and PE at 3 time points: 1. before MAT incubation, 2. after 1 hour MAT incubation and 3. after 1 hour of washout. DbHET mice were subdivided into 6-10 and 18-22 weeks groups similarly to previous experiments. As shown in **Fig.3-10-B and Fig.3-11-B**, 1 hour exposure to MAT significantly enhanced ACh-induced relaxation in MA from DbHET mice at both ages. This was reflected by a significant difference of logEC50 values between time control and MAT incubation (**Fig.3-10-D and Fig.3-11-D)**. Further, 1 hour exposure to MAT also significantly reduced PE-induced vasoconstriction in MA from DbHET mice at both ages (**Fig.3-10-F and Fig. 3-11-F).** A significant difference in logEC50 values between time control and MAT incubation supported the anti-contractile property of MAT from DbHET mice, shown in **Fig.3-10-H and Fig. 3-11-H.** Collectively, MAT from DbHET mice enhanced vasorelaxation and maintained its anti-contractile property, which was not affected by the age. Moreover, those effects from MAT were reversed by washing.

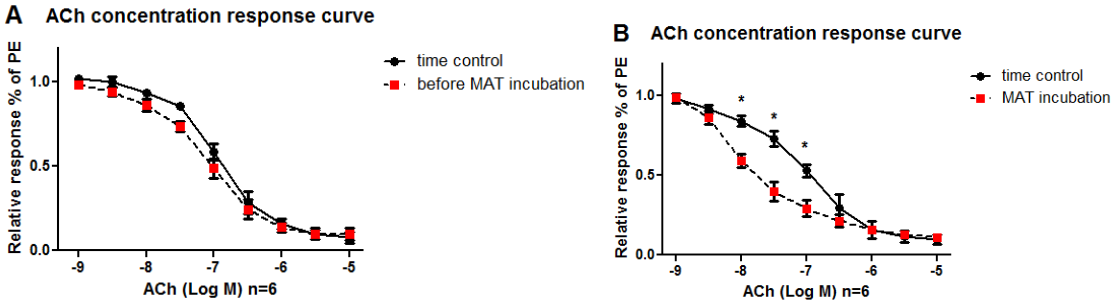

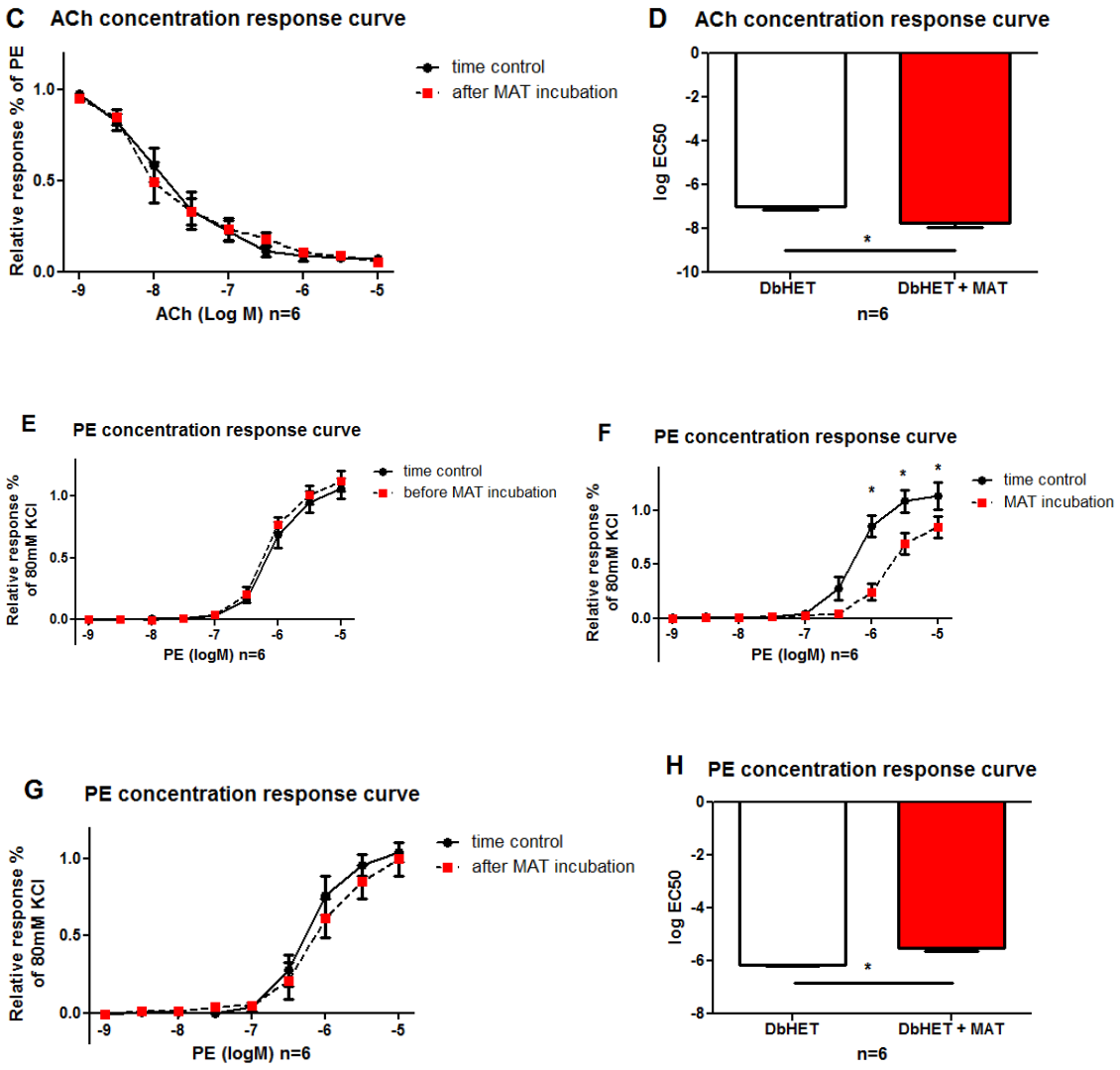

Figure. 3-10. ACh and PE concentration-response curves: effect of MAT co-incubation in DbHET mice (6-10 weeks). (A and **E)** There were no significant differences in ACh **(A)** or PE **(E)** concentration response between time control and MA intended for MAT incubation, termed “before MAT incubation”. **(B** and **F)** following 1 hour MAT co-incubation, MA rings exhibited enhanced ACh-induced vasorelaxation **(B)** and reduced PE-induced vasoconstriction responses **(F)**, compared to the time control in the absence of MAT. **(C** and **G).** After repeated washing (every 10 minutes for 1 hour) of ring segments exposed to MAT, ACh-induced vasorelaxation **(C)** and PE-induced vasoconstriction **(G)** were similar to those of time controls. **(D** and **H)** MA with MAT incubation showed significantly different LogEC50 values for ACh **(D)** and PE **(H)** concentration response curves compared to time controls. *: $P < 0.05$. Panels **(B)** and **(F),** Two-way ANOVA; Panels **(D)** and **(H)**, student *t*-test. All data are presented as mean± SEM.

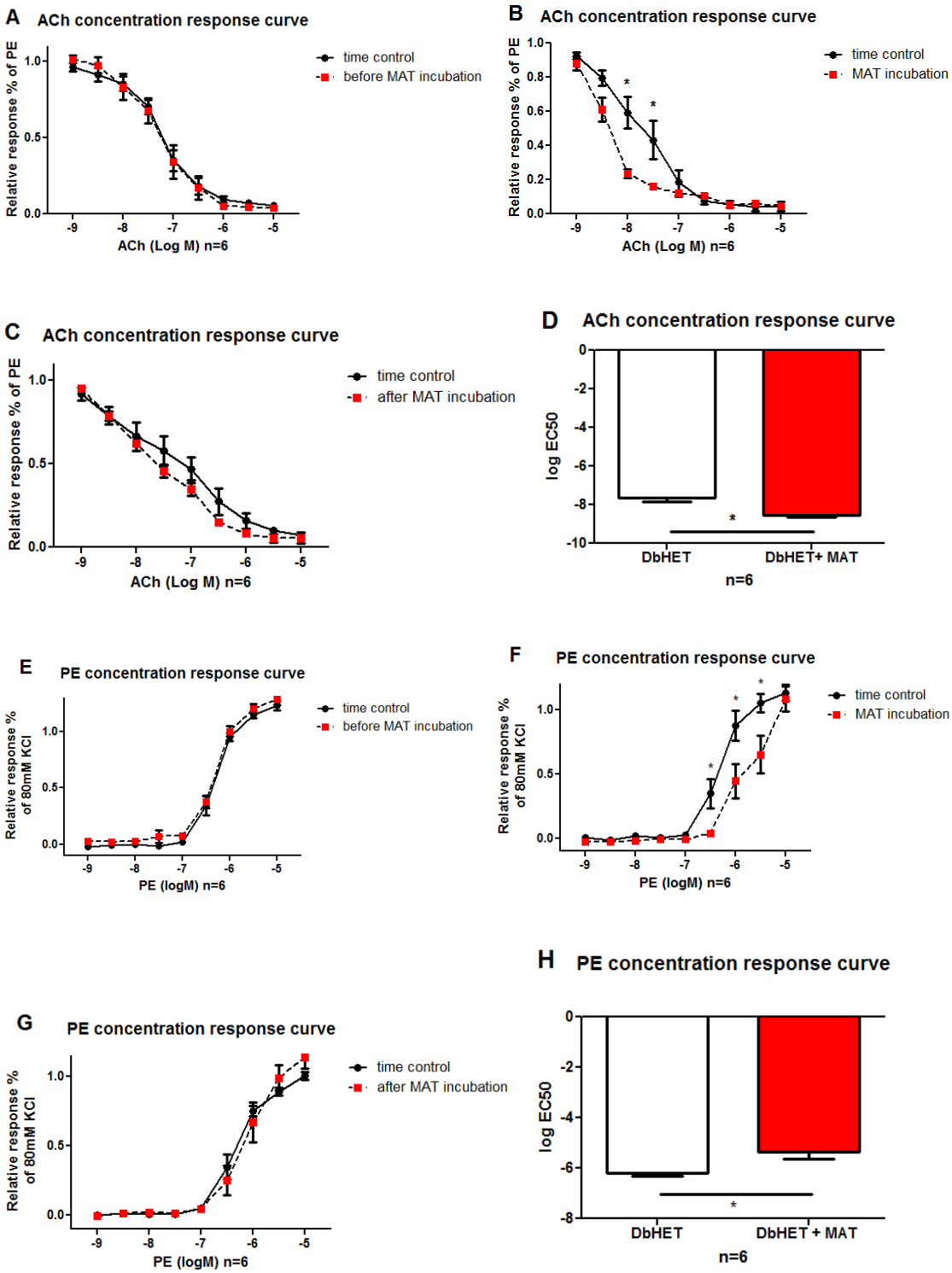
A
ACh concentration response curve
Relative response % of PE
ACh (Log M) n=6
time control
before MAT incubation
B
ACh concentration response curve
Relative response % of PE
ACh (Log M) n=6
time control
MAT incubation
C
ACh concentration response curve
Relative response % of PE
ACh (Log M) n=6
time control
after MAT incubation
D
ACh concentration response curve
log EC50
DbHET
DbHET+ MAT
n=6
E
PE concentration response curve
Relative response % of 80mM KCl
PE (logM) n=6
time control
before MAT incubation
F
PE concentration response curve
Relative response % of 80mM KCl
PE (logM) n=6
time control
MAT incubation
G
PE concentration response curve
Relative response % of 80mM KCl
PE (logM) n=6
time control
after MAT incubation
H
PE concentration response curve
log EC50
DbHET
DbHET + MAT
n=6

Figure. 3-11. ACh and PE concentration-response curves: effect of MAT co-incubation in DbHET mice (18-22 weeks). (A and **E)** There was no significant difference of ACh induced vasorelaxation**(A)** or PE induced vasoconstriction **(E)** response between time control and "before MAT incubation" group. **(B** and **F)** Significant increase of ACh induced vasorelaxation **(B)** and reduction of PE induced vasoconstriction **(F)** responses were observed in MAT incubation group. **(C** and **G).** After repeated washing (every 10 minutes for 1 hour) of ring segments exposed to MAT, ACh-induced vasorelaxation **(C)** and PE-induced vasoconstriction **(G)** were similar to those of time controls. **(D** and **H)** MA with MAT incubation showed significantly different LogEC50 values for ACh **(D)** and PE **(H)** concentration response curves compared to time controls. *: $P < 0.05$. In **(B)** and **(F)** panels**,** Two-way ANOVA. In **(D)** and **(H)** panels, student *t*-test. All data presented as mean± SEM.

Effect of MAT incubation on vascular reactivity in db/db mice at 6-10 and 18-22 weeks

Published studies have shown that the anti-contractile function derived from PVAT is impaired in obese animal models (Meijer, Serne et al. 2011, Lastra and Manrique 2015). Moreover, a recent investigation has also revealed that insulin-induced vasodilation of muscle resistance arteries was abrogated by the presence of PVAT from *db/db* mice (Meijer, Bakker et al. 2013). On the basis of above evidence, it was considered possible that MAT from *db/db* mice would abolish the anti-contractile property and the enhancement of vasorelaxation on MA from *db/db* mice. Since T2DM is a chronic progressive disease, it was also considered that the influence of MAT from *db/db* mice may exhibit a progressive nature. To confirm these hypotheses, the same study protocol as DbHET mice was adopted in the following experiments. *db/db* mice were divided into 6-10 and 18-22 weeks age groups. As shown in **Fig.3-12,** 1 hour MAT co-incubation did not affect ACh-induced vasorelaxation (**Fig.3-12-B**) or PE-induced vasoconstriction (**Fig.3-12-F**) responses compared to time controls in *db/db* mice at 6-10 weeks. Calculation of logEC50 values (**Fig.3-12-D and H)** further supported the above findings. After washing, no significant differences in ACh-induced vasorelaxation (**Fig.3-12-C**) or PE-induced vasoconstriction (**Fig.3-12-G**) responses were observed between time control and MAT incubation MA. Similarly, 1 hour MAT incubation still did not change ACh induced vasorelaxation and PE induced vasoconstriction in *db/db* mice at 18-22 weeks, shown in **Fig. 3-13.** Collectively,

db/db mice at both 6-10 and 18-22 weeks did not exhibit the anti-contractile property and enhancement of ACh induced vasorelaxation derived from MAT.

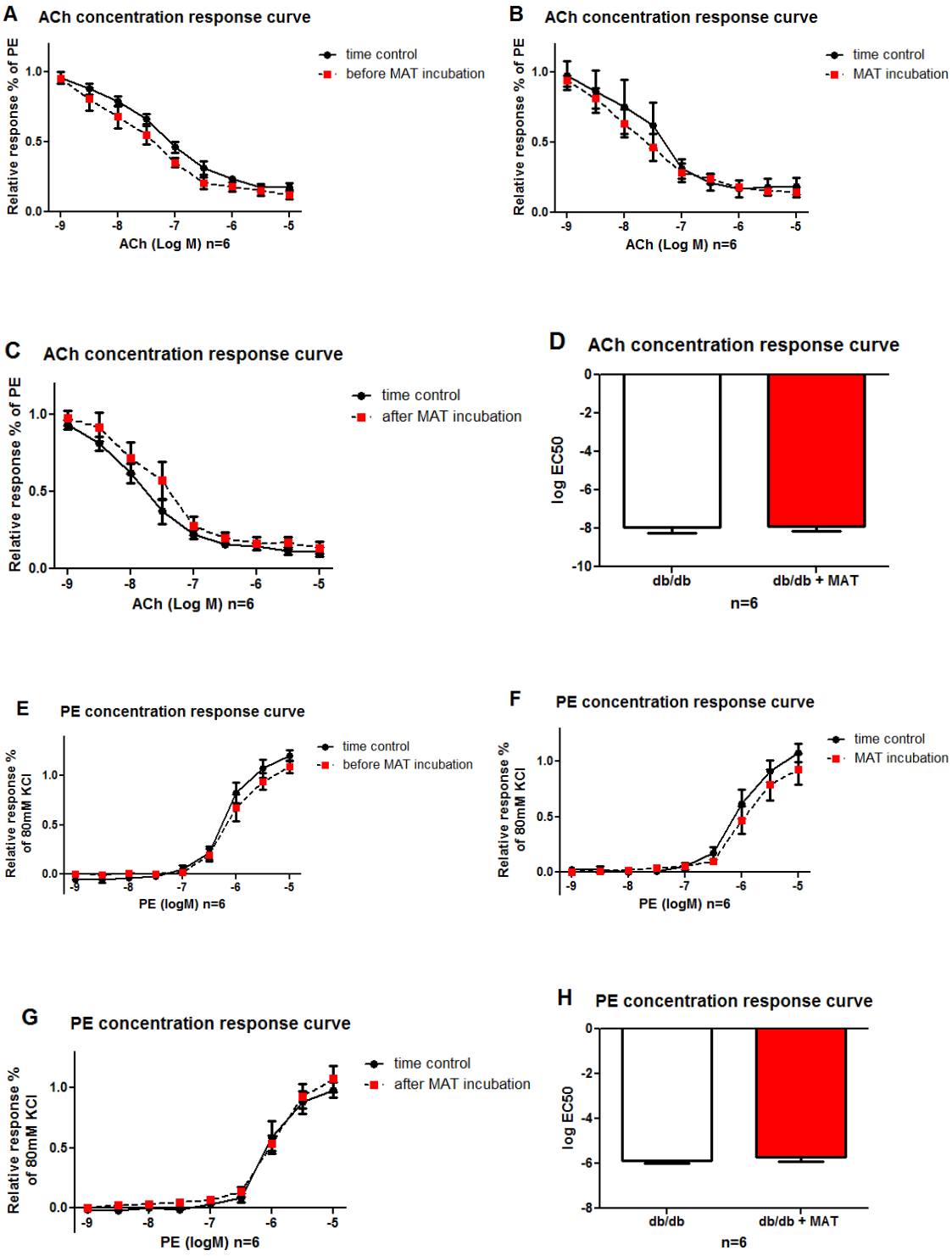

Figure.3-12. ACh and PE concentration response curves – effect of MAT co-incubation in *db/db* mice (6-10 weeks). (A and **E)** There was no significant difference of ACh **(A)** or PE**(E)** concentration response curve between time control and "before MAT incubation" group. **(B** and **F)** There was still no significant difference of ACh induced vasorelaxation **(B)** or PE induced vasoconstriction **(F)** response between time control and MAT incubation group. **(C** and **G)** After repeated washing (every 10 minutes for 1 hour) of ring segments, ACh-induced vasorelaxation **(C)** and PE-induced vasoconstriction **(G)** were similar to those of time controls. **(D** and **H)** No significant logEC50 difference of ACh **(D)** or PE **(H)** concentration response curve was observed between time control and MAT incubation. All data presented as mean± SEM.

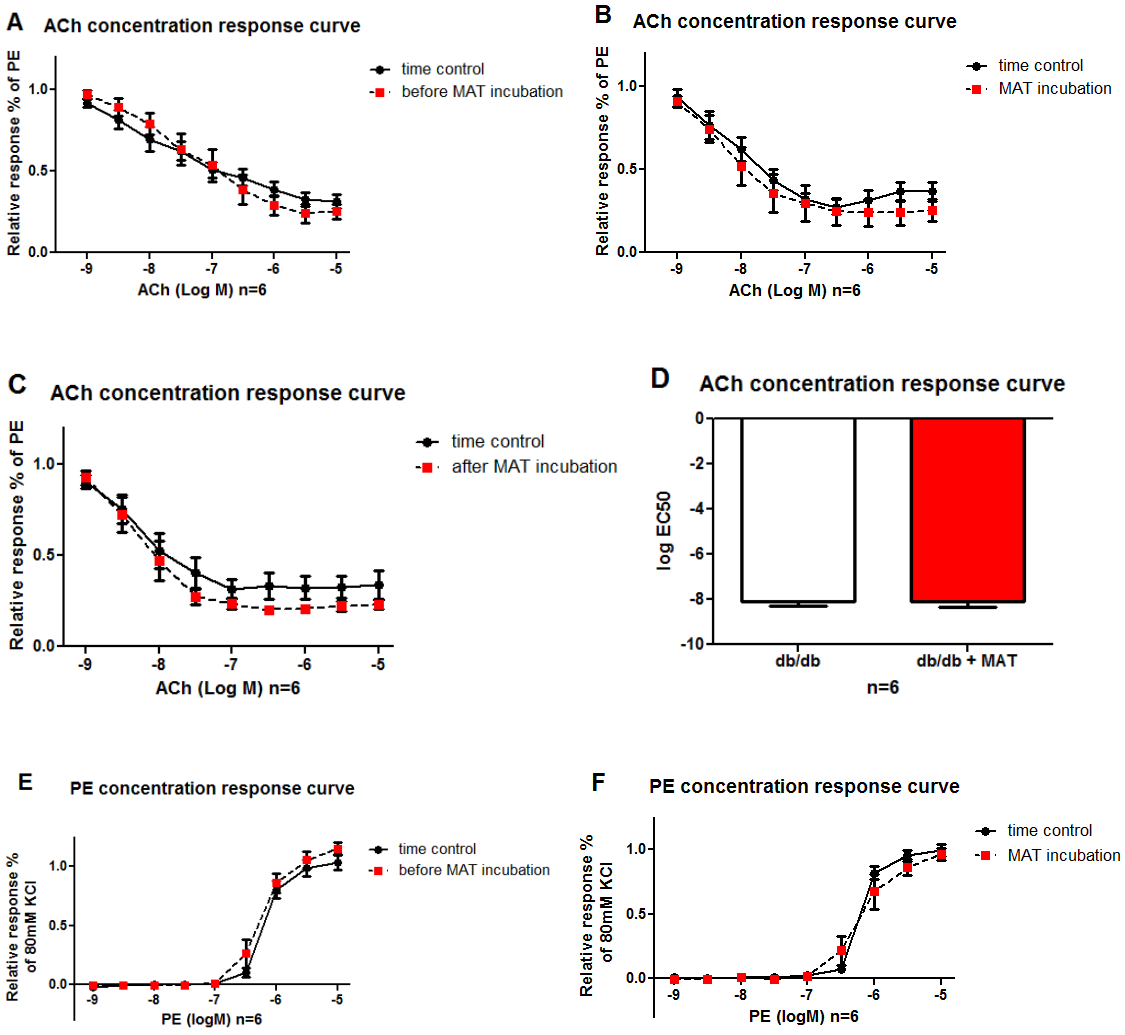

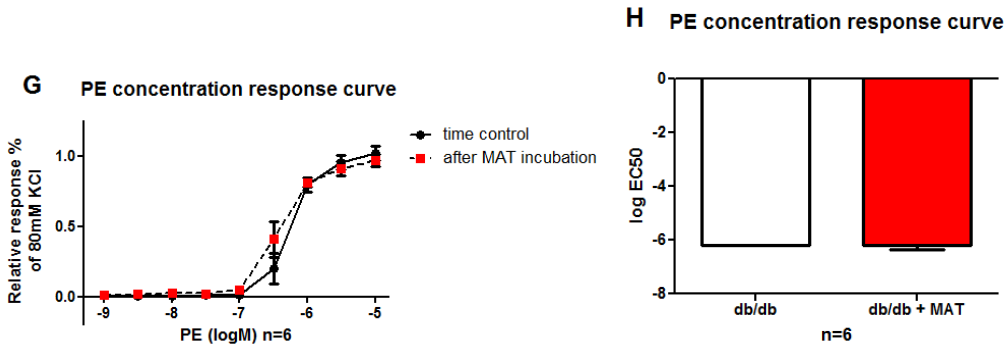

Figure.3-13. ACh and PE concentration-response curves: effect of MAT co-incubation in *db/db* mice (18-22 weeks). (A and **E)** There was no significant difference of ACh **(A)** or PE **(E)** concentration response curve between time control and "before MAT incubation" MA. **(B** and **F)** There was no significant difference of ACh induced vasorelaxation **(B)** or PE induced vasoconstriction **(F)** response between time control and MAT incubation MA. **(C** and **G)** After 1 hour washing procedure, ACh-induced vasorelaxation **(C)** and PE-induced vasoconstriction **(G)** were similar to those of time controls. **(D** and **H)** No significant logEC50 difference of ACh **(D)** or PE **(H)** concentration response curve was observed between time control and MAT incubation. All data presented as mean± SEM.

Effect of MAT incubation on vascular reactivity in DbHET $^{Flt3l-/-}$ mice at 6-10 and 18-22 weeks

Our earlier data showed that VAT from DbHET $^{Flt3l-/-}$ mice was deficient of dendritic cells. This raises the question as to whether dendritic cell depletion in adipose tissue would affect the vascular function in DbHET $^{Flt3l-/-}$ mice. In order to address this, the vascular function protocol, used above, was applied to studies of DbHET $^{Flt3l-/-}$ mice at both 6-10 and 18-22 weeks. 1 hour MAT co-incubation from DbHET $^{Flt3l-/-}$ mice at both 6-10 (**Fig.3-14**) and 18-22 (**Fig.3-15**) weeks significantly enhanced ACh induced vasorelaxation and reduced PE induced vasoconstriction. Calculated logEC50 values for both ACh (**Fig.3-14-D and Fig.3-15-D**) and PE concentration-response curves (**Fig.3-14-H and Fig. 3-15-H**) showed significant differences between time control and MAT incubation, supporting the above findings. The 1 hour wash procedure abolished the differences between time controls and arterial rings undergoing MAT incubation at both 6-10 (**Fig.3-14-C** and **G**) and 18-22(**Fig.3-15-C** and **G**) weeks. Collectively, MAT from DbHET $^{Flt3l-/-}$ mice at both 6-10 and 18-22 weeks enhanced vasorelaxation and exhibited anti-contractile

property, which could be removed by washing. These findings were, therefore, considered to be similar to DbHET mice.

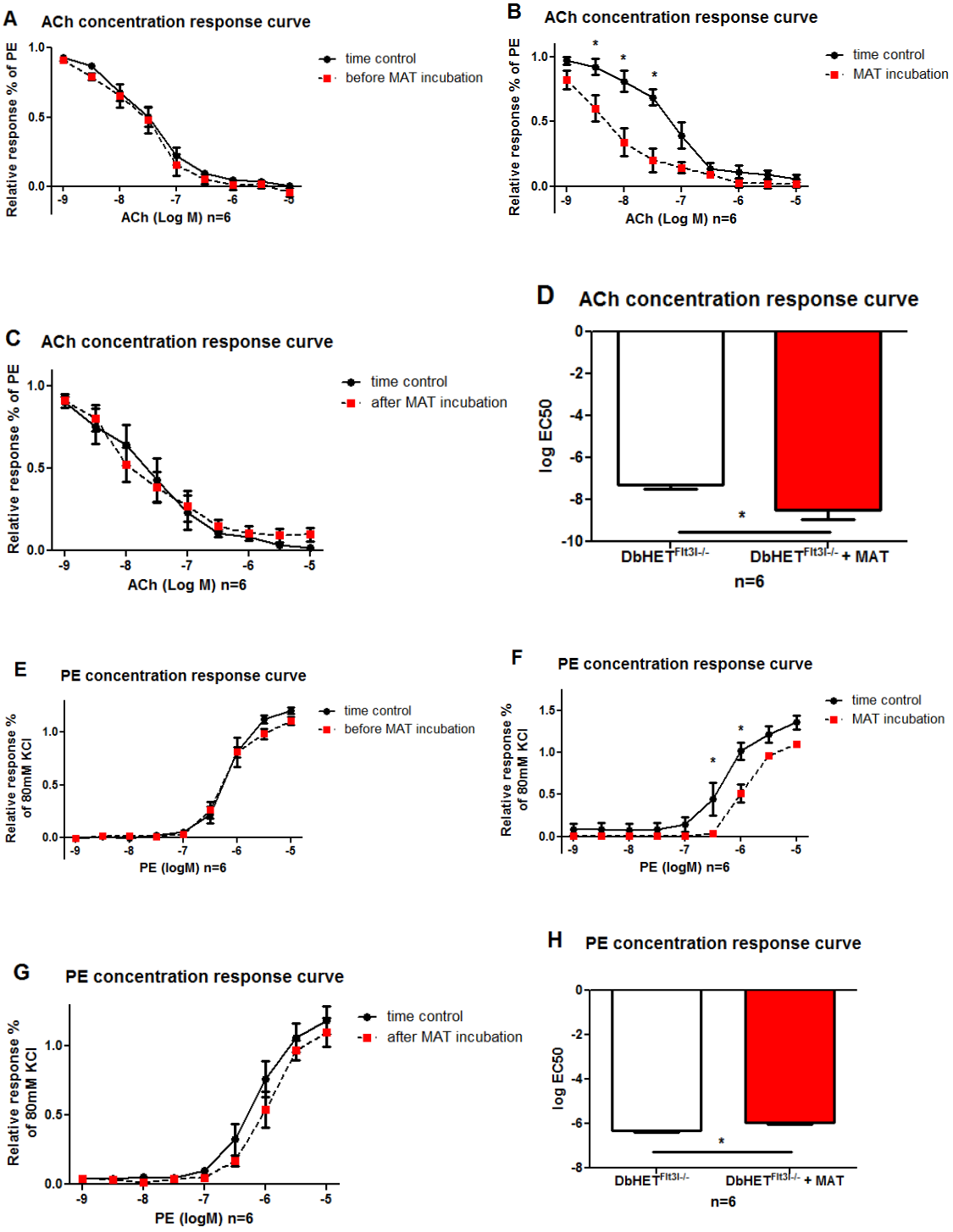

Figure.3-14. ACh and PE concentration-response curves: effect of MAT co-incubation in DbHET $^{Flt3l-/-}$ mice (6-10 weeks). (A and **E)** There was no significant difference of ACh **(A)** or PE **(E)** concentration response curve between time control and "before MAT incubation" MA. **(B** and **F)** Significant increase of ACh induced vasorelaxation **(B)** and reduction of PE induced vasoconstriction **(F)** responses were found in MAT incubation group. **(C** and **G)** After repeated 1 hour washing of ring segments exposed to MAT, ACh-induced vasorelaxation **(C)** and PE-induced vasoconstriction **(G)** were similar to those of time controls. **(D** and **H)** MA with MAT incubation showed significantly different LogEC50 values for ACh **(D)** and PE **(H)** concentration response curves compared to time controls. *: $P < 0.05$. In **(B)** and **(F)** panels**,** Two-way ANOVA. In **(D)** and **(H)** panels, student *t*-test. All data presented as mean± SEM.

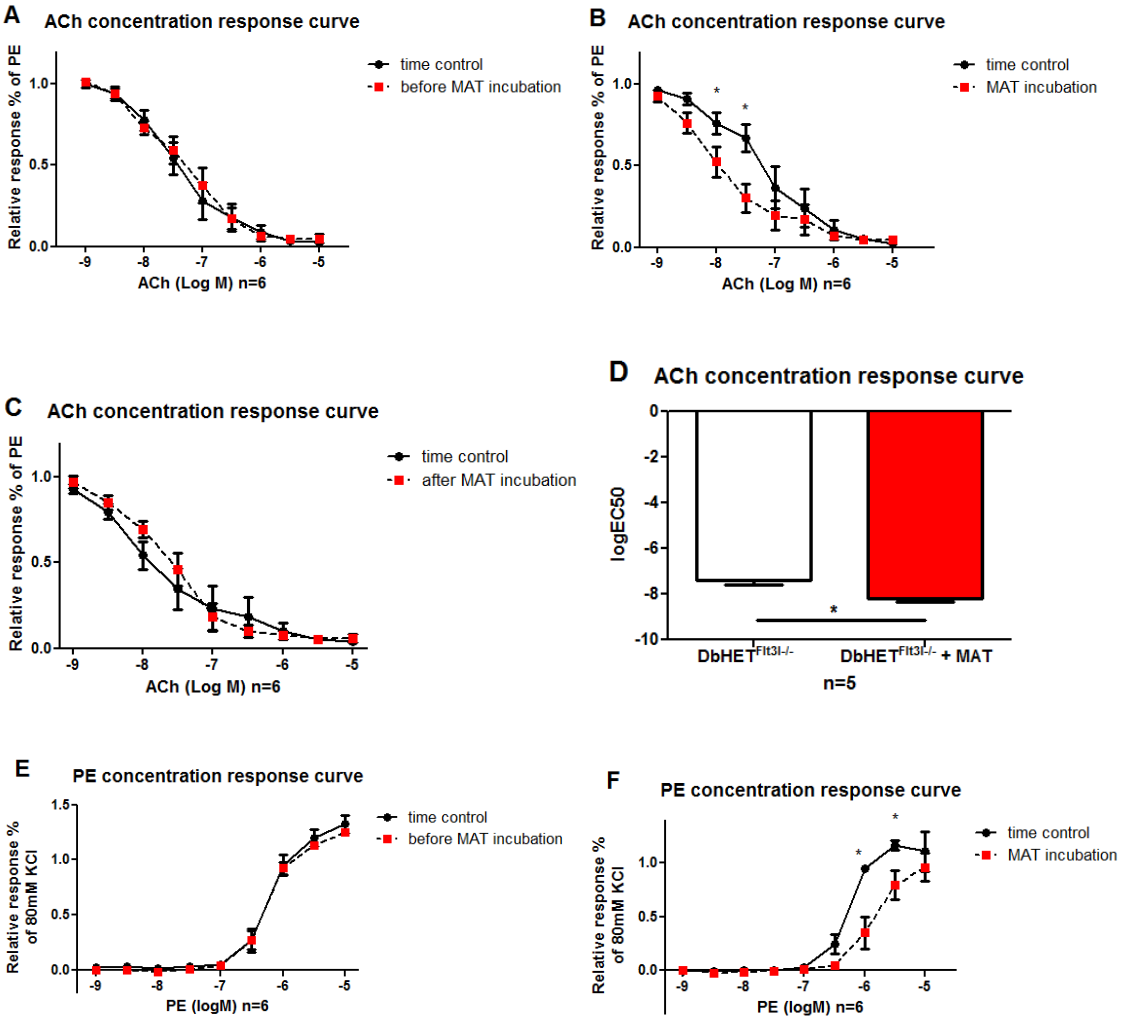

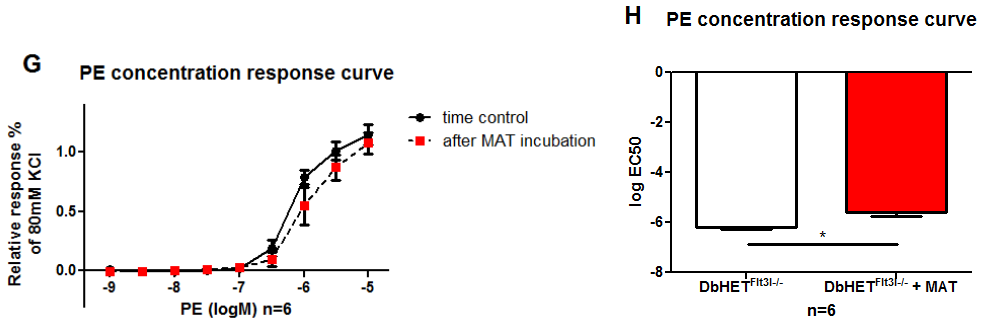

Figure.3-15. ACh and PE concentration-response curves: effect of MAT co-incubation in DbHET $^{Flt3l-/-}$ mice (18-22 weeks). (A and **E)** There was no significant difference of ACh **(A)** or PE **(E)** concentration response curve between time control and "before MAT incubation" MA. **(B** and **F)** Significant increase of ACh induced vasorelaxation **(B)** and reduction of PE induced vasoconstriction **(F)** responses were found in MAT incubation group. **(C** and **G)** After repeated 1 hour washing of ring segments exposed to MAT, ACh-induced vasorelaxation **(C)** and PE-induced vasoconstriction **(G)** were similar to those of time controls. **(D** and **H)** MA with MAT incubation showed significantly different LogEC50 values for ACh **(D)** and PE **(H)** concentration response curves compared to time controls. *: $P < 0.05$. In **(B)** and **(F)** panels**,** Two-way ANOVA. In **(D)** and **(H)** panels, student *t*-test. All data presented as mean± SEM.

Effect of MAT incubation on vascular reactivity in db^{Flt3l-}/db^{Flt3l-} mice at 6-10 and 18-22 weeks

Previous studies have shown that the pro-inflammatory factor TNF-α decreases NO bioavailability and induces the production of reactive oxygen species, leading to endothelial dysfunction in T2DM (Zhang, Park et al. 2009, Zhang and Zhang 2012). Moreover, overproduction of TNF-α and IL-6 contributes to the loss of anti-contractile function of PVAT in a mouse model of obesity (Even, Dulak-Lis et al. 2014). Our previous qPCR data have shown that *db/db* mice had elevated mRNA levels of TNF-α and IL-6 in VAT and MAT. Dendritic cell depletion successfully decreased TNF-α and IL-6 production in both VAT and MAT from *db^{Flt3l-}/db^{Flt3l-}* mice. We therefore hypothesized that dendritic cell depletion would restore anti-contractile activity of MAT in *db/db* mice at both early and late stages of T2DM. In order to confirm this hypothesis, the same vascular function protocol as *db/db* mice was used in studies of *db^{Flt3l-}/db^{Flt3l-}* mice. Shown in **Fig.3-16, a** 1 hour co-incubation with MAT significantly enhanced arterial

ring ACh-induced vasorelaxation (**Fig.3-16-B**) and reduced PE induced vasoconstriction (**Fig.3-16-F**) responses in *db*$^{Flt3l-}$/*db*$^{Flt3l-}$ mice at 6-10 weeks. LogEC50 values for MA ring ACh (**Fig.3-16-D**) and PE (**Fig.3-16-H**) concentration curves showed significant differences between time control and MAT incubation. A 1 hour wash abolished these differences (**Fig.3-16-C** and **G**). Interestingly, *db*$^{Flt3l-}$/*db*$^{Flt3l-}$ mice at 18-22 weeks, 1 hour co-incubation with MAT significantly enhanced arterial ring ACh-induced vasorelaxation (**Fig.3-17-B**), but had no effect on PE induced vasoconstriction (**Fig.3-17-F**), which was supported by the calculation of LogEC50 values **(Fig.3-17-D and H**). The following 1 hour washing abolished those differences (**Fig.3-17-C** and **G**). Collectively, MAT from *db*$^{Flt3l-}$/*db*$^{Flt3l-}$ mice at 6-10 weeks augmented vasorelaxation and maintained anti-contractile activity, in a manner that could be reversed by wash out. However, MAT from *db*$^{Flt3l-}$/*db*$^{Flt3l-}$ mice at 18-22 weeks augmented vasorelaxation that could be abolished by washing, but lost anti-contractile activity, compared to *db*$^{Flt3l-}$/*db*$^{Flt3l-}$ mice at 6-10 weeks.

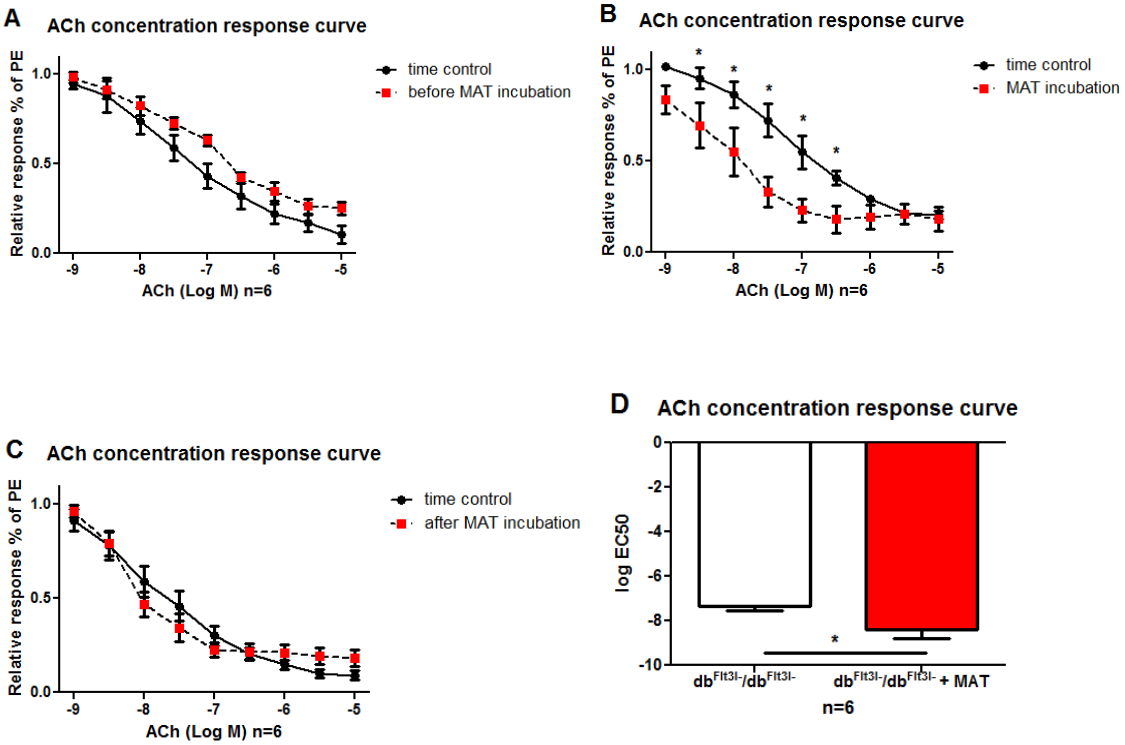

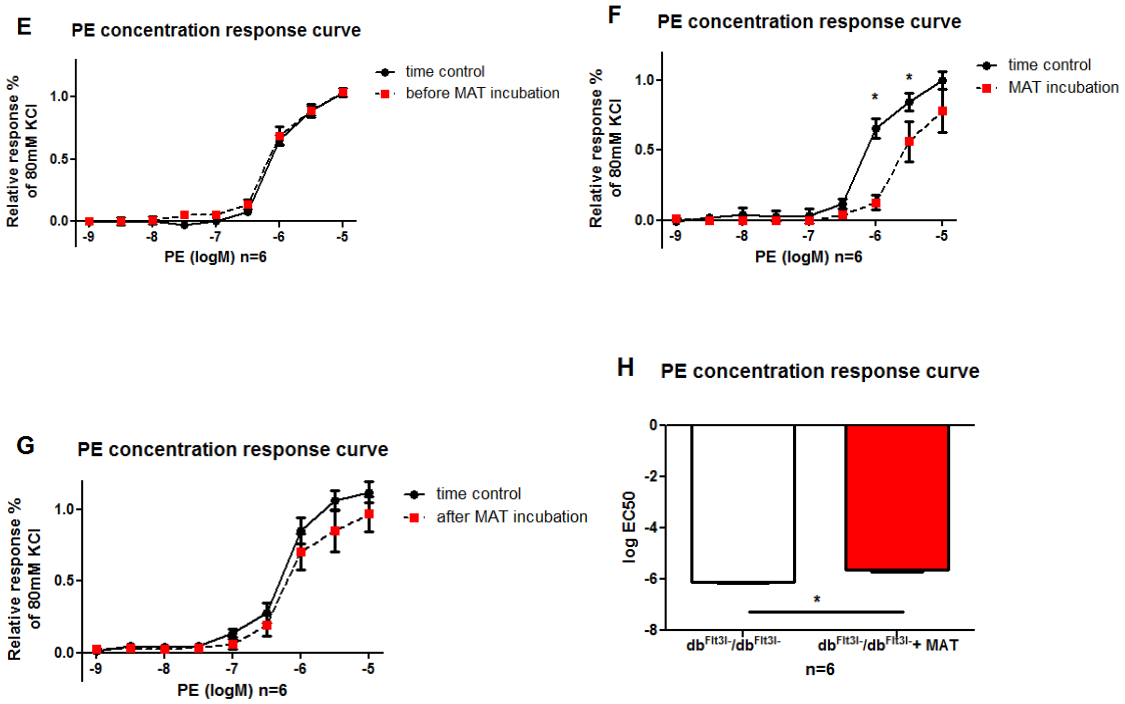

Figure.3-16. ACh and PE concentration-response curves: effect of MAT co-incubation in *db*$^{Flt3l-}$/*db*$^{Flt3l-}$ mice (6-10 weeks). (A and **E)** There was no significant difference of ACh **(A)** or PE **(E)** concentration response curve between time control and "before MAT incubation" MA. **(B** and **F)** Significant increase of ACh induced vasorelaxation **(B)** and reduction of PE induced vasoconstriction **(F)** responses were found in MAT incubation, compared to time control. **(C** and **G)** After repeated 1 hour washing of ring segments exposed to MAT, ACh-induced vasorelaxation **(C)** and PE-induced vasoconstriction **(G)** were similar to those of time controls. **(D** and **H)** MA with MAT incubation showed significantly different LogEC50 values for ACh **(D)** and PE **(H)** concentration response curves compared to time controls. *: $P < 0.05$. In **(B)** and **(F)** panels**,** Two-way ANOVA. In **(D)** and **(H)** panels, student *t*-test. All data presented as mean± SEM.

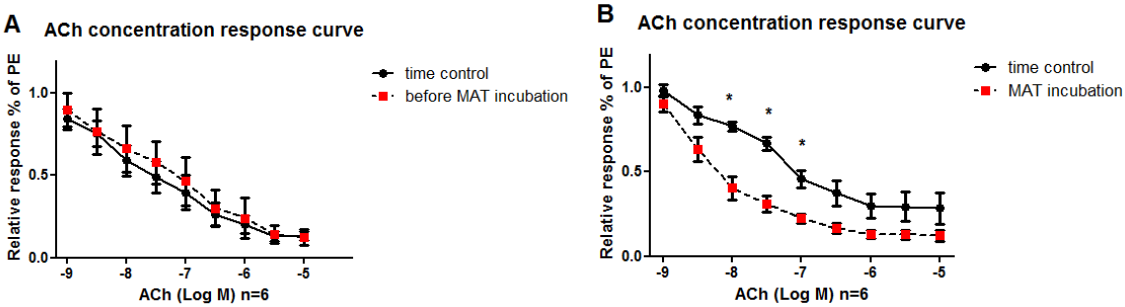

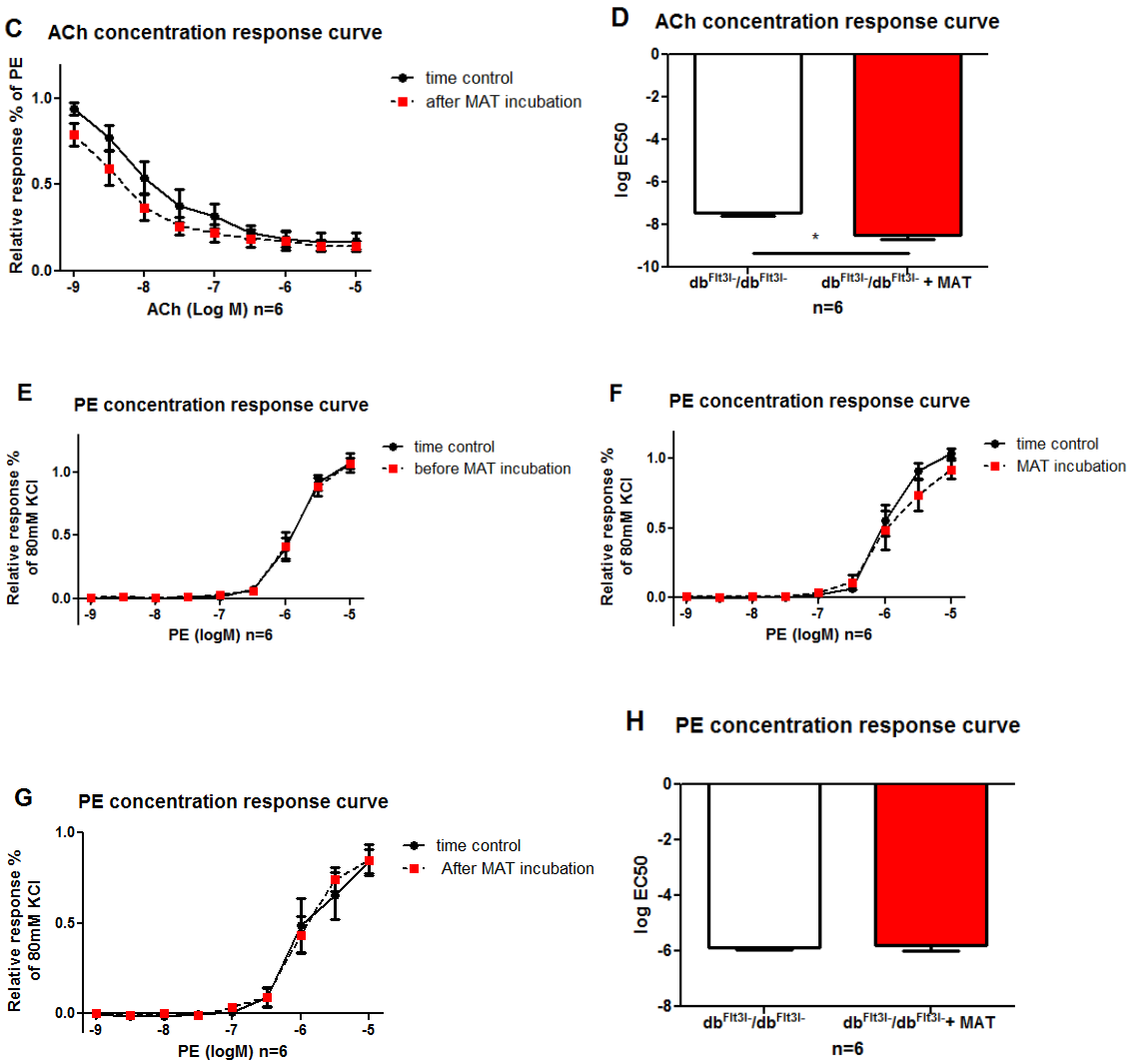

Figure.3-17. ACh and PE concentration-response curves: effect of MAT co-incubation in *db*$^{Flt3l-}$/*db*$^{Flt3l-}$ mice (18-22 weeks). **(A** and **E)** There was no significant difference of ACh **(A)** or PE **(E)** concentration response curve between time control and "before MAT incubation" MA. **(B)** A significant increase of ACh induced vasorelaxation response was found in MAT incubation. **(C** and **G)** After repeated 1 hour washing of ring segments exposed to MAT, ACh-induced vasorelaxation **(C)** and PE-induced vasoconstriction **(G)** were similar to those of time controls. **(D)** MA with MAT incubation showed significantly different LogEC50 values for ACh concentration response curve compared to time control. **(F** and **H)** Interestingly, no significant difference of PE induced vasoconstriction was observed between time control and MAT incubation MA **(F)**, which was supported by their logEC50 values **(H)**. *: $P < 0.05$. In **(B)** panel**,** Two-way ANOVA. In **(D)** panel, student *t*-test. All data presented as mean± SEM.

MAT transfer assay between DbHET and db/db mice at 18-22 weeks

To further confirm that the impairment of vascular function with MAT incubation in *db/db* mice was due to dysfunction of the adipose tissue, we conducted MAT transfer assay experiments. As shown in **Fig.3-18-A,** ACh induced vasorelaxation was enhanced in DbHET mice's MA with MAT incubation from the same mice, which was consistent with previous data in **Fig.3-11.** However, if MA rings from DbHET mice were incubated with MAT from *db/db* mice, the augmentation of ACh-induced relaxation was abolished. Calculated logEC50 values for ACh concentration response curves did not show a significant difference between time control and *db/db* MAT incubation (**Fig.3-18-B).** Consistent with previous data in **Fig.3-11,** PE-induced vasoconstriction was reduced in MA rings from DbHET mice incubated with their own adipose tissue (**Fig.3-18-C**). When the MA was incubated with MAT from *db/db* mice, this reduction of vasoconstriction was still preserved. However, this effect was decreased in MA incubated with MAT from *db/db* mice, compared to MA incubated with MAT from DbHET mice (**Fig.3-26-D**). Taken together, acute incubation of normal vessels with MAT from *db/db* mice impaired the augmentation of ACh-induced relaxation and the reduction of PE-induced vasoconstriction, when exposed to fat from non-diabetic animals.

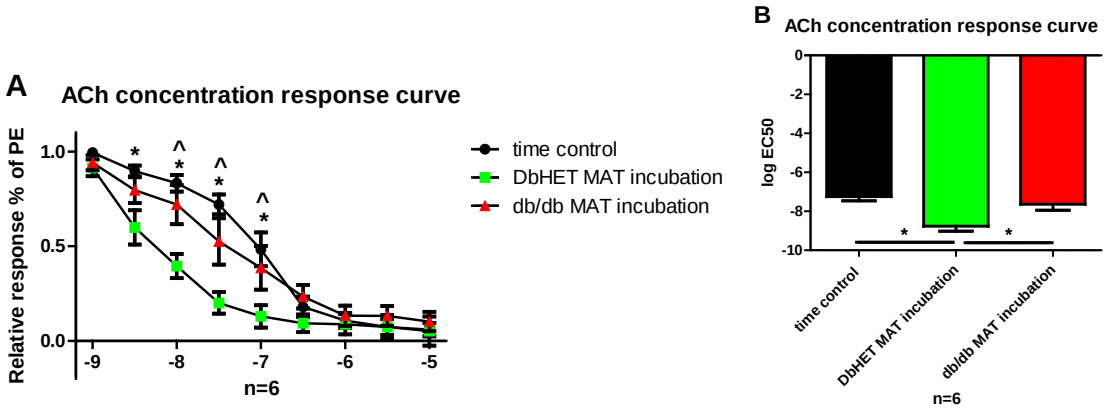

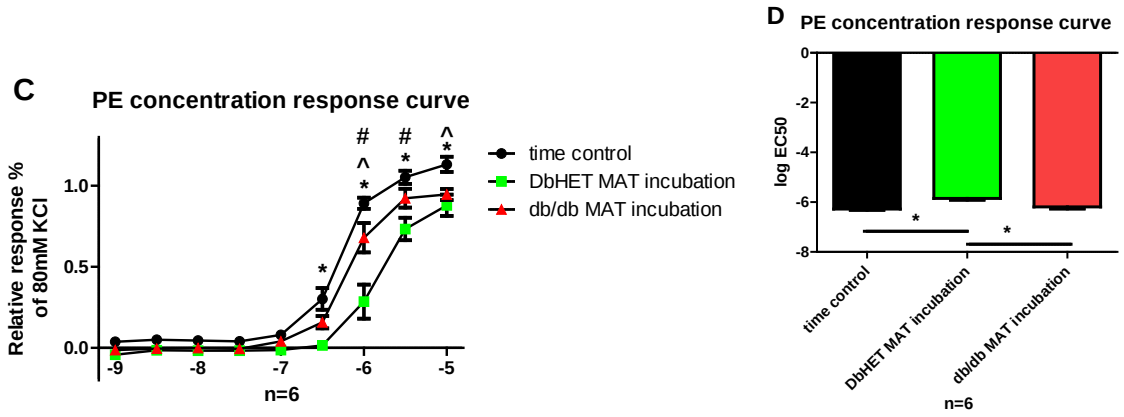

Figure. 3-18. Effect of MAT co-incubation on PE and ACh concentration-responses in DbHET and *db/db* mice (at 18-22 weeks). (A) ACh induced vasorelaxation was increased in MA with MAT incubation from DbHET mice, but this effect was abolished in MA with MAT incubation from *db/db* mice. **(B and D)** Significant logEC50 differences of ACh **(B)** and PE **(D)** concentration response were found between time control and DbHET MAT incubation, as well as between DbHET MAT and *db/db* MAT incubation. **(C)** PE induced vasoconstriction was decreased in MA with MAT incubation from DbHET mice. This effect was still preserved yet impaired in *db/db* MAT incubation. All data presented as mean± SEM. In panel **(A** and **C)**, Two-way ANOVA was used. *: $P < 0.05$. time control v.s. DbHET MA+ MAT from DbHET mice. ^: $P < 0.05$. time control v.s. DbHET MA+ MAT from *db/db* mice. #: $P < 0.05$. DbHET MA+ MAT from DbHET mice v.s. DbHET MA+ MAT from *db/db* mice. In panel **(B** and **D)**, One-way ANOVA was used. *: $P < 0.05$.

MAT transfer assay between DbHET$^{Flt3l-/-}$ and db^{Flt3l-}/db^{Flt3l-} mice at 18-22 weeks

Additional studies were conducted to examine the effects of MAT from *db^{Flt3l-}/db^{Flt3l-}* mice on normally functioning vessels. First order MA from DbHET$^{Flt3l-/-}$ mice were exposed to MAT from either DbHET$^{Flt3l-/-}$ or *db^{Flt3l-}/db^{Flt3l-}* mice. As shown in **Fig. 3-19**, MA rings co-incubated with MAT from DbHET$^{Flt3l-/-}$ mice exhibited significant enhancement of ACh-induced relaxation and an attenuation of PE-induced vasoconstriction responses, compared to time control group. Calculated logEC50 values also showed a significant difference between time control and MAT incubation from DbHET$^{Flt3l-/-}$ mice. Unlike MAT from *db/db* mice (**Fig. 3-18**), MAT incubation from *db^{Flt3l-}/db^{Flt3l-}* mice continued to display an enhancement of ACh induced relaxation and comparable reduction in PE-induced constriction responses to MAT from DbHET$^{Flt3l-/-}$ mice. The

logEC50 values further confirmed the comparable relaxation and constriction response curves between MAT incubation from DbHET$^{Flt3l-/-}$ and *db*$^{Flt3l-}$/*db*$^{Flt3l-}$ mice. Combined with the data shown in **Fig.3-18**, it is suggested that MAT from *db/db* mice markedly impairs the augmentation of relaxation and anti-contractile responses in normal MA (i.e. when exposed to normal adipose tissue). However, genetic depletion of dendritic cells in MAT of diabetic mice significantly prevents these effects.

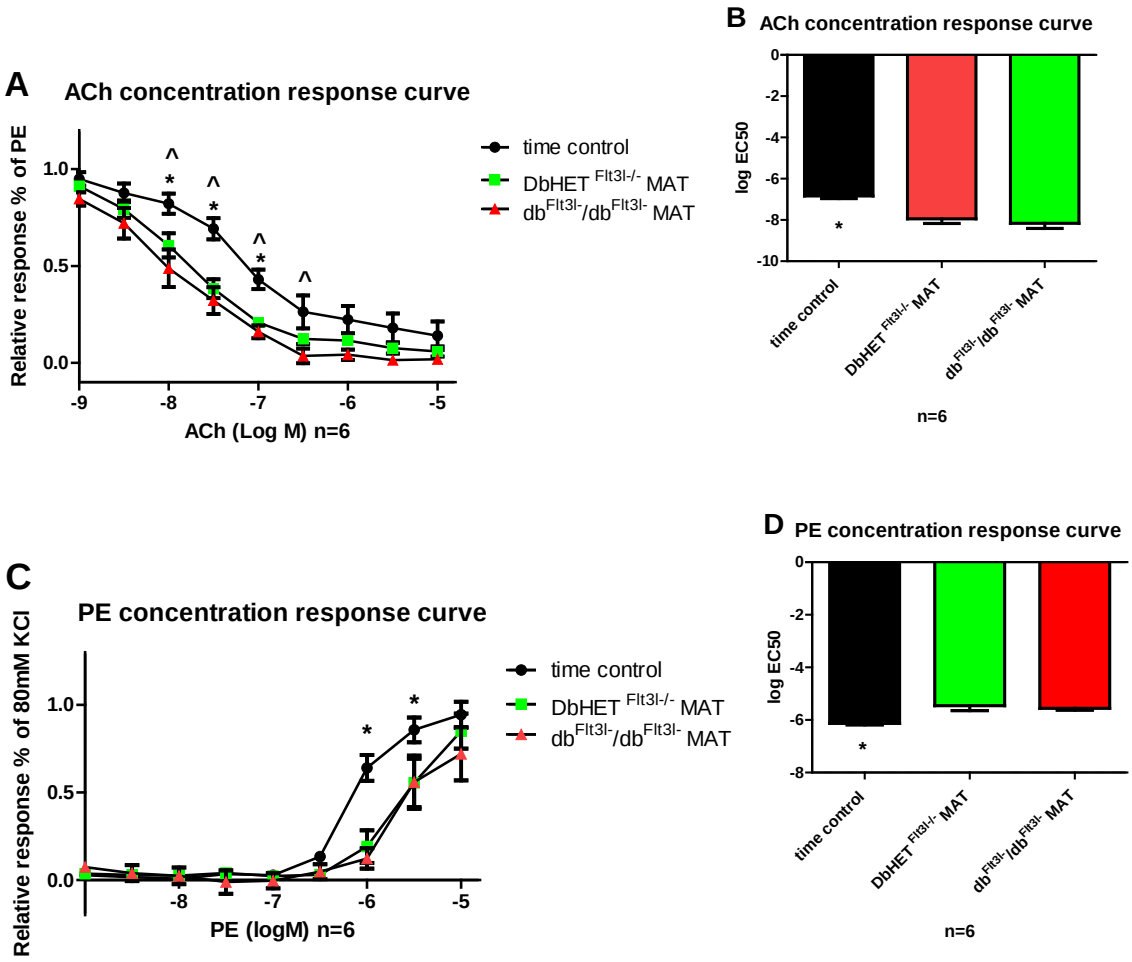

Figure. 3-19. Effect of MAT co-incubation on PE and ACh concentration-responses in DbHET $^{Flt3l-/-}$ and db^{Flt3l-}/ db^{Flt3l-}mice (at 18-22 weeks). (A and C) ACh induced vasorelaxation was increased **(A)** and PE induced vasoconstriction was reduced **(C)** in MA with MAT incubation from both DbHET$^{Flt3l-/-}$ and *db*$^{Flt3l-}$/*db*$^{Flt3l-}$ mice. Two-way ANOVA was used. In **(A)** *: time control v.s. DbHET$^{Flt3l-/-}$ mice. ^: time control v.s. *db*$^{Flt3l-}$/*db*$^{Flt3l-}$ mice. In **(C)** *: time control v.s. DbHET$^{Flt3l-/-}$ or *db*$^{Flt3l-}$/*db*$^{Flt3l-}$ mice. **(B and D)** Significant logEC50 differences of ACh **(B)** and PE **(D)** concentration response were found between time control and DbHET$^{Flt3l-/-}$ or *db*$^{Flt3l-}$/*db*$^{Flt3l-}$ mice's MAT incubation. One-way ANOVA was used. *: time control v.s. DbHET$^{Flt3l-/-}$ or *db*$^{Flt3l-}$/*db*$^{Flt3l-}$ mice. All data presented as mean± SEM.*, ^: $P < 0.05$.

3.5. Discussion

The goal of the present study was to determine the contribution of dendritic cells to the development of chronic inflammation and vascular dysfunction associated with T2DM. To address this hypothesis, a novel murine model of T2DM combined with genetic deletion of dendritic cells, db^{Flt3l-}/ db^{Flt3l-} mouse, was first created and then used in our subsequent studies. Our key findings can be summarized as follows: (1) Dendritic cell depletion reduced the production of pro-inflammatory factors in PVAT from *db/db* mice. (2) Augmentation of vasorelaxation and anti-contractile responses exerted by MAT were lost at both early (6-10 weeks) and later (18-22 weeks) stages of T2DM. (3) Dendritic cell depletion restored these characteristics of adipose tissue despite maintenance of obesity at the early stage of T2DM. However, at the later stage of T2DM, dendritic cell depletion restored the ability of adipose tissue to augment vasorelaxation while its anti-contractile activity was lost.

Murine model of T2DM depleted of dendritic cells

Dendritic cells have been studied for over four decades; however, no cell surface protein marker until now has been discovered to be uniquely expressed in those immune cells. This situation explains the lack of specificity in dendritic cell identification in different murine models. The most commonly used model is the CD11c-DTR (diphtheria toxin receptor) transgenic mouse, which can be transiently and efficiently depleted of $CD11c^+$ cell populations throughout the body (Hochweller, Striegler et al. 2008, Patsouris, Li et al. 2008). The identity of $CD11c^+$ cells is altered within different locations (Mortensen 2012). In peripheral tissues, such as adipose tissue, it has been questioned as to whether $CD11c^+$ cells specifically represent dendritic cells. This cell population likely includes dendritic cells, macrophages and some types of monocytes. Our flow cytometry data shown in **Fig 3-4** supported the notion that $CD11c^+$ cells in adipose tissue are composed of dendritic cells and macrophages. Another important limitation of the CD11c-DTR murine model is that administration of a single dose of DT can maintain $CD11c^+$ cell depletion in peripheral tissues for a short period of time (approximately 2 days), after which, $CD11c^+$ cell

populations begin to recover (Bar-On and Jung 2010). In order to maintain the low expression of $CD11c^+$ cells in peripheral tissues and at the same time mimic the chronic progression of T2DM, repeated administration of DT would have to be applied to the same mouse for a period of weeks to months. Since DT can be fatal in mice, this procedure is likely to exhibit a variable phenotype and high mortality rate in CD11c-DTR mice (Bar-On and Jung 2010). To address these issues, we used an alternate murine model with dendritic cell depletion, $Flt3l^{-/-}$ mice (Stefanovic-Racic, Yang et al. 2012). Flt3l (ligand for FMS-like tyrosine kinase 3) is a growth factor for hematopoietic progenitor cells in mice (McKenna, Stocking et al. 2000). Lack of Flt3l has been reported to reduce dendritic cell number in murine lymphoid organs (McKenna, Stocking et al. 2000). Compared to CD11c-DTR mice, $Flt3l^{-/-}$ mice are genetically depleted of dendritic cells without the need for any chemical administration, making them potentially more suitable for studying the chronic progression of T2DM. Our flow cytometry data in **Fig. 3-4** demonstrated that this ablation can reduce dendritic cell population in VAT without any apparent influence on the M1 macrophage population. Therefore, we created a T2DM murine model without dendritic cells, db^{Flt3l-}/db^{Flt3l-} mice, by cross-breeding $Flt3l^{-/-}$ and DbHET mice. The flow cytometry data in **Fig. 3-4** and **Fig. 3-5** showed that $CD11c^+F4/80^-$ and $CD83^+CD86^+$ dendritic cell populations were increased in VAT from *db/db* mice in comparison with DbHET mice. However, after Flt3l depletion, dendritic cells were dramatically decreased in VAT from db^{Flt3l-}/db^{Flt3l-} mice in comparison with *db/db* mice. In contrast, $CD11c^+F4/80^+$ M1 macrophages were increased in VAT from *db/db* mice compared to DbHET mice, whereas Flt3l depletion did not alter macrophage population in db^{Flt3l-}/db^{Flt3l-} mice. As predicted, dendritic cell and macrophage populations were comparable between DbHET and $DbHET^{Flt3l-/-}$ mice. On the basis of these observations, we concluded that $DbHET^{Flt3l-/-}$ and db^{Flt3l-}/db^{Flt3l-} mice are suitable murine models to study the effect of dendritic cells on vascular dysfunction caused by T2DM.

Metabolic effects of dendritic cell depletion

Our data in **Fig. 3-1** and **Fig. 3-2** showed that T2DM mice exhibit increased total body weights as well as larger adipose tissue depots (intestinal mesentery, VAT, MAT, AH and ATA).

Further, *db/db* mice showed markedly higher non-fasting glucose levels compared to healthy mice at both early and late stages of T2DM. The depletion of dendritic cells decreased intestinal mesentery and VAT weights, as well as non-fasting glucose levels in diabetic mice only at the late stage of T2DM, whereas at the early stage of T2DM, dendritic cell depletion did not affect phenotypic parameters in diabetic mice. $Flt3l^{-/-}$ mice have been reported to be characterized by a higher metabolic rate compared to wild type mice (Stefanovic-Racic, Yang et al. 2012). Therefore, it is possible that db^{Ftl3l-}/ db^{Ftl3l-} mice would still maintain this higher metabolic rate and as a consequence, exhibit reduced adipose tissue weight. Previous reports have shown that ablation of $CD11c^{+}$ cells can normalize glucose homeostasis and insulin reactivity by reduction of the inflammatory environment in insulin-resistant mice (Patsouris, Li et al. 2008). Our qPCR data in **Fig. 3-6** and **Fig. 3-7** revealed that dendritic cell depletion significantly reduced pro-inflammatory factors TNF-α and IL-6 production in diabetic adipose tissue. Glucose and insulin tolerance tests (**Fig.3-3)** show that, in our studies, dendritic cell depletion markedly reduces glucose levels in *db/db* mice, which remained yet significantly higher than healthy controls. These results thus suggest that dendritic cells partially contribute to the high glucose levels and insulin resistance seen in *db/db* mice. As our strategy was aimed at depleting only dendritic cells, other immune cells may contribute to the development of insulin resistance and glucose elevation in diabetic mice – a particular candidate being macrophages, which were not altered by the $Flt3^{-/-}$ ablation. Of further importance in interpreting the current studies, pro-inflammatory M1 macrophages still accumulated in adipose tissue of the db^{Ftl3l-}/ db^{Ftl3l-} mice (**Fig. 3-4).** Evidence has indicated that M1 macrophages disrupt insulin-stimulated glucose transport and further differentiation of adipocytes which results in hypertrophy of adipose tissue (Xie, Ortega et al. 2010). This may explain the observation of a partial change of phenotype in the current studies where intestinal mesentery and VAT weights were heavier in db^{Ftl3l-}/ db^{Ftl3l-} mice than healthy controls, despite lighter than those of *db/db* mice.

Changes in inflammatory mediators following dendritic cell depletion

Fig. 3-6 supports the argument that chronic inflammation in adipose tissue is initiated at an early stage of T2DM (6-10 weeks of age). In regard to specific mediators, mRNA levels for the pro-inflammatory factors, TNF-α and IL-6, were increased in VAT and MAT while mRNA levels for the anti-inflammatory mediator, adiponectin, was decreased in VAT from diabetic mice. However, mRNA levels of adiponectin in MAT along with the anti-inflammatory mediator IL-10 in VAT and MAT were not changed in diabetic mice. Depletion of dendritic cells significantly decreased TNF-α mRNA levels in VAT and MAT, as well as IL-6 mRNA level in MAT from diabetic mice, without any influence on adiponectin and IL-10 mRNA levels. As shown in **Fig. 3-7,** chronic inflammation in adipose tissue appeared to worsen at the later stage of T2DM (18-22 weeks). TNF-α and IL-6 mRNA levels were increased while adiponectin mRNA levels were decreased in VAT and MAT from diabetic mice. **Fig. 3-8** provided a piece of evidence on increased levels of TNF-α protein expression in diabetic VAT, compared to healthy controls, whereas the depletion of dendritic cells significantly decreased TNF-α protein expression in *db/db* mice. Interestingly, IL-10 mRNA levels were increased in VAT and MAT from diabetic mice. Depletion of dendritic cells significantly decreased mRNA levels for TNF-α and IL-6 in VAT and MAT, as well as for IL-10 in MAT from diabetic mice, without any influence of other tested factors. Available evidence has demonstrated that IL-10 is a compensatory cytokine which suppresses the production of pro-inflammatory factors, including TNF-α and IL-6 (Doughty, Carcillo et al. 1998, Sinuani, Beberashvili et al. 2013). This might explain the increase of IL-10 production (as an attempt to inhibit production of inflammatory cytokines) in adipose tissue from diabetic mice compared to healthy controls. In the case of dendritic cell depletion, the decrease in production of TNF-α and IL-6 in diabetic adipose tissue reduced the drive for IL-10 production. Collectively, the results of the current studies revealed that depletion of dendritic cells significantly decreased the production of pro-inflammatory factors, TNF-α and IL-6, in diabetic PVAT, resulting in attenuation of chronic inflammation caused by T2DM.

Vascular function in T2DM

It is well accepted that PVAT plays an important role in vascular homeostasis through paracrine and/or endocrine routes (Szasz, Bomfim et al. 2013, Ozen, Daci et al. 2015). The exact mechanism of this effect has been the subject of considerable recent research. Under physiological conditions, large quantities of metabolically vasoactive molecules, such as adiponectin, H_2S and NO are generated from PVAT. These factors have been shown to be responsible for the promotion of vasorelaxation and reduction of vasoconstriction, the latter often described as an "anti-contractile" function of adipose tissue (Brown, Zhou et al. 2014, Ozen, Daci et al. 2015). Accumulating evidence has revealed that this anti-contractile function from adipose tissue is lost in obese mice (Even, Dulak-Lis et al. 2014, Lastra and Manrique 2015). Enhancement of vasoconstriction, as opposed to vasorelaxation, in the presence of adipose tissue has also been found in murine high fat diet-induced obese models (Ma, Ma et al. 2010). One of the underlying mechanisms to explain the above phenomena is related to the overproduction of pro-inflammatory factors and decreased generation of anti-inflammatory mediators in obese perivascular adipose tissue (Greenstein, Khavandi et al. 2009, Vachharajani and Granger 2009). Application of cytokines TNF-α or IL-6, or an antagonist of adiponectin, to PVAT around healthy vasculature significantly reduces dilator activity (Greenstein, Khavandi et al. 2009). Since our qPCR data in **Fig.3-6** and **Fig.3-7** have shown that higher mRNA levels of TNF-α and IL-6 and lower mRNA level of adiponectin are generated in VAT and MAT from *db/db* mice compared to DbHET controls, it is possible that *db/db* mice would have impaired vascular function compared to that of the DbHET mice. Consistent with our hypothesis, the vascular function data revealed that incubation with MAT from DbHET mice enhanced vasorelaxation and anti-contractile effects on MA (**Fig.3-10** and **Fig.3-11**), whereas MAT from *db/db* mice lost such reactivity. As this occurred at both 6-10 and 18-22 weeks, it is believed to be an early event in the development of diabetes-induced vascular dysfunction (**Fig.3-12** and **Fig.3-13**). Therefore, it is believed that the impairment of vasorelaxation augmentation and anti-contractile reactivity in *db/db* mice might be attributable to either MAT dysfunction or vascular damage. In order to test this hypothesis, MAT transfer experiments were conducted by incubation of DbHET mice's MAs with either MAT from DbHET mice or MAT from *db/db* mice. Our data showed (**Fig.3-18)** that 1

hour incubation of MAT from *db/db* mice with healthy MA reduced the anti-contractile property and abolished the enhancement of vasorelaxation when compared to MAT incubation with control mice. These data suggested that MAT dysfunction contributed to the impairment of vasorelaxation augmentation and anti-contractile reactivity in *db/db* mice, which was consistent with other studies (Wang, Luo et al. 2012, Meijer, Bakker et al. 2013).

Accumulated evidence has shown that incubating coronary arteries with TNF-α for 1 hour (Park, Yang et al. 2011) or intraperitoneal injection of IFN-γ for 5 days (Zhang, Potter et al. 2011) leads to the impairment of endothelial dependent vasodilation and cause vascular dysfunction. Thus, it was considered possible that in the long-term presence of inflamed MAT, the adjacent vasculature in vivo would be eventually damaged by inflammatory cytokines secreted from MAT. That would partially explain the finding that *db/db* mice had impaired endothelial dependent vasorelaxation of isolated MA than DbHET mice at 18-22 weeks (**Fig.3-9)**. Moreover, we divided *db/db* mice into 6-10 and 18-22 weeks groups. From **Fig.3-9, Fig.3-12** and **Fig.3-13**, we have found out that the impairment of vasorelaxation augmentation and anti-contractile reactivity was observed in *db/db* mice at both age groups, whereas MA from *db/db* mice caused endothelial dysfunction only at 18-22 weeks. The precedence of MAT inflammation over vascular dysfunction in *db/db* mice provided another causal linkage between MAT inflammation and vascular dysfunction in T2DM. Taken together, *db/db* mice had impaired augmentation of vasorelaxation and anti-contractile reactivity from inflamed MAT at both early and late stage of T2DM, but endothelial - dependent vasorelaxation was blunted only at late stage of T2DM.

Vascular function influenced by dendritic cell depletion

Our qPCR data (**Fig.3-6** and **Fig.3-7**) have shown that dendritic cell depletion significantly reduced TNF-α and IL-6 production in VAT and MAT from *db/db* mice. Consistent with these data, dendritic cell depletion preserved the augmentation of vasorelaxation and anti-contractile function in *db/db* mice at 6-10 weeks, but only preserved the augmentation of vasorelaxation in *db/db* mice at 18-22 weeks (**Fig.3-16 and Fig.3-17**). In the MAT transferring experiments shown in **Fig. 3-19**, MAT incubation from db^{Ftl3l-}/ db^{Ftl3l-} mice at 18-22 weeks maintained both the augmentation

of vasorelaxation and reduction of vasoconstriction on healthy MA, to the similar extent with MAT incubation from DbHET$^{Flt3l-/-}$ mice. However, this finding was different from previous result that MAT incubation from *db*$^{Ftl3l-}$/ *db*$^{Ftl3l-}$ mice at 18-22 weeks only preserved the augmentation of vasorelaxation rather than the anti-contractile function on MA from *db*$^{Ftl3l-}$/ *db*$^{Ftl3l-}$ mice. This difference was because the tested MA was from different mice. The MAT transfer experiment used MA from DbHET$^{Flt3l-/-}$ mice while the other one was from *db*$^{Ftl3l-}$/ *db*$^{Ftl3l-}$ mice. As shown in **Fig.3-9,** vascular contractility response was significantly lower in *db*$^{Ftl3l-}$/ *db*$^{Ftl3l-}$ mice, compared to DbHET$^{Flt3l-/-}$ mice. This reduction of MA contractility could cover the anti-contractile function from MAT incubation. It has been reported that adiponectin is essential for the maintenance of vascular smooth muscle cell contractility (Ding, Carrão et al. 2012). The low level of adiponectin can decrease the production of contractile proteins in smooth muscle cells and alter their contractile phenotype. Our qPCR data has shown that adiponectin levels in diabetic adipose tissue were not rescued after dendritic cell depletion. Therefore, it is possible that the contractile response of MA from *db*$^{Ftl3l-}$/ *db*$^{Ftl3l-}$ mice was lower than MA from DbHET$^{Flt3l-/-}$ mice. However, in **Fig.3-9,** the contractility of MA from *db*$^{Ftl3l-}$/ *db*$^{Ftl3l-}$ mice was still lower than MA from *db/db* mice. The exact mechanism was still unknown. Collectively, dendritic cell depletion preserved the augmentation of vasorelaxation and anti-contractile function from MAT at the early stage of T2DM, while at the late stage of T2DM, only the augmentation of vasorelaxation from MAT was maintained. These vascular effects after dendritic cell depletion effectively contributed to the restoration of endothelial dependent vasorelaxation in T2DM mice.

In conclusion, our study has shown that (**Fig.3-20**) *db/db* mice had higher blood glucose levels and increased PVAT weights with dendritic cell accumulation, compared to healthy mice. Moreover, elevated production of pro-inflammatory cytokines and reduced production of anti-inflammatory factors were found in VAT and MAT from *db/db* mice compared to healthy controls. This imbalanced production has led to the impairment of vasorelaxation augmentation and anti-contractile reactivity derived from *db/db* mice's inflamed MAT, which further attenuated endothelial dependent vasorelaxation of MA. After dendritic cells were depleted, both PVAT weights and blood glucose levels were decreased in *db*$^{Ftl3l-}$/ *db*$^{Ftl3l-}$ mice. Moreover, pro-

inflammatory cytokines production was significantly reduced in MAT from db^{Ftl3l-}/ db^{Ftl3l-} mice, which facilitated the restoration of vasorelaxation augmentation and anti-contractile reactivity from MAT. This effect successfully restored endothelial dependent vasorelaxation of MA in db^{Ftl3l-}/ db^{Ftl3l-} mice. These findings suggest that dendritic cells are the upstream sources of pro-inflammatory factors generation. Our study is the first to unveil the role of dendritic cells on the regulation of vascular function in T2DM mice, which indicates a novel mechanism of cardiovascular disorders associated with T2DM and provides a potential therapeutic target for this vascular damage in the development of T2DM.

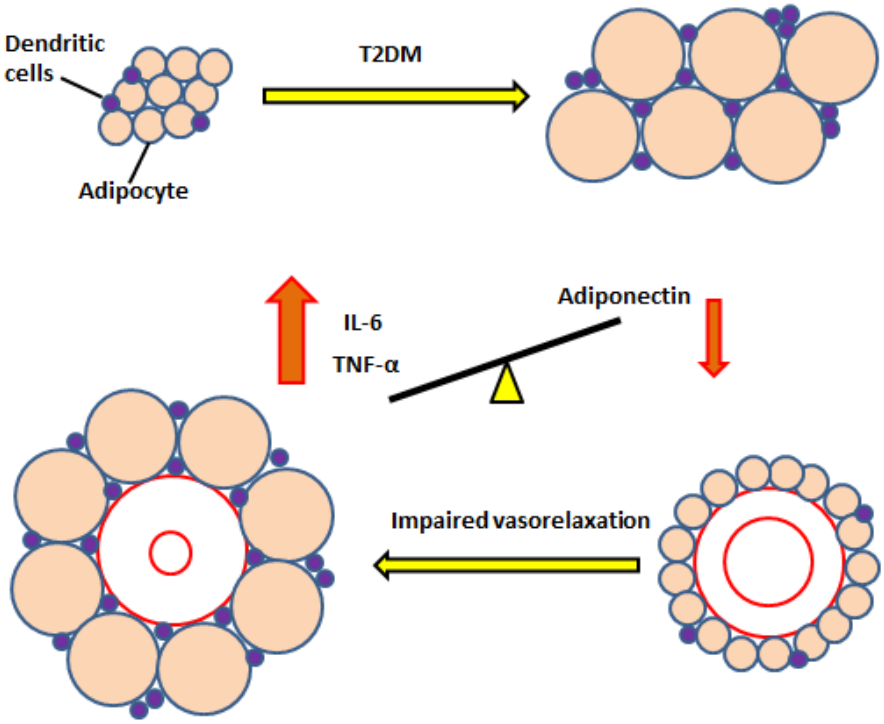

Figure. 3-20. Schematic diagram outlining the role of dendritic cells in vascular dysfunction associated with T2DM. In T2DM, more dendritic cells were recruited into perivascular adipose tissue and promoted the overproduction of pro-inflammatory cytokines TNF-α and IL-6 in obese adipose tissue. Under the influence of inflamed perivascular adipose tissue, adjacent vessels displayed impaired vasorelaxation response and endothelial dysfunction.

3.6. REFERENCES

Agabiti-Rosei, C., C. De Ciuceis, et al. (2014). "Anticontractile activity of perivascular fat in obese mice and the effect of long-term treatment with melatonin." J Hypertens **32**(6): 1264-1274.

Bar-On, L. and S. Jung (2010). "Defining in vivo dendritic cell functions using CD11c-DTR transgenic mice." Methods Mol Biol **595**: 429-442.

Brown, N. K., Z. Zhou, et al. (2014). "Perivascular Adipose Tissue in Vascular Function and Disease A Review of Current Research and Animal Models." Arteriosclerosis, thrombosis, and vascular biology **34**(8): 1621-1630.

Chang, L., H. Milton, et al. (2013). "Paradoxical roles of perivascular adipose tissue in atherosclerosis and hypertension." Circ J **77**(1): 11-18.

Cheng, Y., J. F. Ndisang, et al. (2004). "Hydrogen sulfide-induced relaxation of resistance mesenteric artery beds of rats." Am J Physiol Heart Circ Physiol **287**(5): 10.

Creely, S. J., P. G. McTernan, et al. (2007). "Lipopolysaccharide activates an innate immune system response in human adipose tissue in obesity and type 2 diabetes." American Journal of Physiology - Endocrinology and Metabolism **292**(3): E740-E747.

Dieterlen, M. T., K. John, et al. (2016). "Dendritic Cells and Their Role in Cardiovascular Diseases: A View on Human Studies." **2016**: 5946807.

Ding, M., A. C. Carrão, et al. (2012). "Vascular smooth muscle cell-derived adiponectin: a paracrine regulator of contractile phenotype." Journal of molecular and cellular cardiology **52**(2): 474-484.

Doughty, L., J. A. Carcillo, et al. (1998). "The compensatory anti-inflammatory cytokine interleukin 10 response in pediatric sepsis-induced multiple organ failure." Chest **113**(6): 1625-1631.

Eringa, E. C., W. Bakker, et al. (2012). "Paracrine regulation of vascular tone, inflammation and insulin sensitivity by perivascular adipose tissue." Vascular pharmacology **56**(5): 204-209.

Esser, N., S. Legrand-Poels, et al. (2014). "Inflammation as a link between obesity, metabolic syndrome and type 2 diabetes." Diabetes Res Clin Pract **105**(2): 141-150.

Even, S. E., M. G. Dulak-Lis, et al. (2014). "Crosstalk between adipose tissue and blood vessels in cardiometabolic syndrome: implication of steroid hormone receptors (MR/GR)." Horm Mol Biol Clin Investig **19**(2): 89-101.

Fernández-Alfonso, M. S., M. Gil-Ortega, et al. (2013). "Mechanisms of perivascular adipose tissue dysfunction in obesity." International journal of endocrinology **2013**.

Fesus, G., G. Dubrovska, et al. (2007). "Adiponectin is a novel humoral vasodilator." Cardiovasc Res **75**(4): 719-727.

Gao, Y. J., C. Lu, et al. (2007). "Modulation of vascular function by perivascular adipose tissue: the role of endothelium and hydrogen peroxide." Br J Pharmacol **151**(3): 323-331.

Goldstein, B. J. and R. Scalia (2004). "Adiponectin: A Novel Adipokine Linking Adipocytes and Vascular Function." The Journal of Clinical Endocrinology & Metabolism **89**(6): 2563-2568.

Grant, R. W. and V. D. Dixit (2015). "Adipose tissue as an immunological organ." Obesity (Silver Spring) **23**(3): 512-518.

Greenstein, A. S., K. Khavandi, et al. (2009). "Local inflammation and hypoxia abolish the protective anticontractile properties of perivascular fat in obese patients." Circulation **119**(12): 1661-1670.

Gu, P. and A. Xu (2013). "Interplay between adipose tissue and blood vessels in obesity and vascular dysfunction." Rev Endocr Metab Disord **14**(1): 49-58.

Guilherme, A., J. V. Virbasius, et al. (2008). "Adipocyte dysfunctions linking obesity to insulin resistance and type 2 diabetes." Nat Rev Mol Cell Biol **9**(5): 367-377.

Hansen, M. and M. H. Andersen (2016). "The role of dendritic cells in cancer." Semin Immunopathol.

Hochweller, K., J. Striegler, et al. (2008). "A novel CD11c.DTR transgenic mouse for depletion of dendritic cells reveals their requirement for homeostatic proliferation of natural killer cells." Eur J Immunol **38**(10): 2776-2783.

Kato, H., H. Kashiwagi, et al. (2006). "Adiponectin acts as an endogenous antithrombotic factor." Arteriosclerosis, thrombosis, and vascular biology **26**(1): 224-230.

Kosteli, A., E. Sugaru, et al. (2010). "Weight loss and lipolysis promote a dynamic immune response in murine adipose tissue." J Clin Invest **120**(10): 3466-3479.

Lastra, G. and C. Manrique (2015). "Perivascular adipose tissue, inflammation and insulin resistance: link to vascular dysfunction and cardiovascular disease." Horm Mol Biol Clin Investig **22**(1): 19-26.

Lee, R. M., C. Lu, et al. (2009). "Endothelium-dependent relaxation factor released by perivascular adipose tissue." J Hypertens **27**(4): 782-790.

Lee, S., Y. Park, et al. (2011). "Exercise training improves endothelial function via adiponectin-dependent and independent pathways in type 2 diabetic mice." Am J Physiol Heart Circ Physiol **301**(2): H306-314.

Lee, S., Y. Yang, et al. (2015). "Heterogeneity in Kv7 channel function in the cerebral and coronary circulation." Microcirculation **22**(2): 109-121.

Liao, X., A. M. Reihl, et al. (2016). "Breakdown of Immune Tolerance in Systemic Lupus Erythematosus by Dendritic Cells." **2016**: 6269157.

Ma, L., S. Ma, et al. (2010). "Perivascular fat-mediated vascular dysfunction and remodeling through the AMPK/mTOR pathway in high-fat diet-induced obese rats." Hypertens Res **33**(5): 446-453.

Macia, L., M. Delacre, et al. (2006). "Impairment of dendritic cell functionality and steady-state number in obese mice." J Immunol **177**(9): 5997-6006.

Malinowski, M., M. A. Deja, et al. (2013). "Mechanisms of vasodilatatory effect of perivascular tissue of human internal thoracic artery." J Physiol Pharmacol **64**(3): 309-316.

McKenna, H. J., K. L. Stocking, et al. (2000). "Mice lacking flt3 ligand have deficient hematopoiesis affecting hematopoietic progenitor cells, dendritic cells, and natural killer cells." Blood **95**(11): 3489-3497.

Meijer, R. I., W. Bakker, et al. (2013). "Perivascular adipose tissue control of insulin-induced vasoreactivity in muscle is impaired in db/db mice." Diabetes **62**(2): 590-598.

Meijer, R. I., E. H. Serne, et al. (2011). "Perivascular adipose tissue and its role in type 2 diabetes and cardiovascular disease." Current diabetes reports **11**(3): 211-217.

Mortensen, R. M. (2012). "Immune Cell Modulation of Cardiac Remodeling." Circulation **125**(13): 1597-1600.

Nguyen, D. M. and H. B. El-Serag (2010). "The epidemiology of obesity." Gastroenterol Clin North Am **39**(1): 1-7.

Oriowo, M. A. (2015). "Perivascular adipose tissue, vascular reactivity and hypertension." Med Princ Pract **24 Suppl 1**: 29-37.

Ozen, G., A. Daci, et al. (2015). "Human perivascular adipose tissue dysfunction as a cause of vascular disease: Focus on vascular tone and wall remodeling." European journal of pharmacology **766**: 16-24.

Park, Y., J. Yang, et al. (2011). "Effect of PAR2 in regulating TNF-alpha and NAD(P)H oxidase in coronary arterioles in type 2 diabetic mice." Basic Res Cardiol **106**(1): 111-123.

Patsouris, D., P.-P. Li, et al. (2008). "Ablation of CD11c-positive cells normalizes insulin sensitivity in obese insulin resistant animals." Cell metabolism **8**(4): 301-309.

Pfaffl, M. W. (2001). "A new mathematical model for relative quantification in real-time RT-PCR." Nucleic Acids Res **29**(9): e45.

Price, J. D. and K. V. Tarbell (2015). "The Role of Dendritic Cell Subsets and Innate Immunity in the Pathogenesis of Type 1 Diabetes and Other Autoimmune Diseases." Front Immunol **6**: 288.

Probst, H., K. Tschannen, et al. (2005). "Histological analysis of CD11c-DTR/GFP mice after in vivo depletion of dendritic cells." Clinical & Experimental Immunology **141**(3): 398-404.

Sinuani, I., I. Beberashvili, et al. (2013). "Role of IL-10 in the progression of kidney disease." World J Transplant **3**(4): 91-98.

Stefanovic-Racic, M., X. Yang, et al. (2012). "Dendritic cells promote macrophage infiltration and comprise a substantial proportion of obesity-associated increases in $CD11c^+$ cells in adipose tissue and liver." Diabetes **61**(9): 2330-2339.

Steinman, R. M. (1991). "The dendritic cell system and its role in immunogenicity." Annual review of immunology **9**(1): 271-296.

Steinman, R. M. (2007). "Dendritic cells: understanding immunogenicity." Eur J Immunol **37 Suppl 1**: S53-60.

Szasz, T., G. F. Bomfim, et al. (2013). "The influence of perivascular adipose tissue on vascular homeostasis." Vascular health and risk management **9**: 105.

Tano, J. Y., J. Schleifenbaum, et al. (2014). "Perivascular adipose tissue, potassium channels, and vascular dysfunction." Arterioscler Thromb Vasc Biol **34**(9): 1827-1830.

Vacas-Cordoba, E., N. Climent, et al. (2014). "Dendrimers as nonviral vectors in dendritic cell-based immunotherapies against human immunodeficiency virus: steps toward their clinical evaluation." Nanomedicine (Lond) **9**(17): 2683-2702.

Vachharajani, V. and D. N. Granger (2009). "Adipose tissue: a motor for the inflammation associated with obesity." IUBMB Life **61**(4): 424-430.

Wang, H., W. Luo, et al. (2012). "Obesity-induced endothelial dysfunction is prevented by deficiency of P-selectin glycoprotein ligand-1." Diabetes **61**(12): 3219-3227.

Wentworth, J. M., G. Naselli, et al. (2010). "Pro-inflammatory $CD11c^{+}CD206^{+}$ adipose tissue macrophages are associated with insulin resistance in human obesity." Diabetes **59**(7): 1648-1656.

Winer, D. A., S. Winer, et al. (2011). "B cells promote insulin resistance through modulation of T cells and production of pathogenic IgG antibodies." Nat Med **17**(5): 610-617.

Winer, S., Y. Chan, et al. (2009). "Normalization of obesity-associated insulin resistance through immunotherapy." Nat Med **15**(8): 921-929.

Withers, S. B., L. Simpson, et al. (2014). "cGMP-dependent protein kinase (PKG) mediates the anticontractile capacity of perivascular adipose tissue." Cardiovasc Res **101**(1): 130-137.

Wojcicka, G., A. Jamroz-Wisniewska, et al. (2011). "Differential effects of statins on endogenous H2S formation in perivascular adipose tissue." Pharmacol Res **63**(1): 68-76.

Xie, L., M. T. Ortega, et al. (2010). "Interactive changes between macrophages and adipocytes." Clin Vaccine Immunol **17**(4): 651-659.

Yang, Q., T. E. Graham, et al. (2005). "Serum retinol binding protein 4 contributes to insulin resistance in obesity and type 2 diabetes." Nature **436**(7049): 356-362.

Zhang, H., Y. Park, et al. (2009). "Role of TNF-alpha in vascular dysfunction." Clin Sci (Lond) **116**(3): 219-230.

Zhang, H., B. J. Potter, et al. (2011). "Interferon-gamma induced adipose tissue inflammation is linked to endothelial dysfunction in type 2 diabetic mice." Basic Res Cardiol **106**(6): 1135-1145.

Zhang, H. and C. Zhang (2012). "Vasoprotection by dietary supplements and exercise: role of TNFalpha signaling." Exp Diabetes Res **2012**: 972679.

Zhang, L., T. Sugiyama, et al. (2011). "The inflammatory changes of adipose tissue in late pregnant mice." J Mol Endocrinol **47**(2): 157-165.

CHAPTER IV

FUTURE DIRECTIONS

In this study, we have shown that during the progression of T2DM, dendritic cells are recruited into PVAT as opposed to within the vascular wall; per se. Dendritic cells were also shown to contribute to the generation of a pro-inflammatory environment in PVAT and impair vasoreactivity of small MA. To further implicate a role for dendritic cells, we used a genetic model ($Flt3^{-/-}$) in which dendritic cell was reduced. Depletion of dendritic cells in *db/db* mice markedly decreased pro-inflammatory cytokine production (despite persistence of marked obesity) and further restored vasorelaxation. The data, however, raise additional questions and suggest a number of future directions. For example, it remains unclear whether pro-inflammatory cytokines are directly secreted by dendritic cells or are secreted by other cell types as a consequence of dendritic cell infiltration. In addition, the attenuation of insulin resistance by dendritic cell depletion outlined in chapter III remains to be fully investigated. From a mechanistic point of view, it is unclear exactly how vascular function was improved by dendritic cell depletion in our model of T2DM (for example is there an impact on particular K^+ channels which have been implicated in the actions of 'ADRF')(Zavaritskaya, Zhuravleva et al. 2013, Noblet, Owen et al. 2015)). Finally, it would be of value to ascertain whether dendritic cell depletion protects T2DM mice from other complications such as cardiac dysfunction or ischemia reperfusion injury. In order to answer some of these questions/future directions, the following experiments are suggested.

4.1. Are dendritic cells the main source for pro-inflammatory cytokine secretion in adipose tissue of T2DM mice?

Under physiological conditions, dendritic cells in the immune system function as professional antigen-presenting cells. In this role, these cells usually first recognize and process foreign antigens in peripheral tissues. Subsequently they migrate to lymphoid organs and present these antigens to effector cells, such as T and B lymphocytes, which then clear the foreign antigens in an effort to maintain immune homeostasis (Banchereau and Steinman 1998). Recent studies have shown that T lymphocytes infiltrate into obese adipose tissue, secrete multiple

cytokine species, and cause adipose tissue inflammation (Nishimura, Manabe et al. 2009). It is, therefore, possible that during the progression of T2DM, dendritic cells accumulate in adipose tissue and activate T lymphocytes to secrete inflammatory cytokines locally. Interestingly, another investigation in diabetic mice reported that adipose tissue-associated dendritic cells lost their antigen-presenting function and switched to a secretory phenotype (Macia, Delacre et al. 2006). These findings suggest that dendritic cells, themselves, can generate and secrete different inflammatory cytokines into adipose tissue. In order to address this controversy and to specifically determine, in a model of T2DM, whether dendritic cells directly or indirectly contribute to the secretion of inflammatory cytokines is proposed in the following experiments.

Since adipose tissue inflammation was shown to be more severe in *db/db* mice at 18-22 weeks compared to that at 6-10 weeks (see **Fig.2-6** and **2-7**), DbHET and *db/db* mice at 18-22 weeks will be used to determine the source of inflammatory cytokine production. Initially, $CD11c^{+}$ $F4/80^{-}$ and $CD83^{+}CD86^{+}$ dendritic cell populations in VAT from both DbHET and *db/db* mice will be detected using flow cytometry (Macia, Delacre et al. 2006). Subsequently, intracellular cytokine detection of TNF-α, IL-6 and IFN-γ in flow cytometry will be applied to the isolated dendritic cell populations. If the dendritic cells resident in T2DM adipose tissue secrete various inflammatory cytokines as we predict, increased protein levels of TNF-α, IL-6 and IFN-γ will be observed in *db/db* compared to DbHET mice. If dendritic cells are not the source of inflammatory cytokines, there will be similar expression of TNF-α, IL-6 and IFN-γ protein between DbHET and *db/db* mice. Our previous data (in chapter II) also have shown that M1 macrophages were accumulated in VAT from *db/db* compared to DbHET mice. It is possible that M1 macrophages would be responsible for the inflammatory cytokine production. In order to demonstrate this hypothesis, the same protocols as above will be employed in $CD11c^{+}$ $F4/80^{+}$ M1 macrophage population in VAT from *db/db* and DbHET mice. If the hypothesis were confirmed to be correct, it is expected that VAT from *db/db* mice would have higher TNF-α, IL-6 and IFN-γ levels than DbHET mice.

4.2. Does genetic depletion of dendritic cells alter insulin sensitivity in peripheral tissues of T2DM mice?

Consistent with the literature, our data show (see **Fig.3-3.**) that *db/db* mice exhibit markedly higher blood glucose levels, compared to DbHET mice, during glucose tolerance tests. Furthermore, insulin resistance tests showed an impaired glucose lowering effect of insulin in *db/db* mice compared to DbHET controls. Interestingly, our studies also showed that genetic depletion of dendritic cells in *db/db* mice significantly decreases blood glucose levels during glucose tolerance tests and improves the glucose lowering effect of insulin. Consistent with this, studies in which $CD11c^{+}$ cells were ablated in high fat fed obese mice demonstrated normalization of muscle, liver, and adipose tissue insulin sensitivity during euglycemic clamp experiments (Patsouris, Li et al. 2008). Thus, it appears that dendritic cell depletion would also improve insulin resistance in the peripheral tissue from *db/db* mice, which would further extend the observation of dendritic cell role in the amelioration of insulin resistance. In order to test this hypothesis the following experiments are proposed.

Firstly, euglycemic clamp studies will be conducted in DbHET, $DbHET^{Flt3l-/-}$, *db/db* and db^{Flt3l-}/ db^{Flt3l-} mice at 18-22 weeks (Hevener, Olefsky et al. 2007). In these studies, the insulin sensitivity of skeletal muscle will be measured by insulin-stimulated glucose disposal rate. The insulin sensitivity of liver will be measured by insulin-mediated suppression of hepatic glucose output and the insulin sensitivity of adipose tissue will be measured by insulin-induced suppression of plasma free fatty acid. Two catheters will be implanted in both jugular veins in the above mice, after which they will be fasted for 5 hours. After fasting, equilibration solution containing tracer (5 µCi/h of [3-^{3}H]D-glucose) will be applied into one catheter until a constant plasma tracer concentration is achieved. After equilibration, blood will be collected via a tail nick to obtain basal sampling. Subsequently infusion of insulin (6.0 mU/kg/min, 0.12 ml/hr) plus tracer (5 µCi/hr) and glucose (50% dextrose) will be initiated until a steady-state blood glucose concentration is achieved. At steady state, additional blood samples will be taken to measure post-clamp plasma free fatty acid levels. It is predicted that insulin-stimulated glucose disposal rate, insulin-mediated

suppression of hepatic glucose output and insulin-induced suppression of plasma free fatty acids levels will be significantly decreased in *db/db* mice, compared to DbHET mice. These results would indicate the presence of insulin resistance in skeletal muscle, liver and adipose tissue of *db/db* mice. It is expected that above parameters will be comparable between DbHET and DbHET$^{Flt3l-/-}$ mice suggesting that normal insulin reactivity is maintained in DbHET mice despite dendritic cell depletion. Given our preliminary glucose and insulin tolerance tests we predict that *db*$^{Flt3l-}$/ *db*$^{Flt3l-}$ mice will exhibit significant restoration of skeletal muscle, liver, and adipose tissue insulin reactivity when compared to *db/db* counterparts, indicating that dendritic cell depletion would protect from T2DM-induced insulin resistance.

Secondly, molecular studies will be performed examining insulin sensitivity of the above four groups of mice. Since it is well known that skeletal muscle and hepatic insulin resistance in T2DM mice are accompanied by increased triglyceride content, it is important to measure enzymes involved in triglyceride metabolism to provide another piece of evidence to support our hypothesis (Liang, Osborne et al. 2004, Anstee and Goldin 2006). To accomplish this, peroxisome proliferator-activated receptor (PPAR) α, acetyl-CoA carboxylase 1 (ACC1), stearoyl CoA desaturase-1 (SCD1) and liver X receptor α (LXR α), which participate in lipogenesis and lipid oxidation processes, will be examined. mRNA and protein expression for these enzymes will be measured in skeletal muscle and liver from DbHET, DbHET$^{Flt3l-/-}$, *db/db* and *db*$^{Flt3l-}$/ *db*$^{Flt3l-}$ mice at 18-22 weeks. It is expected that mRNA and protein expressions of PPAR-α, ACC1, SCD1 and LXR-α will be increased in *db/db* mice compared to DbHET mice. However, it is anticipated that those levels will be decreased in *db*$^{Flt3l-}$/ *db*$^{Flt3l-}$ mice after dendritic cell depletion, whereas those enzyme levels will be comparable between DbHET and DbHET$^{Flt3l-/-}$ mice.

In summary, this quantification of insulin sensitivity of skeletal muscle, liver and adipose tissue, along with alterations of molecular enzymes will present another perspective to unveil the effect of dendritic cell depletion on the amelioration of insulin resistance in T2DM mice. Combined with glucose and insulin tolerance tests in chapter III, these studies will increase knowledge as to the role of dendritic cells in the insulin resistance in T2DM.

4.3 Does expression of Kv channels change in T2DM when vascular function is restored by dendritic cell depletion?

Previous studies have shown that the anti-contractile activity provided by perivascular adipose tissue involves the activation of vascular smooth muscle potassium ion channels. In particular, Kv (voltage-dependent potassium) channels have been suggested to play a major role (Gollasch 2012). Specifically, it has been proposed that release of ADRF (adipocyte-derived relaxing factors) from perivascular adipose tissue stimulates the opening of Kv channel and decreases calcium influx into vascular smooth muscle cells, leading to vasorelaxation or the 'anti-contractile' effect (Gao, Lu et al. 2007, Gollasch 2012). In pathological conditions, such as hypertension, both the expression of Kv channels is decreased and the anti-contractile action of perivascular adipose tissue is impaired (Oriowo 2014). However, little research has focused on Kv channel expression in mesenteric arteries of T2DM mice. In addition, little is known about whether the expression of Kv channel is associated with blunted anti-contractile function induced by obese perivascular adipose tissue. Previous investigations have demonstrated that ARDF release is impaired in obese perivascular adipose tissue (Estacio, Jeffers et al. 2000). Combined with the findings in chapter III that the anti-contractile function derived from diabetic mesenteric adipose tissue was impaired, it is possible that the expression of Kv channels is decreased in the vasculature of T2DM mice. Thus, the low level of Kv channels in the diabetic vasculature would lead to the loss of anti-contractile function of perivascular adipose tissues. Since our previous data in Chapter III has indicated that genetic depletion of dendritic cells restores anti-contractile and vasorelaxation augmentation effects of diabetic perivascular adipose tissue, it is possible that genetic depletion of dendritic cells would also restore Kv channel expression on vasculature, resulting in restoration of vascular function.

In order to test above hypothesis, the following experiments are proposed. First order mesenteric arteries from DbHET, DbHET$^{Flt3l-/-}$, *db/db* and *db*$^{Flt3l-}$/ *db*$^{Flt3l-}$ mice at 18-22 weeks will be harvested. Western blotting will be conducted on the above vessels to detect the protein levels of Kv channels. To assess function, the Kv channel blocker 4-aminopyridine (4-AP) will be added

to MAT/mesenteric artery co-incubations in db^{Flt3l-}/ db^{Flt3l-} mice, whereas Kv channel agonist retigabine will be applied to MAT incubation with mesenteric arteries in *db/db* mice (Lee, Yang et al. 2015). It is anticipated that Kv channel protein levels in mesenteric arteries will be decreased in *db/db* mice compared to DbHET controls. Depletion of dendritic cells has been shown to largely reduce pro-inflammatory cytokines production in chapter III. Therefore, depletion of dendritic cells would significantly restore Kv channel expression on mesenteric arteries in db^{Flt3l-}/ db^{Flt3l-} mice. It is also possible that administration of 4-AP will impair the anti-contractile and vasorelaxation augmentation effects from MAT in db^{Flt3l-}/ db^{Flt3l-} mice. Activation of Kv channels by retigabine will partially restore the anti-contractile and vasorelaxation augmentation responses on mesenteric arteries from *db/db* mice. However, it has been reported that the increasing protein expression of Kv channels on arteries is not always associated with the increment of Kv channel activity, due to the increasing expression of an inhibitory subunit in Kv channel (Lee, Yang et al. 2015). In that case, the restored expression of Kv channels in db^{Flt3l-}/ db^{Flt3l-} mice probably would not improve the vascular dysfunction caused by T2DM. If so, other mechanisms would be indicated, such as the restoration of calcium-dependent potassium channel on diabetic mesenteric arteries(Weston, Egner et al. 2013). Similar protocols will be adopted as above.

4.4. Does depletion of dendritic cells protect diabetic mice from ischemia /reperfusion injury?

It is well known that T2DM is a metabolic disease accompanied with an increase incidence of cardiovascular disorders, including myocardial infarction and congestive heart failure (Greer, Ware et al. 2006). These cardiovascular outcomes have been shown to be related to vascular dysfunction of small resistance arteries in diabetic mice, such as coronary arteries (Guo, Su et al. 2005, Moien-Afshari, Ghosh et al. 2008). Our previous data (see **Fig.3-7**) have shown that when dendritic cells were genetically depleted, endothelial-dependent vasorelaxation responses were restored in *db/db* mice. It is, therefore, hypothesized that dendritic cell depletion may also decrease ischemia/ reperfusion injury in *db/db* mice, resulting in a decrease in cardiovascular events caused by T2DM. In support of this, one of the molecular mechanisms implicated in

ischemia/ reperfusion injury is the increased production of the pro-inflammatory cytokine TNF-α (Zhang, Park et al. 2009). Of relevance, our qPCR data (see **Fig. 3-5** and **Fig.3-6**) have shown that dendritic cell depletion decreased the production of TNF-α in adipose tissue from *db/db* mice. Collectively, these data provides another piece of evidence to support the hypothesis that dendritic cell depletion would protect *db/db* mice from ischemia/ reperfusion injury.

In order to test the above hypothesis, DbHET, DbHET$^{Flt3l-/-}$, *db/db* and *db*$^{Flt3l-}$/ *db*$^{Flt3l-}$ mice at 18-22 weeks will be used in the following experiments. Mice will be subjected to escalating durations of left coronary artery ischemia surgery (30, 45 and 60 minutes) as described in previous studies (Greer, Ware et al. 2006). Mice will be allowed to undergo reperfusion for 28 days and waif for the development of heart failure. After reperfusion, we will assess the survival rate of the mice and left ventricular contractile function using high frequency echocardiography. Left ventricle tissue from above mice will be harvested for measurement of TNF-α protein expression. It is expected that all the mice will have decreased survival rate in parallel with the increasing duration of ischemia (from 30 to 60 minutes). Amongst the experimental groups, *db/db* mice will likely exhibit significantly lower survival rates at each time of ischemia compared to DbHET controls. Conversely, *db*$^{Flt3l-}$/ *db*$^{Flt3l-}$ mice will exhibit prolonged survival rates in comparison with *db/db* mice. Further it is anticipated that there will be no significant difference in survival rates between DbHET and DbHET$^{Flt3l-/-}$ mice. Left ventricular end-diastolic dimension, left ventricular end-systolic dimensions and left ventricular fractional shortening parameters are predicted to be similar in DbHET and DbHET$^{Flt3l-/-}$ mice following ischemia/ reperfusion injury. In contrast, increased left ventricular end-diastolic and end-systolic dimensions along with decreased left ventricular fractional shortening parameters are expected to be observed in *db/db* mice compared to DbHET mice and again parallel the duration of ischemia. These results would be consistent with an increased propensity for deterioration of left ventricular function and development of heart failure in *db/db* mice. However, *db*$^{Flt3l-}$/ *db*$^{Flt3l-}$ mice would exhibit partially decreased left ventricular end-diastolic and end-systolic dimensions, along with partially increased left ventricular fractional shortening parameters, compared to *db/db* mice. These results would suggest that dendritic cell depletion restores left ventricular function and protects

db/db mice from further heart failure development. Western blotting studies are predicted to show increased TNF-α protein levels in the left ventricles of *db/db* mice compared to DbHET controls, whereas TNF-α levels will be decreased in db^{Flt3l-}/ db^{Flt3l-} mice compared to *db/db* mice. Immunofluorescence staining of TNF-α levels in left ventricles from above mice not only would further support western blotting findings, but also could reveal the location of TNF-α protein distribution in the left ventricles. These results would provide molecular basis for cardiac function changes in above mice.

To sum up, in the future experiments, we will further explore more activities of dendritic cells in the development of T2DM. Firstly, we will determine whether dendritic cells have secretory function and directly release pro-inflammatory cytokines into diabetic adipose tissue. Secondly, we will study whether this pro-inflammatory secretion profile of dendritic cells would be responsible for the reduction of peripheral insulin sensitivity in diabetic mice. Thirdly, we will confirm whether the depletion of dendritic cells, reduction of inflammatory state and improvement of insulin sensitivity in perivascular adipose tissue, would restore Kv channel expression on mesenteric arteries. Last, we will test whether depletion of dendritic cells, reduction of inflammatory state along with improvement of insulin sensitivity and Kv channel expression, would reduce the damage of ischemia/reperfusion injury in diabetic mice. Through those four hypotheses, the role of dendritic cells in vascular dysfunction and insulin resistance caused by T2DM would be further revealed. The result would provide a novel therapeutic target for the treatment of T2DM.

4.5. REFERENCES

Anstee, Q. M. and R. D. Goldin (2006). "Mouse models in non-alcoholic fatty liver disease and steatohepatitis research." International journal of experimental pathology **87**(1): 1-16.

Banchereau, J. and R. M. Steinman (1998). "Dendritic cells and the control of immunity." Nature **392**(6673): 245-252.

Estacio, R. O., B. W. Jeffers, et al. (2000). "Effect of blood pressure control on diabetic microvascular complications in patients with hypertension and type 2 diabetes." Diabetes Care **23**: B54.

Gao, Y. J., C. Lu, et al. (2007). "Modulation of vascular function by perivascular adipose tissue: the role of endothelium and hydrogen peroxide." British journal of pharmacology **151**(3): 323-331.

Gollasch, M. (2012). "Vasodilator signals from perivascular adipose tissue." British journal of pharmacology **165**(3): 633-642.

Greer, J. J., D. P. Ware, et al. (2006). "Myocardial infarction and heart failure in the db/db diabetic mouse." American Journal of Physiology-Heart and Circulatory Physiology **290**(1): H146-H153.

Greer, J. J., D. P. Ware, et al. (2006). "Myocardial infarction and heart failure in the db/db diabetic mouse." Am J Physiol Heart Circ Physiol **290**(1): 19.

Guo, Z., W. Su, et al. (2005). "COX-2 up-regulation and vascular smooth muscle contractile hyperreactivity in spontaneous diabetic db/db mice." Cardiovascular Research **67**(4): 723-735.

Hevener, A. L., J. M. Olefsky, et al. (2007). "Macrophage PPAR gamma is required for normal skeletal muscle and hepatic insulin sensitivity and full antidiabetic effects of thiazolidinediones." J Clin Invest **117**(6): 1658-1669.

Lee, S., Y. Yang, et al. (2015). "Heterogeneity in Kv7 channel function in the cerebral and coronary circulation." Microcirculation **22**(2): 109-121.

Liang, Y., M. C. Osborne, et al. (2004). "Reduction in glucagon receptor expression by an antisense oligonucleotide ameliorates diabetic syndrome in db/db mice." Diabetes **53**(2): 410-417.

Macia, L., M. Delacre, et al. (2006). "Impairment of dendritic cell functionality and steady-state number in obese mice." J Immunol **177**(9): 5997-6006.

Moien-Afshari, F., S. Ghosh, et al. (2008). "Exercise restores endothelial function independently of weight loss or hyperglycaemic status in db/db mice." Diabetologia **51**(7): 1327-1337.

Nishimura, S., I. Manabe, et al. (2009). "$CD8^+$ effector T cells contribute to macrophage recruitment and adipose tissue inflammation in obesity." Nature medicine **15**(8): 914-920.

Oriowo, M. A. (2014). "Perivascular adipose tissue, vascular reactivity and hypertension." Medical Principles and Practice **24**(Suppl. 1): 29-37.

Patsouris, D., P.-P. Li, et al. (2008). "Ablation of CD11c-positive cells normalizes insulin sensitivity in obese insulin resistant animals." Cell metabolism **8**(4): 301-309.

Zhang, H., Y. Park, et al. (2009). "Role of TNF-α in vascular dysfunction." Clinical Science **116**(3): 219-230.

VITA

Tianyi Qiu was born in October 31, 1984 in Liaoning province, China. She attended Medical School of Wuhan University at 2002. She received her Medical Degree in 2009. During the 7 years medical training, she witnessed the sufferings from microvascular diseases, such as atherosclerosis, diabetes, and some nephropathies. This experience raised her interest in the pathogenesis of those diseases and she tried to find a therapeutic method to save those lives. That is the main reason why she applied Medical Pharmacology and Physiology of University of Missouri, Columbia, which is famous for the study of microcirculation physiology. After this years' Ph.D. training, she acquired the basic techniques to conduct microcirculation research and gained more knowledge into the vascular function of type 2 diabetes. She hopes that these learned skills would one day be used to explore more mechanisms behind type 2 diabetes.